

Tectonomagnetic Modeling on the Basis of the Linear Piezomagnetic Effect

Yoichi SASAI

Earthquake Research Institute, University of Tokyo

(Received September 27, 1991)

Table of Contents

Abstract	586
1. Introduction.....	587
2. Basic Theory	596
2.1 The Linear Piezomagnetic Effect	598
2.2 Basic Equation	601
2.3 Representation Theorem	603
2.4 The Seismomagnetic Moment	607
2.5 The Stacey-Nagata Piezomagnetic Solid	610
2.6 Predominance of the Piezomagnetic Effect —the Mogi Model as an Example—.....	611
3. Piezomagnetic Field Associated with the Mogi Model.....	615
3.1 Point Source Problem—A Paradox	616
3.2 Finite Spherical Source Solution.....	626
3.3 Point Source Solution as a Limiting Case of Finite Spherical Source.....	634
4. Green's Function Approach to Tectonomagnetic Problems....	640
4.1 Formulation	641
4.2 Fundamental Piezomagnetic Potentials	644
4.3 Dam Magnetic Effect.....	654
5. Dislocation Source Problems	659
5.1 Volterra's Formula for the Piezomagnetic Field	660
5.2 Elementary Piezomagnetic Potentials.....	662
5.3 Multiple Tension-Crack Model	674
5.4 Magnetic Change due to Vertical Strike-Slip and Tensile Faults.....	681
Acknowledgements	691
Appendix A: Derivation of the Isotropic Piezomagnetic Law....	691
Appendix B: The Double Fourier Transforms.....	693
Appendix C: The Integrals of Lipschitz-Hankel Type	696
Appendix D: Three Constituents of the Elementary Piezomagnetic Potentials.....	701
Appendix E: Piezomagnetic Potential due to Vertical Strike-Slip and Tensile Faults.....	708
References	715

Abstract

Modeling of tectonomagnetic changes is formulated in a unified way. First the linear relationship between magnetization and stress is obtained for a general 3-dimensional stress state. It is deduced by applying the principle of superposition to experimental results of uniaxial compression tests. The isotropic piezomagnetic law thus obtained has two independent parameters, which is equivalent to the law proposed by ZLOTNICKI *et al.* (1981). The ordinary piezomagnetic law (STACEY, 1964; NAGATA, 1970a) with a single parameter, i.e. the stress sensitivity, is a particular case of this extended formula. Because of its simplicity and validity as an average for aggregates of various rocks, the single parameter formula is applied in the following calculations. The basic equation is derived by connecting the Gaussian law for the magnetic field and the Cauchy-Navier equation for static elastic equilibrium through constitutive relationships, i.e. the piezomagnetic law and the Hooke law for isotropic elasticity. It is a Poisson's equation with a source term expressed in terms of the displacement. The representation theorem is obtained for the solution: the tectonomagnetic field is given by surface integrals of the displacement and its normal derivatives over the strained body. Applying the theorem to a medium including a dislocation surface within it, we find that the dislocation surface behaves as a magnetic sheet. For Volterra dislocations, the magnetic sheet becomes simply a double layer, of which the moment is given by the inner product of the displacement discontinuity and the magnetization vector. The seismomagnetic moment thus defined is useful to intuitively realize coseismic magnetic changes. In the following calculations, the model earth considered is the simplest one: a homogeneous and isotropic elastic half-space having a uniformly magnetized top layer with a constant stress sensitivity.

The piezomagnetic field associated with the Mogi model is investigated in detail. Two mathematical techniques are introduced, which are frequently used throughout this study: i.e. the double Fourier (or Hankel) transforms and the Lipschitz-Hankel type integrals. The piezomagnetic field associated with the inflation of a finite spherical pressure source is solved with the aid of these two methods. The point source solution is also obtained, and subsequently used as a Green's function for the multiple Mogi model in Chapter 5. The way we obtained the point source solution becomes the prototype of constructing Green's functions in the following chapters. In the case of integrals containing a singular point of the stress field, we must take a limit in a special way: i.e. to enclose the singular point with a closed surface which satisfies the boundary conditions and then to shrink the surface to that point.

A variety of tectonic models can be formed by superposing the displacement field solutions of single forces acting at points in an

elastic half-space. Piezomagnetic changes associated with the same models are given as well by the linear combination of fundamental piezomagnetic potentials, which arise from stress-induced magnetization produced by unit single forces acting at points. The method is adaptable to surface load and volume source problems. As an application example, piezomagnetic change is calculated for a uniform circular load. Comparing the calculations with some observations of the dam-magnetic effect, we suggest that the *in situ* value of the stress sensitivity of the upper crust is an order of magnitude greater than that of stiff rocks which are usually tested in rock-magnetic experiments.

Finally the dislocation problems are considered. The same integral representation as the Volterra formula for the elastic field is derived for the piezomagnetic field. The elementary piezomagnetic potentials are defined as the potentials produced by a point dislocation. The effect of divergent stresses around a point dislocation is evaluated as follows: we enclose the point dislocation with a small thin disk parallel to the infinitesimal dislocation surface, diminish the thickness of the disk and then its radius. Elementary potentials consists of dipoles and multipoles at the position of point dislocation and their mirror images with respect to the Curie depth. However, some types of strain nuclei lack magnetic source equivalents at the dislocation position. Hence the seismomagnetic effect accompanying some kinds of fault motion becomes much weaker than that anticipated from the seismomagnetic moment. An important application of the theory is the multiple tension-crack model, which is a versatile model for crustal dilatancy or crustal deformation of volcanic origin. Another application is the piezomagnetic change associated with faulting. Formulas for a vertical rectangular fault with shearing as well as tensile fault motion are presented.

1. Introduction

Does the geomagnetic field change in association with or prior to an earthquake?—The question was raised even in the cradle stage of seismology. In 1891, just a hundred years ago, the Mino-Owari earthquake of M 8.0 occurred in the central part of Japan, which was one of the most severe and damaging earthquakes inland in Japan (7,232 people were killed). TANAKADATE and NAGAOKA (1893) conducted resurveys of geomagnetic measurement over a wide area, and found an enormous change in the geomagnetic field, especially in the horizontal component, at a survey point in Nagoya city closest to the focal zone. The observed change, almost 1,000 nT in magnitude, was too large as compared with our present day standard of observations (RIKITAKE, 1968). However, their physical understanding of the possible cause of such a “seismo-

magnetic effect" is common to ours. They stated: "Whether this disturbance is due to the change of magnetic conditions of the earth's crust in the vicinity caused by strain, or to the change in conductivity for earth currents, or, again, is the result of the dislocation of the magnetic crust, is more than we can decide from the scanty data which we now possess. These points will undoubtedly afford most interesting subjects of research in the future." (TANAKADATE and NAGAOKA, 1893, p. 176.)

In Japan many efforts have been made to observe magnetic changes associated with earthquakes and volcanic eruptions (e.g. KATO, 1939; TAZIMA, 1966). Magnetic observations in volcanos detected significant changes. In the 1940 eruptions of Miyakejima Volcano, a few independent magnetic observations detected mutually consistent and outstanding changes in the geomagnetic field (KATO, 1940; TAKAHASI and HIRANO, 1941a, b; NAGATA, 1941; MINAKAMI, 1941). In the 1950 eruption of Izu-Oshima Volcano, remarkable changes in the geomagnetic dip were detected (RIKITAKE, 1951). During the decade after the 1950 eruption, continuous observations of magnetic declination were made in Izu-Oshima Volcano. Geothermal processes within the volcano were discussed on the basis of magnetic data (YOKOYAMA, 1956, 1969). After 12 years' repose, Izu-Oshima Volcano erupted again in November 1986. A variety of magnetic changes were observed: long-term (ca. 10 years), intermediate (ca. 3 years) and short-term (ca. 1 month) precursory changes as well as coeruptive and post-eruption magnetic changes (YUKUTAKE *et al.*, 1990a, b; SASAI *et al.*, 1990; HAMANO *et al.*, 1990). Hence, magnetic observation is regarded as a useful means to monitor the activity of Izu-Oshima Volcano (YUKUTAKE, 1990).

These magnetic changes associated with volcanic activity are probably caused by thermal demagnetization or remagnetization due to temperature changes of rocks. NAGATA's (1943) pioneer study on TRM was strongly motivated by a wish to establish the physical basis for interpreting his own magnetic observations at the time of the Miyakejima eruptions in 1940.

As compared with volcanomagnetic observations, earthquake-related magnetic changes were less reliable. KATO and UTASHIRO (1949) reported on a coseismic change in the geomagnetic declination amounting to 35 nT associated with the 1946 Nankaido earthquake of M 8.0. The result was obtained at a magnetic observatory through absolute measurements made every 5 days, which was a rare example of reliable observations in the first half of this century. Development of highly sensitive, spin precession magnetometers made a breakthrough in seismomagnetic observations (BREINER, 1964). In particular, reliable data are available since proton precession magnetometers were widely introduced in the 1960's (RIKITAKE,

1968).

The total intensity change during the Matsushiro earthquake swarm is typical of such observations (RIKITAKE *et al.*, 1968). The number of observed seismomagnetic events has been increasing since then: the Izu-Oshima-Kinkai earthquake of M 7.0 in 1978 (OHCHI *et al.*, 1979: preseismic change), the Higashi-Izu earthquake of M 4.9 in 1978 (SASAI and ISHIKAWA, 1980a: pre- and coseismic), near the Yamasaki-fault earthquake of M 5.6 in 1984 (SUMITOMO and NORITOMI, 1986: post-seismic). We failed, however, to catch the coseismic change even within 10 km from the earthquake fault: the East-Off Izu Peninsula earthquake of M 6.7 in 1980 (SASAI and ISHIKAWA, 1980b). Remarkable changes are also found in association with the anomalous crustal uplift in the eastern part of the Izu Peninsula (SASAI, 1989; SASAI and ISHIKAWA, 1991).

In the United States a telemetered magnetometer array was established along the San Andreas fault (JOHNSTON *et al.*, 1976), which was used to observe the 1974 Thanksgiving Day earthquake of M 5.4 (SMITH and JOHNSTON, 1976: preseismic), aseismic magnetic event near San Juan Bautista in 1975 (JOHNSTON, 1978) and the North Palm Springs earthquake of M 5.9 in 1986 (JOHNSTON and MUELLER, 1987: coseismic). Moreover, enormous changes were detected by repeat surveys over the southern California downwarp (JOHNSTON *et al.*, 1979).

In the People's Republic of China, magnetic measurement is an important tool for earthquake forecasting. Remarkable changes were observed before the 1976 Tangshan earthquake of M 7.8 (ZHAN, 1989). Observations of local magnetic changes with special reference to the earthquake prediction study have been extensively carried out in Soviet central Asia (SHAPIRO *et al.*, 1978). No coseismic change was observed at the time of the Gazly earthquake of M 7.3 in 1976 (SHAPIRO and ABDULLABEKOV, 1978). However, a remarkable magnetic precursor up to +23 nT was detected 3 days prior to the 1978 Alay earthquake of M 7.0: the earthquake warning was actually issued on the basis of this anomalous magnetic change (SHAPIRO and ABDULLABEKOV, 1982). In Turkey, search for magnetic precursors to earthquake has been made in the most active fault zone, i.e. the north Anatolian fault system (ISPIR and UYAR, 1976). Recently magnetic observations are being intensively carried out in this region (ISIKARA and HONKURA, 1988; UHRENBACHER, 1988).

Variation of magnetization caused by applied stresses is called the piezomagnetic effect. This is the inverse effect of magnetostriction, in which the magnetic substance is strained under an applied magnetic field. We should recall that TANAKADATE and NAGAOKA (1893) first proposed "the change of magnetic conditions of the earth's crust caused by strain" as a possible cause of seismomagnetic change. Actually, Hantaro Naga-

oka's (1865-1950) first scientific work was some experiments on the magnetostriction of ferromagnetic materials (e.g. NAGAOKA, 1889). The piezomagnetic effect of rocks was first experimentally confirmed on the magnetic susceptibility by KALASHNIKOV and KAPITSA (1952). The same phenomenon was ascertained for the hard remanent magnetization such as TRM of rocks by OHNAKA and KINOSHITA (1968). These experimental results were summarized by NAGATA (1970a).

Since earthquake faulting occurs almost isothermally, the cause of magnetic changes associated with earthquakes is considered to be stress rather than temperature. STACEY (1964) proposed the term "seismomagnetic effect" for such magnetic changes. Moreover, we have some examples of magnetic changes related to volcanic activity as most probably due to stresses because of their rapid time variations: e.g. magnetic changes at Mt. Ruapehu, New Zealand (JOHNSTON and STACEY, 1969), coeruptive change at Kilauea Volcano, Hawaii (DAVIS *et al.*, 1974, 1979), the change accompanied by the catastrophic blast of Mt. St. Helens on May 18, 1980 (JOHNSTON *et al.*, 1981), and changes at the time of fissure eruption in Izu-Oshima Volcano on Nov. 21, 1986 (SASAI *et al.*, 1990). Intrusion of magma or stress build-up in the reservoir could produce magnetic changes owing to the piezomagnetic effect. Hence STACEY *et al.* (1965) called such magnetic changes the "volcanomagnetic effect".

Another new idea was proposed for the origin of magnetic changes associated with tectonic events: the electrokinetic effect due to underground water flow (MIZUTANI *et al.*, 1976). MIZUTANI and ISHIDO (1976) claimed that the magnetic changes during the Matsushiro swarm earthquakes were well explained by this effect because a huge amount of ground water gushed out in the final stage of the swarm activity. The streaming potential due to ground water flow can be the most probable cause of self potential changes related to tectonic activity (FITTERMAN, 1978; ISHIDO and MIZUTANI, 1981). The associated earth currents could produce the magnetic field (FITTERMAN, 1979). Recent theoretical studies show that the electrokinetic effect is rather too weak to produce an observable magnetic field if ordinary values of earth resistivity and water flow speed are assumed (FITTERMAN, 1981; MURAKAMI, 1989). However, there still remains a possibility that this effect can contribute to magnetic changes, especially in hydrothermal volcanic regions (e.g. ZLOTNICKI and LE MOUËL, 1988).

The study of magnetic changes associated with various kinds of tectonic activity such as earthquakes, volcanic eruptions, gradual crustal movement and so on was named "Tectonomagnetism" by NAGATA (1969). The term "tectonomagnetism" is sometimes given the narrow meaning of only the study of magnetic fields of piezomagnetic origin. We should,

however, regard it as "the study of generating mechanisms of various tectonic events through geomagnetic observations". The origin of magnetic changes may be either stress, temperature or ground water, or a combination of them. One of the ultimate objectives of tectonomagnetism is to contribute to earthquake prediction and volcanic eruption forecasting.

Tectonomagnetism is part of a wider field of study, i.e. "Tectono-Electro-Magnetics (TEM)". TEM is the study of all kinds of electromagnetic phenomena associated with tectonic activity. Apart from (a) quasi-static magnetic changes (tectonomagnetism), we have a variety of electromagnetic observations: i.e. (b) changes in the earth's resistivity (e.g. YANAGIHARA, 1972; MAZZELLA and MORRISON, 1974; YAMAZAKI, 1977; HONKURA and TAIRA, 1983; YUKUTAKE *et al.*, 1987), (c) anomalous changes in self potential (e.g. CORWIN and MORRISON, 1977, VAROTSOS and ALEXOPOULOS, 1984a, b; MIYAKOSHI, 1986), and (d) electromagnetic emissions including 'earthquake light' (e.g. TERADA, 1931; GOKHBERG *et al.*, 1982). Tectono-Electro-Magnetics is based on observations of mechanical phenomena in the crust with electromagnetic means and aims at clarifying the generating mechanisms of tectonic events.

Now let us briefly review experimental and theoretical studies of the piezomagnetic effect of rocks. There are two sorts of stress-induced magnetization change: reversible and irreversible ones (NAGATA, 1970a). One of the prominent irreversible changes is that the remanent magnetization decreases under applied stresses: this can be a cause of coseismic magnetic change (e.g. Shock Remanent Magnetization (SRM): NAGATA, 1971). In the case of reversible piezomagnetic change, the induced piezomagnetism is approximately proportional to applied stress. This linearity makes it easy for us to compute the piezomagnetic field. Actually tectonomagnetic modeling has hitherto been limited to models based on the linear piezomagnetic effect.

Many experimental studies have been reported: e.g. KAPITSA (1955), KINOSHITA (1968), NAGATA and CARLETON (1968), KEAN *et al.* (1976). Physical interpretations of the piezomagnetic effect of rocks have been attempted (e.g. KERN, 1961; STACEY, 1962; KINOSHITA, 1969; NAGATA 1970b; STACEY and JOHNSTON, 1972; HODYCH, 1976, 1977). For ferromagnetic minerals with single domain structure, the reversible change can be explained by rotation of spontaneous magnetization. Most minerals have multi-domain structure, in which movement of the 90° domain wall occurs at a certain stress level to bring about irreversible changes. NRM's of some rock samples often show quite complicated behavior against applied stresses (HENYEV *et al.*, 1978; REVOL *et al.*, 1978; HAO *et al.*, 1990).

The dependence of stress sensitivity on the hydrostatic pressure was

investigated (NAGATA and KINOSHITA, 1967; NULMAN *et al.*, 1978). The stress sensitivity, i.e. the proportionality constant of induced magnetization vs. stress, increases with increasing hydrostatic pressure. However, it sharply decreases with temperature around 300°C, far below the Curie point (POZZI, 1977). CARMICHAEL (1977) argued that the upper 15 km of the lithosphere is likely to be the most important in yielding observable piezomagnetic field anomalies for earthquake prediction. As a first order approximation, it seems to be valid that the uppermost crust is uniformly magnetized with a constant stress sensitivity.

The effect of dilatancy on the remanent magnetization of rocks was investigated by MARTIN *et al.* (1978). The onset of dilatancy produces changes in the rate of magnetization changes. However, the rate of change itself becomes smaller, which implies that the dilatancy-related magnetic change should be small. On the other hand, in the case of porous rock samples, the stress sensitivity is one order of magnitude greater than that of stiff rocks (HAMANO, 1983; HAMANO *et al.*, 1989). This fact, together with world-wide observations of the dam magnetic effect, suggests that the *in situ* stress sensitivity of the upper crust may be on the order of $1 \times 10^{-8} \text{ bar}^{-1}$ (see section 4.3).

In the tectonomagnetic modeling, we seek a general linear relationship among magnetization changes and stress components. ZLOTNICKI *et al.* (1981) proposed a tensorial formulation for the linear piezomagnetic law. The simplest form is given for isotropic piezomagnetic material, which is described with two independent parameters. How to derive these parameters from results of uniaxial compression experiments will be discussed in section 2.1.

Let us review the history of calculations on the tectonomagnetic field raised by the linear piezomagnetic effect. STACEY (1964) was the pioneer of such study. He assumed a hypothetical distribution of coseismic stress drop due to a vertical transect fault to estimate the seismomagnetic effect. The modeling procedure was: (a) to give the stress field at each point in the magnetized region, (b) to compute stress-induced magnetization, and (c) to calculate the magnetic field by applying the dipole law of force. In (c), he performed numerical integrations by subdividing the magnetized medium into small volume elements. Step (b) was extended to a formula for a general 3-dimensional stress state by STACEY *et al.* (1965) in their calculation of the volcanomagnetic effect. As the stresses around a magma reservoir, they utilized the stress field solution around a spherical cavity in an infinite elastic medium under a uniform external stress applied at infinity. Thus STACEY (1964) and STACEY *et al.* (1965) demonstrated that we can reasonably expect observable magnetic changes due to stresses associated with earthquakes and

volcanic activity. The work done by Stacey and his coworkers became the prototype of tectonomagnetic modeling.

Once the elementary way of modeling was established, the next step was to investigate more physically realistic models. YUKUTAKE and TACHINAKA (1967) calculated piezomagnetic changes due to an infinitely long cylinder under hydrostatic pressure from inside, embedded horizontally in a semi-infinite medium. This was the first mechanically valid model since the stress-free boundary conditions at the earth's surface were properly taken into account. Only a few nT change in the total intensity was expected for an internal pressure of 100 bars. This suggested that stress-induced magnetic changes would be smaller as compared with those anticipated so far.

Piezomagnetic changes due to a fault model based on the elasticity theory of dislocations were first calculated by SHAMSI and STACEY (1969). They proposed a 2-dimensional vertical strike-slip fault for the 1906 San Francisco earthquake and a dip-slip fault for the 1964 Alaska earthquake. Their model is called the linear slip model since the dislocations are degraded linearly to zero toward the deeper edge for a strike-slip and toward both edges for a dip-slip fault. The maximum change in total intensity was expected to be a few nT and was prominent only above the fault. TALWANI and KOVACH (1972) estimated magnetic changes due to stress concentration around the edge of a semi-infinitely long vertical strike-slip fault. HILDENBRAND (1975) investigated some 2-dimensional vertical faults including uniform and linear slip models. These studies show that the seismomagnetic effect could be observed only near an earthquake fault.

Computational difficulty increases in the case of 3-dimensional models. DAVIS (1974) calculated piezomagnetic changes caused by a square-shaped load. The dam magnetic effect, i.e. magnetic field produced by water load during the filling of a reservoir, was estimated by approximating the shape of the actual reservoir with squares. DAVIS (1976) calculated the piezomagnetic field of the Mogi model in volcanology (MOGI, 1958). He compared his results with observations in Kilauea Volcano. Davis' work became a breakthrough to 3-D modeling. JOHNSTON (1978) computed piezomagnetic field changes due to a vertical rectangular strike-slip fault to interpret an aseismic magnetic change along the San Andreas fault. OHSHIMAN (1980) developed a numerical integration program for seismomagnetic calculation of an inclined rectangular shear fault. These 3-D fault models incorporated stress field solutions based on the elasticity theory of dislocations (e.g. CHINNERY, 1963; MARUYAMA, 1964; IWASAKI and SATO, 1979).

All these model calculations followed STACEY's (1964) method. We

may call it the volume element method. It has some difficulties: (1) the incremental magnetization is a complicated function of stress components, (2) the only way to improve the accuracy of numerical integration is to diminish the size of volume elements, which requires enormous computation time in the 3-D models. Defect (1) prevents us from finding analytical solutions, while (2) makes it practically impossible to assess computational errors. SASAI (1979) obtained an analytic solution for the piezomagnetic field due to the Mogi model in the point source case. His work was done following HAGIWARA (1977a), who presented an analytic solution for the gravity change in the Mogi model with the aid of Fourier transforms. SASAI (1979) solved the difficulty (1) to find that the stress-induced magnetization in the case of an axially symmetric stress field can be expressed by a simple linear combination of stress components.

RIKITAKE (1966) first pointed out that the piezomagnetic law should be represented by a linear combination of stress or strain components. He proposed that these coefficients should be experimentally determined. Such experiments were not, however, attempted because of technical difficulty. SASAI (1980) proved that the extended piezomagnetic law by STACEY *et al.* (1965) can be reduced to a simple linear combination among stress components. This linear relationship made it possible for us to develop an analytic approach to tectonomagnetic modeling. With the aid of this formula, SASAI (1980) presented a unified treatment of tectonomagnetic models related to dislocations. As an application example, he showed that the piezomagnetic potential due to a vertical rectangular strike-slip fault could be expressed in terms of elementary functions. Moreover, the potential thus obtained had the same functional form as some of the displacement field. SASAI (1980) made an effort to represent the piezomagnetic potential with the displacement field of the strained body.

Independently of SASAI's (1980) work, BONAFEDE and SABADNI (1980) published a general treatment of tectonomagnetic modeling. From thermodynamical considerations, they derived constitutive relations of aeolotropic magnetoelastic materials. They formulated tectonomagnetic modeling as a coupled problem of two differential equations, i.e. the elastodynamic and Ampère-Maxwell equations, both of which were combined through the Hooke law and the generalized piezomagnetic law. On the assumption that the Green function exists *a priori* for such a coupled differential equations system, they derived a representation theorem for the piezomagnetic vector potentials. Applying the theorem to a magnetoelastic body including a dislocation surface within it, they showed that the magnetic field caused by dislocation sources is equivalent to that of a distribution of magnetic dipoles along the dislocation surface, of

which intensities are proportional to the dislocation moment density through a set of piezomagnetic coefficients. They call these dipoles the magnetic source equivalents.

BONAFEDE and SABADINI's (1980) result is the most general representation of tectonomagnetic field in terms of the displacement field of aeolotropic magnetoelastic materials. However, we cannot actually calculate the piezomagnetic field because we do not know the definite form of Green's function for a general aeolotropic medium. Even if isotropic elasticity is assumed, their formula is mathematically complex because the magnetic field is described in terms of a vector rather than a scalar potential and the magnetoelastic coupling terms remain. In the case of crustal rocks and the Earth's magnetic field, the coupling terms are negligible.

SASAI (1983) presented a surface integral representation of the piezomagnetic potential produced by a homogeneous and isotropic magnetoelastic body with uniform magnetization. It is given by an integral of the displacement and its normal derivatives over the strained body. We may call it the representation theorem for a tectonomagnetic field. Applying the theorem to a magnetoelastic medium containing a dislocation surface within it, we find that the dislocation surface behaves as a sheet magnet. It corresponds to the magnetic source equivalents as defined by BONAFEDE and SABADINI (1980).

SASAI (1986a) obtained the fundamental piezomagnetic potentials, i.e. magnetic potentials produced by a single force operative at a point in a semi-infinite medium. Piezomagnetic changes due to mechanical models which are constructed by a single force distribution are equivalent to those which are obtained by arranging the fundamental piezomagnetic potentials in the same way as the single force distribution. This leads to analytic solutions for the piezomagnetic field of the surface load problem. Actually SASAI (1986a) presented the magnetic field produced by a uniform circular load expressed by complete elliptic integrals. Thus we find that all the problems which have been solved so far numerically with the volume element method have analytic expressions.

Recently, SUZUKI and OSHIMAN (1990) reexamined the piezomagnetic field due to the Mogi model with the numerical volume integrals and reproduced DAVIS' (1976) result for the finite spherical source. They also reproduced SASAI's (1979) result for the point source case (the type I solution). They pointed out that both the results were very different from each other. Spurred by their work, SASAI (1991) investigated an analytical expression of the solution for the finite spherical source. He found that the limit as the source radius was reduced led to a result different from the type I solution, which was called type II. It was

concluded that type II was appropriate as the point source solution. In evaluating the effect of the divergent stress field at a singular point, we should integrate over the medium excluding a small area around the point, and then take the limit as the closed surface shrinks.

This implies that we should reexamine the Green's functions for the piezomagnetic field in the dislocation problems (SASAI, 1980) and single force source problems (SASAI, 1986a). In the following chapters we will reformulate these Green's functions by adopting type II solutions. Thus we can develop a unified way of tectonomagnetic modeling on the basis of the linear piezomagnetic effect. We should emphasize, however, that the method described in this paper essentially follows the framework of tectonomagnetic modeling devised by STACEY (1964).

The main contributions from the present study consist of four chapters. In Chapter 2, the basic theory is formulated. The generalized piezomagnetic law for isotropic magnetoelastic material which is an extended version of the result by SASAI (1980), is derived. The basic equation and the representation theorem for the solution are given (SASAI, 1983). The correspondence among piezomagnetic potential vs. displacement and piezomagnetic field vs. strain is presented; the concept of the "seismomagnetic moment" is proposed (SASAI, 1983). It will be shown that the piezomagnetic effect is the predominant factor among various causes of magnetic change associated with the mechanical distortion (SASAI, 1985).

In Chapter 3, the piezomagnetic field associated with the Mogi model will be fully investigated. This chapter is based on SASAI (1979, 1991). In particular, we discuss how to deal with the divergent stress field around a point source. Two mathematical tools, i.e. the double Fourier (or Hankel) transform and the integral of Lipschitz-Hankel type, are introduced. They will be frequently used throughout this study. In Chapter 4, we will investigate the mechanical models given by the distribution of single forces in a semi-infinite solid. This chapter is based on SASAI (1986a). The dam magnetic effect will be effectively calculated by the Green's function method. In Chapter 5, we will treat the dislocation problems. Volterra's formula for the piezomagnetic potentials is presented. We present some corrections to SASAI's (1980) results for elementary piezomagnetic potentials. The theory will be applied to the multiple tension-crack model (SASAI, 1986b) and fault models.

Chapter 2. Basic Theory

In this chapter, we formulate a theoretical basis for tectonomagnetic modeling. In the first section we derive a linear relationship between

magnetization changes and applied stresses in the three dimensional stress state. This constitutive law is based on two independent piezomagnetic parameters. Although the traditional formula for the piezomagnetic effect of rock samples has been described with a single parameter, i.e. stress sensitivity, the new piezomagnetic law is verified by recent experiments as well as by some theoretical considerations.

In the second section we represent the piezomagnetic law by the displacement field, using Hooke's law. The fundamental equations for tectonomagnetic problems are the Cauchy-Navier equation for the displacement under static equilibrium and the Gauss-Maxwell equation for the magnetic field. Both these equations are combined to deduce the basic equation for the tectonomagnetic field. We use the scalar potential to deal with the static magnetic field produced by rock magnetization. This simplifies the formulation as compared with the use of the vector potential.

In section 3 we will derive a representation theorem for the solution of the basic equation in the form of a surface integral. Then we find that the magnetic potential corresponds to the displacement, and the piezomagnetic field to the strain. One nanotesla change in the tectonomagnetic field is expected to correspond to the earth's strain of a few microstrain.

The elasticity theory of dislocations was introduced to successfully interpret crustal deformations produced by earthquake and volcanic activity. We also consider dislocation problems in the magnetoelastic continuum. In the fourth section we apply the representation theorem to such cases. We will demonstrate that an equivalent magnet emerges along a dislocation surface. This magnetic source equivalent has an intensity proportional to the moment tensor of dislocations, which leads us to the idea of the "seismomagnetic moment". This concept is convenient to intuitively recognize the seismomagnetic effect.

In the final section we will investigate the relative importance of the piezomagnetic effect in the tectonomagnetic field. The Mogi model is taken as an example. Factors of the magnetic change associated with mechanical distortion of the magnetoelastic medium are: (a) the change due to spatial movement of the observation site in the earth's main field (the Free-air change), (b) the change produced by deformation of the ground surface (the Bouguer change), (c) increase or decrease of magnetic mass in the source and (d) the piezomagnetic effect. We will find that the piezomagnetic effect is the only major contribution to the mechanically produced magnetic field changes.

2.1 The Linear Piezomagnetic Effect

The magnetization of rocks containing ferromagnetic minerals varies when mechanical stresses are applied. This phenomenon is called the piezomagnetic effect, which is the inverse effect of magnetostriction. It was discovered by laboratory experiment for induced magnetization by KALASHNIKOV and KAPITZA (1952), and for remanent magnetization by OHNAKA and KINOSHITA (1968). The magnetization changes reversibly and/or irreversibly against applied stresses. Experimental and theoretical studies on piezomagnetism of rocks were summarized by NAGATA (1970a) and by STACEY and BANERJEE (1974). In this study we are concerned with only the reversible piezomagnetic effect.

The magnetization of rocks behaves under mechanical stresses as follows:

$$J^{\parallel} = \frac{J_0^{\parallel}}{(1 - \beta_1 \sigma)} \approx J_0^{\parallel} (1 + \beta_1 \sigma) \quad (2.1a)$$

$$J^{\perp} = \frac{J_0^{\perp}}{(1 - \beta_2 \sigma)} \approx J_0^{\perp} (1 + \beta_2 \sigma) \quad (2.1b)$$

in which the superscripts \parallel and \perp represent the magnetization components parallel and perpendicular to the applied stress direction respectively, while the subscript 0 indicates the initial value of magnetization under no stress. We denote the incremental magnetization by ΔJ . We have

$$\Delta J^{\parallel} = \beta_1 \sigma J_0^{\parallel} \quad (2.2a)$$

$$\Delta J^{\perp} = \beta_2 \sigma J_0^{\perp} \quad (2.2b)$$

We follow the standard sign convention of stress in the elasticity theory: i.e. compression is negative. It is opposite to the traditional one employed in studies of piezomagnetism because laboratory experiments started as uniaxial compression test in its early history. However, tectonomagnetic modeling has developed in close contact with elasticity theory, hence the new sign convention is reasonable.

It has usually been assumed that the following relation holds good (STACEY, 1964; NAGATA, 1970a):

$$\Delta J^{\parallel} = \beta \sigma J_0^{\parallel} \quad (2.3a)$$

$$\Delta J^{\perp} = -\frac{1}{2} \beta \sigma J^{\perp} \quad (2.3b)$$

STACEY, BARR and ROBSON (1965) extended this formula (2.3) to a general three-dimensional stress state as

$$\Delta J_i e_i = \beta J_i \left(\sigma_i - \frac{\sigma_j + \sigma_k}{2} \right) e_i \quad (2.4)$$

$$(i, j, k = 1, 2, 3; i \neq j \neq k)$$

where J_i and ΔJ_i are the magnetization and its increment in the i -th principal direction, while e_i indicates a unit vector direction of the principal stress σ_i . SASAI (1980) derived a modified formula which is equivalent to eq. (2.4):

$$\Delta J = \frac{3}{2} \beta T' J \quad (2.5)$$

T' is the stress deviation tensor, which is related to the stress tensor T and the average stress σ_0 as follows:

$$T = \sigma_0 + T' \quad (2.6a)$$

$$\sigma_0 = \frac{1}{3} (\tau_{xx} + \tau_{yy} + \tau_{zz}) \quad (2.6b)$$

Eqs. (2.5) and (2.6) imply that piezomagnetism of rocks is produced only by deviatoric stresses. This is in contrast to the gravity field due to density changes, which responds only to hydrostatic pressure σ_0 . This is the direct consequence of eqs. (2.3), where the magnetization change rate in the perpendicular direction is exactly half of that parallel to the stress. In view of the fact that piezomagnetism is the inverse effect of magnetostriction and that volumetric magnetostriction of ferromagnetic minerals is almost zero, this result (2.5) is quite acceptable. This experimental result has been interpreted in terms of the "rotation of spontaneous magnetization" model (i.e. single domain theory: NAGATA 1970b; HODYCH, 1976, 1977) and/or with the aid of thermodynamic consideration (STACEY and JOHNSTON, 1972). However, many authors including KALASHNIKOV and KAPITZA (1952) have been aware that the relationship (2.3) is valid only as an average.

ZLOTNICKI, POZZI and CORNET (1981) proposed the most generalized formula of the linear piezomagnetic effect as follows:

$$\Delta J_i = P_{ijkn} \tau_{kn} J_j \quad (2.7)$$

in which Einstein's summation convention applies. P_{ijkn} is a component of a fourth rank tensor. Only 36 components out of 81 are independent from symmetry considerations of stress tensor. Their experiments were done only for remanent magnetization of rocks. They went further to deduce the following formula for the isotropic piezomagnetic material:

$$\Delta J_i = (P_1 \tau_{kk} \delta_{ij} + 2P_2 \tau_{ij}) J_j \quad (2.8)$$

Eq. (2.8) is analogous to Hooke's law for isotropic elasticity. We can modify it to correspond to eq. (2.5) as follows:

$$\Delta J = (3P_1 + 2P_2)\sigma_0 J + 2P_2 T' J \quad (2.9)$$

Eq. (2.9) coincides with eq. (2.5) only if

$$P_2 = \frac{3}{4}\beta, \quad P_1 = -\frac{2}{3}P_2 = -\frac{1}{2}\beta \quad (2.10)$$

Eq. (2.9) implies that the piezomagnetic effect can be caused not only by deviatric stresses but also by hydrostatic pressure. ZLOTNICKI *et al.* (1981) interpreted the observations as due to the movement of a magnetic domain wall caused by local stress concentration under hydrostatic pressure (i.e. multi-domain theory).

BONAFEDE and DRAGONI (1986) derived the same formula as eq. (2.7) for induced magnetization. They obtained the result from thermodynamical considerations, namely by taking account of the Helmholtz free energy of magnetoelastic substances. They proved that eq. (2.8) holds in the case of isotropic piezomagnetism. It is important from a geophysical viewpoint that the thermodynamical discussion verifies eq. (2.8). This implies that an aggregate of crystalline rocks obeying different piezomagnetic laws behaves as a whole as if it were a single isotropic material. This is analogous to the fact that the Earth behaves, to the first order approximation, as an isotropic elastic body although the Earth itself consists of various materials with complicated mechanical anisotropy.

Now we will demonstrate that the experimental result (2.2) does give the same formula as eq. (2.8). Following STACEY *et al.* (1965), we extend eqs. (2.2) to a three-dimensional stress state. Suppose that rock samples cut in any arbitrary direction always yield the same stress-induced magnetization as in eqs. (2.2). We may regard such rocks as "piezomagnetically isotropic". Superposing contributions from the three principal directions, we obtain the incremental magnetization in the i -th principal stress direction as follows:

$$\Delta J_i e_i = J_i \{ \beta_2 (\sigma_j + \sigma_k) + \beta_1 \sigma_i \} e_i \quad (2.11)$$

By making use of the characteristics of the modal matrix, or the principal axis transformation matrix, we can reduce eq. (2.11) to the following:

$$\Delta J = \{ (\beta_1 + 2\beta_2)\sigma_0 + (\beta_1 - \beta_2)T' \} J \quad (2.12)$$

The derivation is given in Appendix A. Eq. (2.12) coincides with eq. (2.5) if $\beta_1 = \beta$ and $\beta_2 = -\frac{1}{2}\beta$. ZLOTNICKI *et al.*'s (1981) parameters are given

by

$$P_1 = \beta_2, \quad P_2 = \frac{1}{2}(\beta_1 - \beta_2) \quad (2.13)$$

Thus we can derive the isotropic piezomagnetic law (2.8) by applying the superposition principle to experimental results. In this chapter we employ formula (2.8) as the fundamental constitutive law for the linear piezomagnetic effect. The traditional formula (2.5) corresponds to a Poisson solid (i.e. $\lambda = \mu$ in Hooke's law, eq. (2.14)) as a particular case of an isotropic elastic material. We will often assume the special case of eq. (2.10) in actual calculations.

2.2 Basic Equation

Isotropic elastic materials are also isotropic in their piezomagnetic properties (BONAFEDE and DRAGONI, 1986). Hence we assume that Hooke's law for isotropic elasticity applies to the substance considered:

$$\tau_{mn} = \lambda \delta_{mn} \operatorname{div} \mathbf{u} + \mu \left(\frac{\partial u_m}{\partial x_n} + \frac{\partial u_n}{\partial x_m} \right) \quad (2.14)$$

λ and μ are Lamè's constants. Substituting eq. (2.14) into (2.9), we can represent the stress-induced magnetization in terms of displacement components as follows:

$$\Delta M_{kl} = \left[\{ (3\lambda + 2\mu)P_1 + 2\lambda P_2 \} \delta_{kl} \operatorname{div} \mathbf{u} + 2\mu P_2 \left(\frac{\partial u_k}{\partial x_l} + \frac{\partial u_l}{\partial x_k} \right) \right] J_k \quad (2.15)$$

Here we specify ΔM_k as the incremental magnetization produced by the k -th component of the initial value and ΔM_{kl} is the l -th component of ΔM_k .

Since the source of the magnetic field is the magnetization alone, there exists a scalar potential W_k . The magnetic field H , the scalar potential W_k , the magnetic induction B and the magnetization ΔM_k are related to each other as follows:

$$H = -\operatorname{grad} W_k \quad (2.16)$$

$$B = H + 4\pi \Delta M_k \quad (2.17)$$

Ampère's law under no electric currents holds automatically by virtue of eq. (2.16). Therefore the fundamental equation for the magnetic field is the Gauss law:

$$\operatorname{div} B = 0 \quad (2.18)$$

From eq. (2.16), (2.17) and (2.18), the magnetic scalar potential should satisfy the following equation:

$$\nabla^2 W_k = 4\pi \operatorname{div} \Delta M_k \quad (k=x, y, z) \quad (2.19)$$

On the other hand, the displacement field of a homogeneous and isotropic elastic body satisfies the equation of static equilibrium under a body force F_k :

$$(\lambda + \mu) \frac{\partial}{\partial x_k} \operatorname{div} \mathbf{u} + \mu \nabla^2 u_k + F_k = 0 \quad (2.20)$$

By taking the divergence of eq. (2.15) and applying eq. (2.20), eq. (2.19) is reduced to

$$\nabla^2 W_k = 4\pi \operatorname{div} \Delta M_k = 4\pi C_k \nabla^2 u_k + 4\pi D_k F_k \quad (2.21)$$

where

$$C_k = -\frac{3\lambda + 2\mu}{\lambda + \mu} \mu P_1 J_k = -2(1 + \nu) \mu P_1 J_k \quad (2.22a)$$

$$D_k = \left(\frac{3\lambda + 2\mu}{\lambda + \mu} P_1 + 2P_2 \right) J_k = 2((1 + \nu)P_1 + P_2) J_k \quad (2.22b)$$

where ν is Poisson's ratio represented by

$$\nu = \frac{1}{2} \frac{\lambda}{\lambda + \mu} \quad (2.22c)$$

This is the basic equation for the tectonomagnetic field. The boundary conditions at the surface of a magnetic body are continuity of the potential itself, of the tangential component of H and of the normal component of B . They are given by

$$W_{k+} = W_{k-} \quad (2.23a)$$

$$\left[\frac{\partial W_k}{\partial t} \right]_{-}^{+} = 0 \quad (2.23b)$$

$$\left[\frac{\partial W_k}{\partial n} \right]_{-}^{+} = -4\pi \Delta M_k \cdot \mathbf{n} \quad (2.23c)$$

where \mathbf{n} denotes the outward normal to the boundary surface S , while t and n are the directions tangential and normal to the surface. Thus the problem is reduced to solving the basic equation (2.21) under the conditions (2.23).

The displacement field is found by solving the Cauchy-Navier equation (2.20) under appropriate boundary conditions. In other words, the equation for the magnetic potential and the one for the displacement are decoupled. This situation exists owing to the following two approximations.

1) In eq. (2.17) we ignore the secondary magnetization induced by the primary piezomagnetic field. Actually this term is two orders of magnitude smaller than the primary one.

2) In eq. (2.14) we neglect the magnetostriction. It is negligibly small compared with the mechanical strain.

2.3 Representation Theorem

The source term on the right hand side of the basic equation (2.21) is not a function of W_k itself. The scalar potential is defined uniquely even within the magnetized area. Then the solution of eq. (2.21) can be given in a well-established way (i.e. Poisson's analysis; see STRATTON (1941), Chapter IV) as follows:

$$W_k(\mathbf{r}) = - \iiint_V \frac{\operatorname{div} \Delta \mathbf{M}_k}{\rho} dV + \iint_S \frac{\Delta \mathbf{M}_k \cdot \mathbf{n}}{\rho} dS \quad (2.24)$$

With the aid of Gauss' theorem we find that eq. (2.24) is equivalent to the dipole law of force:

$$W_k(\mathbf{r}) = \iiint_V \Delta \mathbf{M}_k \cdot \nabla \left(\frac{1}{\rho} \right) dV \quad (2.25)$$

The volume V surrounded by S is assumed to be a uniformly magnetized, homogeneous and isotropic elastic body.

The function $(4\pi\rho)^{-1}$ is the fundamental solution of the Laplace-Poisson type equation, which satisfies

$$\nabla^2 \left[\frac{1}{4\pi\rho} \right] = -\delta(\mathbf{r} - \mathbf{r}') \quad (2.26)$$

$$\rho = |\mathbf{r} - \mathbf{r}'|$$

Substituting the third identity of eq. (2.21) into eq. (2.24) and applying Green's theorem, we obtain

$$W_k(\mathbf{r}) = 4\pi C_k u_k(\mathbf{r}) \theta(\mathbf{r} \in V) + D_k \iiint_V \frac{F_k}{\rho} dV$$

$$+ \iint_S \left[\left\{ -C_k \frac{\partial u_k(\mathbf{r}')}{\partial n'} + \Delta \mathbf{M}_k \cdot \mathbf{n}' \right\} \frac{1}{\rho} + C_k u_k(\mathbf{r}') \frac{\partial}{\partial n'} \left(\frac{1}{\rho} \right) \right] dS \quad (2.27)$$

where

$$\theta(r \in V) = \begin{cases} 1 & (r \in V) \\ 0 & (r \notin V) \end{cases} \quad (2.28)$$

For ΔM_k , we may rewrite eq. (2.15) as follows:

$$\Delta M_i^k = A_k \delta_{ki} \operatorname{div} \mathbf{u}(\mathbf{r}') + B_k \left(\frac{\partial u_k}{\partial x_i} + \frac{\partial u_i}{\partial x_k} \right) \quad (2.29a)$$

$$A_k = \{(3\lambda + 2\mu)P_1 + 2\lambda P_2\}J_k = 2\mu \left(\frac{1+\nu}{1-2\nu}P_1 + \frac{2\nu}{1-2\nu}P_2 \right)J_k \quad (2.29b)$$

$$B_k = 2\mu P_2 J_k \quad (2.29c)$$

Eq. (2.27) is a representation theorem for the tectonomagnetic field.

The first term on the right hand side of eq. (2.27) appears only when the observation point is located within the magnetized area. A bore-hole magnetometer has been developed in recent years for monitoring earthquakes and volcanoes. This term is important for tectonomagnetic observations under the ground. It represents the nature of the tectonomagnetic field the most plainly: the potential is simply proportional to the displacement. The total field change due to this term is given by

$$\Delta F = -4\pi C_0 \frac{\partial u_f}{\partial f} \quad (2.30)$$

where

$$u_f = u_x \cos I_0 + u_z \sin I_0 \quad (2.31a)$$

$$\frac{\partial}{\partial f} = \mathbf{e}_f \cdot \nabla = \cos I_0 \frac{\partial}{\partial x} + \sin I_0 \frac{\partial}{\partial z} \quad (2.31b)$$

$$C_0 = -\frac{3\lambda + 2\mu}{\lambda + \mu} \mu P_1 J \quad (2.31c)$$

J and I_0 are the average magnetization and the inclination of the ambient magnetic field. The unit vector \mathbf{e}_f indicates the direction of the ambient field, which is assumed parallel to that of J . For a model earth with material constants $\beta = 1.0 \times 10^{-4}$ per bar, $J = 1.0$ A/m and $\lambda = \mu = 3.5 \times 10^5$ bar, 1 nT change in the total intensity corresponds to a strain change of 1.8×10^{-5} . This gives a measure of the sensitivity of a magnetometer as a strain gauge. Since we follow the standard sign convention of stress, simple extension along the \mathbf{e}_f axis decreases the total intensity.

Across the boundary surface, it appears as if a gap in the potential value $4\pi C_k\{u_k(r)\}$ might occur owing to the vanishing of the first term in eq. (2.27) outside the body. This is completely compensated for by a jump in the potential across the double layer, the latter term in the surface integral of eq. (2.27). According to the well-known theorem across a double layer potential (KELLOGG, 1929), the value of the jump is equivalent to 4π times the intensity at the cross point, i.e. $4\pi C_k\{u_k(r)\}$. Thus the magnetic potential is continuous at the boundary surface. However, the normal component of the magnetic field varies discontinuously across the boundary.

Magnetic measurements are usually made in free space, where the analogy between the strain and the piezomagnetic field fails. The surface magnetic field, however, contains some information on the crustal strain just at the observation site. Let us investigate the contribution of the surface integral in eq. (2.27) along the earth's surface. We take the x axis in the magnetic north direction and the z axis positive downward. We specify the plane $z=0$ as the earth's surface and denote the surface integral by $W_k^{(0)}$:

$$W_k^{(0)} = \iint_{-\infty}^{\infty} \left[\left\{ C_k \frac{\partial u_k}{\partial z'} - \Delta M_{kz} \right\} \frac{1}{\rho} - \{ C_k u_k(r') \} \frac{\partial}{\partial z'} \left(\frac{1}{\rho} \right) \right]_{z'=0} dx' dy' \quad (2.32)$$

Taking account of the stress-free boundary conditions, i.e.

$$\begin{aligned} \tau_{xz} &= \mu \left[\frac{\partial u_z}{\partial x'} + \frac{\partial u_x}{\partial z'} \right]_{z'=0} = 0 \\ \tau_{zz} &= \left[\lambda \operatorname{div} \mathbf{u} + 2\mu \frac{\partial u_z}{\partial z'} \right]_{z'=0} = 0 \end{aligned}$$

We have

$$W_x^{(0)} = C_x \iint_{-\infty}^{\infty} \left[\frac{\partial u_x}{\partial z'} \frac{1}{\rho} - u_x(r') \frac{\partial}{\partial z'} \left(\frac{1}{\rho} \right) \right]_{z'=0} dx' dy' \quad (2.33a)$$

$$W_z^{(0)} = C_z \iint_{-\infty}^{\infty} \left[-\frac{\lambda+2\mu}{\lambda} \frac{\partial u_z}{\partial z'} \frac{1}{\rho} - u_z(r') \frac{\partial}{\partial z'} \left(\frac{1}{\rho} \right) \right]_{z'=0} dx' dy' \quad (2.33b)$$

Note that the piezomagnetic parameter P_2 originally involved in ΔM_{kz} disappears in the final results eqs. (2.33).

Now we apply two theorems on the derivatives of single and double layer potential when a point approaches the source layer. Proper conditions should be assumed for the curvature of the layer and the smoothness of the density distribution (KELLOGG, 1929). The normal derivatives of a single layer potential $U^{(S)}$ with a surface density $\sigma(p)$ on the posi-

tive and negative side of the layer are given by

$$\left[\frac{\partial U^{(s)}}{\partial n} \right]_+ = -2\pi\sigma(\mathbf{p}) + \iint_s \sigma(\mathbf{p}') \frac{\partial}{\partial n'} \left(\frac{1}{\rho} \right) dS' \quad (2.34a)$$

$$\left[\frac{\partial U^{(s)}}{\partial n} \right]_- = 2\pi\sigma(\mathbf{p}) + \iint_s \sigma(\mathbf{p}') \frac{\partial}{\partial n'} \left(\frac{1}{\rho} \right) dS' \quad (2.34b)$$

On the other hand, tangential derivatives of a double layer potential $U^{(d)}$ with a surface moment density $\mu(\mathbf{p})$ have a similar property (COURANT and HILBERT, 1937):

$$\left[\frac{\partial U^{(d)}}{\partial t} \right]_+ = 2\pi \frac{\partial \mu(\mathbf{p})}{\partial t} + \iint_s \mu(\mathbf{p}') \frac{\partial^2}{\partial t \partial n'} \left(\frac{1}{\rho} \right) dS' \quad (2.35a)$$

$$\left[\frac{\partial U^{(d)}}{\partial t} \right]_- = -2\pi \frac{\partial \mu(\mathbf{p})}{\partial t} + \iint_s \mu(\mathbf{p}') \frac{\partial^2}{\partial t \partial n'} \left(\frac{1}{\rho} \right) dS' \quad (2.35b)$$

Since the source layer is simply a plane, integral terms in eqs. (2.34) and eqs. (2.35) vanish.

Applying these formulas to derivatives of $W_x^{(0)}$ and $W_z^{(0)}$, we obtain the magnetic field arising from the free surface potential $W_k^{(0)}$:

$$\Delta X^{(0)} = -2\pi C_0 \frac{\partial u_f}{\partial x} - C_0 \frac{\partial U_p^{(0)}}{\partial x} \quad (2.36a)$$

$$\Delta Y^{(0)} = -2\pi C_0 \frac{\partial u_f}{\partial y} - C_0 \frac{\partial U_p^{(0)}}{\partial y} \quad (2.36b)$$

$$\Delta Z^{(0)} = -2\pi C_0 \frac{\partial u_p}{\partial z} - C_0 \frac{\partial U_f^{(0)}}{\partial z} \quad (2.36c)$$

where

$$u_p = u_f - \frac{2(\lambda + \mu)}{\lambda} u_z \sin I_0 \quad (2.37a)$$

$$U_p^{(0)} = \iint_{-\infty}^{\infty} \left[\frac{\partial u_p}{\partial z'} \frac{1}{\rho} \right]_{z'=+0} dx' dy' \quad (2.37b)$$

$$U_f^{(0)} = \iint_{-\infty}^{\infty} \left[u_f \frac{\partial}{\partial z'} \left(\frac{1}{\rho} \right) \right]_{z'=+0} dx' dy' \quad (2.37c)$$

The contribution to the total intensity is given by

$$\Delta F^{(0)} = -2\pi C_0 \left[\frac{\partial u_f}{\partial f} - \frac{2(\lambda + \mu)}{\lambda} \frac{\partial u_z}{\partial z} \sin I_0 \right]$$

$$-C_0 \left[\frac{\partial U_p^{(0)}}{\partial x} \cos I_0 + \frac{\partial U_f^{(0)}}{\partial z} \sin I_0 \right] \quad (2.38)$$

The first term of eq. (2.38) represents a linear combination of the surface strain components just at the observation site.

If the first term of $\Delta F^{(0)}$ in eq. (2.38) is a representative of the resultant total intensity as estimated from the total piezomagnetic potential (2.27), the tectonomagnetic observation is nothing but a kind of strain measurement. However, things are different from such simple circumstances. In the next chapter we will apply the representation theorem to obtain the piezomagnetic field associated with the Mogi model as an example. We will find that the terms in eq. (2.27) have the same order of magnitude: some cancel and other augment each other. Moreover, the latter integral terms in eq. (2.38) are comparable with first one. In the special case of the Mogi model, $\Delta F^{(0)}$ is actually zero: the first and the latter terms completely cancel each other.

Thus we cannot say anything definite about the strain change just at the observation site from the magnetic measurement. Although the direct correspondence between the piezomagnetic field and the pointwise strain fails in free space, we may say that a few nT changes are expected around the strain field of 10^{-5} with a magnetization of 1 A/m.

2.4 The Seismomagnetic Moment

We have derived eq. (2.27) with the aid of Green's theorem. This requires that the displacement field $u(r)$ and its first order derivatives must be continuous in $V+S$, while its second order derivatives be piecewise continuous within V . When the magnetoelastic medium V involves an internal dislocation surface Σ , eq. (2.27) no longer holds as it is. In this case, we divide V into two parts with a surface S' including Σ , as shown in Fig. 1. Then we apply the formula (2.27) to each part separately and add the two parts. The unit normal is assigned to point outward. We define

$$\nu = \nu_- = -\nu_+ \quad \text{on } \Sigma \quad (2.39a)$$

$$n_{S'+} = -n_{S'-} \quad \text{on } S' \text{ besides } \Sigma \quad (2.39b)$$

The contribution of the surface integral from S' except for Σ becomes zero owing to (2.39b). Hence we have

$$W_k = W_k^{(\Sigma)} + W_k^{(S)} + W_k^{(F)} \quad (2.40)$$

where

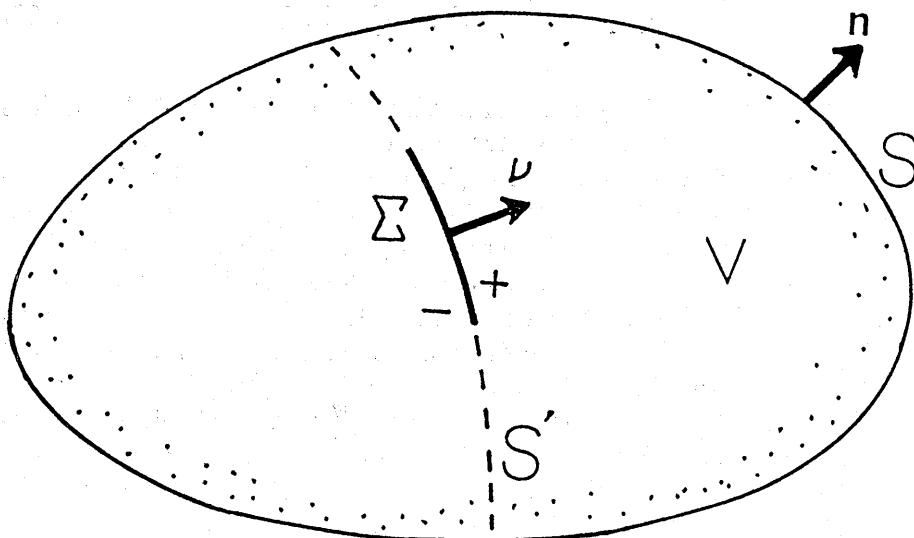


Fig. 1. A magnetoelastic body V with its surface S and an internal dislocation surface Σ . \mathbf{n} and $\boldsymbol{\nu}$ are unit normal vectors. S' is a subdivisive surface including Σ .

$$W_k^{(\Sigma)} = \iint_{\Sigma} \left\{ \left[C_k \operatorname{grad} u_k(\mathbf{r}') - \Delta \mathbf{M}_k \right]_{-}^{+} \cdot \boldsymbol{\nu} \frac{1}{\rho} - \left[C_k u_k(\mathbf{r}') \right]_{-}^{+} \frac{\partial}{\partial \nu'} \left(\frac{1}{\rho} \right) \right\} d\Sigma \quad (2.41)$$

$$W_k^{(S)} = \iint_S \left\{ \left[-C_k \operatorname{grad} u_k(\mathbf{r}') + \Delta \mathbf{M}_k \right] \cdot \mathbf{n} \frac{1}{\rho} + \left[C_k u_k(\mathbf{r}') \right] \frac{\partial}{\partial n'} \left(\frac{1}{\rho} \right) \right\} dS \quad (2.42)$$

and

$$W_k^{(F)} = D_k \iiint_V \frac{F_k}{\rho} dV \quad (2.43)$$

The symbol $[]_{\pm}$ represents the discontinuity of the quantity within the bracket.

Let us investigate the characteristics of the dislocation-related potential $W_k^{(\Sigma)}$. In the case of natural dislocation events within the Earth such as seismic faulting, dyke formation by intrusive magmas and so on, no external force acts upon the dislocation surface. Hence the traction across Σ should be continuous. Then we obtain

$$W_k^{(\Sigma)} = \iint_{\Sigma} \left\{ \left(C_k \operatorname{grad} u_k(\mathbf{r}') - (3\lambda + 2\mu) P_1 J_k \operatorname{div} \mathbf{u} \mathbf{e}_k \right)_{-}^{+} \cdot \boldsymbol{\nu} \frac{1}{\rho} - \left[C_k u_k(\mathbf{r}') \right]_{-}^{+} \frac{\partial}{\partial \nu} \left(\frac{1}{\rho} \right) \right\} d\Sigma \quad (2.44)$$

Moreover we often prefer a simple model, in which all the stress components are continuous across the dislocation surface, as is the case with the Volterra dislocations. In this special case, all the spatial derivatives of the displacement become continuous, and the single layer term in eq. (2.44) vanishes. Eq. (2.44) reduces to

$$W_k^{(\Sigma)} = -C_k \iint_{\Sigma} \left[u_k(r') \right]_{-}^{+} \frac{\partial}{\partial \nu} \left(\frac{1}{\rho} \right) d\Sigma \quad (2.45)$$

Summing up for $k=x, y, z$, we have a resultant potential $W^{(\Sigma)}$ as follows:

$$W^{(\Sigma)} = \iint_{\Sigma} m \frac{\partial}{\partial \nu} \left(\frac{1}{\rho} \right) d\Sigma \quad (2.46)$$

where

$$m = -C_0 e_J \cdot \Delta u \quad (2.47)$$

e_J is the unit vector in the magnetized direction, and Δu the vectorial representation of the displacement discontinuity. Thus the piezomagnetic field accompanying a dislocation surface is equivalent to that of a double layer Σ , whose magnetic moment is given by (2.47).

At far-field distances, where we may regard the earthquake fault as a point source, we have an expression:

$$W^{(\Sigma)} = M \frac{\partial}{\partial \nu} \left(\frac{1}{\rho} \right) \quad (2.48)$$

where

$$M = \frac{3\lambda + 2\mu}{\lambda + \mu} P_1 J M_0 \cos \phi \quad (2.49)$$

M_0 is the seismic moment (i.e. $M_0 = \mu \Delta u A$; A is the fault area. See text: e.g. AKI and RICHARDS, 1980). ϕ indicates the angle between the magnetization and the slip vector. The magnetic moment given by eq. (2.47) or eq. (2.49) is suitable for measuring the seismomagnetic effect. We may call M the *total seismomagnetic moment* and m the *seismomagnetic moment density*. This concept can be naturally extended to tensile faults produced by intrusive magma (OKADA, 1986).

The important result in this section is that the dislocation surface within a magnetoelastic body forms the sources and sinks of the magnetic lines of force. The surface magnetic source distribution in eq. (2.44) corresponds to the *magnetic source equivalents* as named by BONAFEDE and SABADINI (1980). In general Somigiana dislocations, we have not

only the double layer but also the single layer. The total sum of these monopoles over the dislocation surface should vanish, or else their counterpart should appear in the surface integral term $W_k^{(S)}$.

The concept of the seismomagnetic moment is useful for intuitively understanding the dislocation-related magnetic field near the source. Eq. (2.47) tells us that the intensity of the seismomagnetic effect strongly depends on the angle between the magnetization and the dislocation vector. In some instances the seismomagnetic moment becomes null, e.g. an East-West oriented shear fault and a North-South oriented tensile fault. It should also be mentioned that bore-hole magnetometers have an advantage for detecting dislocation-related magnetic changes because they are in general located closer to the magnetic sources.

2.5 The Stacey-Nagata Piezomagnetic Solid

Our formulation has so far been based on the piezomagnetic law eq. (2.8) with two independent parameters P_1 and P_2 . The law of one parameter eq. (2.3) by STACEY (1964) and NAGATA (1970a) and accordingly eq. (2.5) by SASAI (1980) can be regarded as a special case of eq. (2.8) by ZLOTNICKI *et al.* (1981) (cf. eq. (2.10)). However, eq. (2.3) is essentially valid for "linear" piezomagnetism for the following two reasons. First, spontaneous magnetization of titanomagnetite bearing rocks changes little under hydrostatic pressure because their volumetric magnetostriction is negligibly small. Secondly, if the piezomagnetism due to hydrostatic pressure is caused by movement of magnetic domain wall, as ZLOTNICKI *et al.* (1981) claimed, the magnetization never recovers to its initial value after applied stresses are removed. The linearity breaks in this case. The irreversible piezomagnetic effect is rather difficult to incorporate into the framework of the linear elasticity theory, hence it is beyond the scope of present study.

On the other hand, a number of laboratory experiments show that the relation (2.3) holds as an average for the magnetic susceptibility and the hard remanent magnetization. Thus we will hereafter model substances for which eq. (2.3) and hence eq. (2.5) hold good. We may call such material the Stacey-Nagata piezomagnetic solid. This is an analogue to the Poisson solid in the case of isotropic elasticity.

The piezomagnetic law for the Stacey-Nagata solid is given simply by

$$\Delta J = \beta S \cdot J \quad (2.50)$$

where

$$S_{jk} = \frac{3}{2} \tau_{jk} - \frac{1}{2} \delta_{jk} \Theta = \mu \left\{ \frac{3}{2} \left(\frac{\partial u_j}{\partial x_k} + \frac{\partial u_k}{\partial x_j} \right) - \delta_{jk} \operatorname{div} \mathbf{u} \right\} \quad (2.51)$$

The representation theorem corresponding to eq. (2.27) is as follows:

$$W_k(r_0) = C_k \iint_S \left[\left\{ -\frac{\partial u_k(r)}{\partial n} + \frac{2(\lambda + \mu)}{3\lambda + 2\mu} \Delta m^{(k)} \cdot n \right\} \frac{1}{\rho} + \{u_k(r)\} \frac{\partial}{\partial n} \left(\frac{1}{\rho} \right) \right] dS \quad (2.52)$$

where

$$\Delta m_i^{(k)} = \frac{3}{2} \left(\frac{\partial u_k}{\partial x_i} + \frac{\partial u_i}{\partial x_k} \right) - \delta_{ki} \operatorname{div} u \quad (2.53)$$

$$C_k = \frac{1}{2} \beta J_k \mu \frac{3\lambda + 2\mu}{\lambda + \mu} \quad (2.54)$$

We will often refer to eqs. (2.50)–(2.54) in the following sections.

2.6 Predominance of the Piezomagnetic Effect —the Mogi Model as an Example—

In tectonomagnetic modeling studies, the piezomagnetic effect and the thermal demagnetization or remagnetization effect have so far been considered. There is, however, another simple cause of magnetic change related to tectonic activities. All tectonic events, such as earthquake faulting, inflation of a magma chamber, formation of a dome, intrusion of magma sheets and so on, are accompanied by the deformation of the earth's surface. This can be regarded as the relative movement of magnetic masses. A question arises: how much does the deformation-related magnetic change amount to? Is it comparable with the piezomagnetic field?

A relevant problem was solved in the field of gravity. HAGIWARA (1977a) presented the gravity change associated with the Mogi model. Hagiwara discriminated four types of contributions to the gravity change; i.e. (1) G1: free-air gravity change accompanying the uplift of the observation site, (2) G2: Bouguer change caused by the excess mass corresponding to the upheaved portion of the free surface, (3) G3: the effect of chamber wall expansion which implies replacement of surrounding mass with gas or magma, and (4) G4: the gravity change produced by density changes within a semi-infinite medium.

SASAI (1985) investigated the same problem for magnetic change due to the Mogi model. Similarly, four ways of generating the magnetic change are conceivable. They are (1) M1: "free-air" magnetic change resulting from movement of the observation site in the earth's main field, (2) M2: magnetic change due to undulation of an initially flat surface, (3) effect of chamber wall expansion corresponding to loss of magnetic mass, and (4) M4: the piezomagnetic field caused by the stress

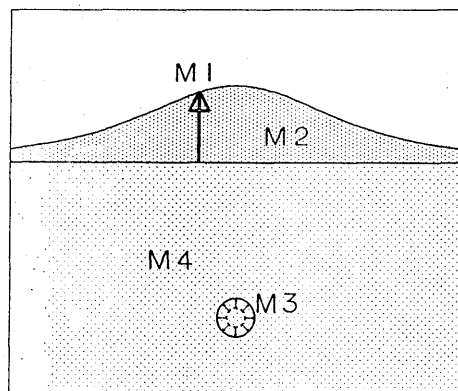


Fig. 2. A schematic representation of the four types of contributions to magnetic change.

change within a magnetic medium. They are schematically depicted in Fig. 2.

The piezomagnetic field due to the Mogi model will be fully investigated in Chapter 3. A brief description of parameters for the Mogi model is given here. Let us take the Cartesian coordinates as follows: x positive north-, y east- and z downward. A small sphere with radius a at a point $A(0, 0, D)$ suffers excess hydrostatic pressure ΔP from inside. The surface uplift $\Delta h(r)$ is given by

$$\Delta h(r) = h_0 \frac{D^3}{R^3} \quad (2.55)$$

$$R = (r^2 + D^2)^{1/2} \quad (2.56)$$

where h_0 is the maximum uplift at the origin. This is related to model parameters as

$$h_0 = \frac{\lambda + 2\mu}{2\mu(\lambda + \mu)} \frac{a^3 \Delta P}{D^2} \quad (2.57)$$

According to SASAI (1985), M1, M2, M3 and M4 are given as follows. Only the final results are quoted here.

'Free Air' Magnetic Change (M1)

The source of the earth's magnetic field is well represented by a geocentric dipole. The magnetic field decreases as the observation site moves away from the dipole. The total intensity change associated with the uplift $\Delta h(r)$ is given by

$$\Delta F^{(M1)} = -\frac{3F_0}{R_E} h_0 \left(\frac{D}{R} \right)^3 \quad (2.58)$$

where F_0 is the geomagnetic total force intensity at the observation site and R_E is the earth's radius. Even for an uplift of 1m high, $\Delta F^{(M1)}$ is at most $0.002 nT$ at mid-latitudes such as in Japan.

Magnetic Terrain Effect (M2)

The surface uplift caused by the Mogi model is symmetric around the z axis. We have a useful formula for calculating the magnetic field of an axially-symmetric body with uniform magnetization, which was originally derived by RIKITAKE (1951) for a circular cone. The total intensity component of the magnetic terrain effect is

$$\Delta F^{(M2)} = 3J \frac{h_0}{D} \{ (F_1 \cos 2\phi - G_1 \cos^2 \phi) \cos^2 I_0 - H_1 \sin 2I_0 \cos \phi + G_1 \sin^2 I_0 \} \quad (2.59)$$

where F_1 , G_1 and H_1 are functions of the observation point and are represented as one-dimensional integrals containing elliptic integrals of the 1st and 2nd kind.

Source Expansion Effect (M3)

The source sphere expands under an internal hydrostatic pressure ΔP by an amount (HAGIWARA, 1977a):

$$\Delta a = \frac{a \Delta P}{4\mu} \quad (2.60)$$

This implies vanishment of a uniformly magnetized shell with radius a and thickness Δa , which brings about total intensity change as

$$\Delta F^{(M3)} = 2\pi \frac{\lambda + \mu}{\lambda + 2\mu} J \frac{h_0}{D} \left\{ \left(\frac{D}{R} \right)^3 + \frac{3}{2} \left(1 - \frac{x}{R} \right) \left(\frac{D}{R} \right)^5 \cos 2I_0 + 3 \left(\frac{D}{R} \right)^5 \sin 2I_0 \right\} \quad (2.61)$$

Piezomagnetic Change (M4)

As for piezomagnetic change we refer to the result in the next chapter. We employ a point source solution of type II, i.e. eqs. (3.55). For a shallow source the influence of the Curie depth is negligible. The total intensity change is given by:

$$\Delta F^{(M4)} = C \left[\frac{1}{2} \left\{ - \left(\frac{D}{R} \right)^3 + 3 \left(\frac{x}{D} \right)^2 \left(\frac{D}{R} \right)^5 \right\} \cos^2 I_0 \right]$$

$$-3 \frac{x}{D} \left(\frac{D}{R} \right)^5 \sin I_0 \cos I_0 + \frac{1}{2} \left\{ - \left(\frac{D}{R} \right)^3 + 3 \left(\frac{D}{R} \right)^5 \right\} \sin^2 I_0 \quad (2.62)$$

where

$$C = 2\pi\mu\beta J \frac{h_0}{D} \quad (2.63)$$

Figures 3(a)-3(d) show total intensity changes along a N-S meridian corresponding to M1 to M4. Model parameters are $\lambda = \mu = 3.5 \times 10^{11}$ cgs, $\beta = 1.0 \times 10^{-4}$ bar $^{-1}$, $J = 1$ A/m, $F_0 = 46,000$ nT, and $I_0 = 46^\circ$. The maximum

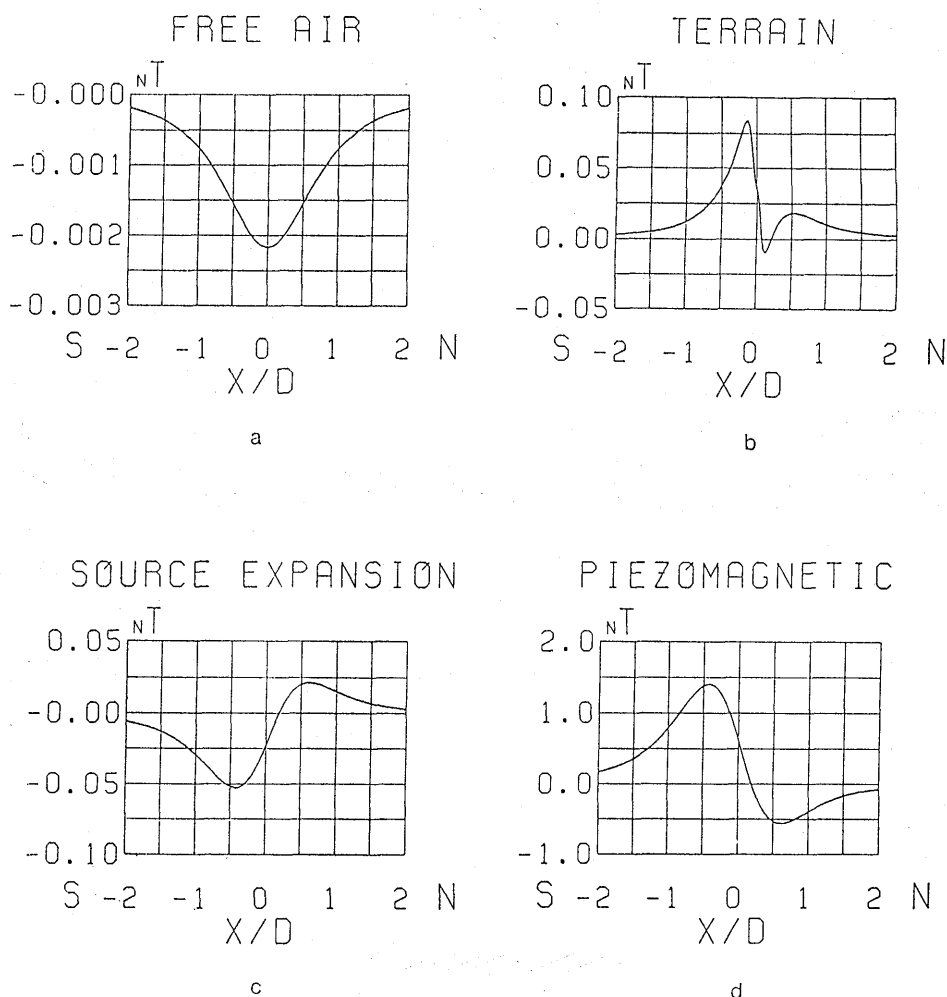


Fig. 3. (a) M1: 'Free air' magnetic change. (b) M2: Magnetic terrain effect. (c) M3: Source expansion effect. (d) M4: Piezomagnetic change.

uplift h_0 and the depth of pressure source D are taken to be 10 cm and 1 km, respectively. In calculating M2, the sensor height is taken as 2.5 m.

Since all the types of contributions are proportional to the ratio $\frac{h_0}{D}$, the relative magnitude of each part remains invariant for any combination of model parameters. Figure 3 tells us

$$|M4| > |M2| \approx |M3| > |M1|$$

For gravity change due to the Mogi model (HAGIWARA, 1977a), $|G1| > |G2| > |G3| > |G4|$ (when the source sphere is filled with gas), or $|G1| > |G2| > |G4| > |G3|$ (when filled with magma). Accordingly, a gravity survey measures mainly height changes caused by mechanical sources, while magnetic observation detects stress changes associated with the same sources. However, if precise leveling is done along with gravity and magnetic measurements, such a data set will surely provide us with definite information on the sources of tectonic events.

As for the Mogi model, the tectonomagnetic field can be regarded almost entirely as of piezomagnetic origin. Moreover, we can expect the piezomagnetic effect to dominate for dislocation models with sources at moderate depth. This is because the dislocation surface behaves as a distribution of multipoles with their intensity proportional to the moment of double-couple force sources (see Chapter 5). Thus we have only to take into account the piezomagnetic effect in most cases of tectonomagnetic modeling.

Chapter 3. Piezomagnetic Field Associated with the Mogi Model

In this chapter we will investigate the piezomagnetic change associated with the Mogi model. A hydrostatically-pumped sphere buried within a semi-infinite elastic medium is called the Mogi model in volcanology (MOGI, 1958). The source sphere is an analogue to a magma reservoir. As has been reviewed in the Introduction, piezomagnetic change associated with the Mogi model has been studied in the history of tectonomagnetic modeling (DAVIS, 1976; SASAI, 1979; SUZUKI and OSHIMAN, 1990; SASAI, 1991).

In applying the representation theorem (2.52), we must evaluate convolution integrals. Two kinds of mathematical tools are introduced for that purpose. One is the double Fourier transform (or Hankel transform) to deal with convolution over an infinite plane. The other is the Lipschitz-Hankel type integrals to estimate potentials accompanied with an axi-symmetric source distribution. Both are closely related to each other through Bessel functions. We will systematically use these two

tools throughout the present study.

First we will derive a point source solution of the problem when the source volume is reduced to zero. However, a paradox appears in that two different solutions are obtained for different ways of taking the limit as the source decreases. We call them type I and type II solutions, respectively.

How to manage the singularity around the source point is crucial in our Green's function approach to tectonomagnetic modeling. In order to identify the cause of the discrepancy between the two kinds of solutions, the finite source problem is further investigated. The type III solution for the finite spherical source is reduced to a one-dimensional integral containing complete elliptic integrals. With the aid of the double exponential formula (DEF: TAKAHASHI and MORI, 1974) we can accurately conduct numerical integrations.

Finally we investigate the limit of type III solution as the source radius decreases to zero. We will find that type II is appropriate as the point source solution. We can then clarify the cause of the discrepancy between the two types of solutions.

3.1 Point Source Problem—A Paradox

Let us take the Cartesian coordinates shown in Fig. 4. A semi-infinite elastic medium occupies $z > 0$. It is also assumed that a layer from $z=0$ to $z=H$ is uniformly magnetized. We assume a small sphere with radius a centered at a point $A(0, 0, D)$, which is acted on by hydrostatic pressure ΔP from inside. Since the spherical pressure source

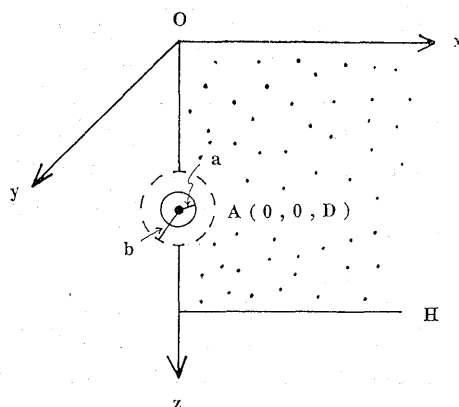


Fig. 4. Coordinate system, a hydrostatically pumped pressure source at $A(0, 0, D)$ with radius a , the thermally demagnetized zone with radius b and the Curie point isotherm at a depth H .

is regarded as a magma chamber, a concentric spherical shell with radius b is assumed to be thermally demagnetized and non-magnetic. Its boundary may coincide with the source sphere: i.e. $b \geq a$. The Curie point isotherm may lie either above, below or even across the demagnetized sphere. The point source problem corresponds to the case in which a and b are infinitesimally small.

The displacement field of the Mogi model is equivalent to that produced by a strain nucleus called the center of dilatation (MINDLIN and CHENG, 1950; YAMAKAWA, 1955). It is given as follows:

$$u_x = \frac{C}{2\mu} \left\{ \frac{x}{R_1^3} + \frac{\lambda+3\mu}{\lambda+\mu} \frac{x}{R_2^3} - \frac{6xz(z+D)}{R_2^5} \right\} \quad (3.1a)$$

$$u_y = \frac{C}{2\mu} \left\{ \frac{y}{R_1^3} + \frac{\lambda+3\mu}{\lambda+\mu} \frac{y}{R_2^3} - \frac{6yz(z+D)}{R_2^5} \right\} \quad (3.1b)$$

$$u_z = \frac{C}{2\mu} \left\{ \frac{z-D}{R_1^3} + \frac{(\lambda-\mu)z - (\lambda+3\mu)D}{(\lambda+\mu)R_2^3} - \frac{6z(z+D)^2}{R_2^5} \right\} \quad (3.1c)$$

where

$$R_1 = \sqrt{x^2 + y^2 + (z-D)^2} \quad (3.2a)$$

$$R_2 = \sqrt{x^2 + y^2 + (z+D)^2} \quad (3.2b)$$

λ and μ are Lamé's constants, while C is the moment of the strain nucleus. Under the condition that a is sufficiently small as compared with D , the moment C is given by

$$C = -\frac{1}{2}a^3 \Delta P \quad (3.3)$$

The first terms on the right hand side of eqs. (3.1) are the displacement field due to a center of dilatation in an infinite medium, while the remainder represent the effect of the free surface. We will hereafter specify the former $u^{(A)}$ and the latter $u^{(B)}$. In the point source problem displacements become singular at the point $A(0,0,D)$. Differentiation of eqs. (3.1) gives the stress field. Applying the piezomagnetic law eq. (2.50), we obtain components of the stress-induced magnetization at an arbitrary point. They are given in SASAI (1979, 1991), which are not reproduced here.

Let us consider the point source problem. We subdivide the magnetized crust into two parts: a layer from the earth's surface to the source depth ($0 < z < D$) and one from the source depth to the Curie point isotherm ($D < z < H$) (see Fig. 5(a)). SASAI (1979) obtained an analytical

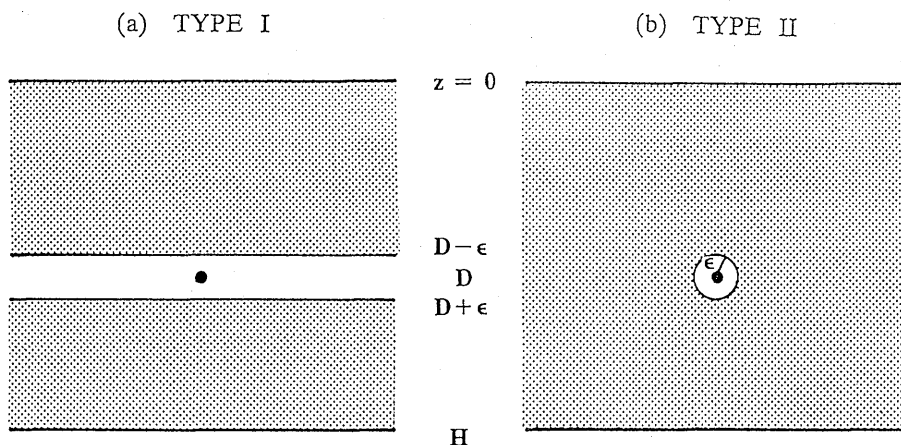


Fig. 5. A schematic representation of integration area (shaded) for (a) type I and (b) type II solution.

solution for this problem. He applied the magnetic dipole law of force, i.e. eq. (2.25), to the stress-induced magnetization and performed volume integrals with the aid of the Fourier transform method. If we apply the representation theorem, eq. (2.52), we may take account of four plane surfaces, i.e. the earth's surface ($z=0$), a horizontal plane just above the source point ($z=D-\epsilon$), a plane just below the source ($z=D+\epsilon$) and the Curie point isotherm ($z=H$). Actually, SASAI (1983) recalculated the piezomagnetic potential of the Mogi model with the aid of eq. (2.52) and arrived at the same result through volumetric integrals. The contribution from the point source is defined as a limit as the distance between two surfaces, $z=D-\epsilon$ and $z=D+\epsilon$ becomes very small. We call it the type I solution.

We may consider another way of integration which is usually adopted in improper integrals. It is to do integration over a region except for a small sphere with radius ϵ centered at $(0, 0, D)$ and then to let $a=b=\epsilon$ approach zero (see Fig. 5(b)). We call this the type II solution. However, it is much easier to do surface integrations according to eq. (2.52) than volumetric ones. We are to evaluate contributions from the earth's surface, the Curie point isotherm and a spherical surface with radius ϵ . The former two have already appeared in the type I solution. Let us investigate these solutions respectively.

Type I solution

The piezomagnetic potential produced by the k -th component of the uniform magnetization consists of three parts:

$$W_k = W_k^{(0)} + W_k^{(P)} + W_k^{(H)} \quad (3.4)$$

in which the superscripts indicate contributions from the free surface (0), the pressure source (P) and the Curie point isotherm (H) respectively. Because of the symmetrical nature of the Mogi model, we may take the x axis in the magnetic north direction without loss of generality. The observation point of the magnetic field is denoted by (x_0, y_0, z_0) .

The contribution from the free surface is represented by

$$\frac{2\mu}{C} W_x^{(0)} = -\frac{2(\lambda+2\mu)}{\lambda+\mu} C_x \iint_{-\infty}^{\infty} \left[\frac{3xD}{R_0^5} \frac{1}{\rho_0} + \frac{x}{R_0^3} \frac{z_0}{\rho_0^3} \right] dx dy \quad (3.5a)$$

$$\frac{2\mu}{C} W_z^{(0)} = \frac{2(\lambda+2\mu)}{\lambda+\mu} C_z \iint_{-\infty}^{\infty} \left[-\left(\frac{1}{R_0^3} - \frac{3D^2}{R_0^5} \right) \frac{1}{\rho_0} + \frac{D}{R_0^3} \frac{z_0}{\rho_0^3} \right] dx dy \quad (3.5b)$$

where

$$R_0 = (x^2 + y^2 + D^2)^{1/2} \quad (3.6a)$$

$$\rho_0 = \{(x_0 - x)^2 + (y_0 - y)^2 + z_0^2\}^{1/2} \quad (3.6b)$$

Similarly, the contribution from the Curie point isotherm is expressed as follows:

$$\begin{aligned} \frac{2\mu}{C} W_x^{(H)} = & C_x \iint_{-\infty}^{\infty} \left[3 \left\{ -\frac{3\lambda+4\mu}{3\lambda+2\mu} \frac{x(H-D)}{R_1^5} + \left(-\frac{\lambda-\mu}{\lambda+\mu} + \frac{6\mu}{3\lambda+2\mu} \right) H \right. \right. \\ & + \left. \left(\frac{\lambda+3\mu}{\lambda+\mu} - \frac{2\mu}{3\lambda+2\mu} \right) D \right\} \frac{x}{R_2^5} + \frac{10(3\lambda+4\mu)}{3\lambda+2\mu} \frac{H(H+D)^2 x}{R_2^7} \Big\} \frac{1}{\rho_H} \\ & - \left\{ -\frac{x}{R_1^3} - \frac{\lambda+3\mu}{\lambda+\mu} \frac{x}{R_2^3} + \frac{6xH(H+D)}{R_2^5} \right\} \frac{z_0 - H}{\rho_H^3} \Big] dx dy \end{aligned} \quad (3.7a)$$

$$\begin{aligned} \frac{2\mu}{C} W_z^{(H)} = & C_z \iint_{-\infty}^{\infty} \left[\left\{ -\frac{3\lambda+4\mu}{3\lambda+2\mu} \left[-\frac{1}{R_1^3} + \frac{3(H-D)^2}{R_1^5} - \frac{\lambda-\mu}{\lambda+\mu} \frac{1}{R_2^3} \right. \right. \right. \\ & + 3 \left(\frac{7\lambda+5\mu}{\lambda+\mu} H + \frac{\lambda-\mu}{\lambda+\mu} D \right) \frac{H+D}{R_2^5} - \frac{30H(H+D)^3}{R_2^7} \Big] \\ & + \frac{8\mu}{3\lambda+2\mu} \left[\frac{1}{R_2^3} - \frac{3(H+D)^2}{R_2^5} \right] \Big\} \frac{1}{\rho_H} - \left\{ -\frac{H-D}{R_1^3} \right. \\ & + \left. \left(-\frac{\lambda-\mu}{\lambda+\mu} H + \frac{\lambda+3\mu}{\lambda+\mu} D \right) \frac{1}{R_2^3} + \frac{6H(H+D)^2}{R_2^5} \right\} \frac{z_0 - H}{\rho_H^3} \Big] dx dy \end{aligned} \quad (3.7b)$$

$W_k^{(0)}$ and $W_k^{(H)}$ are convolution integrals, which can be evaluated by the Fourier transform method. All the integrands in the convolution integrals are axially symmetric functions and their derivatives with respect to x or y . Fourier transforms of such functions can be reduced

to Hankel transforms. A convolution integral in the space domain is converted into a product of Fourier transforms in the wave number domain. Moreover, differential operation with respect to x or y is simply multiplication of ik_1 or ik_2 in the transformed space. Such unique properties of the Fourier transform are briefly summarized in Appendix B. All the Fourier transforms and their inverses required in this study are found in SASAI (1979) and SASAI (1980).

Thus we can evaluate the integrals in eqs. (3.5) and eqs. (3.7). We obtain

$$W_x^{(0)} = 0 \quad (3.8a)$$

$$W_z^{(0)} = 0 \quad (3.8b)$$

and

$$\begin{aligned} \frac{2\mu}{C} W_x^{(H)} = 4\pi C_x \left[-\frac{\mu}{3\lambda+2\mu} \frac{x_0}{\rho_3^3} + \frac{6(\lambda+\mu)}{3\lambda+2\mu} H \frac{3x_0 D_3}{\rho_3^5} \right. \\ \left. + \begin{cases} -\frac{3(\lambda+\mu)}{3\lambda+2\mu} \frac{x_0}{\rho_2^3} & (H > D) \\ \frac{\mu}{3\lambda+2\mu} \frac{x_0}{\rho_1^3} & (H < D) \end{cases} \right] \quad (3.9a) \end{aligned}$$

$$\begin{aligned} \frac{2\mu}{C} W_z^{(H)} = 4\pi C_z \left[\frac{\mu}{3\lambda+2\mu} \frac{D_3}{\rho_3^3} + \frac{6(\lambda+\mu)}{3\lambda+2\mu} H \left(-\frac{1}{\rho_3^3} + \frac{3D_3^2}{\rho_3^5} \right) \right. \\ \left. + \begin{cases} -\frac{3(\lambda+\mu)}{3\lambda+2\mu} \frac{D_2}{\rho_2^3} & (H > D) \\ -\frac{\mu}{3\lambda+2\mu} \frac{D_1}{\rho_1^3} & (H < D) \end{cases} \right] \quad (3.9b) \end{aligned}$$

where

$$\rho_i = (x_0^2 + y_0^2 + D_i^2)^{1/2} \quad (3.10a)$$

$$D_1 = D - z_0, \quad D_2 = 2H - D - z_0, \quad D_3 = 2H + D - z_0 \quad (3.10b)$$

Since outward normals of the surfaces $z = D - \epsilon$ and $z = D + \epsilon$ face each other, $W_k^{(P)}$ is given by

$$W_k^{(P)} = \lim_{\epsilon \rightarrow 0} \left\{ W_k^{(H=D-\epsilon)} - W_k^{(H=D+\epsilon)} \right\} \quad (3.11)$$

Substituting eqs. (3.9), we obtain

$$\frac{2\mu}{C} W_x^{(P)} = 4\pi C_x \frac{3\lambda+4\mu}{3\lambda+2\mu} \frac{x_0}{\rho_1^3} \quad (3.12a)$$

$$\frac{2\mu}{C} W_z^{(P)} = 4\pi C_z \frac{D_1}{\rho_1^3} \quad (3.12b)$$

Those terms containing ρ_3 in eqs. (3.9) are contributions from $u^{(B)}$. They cancel each other in the limiting operation (3.11). However, not all the terms arising from $u^{(A)}$ survive in eqs. (3.12). A close inspection tells us that the single layer potential remains in $W_z^{(P)}$ and the double layer in $W_z^{(P)}$. Thus the magnitude of the source sphere contribution is different for the horizontal and vertical magnetization cases respectively.

Combining eqs. (3.8), (3.9) and (3.12), we obtain the type I solution as follows:

$$\begin{aligned} \frac{2\mu}{C} W_z = 4\pi C_z \left[\frac{\mu}{3\lambda + 2\mu} \left(\frac{x_0}{\rho_1^3} - \frac{x_0}{\rho_3^3} \right) + \frac{6(\lambda + \mu)}{3\lambda + 2\mu} H \frac{3x_0 D_3}{\rho_3^5} \right. \\ \left. + \begin{cases} \frac{3(\lambda + \mu)}{3\lambda + 2\mu} \left(\frac{x_0}{\rho_1^3} - \frac{x_0}{\rho_2^3} \right) & (H > D) \\ 0 & (H < D) \end{cases} \right] \quad (3.13a) \end{aligned}$$

$$\begin{aligned} \frac{2\mu}{C} W_z = 4\pi C_z \left[-\frac{\mu}{3\lambda + 2\mu} \left(\frac{D_1}{\rho_1^3} - \frac{D_3}{\rho_3^3} \right) + \frac{6(\lambda + \mu)}{3\lambda + 2\mu} H \left(-\frac{1}{\rho_3^3} + \frac{3D_3^2}{\rho_3^5} \right) \right. \\ \left. + \begin{cases} \frac{3(\lambda + \mu)}{3\lambda + 2\mu} \left(\frac{D_1}{\rho_1^3} - \frac{D_2}{\rho_2^3} \right) & (H > D) \\ 0 & (H < D) \end{cases} \right] \quad (3.13b) \end{aligned}$$

Type II Solution

We evaluate the surface integral (2.52) over a spherical surface of radius b as shown in Fig. 6. Let us take the spherical coordinates (R_1, θ, ϕ) with origin at $A(0, 0, D)$ and polar axis in the z direction. An observation point $Q(r_0)$ in free space is given by $Q(\rho_1, \theta_0, \phi_0)$, while a moving point $P(r) = P(b, \theta, \phi)$ sweeps the source sphere. Then we have

$$\rho = \sqrt{\rho_1^2 + R_1^2 - 2\rho_1 R_1 \cos \gamma} \quad (3.14)$$

in which γ is the angle between AP and AQ. $\cos \gamma$ is given by

$$\cos \gamma = \cos \theta \cos \theta_0 + \sin \theta \sin \theta_0 \cos(\phi - \phi_0) \quad (3.15)$$

ρ_1 and R_1 are defined by eq. (3.10a) and eq. (3.2a) in original Cartesian coordinates. We write the contribution from the spherical surface $R_1 = b$ as $W_k^{(K)}$. Since the outward normal is given by $n = -e_{R_1}$, we have

$$W_k^{(K)} = C_k \int_0^{2\pi} d\phi \int_0^\pi \left[F_{1k} \cdot G_1 + F_{2k} \cdot G_2 \right] \sin \theta d\theta \quad (3.16)$$

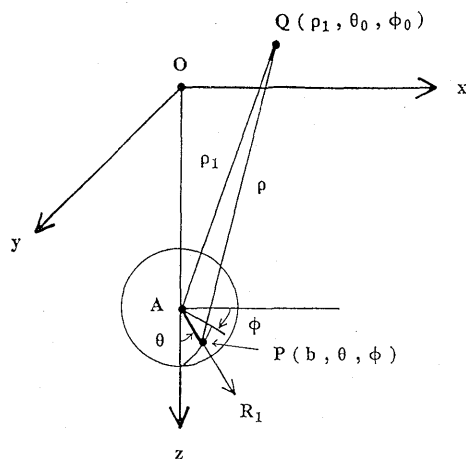


Fig. 6. Spherical coordinate system for integration over a spherical cap.

where

$$F_{1k} = b^2 \left[\frac{\partial u_k}{\partial R_1} - \frac{3(\lambda + \mu)}{3\lambda + 2\mu} \Delta m^{(k)} \cdot e_{R_1} \right]_{R_1=b} \quad (3.17a)$$

$$F_{2k} = b^2 \left[u_k \right]_{R_1=b} \quad (3.17b)$$

and

$$G_1 = \left[\frac{1}{\rho} \right]_{R_1=b} \quad (3.18a)$$

$$G_2 = \left[-\frac{\partial}{\partial R_1} \left(\frac{1}{\rho} \right) \right]_{R_1=b} \quad (3.18b)$$

F_{1k} 's and F_{2k} 's give density distributions of single and double layer potentials respectively. We may discriminate those arising from $u^{(A)}$ and $u^{(B)}$.

$$\frac{2\mu}{C} F_{1x}^{(A)} = \frac{2(3\lambda + 4\mu)}{3\lambda + 2\mu} \frac{\sin \theta \cos \phi}{b} \quad (3.19a)$$

$$\begin{aligned} \frac{2\mu}{C} F_{1x}^{(B)} = & 2b^2 \sin \theta \cos \phi \left[\left(\frac{2(3\lambda + 7\mu)}{3\lambda + 2\mu} - \frac{\lambda + 3\mu}{\lambda + \mu} \right) \frac{1}{S^3} \right. \\ & + 3 \left\{ 2 \left(s^2 + \frac{3\lambda + 4\mu}{\lambda + \mu} Ds + \frac{\lambda + 2\mu}{\lambda + \mu} D^2 \right) - 2 \frac{(9\lambda + 10\mu)}{3\lambda + 2\mu} (s + D)^2 + \frac{12(\lambda + \mu)}{3\lambda + 2\mu} D^2 \right\} \frac{1}{S^5} \\ & \left. + \frac{30(3\lambda + 4\mu)}{3\lambda + 2\mu} \frac{Ds(s + D)^2}{S^7} \right] \end{aligned} \quad (3.19b)$$

$$\frac{2\mu}{C} F_{2x}^{(A)} = \sin \theta \cos \phi \quad (3.19c)$$

$$\frac{2\mu}{C} F_{2x}^{(B)} = b^3 \sin \theta \cos \phi \left\{ \frac{\lambda + 3\mu}{\lambda + \mu} \frac{1}{S^3} - \frac{6s(s+D)}{S^5} \right\} \quad (3.19d)$$

$$\frac{2\mu}{C} F_{1z}^{(A)} = \frac{2(3\lambda + 4\mu)}{3\lambda + 2\mu} \frac{\cos \theta}{b} \quad (3.19e)$$

$$\begin{aligned} \frac{2\mu}{C} F_{1z}^{(B)} = & 2b \left[\left(-\frac{\lambda - \mu}{\lambda + \mu} s + \frac{\lambda + 5\mu}{\lambda + \mu} D \right) \frac{1}{S^3} + \left(10s + 3 \frac{2\lambda + 5\mu}{3\lambda + 2\mu} D \right) \frac{1}{S^3} \right. \\ & + 3 \left(\frac{\lambda - \mu}{\lambda + \mu} s - \frac{\lambda + 3\mu}{\lambda + \mu} D \right) \frac{D(s+D)}{S^5} + 3(2s^2 + 7Ds + D^2) \frac{s+D}{S^5} \\ & - \frac{9(\lambda + \mu)}{3\lambda + 2\mu} \frac{(13s+D)(s+D)^2}{S^5} - 3 \left(\frac{21\lambda + 11\mu}{3\lambda + 2\mu} s + \frac{3\lambda - 7\mu}{3\lambda + 2\mu} D \right) \frac{s^2 - D^2}{S^5} \\ & \left. - \frac{30Ds(s+D)^3}{S^7} + \frac{180(\lambda + \mu)}{3\lambda + 2\mu} \frac{s^2(s+D)^3}{S^7} \right] \quad (3.19f) \end{aligned}$$

$$\frac{2\mu}{C} F_{2z}^{(A)} = \cos \theta \quad (3.19g)$$

$$\frac{2\mu}{C} F_{2z}^{(B)} = b^2 \left[\left(\frac{\lambda - \mu}{\lambda + \mu} s - \frac{\lambda + 3\mu}{\lambda + \mu} D \right) - \frac{6s(s+D)^2}{S^5} \right] \quad (3.19h)$$

where s and S are z and R_2 in polar coordinates when P moves on the source sphere:

$$s = b \cos \theta + D \quad (3.20a)$$

$$S = \sqrt{b^2 + 4bD \cos \theta + 4D^2} = \sqrt{b^2 + 4Ds} \quad (3.20b)$$

ρ^{-1} can be expanded as follows:

$$\frac{1}{\rho} = \sum_{n=0}^{\infty} \frac{R_1^n}{\rho_1^{n+1}} P_n(\cos \gamma) \quad (3.21)$$

Thus the single layer potential G_1 on the sphere with unit intensity and the double layer potential G_2 can be given by

$$G_1 = \sum_{n=0}^{\infty} \frac{b^n}{\rho_1^{n+1}} P_n(\cos \gamma) \quad (3.22a)$$

$$G_2 = \sum_{n=1}^{\infty} \frac{nb^{n-1}}{\rho_1^{n+1}} P_n(\cos \gamma) \quad (3.22b)$$

To compute (3.16), we may use the following integration theorem of spherical harmonics.

$$\begin{aligned} & \int_0^{2\pi} d\phi \int_0^\pi Y_n(\theta, \phi) P_m(\cos \gamma) \sin \theta d\theta \\ &= \begin{cases} \frac{4\pi}{2n+1} Y_n(\theta_0, \phi_0) & (n=m) \\ 0 & (n \neq m) \end{cases} \end{aligned} \quad (3.23)$$

$Y_n(\theta, \phi)$ is an arbitrary spherical harmonic function.

By applying this theorem, we can readily evaluate integrals involving $u^{(A)}$ term. As for (B) terms we have an infinite series of $P_n(\cos \theta_0)$. This solution is less useful because of its poor convergence. However, all the (B) terms are multiplied by a factor b , so that they vanish in the limit of b approaching zero. As far as the point source problem is concerned, we may disregard the contribution from $u^{(B)}$. We will give different expressions for the (B) terms in the next section.

With the aid of the theorem (3.23) we obtain the pressure source contribution as follows.

$$\begin{aligned} \frac{2\mu}{C} W_x^{(K)} &= C_x \left\{ \frac{2(3\lambda+4\mu)}{3\lambda+2\mu} \frac{1}{b} \sin \theta_0 \cos \phi_0 \frac{b}{\rho_1^2} - \sin \theta_0 \cos \phi_0 \frac{1}{\rho_1^2} \right\} \times \frac{4\pi}{3} \\ &= 4\pi C_x \frac{\lambda+2\mu}{3\lambda+2\mu} \frac{\sin \theta_0 \cos \phi_0}{\rho_1^2} = 4\pi C_x \frac{\lambda+2\mu}{3\lambda+2\mu} \frac{x_0}{\rho_1^3} \end{aligned} \quad (3.24a)$$

and quite similarly

$$\begin{aligned} \frac{2\mu}{C} W_z^{(K)} &= C_z \left\{ \frac{2(3\lambda+4\mu)}{3\lambda+2\mu} \frac{1}{b} \cos \theta_0 \frac{b}{\rho_1^2} - \cos \theta_0 \frac{1}{\rho_1^2} \right\} \times \frac{4\pi}{3} \\ &= 4\pi C_z \frac{\lambda+2\mu}{3\lambda+2\mu} \frac{\cos \theta_0}{\rho_1^2} = 4\pi C_z \frac{\lambda+2\mu}{3\lambda+2\mu} \frac{-D_1}{\rho_1^3} \end{aligned} \quad (3.24b)$$

The solutions (3.24) have nothing to do with the source radius b . Thus they survive when the radius b approaches zero.

Combining eqs. (3.8), (3.9) and (3.24), we obtain the type II solution as follows:

$$\begin{aligned} \frac{2\mu}{C} W_x &= 4\pi C_x \left[\frac{\mu}{3\lambda+2\mu} \left(\frac{x_0}{\rho_1^3} - \frac{x_0}{\rho_3^3} \right) + \frac{6(\lambda+\mu)}{3\lambda+2\mu} H \frac{3x_0 D_3}{\rho_3^5} \right. \\ &\quad \left. + \begin{cases} \frac{\lambda+\mu}{3\lambda+2\mu} \left(\frac{x_0}{\rho_1^3} - \frac{3x_0}{\rho_2^3} \right) & (H > D) \\ 0 & (H < D) \end{cases} \right] \end{aligned} \quad (3.25a)$$

$$\frac{2\mu}{C} W_z = 4\pi C_z \left[-\frac{\mu}{3\lambda + 2\mu} \left(\frac{D_1}{\rho_1^3} - \frac{D_3}{\rho_3^3} \right) + \frac{6(\lambda + \mu)}{3\lambda + 2\mu} H \left(-\frac{1}{\rho_3^3} + \frac{3D_3^2}{\rho_3^5} \right) \right. \\ \left. + \begin{cases} -\frac{\lambda + \mu}{3\lambda + 2\mu} \left(\frac{D_1}{\rho_1^3} + \frac{3D_2}{\rho_2^3} \right) & (H > D) \\ 0 & (H < D) \end{cases} \right] \quad (3.25b)$$

As shown in eqs. (3.24), both the source terms produced by J_x and J_z are identical. This feature is naturally expected because $u^{(A)}$ has spherical symmetry. In other words, type I solution, eqs. (3.13), lacks something. We should investigate the cause of the discrepancy between the two. Moreover, in type II solution, the source term $W_k^{(K)}$ suddenly emerges when the Curie depth H becomes larger than the source depth D . We have to analyze such transitional behavior for type II solution. These issues will be discussed in section 3.3.

DAVIS (1976) computed piezomagnetic changes for Kilauea Volcano with model parameters as follows: $D=4$ km, $a/D=1/4$, $\Delta P=1$ kbar, $\lambda=\mu=3 \times 10^5$ bar, $\beta=2 \times 10^{-4}$ bar $^{-1}$, $J=5 \times 10^{-3}$ A/m, magnetic dip $I_0=35^\circ$, and declination $D_0=11^\circ$ east. Total field changes associated with the corresponding point source model are shown in Fig. 7(a) for type I and in Fig. 7(b) for type II solution respectively. Both are apparently quite different. Which type of solution is appropriate?

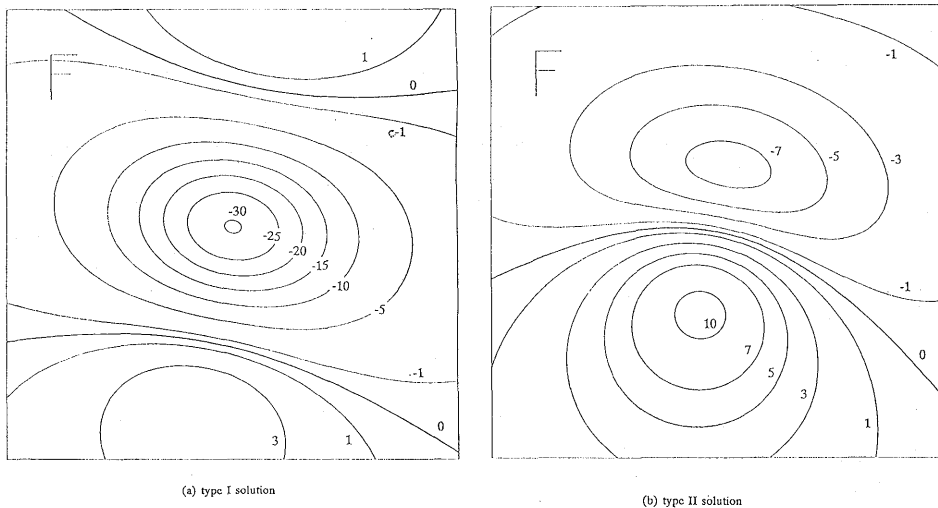


Fig. 7. Computed total intensity changes for Kilauea Volcano with the same model parameters as DAVIS' (1976) for (a) type I solution and (b) type II solution. Unit in nT.

3.2 Finite Spherical Source Solution

Now let us consider the case when the Curie point isotherm intersects the thermally demagnetized source sphere. We cannot apply theorem (3.23) in evaluating $W_k^{(K)}$, i.e. integrals over a spherical cap. Nor can we use Fourier transforms to calculate $W_k^{(H)}$, because the horizontal plane with infinite extent has a circular hole. We are now to formulate such a case. The formulation allows for integration either over the whole spherical surface or an infinite plane without a hole as a special case.

Contribution from Spherical Cap

We take the same spherical coordinates as those in Fig. 6. The integral over a spherical cap is defined in eq. (3.16) by letting the lower limit of θ vary from 0 to Θ as below.

$$\Theta = \begin{cases} \cos^{-1} \frac{H-D}{b} & (|H-D| < b) \\ 0 & (|H-D| \geq b) \end{cases} \quad (3.26)$$

Integrating with respect to ϕ , we obtain the following expression in place of eq. (3.16):

$$W_k^{(K)} = C_k \int_{\Theta}^{\pi} \sin \theta d\theta [F_{1k}(\theta) \cdot G_{1k}(\theta; r_0) + F_{2k}(\theta) \cdot G_{2k}(\theta; r_0)] \quad (3.27)$$

where

$$F_{1x}(\theta) = \{F_{1x}^{(A)} + F_{1x}^{(B)}\} / \cos \phi \quad (3.28a)$$

$$F_{2x}(\theta) = \{F_{2x}^{(A)} + F_{2x}^{(B)}\} / \cos \phi \quad (3.28b)$$

$$F_{1z}(\theta) = \{F_{1z}^{(A)} + F_{1z}^{(B)}\} \quad (3.28c)$$

$$F_{2z}(\theta) = \{F_{2z}^{(A)} + F_{2z}^{(B)}\} \quad (3.28d)$$

and

$$G_{1x}(\theta; r_0) = \int_0^{2\pi} \frac{\cos \phi}{\rho_b} d\phi = 2 \cos \phi_0 \cdot \Phi_2 \quad (3.29a)$$

$$\begin{aligned} G_{2x}(\theta; r_0) &= \int_0^{2\pi} \frac{b - \rho_1 \cos \gamma}{\rho_b^3} \cos \phi d\phi \\ &= 2 \cos \phi_0 \{2(b - \zeta_0 \cos \theta) \cdot \Phi_4 - r_0 \sin \theta \cdot (\Phi_3 + \Phi_5)\} \end{aligned} \quad (3.29b)$$

$$G_{1z}(\theta; r_0) = \int_0^{2\pi} \frac{1}{\rho_b} d\phi = 2\Phi_1 \quad (3.29c)$$

$$G_{2x}(\theta; r_0) = \int_0^{2\pi} \frac{b - \rho_1 \cos \gamma}{\rho_b^3} d\phi$$

$$= 2(b - \zeta_0 \cos \theta) \cdot \Phi_3 - 2r_0 \sin \theta \cdot \Phi_4 \quad (3.29d)$$

ρ_b is given as $\rho(R_1=b)$ in eq. (3.14). $F_{1k}^{(A)}$'s and $F_{2k}^{(B)}$'s have already been given in eqs. (3.19). Notice that a common factor $\cos \phi$ in F_{1x} and F_{2x} is included within G_{1x} and G_{2x} for the first integration as to ϕ . Φ_n 's in eqs. (3.29) are defined by the following integrals:

$$\Phi_1 = \int_0^\pi \frac{1}{\rho_\phi} d\phi, \quad \Phi_2 = \int_0^\pi \frac{\cos \phi}{\rho_\phi} d\phi \quad (3.30a)$$

$$\Phi_3 = \int_0^\pi \frac{1}{\rho_\phi^3} d\phi, \quad \Phi_4 = \int_0^\pi \frac{\cos \phi}{\rho_\phi^3} d\phi, \quad \Phi_5 = \int_0^\pi \frac{\cos 2\phi}{\rho_\phi^3} d\phi \quad (3.30b)$$

ρ_ϕ is rewritten from ρ_b as a function of $\phi = \phi - \phi_0$:

$$\rho_\phi = (b^2 - 2b\rho_1 \cos \theta \cos \theta_0 + \rho_1^2 - 2b\rho_1 \sin \theta \sin \theta_0 \cos \phi)^{1/2}$$

$$= \{b^2 \sin^2 \theta - 2r_0 b \sin \theta \cos \phi + r_0^2 + (b \cos \theta - \zeta_0)^2\}^{1/2} \quad (3.31)$$

where

$$\zeta_0 = \rho_1 \cos \theta_0 = z_0 - D \quad (3.32)$$

r_0 is the horizontal distance from the observation point in the original Cartesian coordinates: i.e. $r_0 = \sqrt{x_0^2 + y_0^2}$.

Since Φ_n 's are not expressible with elementary functions, we have to integrate numerically with respect to θ . We seek to obtain expressions for the magnetic field components in the form of integrals with respect to θ , by differentiating potentials (3.27). Thus we have

$$\Delta F_k^{l(K)} = C_k \int_\theta^\pi \sin \theta d\theta [F_{1k}(\theta) \cdot G_{1k}^l + F_{2k}(\theta) \cdot G_{2k}^l] \quad (3.33)$$

$\Delta F_k^{l(K)}$ implies the l -th component of the magnetic field arising from the potential $W_k^{(K)}$. For example, G_{1x}^x is given by

$$G_{1x}^x = 2r_0 \cos^2 \phi_0 \cdot \Phi_4 - b \sin \theta \cdot (\Phi_3 + \cos 2\phi_0 \cdot \Phi_5) \quad (3.34a)$$

while G_{2x}^x is

$$G_{2x}^x = \sin \theta \cdot (\Phi_3 + \cos 2\phi_0 \cdot \Phi_5) + 6r_0 \cos^2 \phi_0 (b - \zeta_0 \cos \theta) \cdot \Phi_7$$

$$- 3r_0^2 \cos^2 \phi_0 \sin \theta \cdot (\Phi_6 + \Phi_8) - 3b \sin \theta (b - \zeta_0 \cos \theta) \cdot (\Phi_6 + \cos 2\phi_0 \cdot \Phi_8)$$

$$+ 3br_0 \sin^2 \theta \left\{ \left(\frac{1}{2} + \cos^2 \phi_0 \right) \cdot \Phi_7 + \frac{1}{2} \cos 2\phi_0 \cdot \Phi_9 \right\} \quad (3.34b)$$

All the G_{1k} 's and G_{2k} 's are given explicitly by SASAI (1991). They are rather intricate functions of Φ_n 's and are not reproduced here. In addition to Φ_n 's ($n=1, 5$), we need the following ones.

$$\Phi_6 = \int_0^\pi \frac{1}{\rho_\phi^5} d\phi, \quad \Phi_7 = \int_0^\pi \frac{\cos \phi}{\rho_\phi^5} d\phi, \quad (3.35a)$$

$$\Phi_8 = \int_0^\pi \frac{\cos 2\phi}{\rho_\phi^5} d\phi, \quad \Phi_9 = \int_0^\pi \frac{\cos 3\phi}{\rho_\phi^5} d\phi \quad (3.35b)$$

Φ_n 's can be expressed with complete elliptic integrals. Following EASON *et al.* (1955), we treat these integrals in a unified way. We first reduce Φ_n to an integral of Lipschitz-Hankel type, which is defined as

$$I(m, n; l) = \int_0^\infty J_m(at) J_n(bt) e^{-ct} t^l dt \quad (3.36)$$

J_m and J_n are Bessel functions. We should replace a , b and c with the following variables.

$$a = b \sin \theta, \quad b = r_0, \quad c = b \cos \theta + D - z_0 \quad (3.37)$$

Transformation of Φ_n into the Lipschitz-Hankel integral is achieved in Appendix C. Next we will express those with complete elliptic integrals. Some integrals of the type in eqs. (3.35) were not given explicitly by EASON *et al.* (1955). All the integrals necessary for the present purpose are tabulated in Appendix C. They are eventually represented by combinations of complete elliptic integrals of the first and second kind. Numerical approximation formulas are available for these two functions (HASTINGS, 1955).

Thus integrands in eqs. (3.33) can be calculated accurately as well as rapidly. As for one dimensional integrals of analytic functions, we have a useful algorithm for numerical integration, i.e. the double exponential formula (TAKAHASI and MORI, 1974). Now we have an analytic expression for integrals over a spherical cap and an effective way of integrating it: the problem is solved.

Contribution from the Curie Surface with a Circular Hole

We take the cylindrical coordinates (u, ϕ, z) with origin $(0, 0, H)$, at the intersection of the z axis with the Curie depth surface (see Fig. 8). Let us consider the surface integral over the magnetized portion of the Curie surface. The integral in the radial direction should be carried out from u_0 to infinity. u_0 is given by

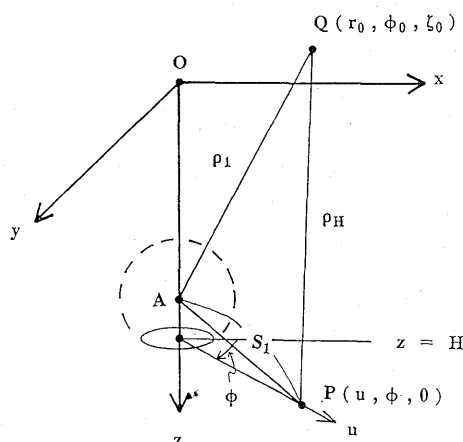


Fig. 8. Cylindrical coordinate system for integration over the Curie surface with a circular hole.

$$u_0 = \begin{cases} \sqrt{b^2 - (H-D)^2} & (|H-D| < b) \\ 0 & (|H-D| \geq b) \end{cases} \quad (3.38)$$

We first conduct integrations with respect to ϕ and obtain

$$W_k^{(H)} = C \int_{u_0}^{\infty} [\{f_{1k}^{(A)}(u) + f_{1k}^{(B)}(u)\} \cdot g_{1k}(u; r_0) + \{f_{2k}^{(A)}(u) + f_{2k}^{(B)}(u)\} \cdot g_{2k}(u; r_0)] u du \quad (3.39)$$

where

$$\frac{2\mu}{C} f_{1x}^{(A)} = 3u \left\{ -\frac{3\lambda + 4\mu}{3\lambda + 2\mu} \frac{H-D}{S_1^5} \right\} \quad (3.40a)$$

$$\begin{aligned} \frac{2\mu}{C} f_{1x}^{(B)} = 3u \left[\left\{ -\left(\frac{\lambda - \mu}{\lambda + \mu} + \frac{6\mu}{3\lambda + 2\mu} \right) H + \left(\frac{\lambda + 3\mu}{\lambda + \mu} - \frac{2\mu}{3\lambda + 2\mu} \right) D \right\} \frac{1}{S_2^5} \right. \\ \left. + \frac{10(3\lambda + 4\mu)}{3\lambda + 2\mu} \frac{H(H+D)^2}{S_2^7} \right] \end{aligned} \quad (3.40b)$$

$$\frac{2\mu}{C} f_{2x}^{(A)} = \frac{u}{S_1^3} \quad (3.40c)$$

$$\frac{2\mu}{C} f_{2x}^{(B)} = u \left[\frac{\lambda + 3\mu}{\lambda + \mu} \frac{1}{S_2^3} - \frac{6H(H+D)}{S_2^5} \right] \quad (3.40d)$$

$$\frac{2\mu}{C} f_{1z}^{(A)} = \frac{3\lambda + 4\mu}{3\lambda + 2\mu} \left\{ \frac{1}{S_1^3} - \frac{3(H-D)^2}{S_1^5} \right\} \quad (3.40e)$$

$$\begin{aligned} \frac{2\mu}{C} f_{1z}^{(B)} = & \frac{3\lambda+4\mu}{3\lambda+2\mu} \left[\frac{\lambda-\mu}{\lambda+\mu} \frac{1}{S_2^3} - 3 \left(\frac{7\lambda+5\mu}{\lambda+\mu} H + \frac{\lambda-\mu}{\lambda+\mu} D \right) \frac{H+D}{S_2^5} \right. \\ & \left. + \frac{30H(H+D)^3}{S_2^7} \right] + \frac{8\mu}{3\lambda+2\mu} \left[\frac{1}{S_2^3} - \frac{3(H+D)^2}{S_2^5} \right] \end{aligned} \quad (3.40f)$$

$$\frac{2\mu}{C} f_{2z}^{(A)} = \frac{H-D}{S_1^3} \quad (3.40g)$$

$$\frac{2\mu}{C} f_{2z}^{(B)} = \left(\frac{\lambda-\mu}{\lambda+\mu} H - \frac{\lambda+3\mu}{\lambda+\mu} D \right) \frac{1}{S_2^3} - \frac{6H(H+D)^2}{S_2^5} \quad (3.40h)$$

in which

$$S_1 = \sqrt{u^2 + (H-D)^2}, \quad S_2 = \sqrt{u^2 + (H+D)^2}. \quad (3.41)$$

The unit single layer potential g_{1k} 's and the unit double layer potential g_{2k} 's are given by

$$g_{1x} = \int_0^{2\pi} \frac{\cos \phi}{\rho_H} d\phi = 2 \cos \phi_0 \cdot \Phi_2 \quad (3.42a)$$

$$g_{2x} = \int_0^{2\pi} \frac{(z_0 - H) \cos \phi}{\rho_H^3} d\phi = 2(z_0 - H) \cos \phi_0 \cdot \Phi_4 \quad (3.42b)$$

$$g_{1z} = \int_0^{2\pi} \frac{1}{\rho_H} d\phi = 2\Phi_1 \quad (3.42c)$$

$$g_{2z} = \int_0^{2\pi} \frac{(z_0 - H)}{\rho_H^3} d\phi = 2(z_0 - H) \cdot \Phi_3 \quad (3.42d)$$

where

$$\begin{aligned} \rho_H = & \{u^2 + (H-z_0)^2 + x_0^2 + y_0^2 - 2u(x_0 \cos \phi + y_0 \sin \phi)\}^{1/2} \\ = & \{u^2 - 2r_0 u \cos \phi + r_0^2 + (H-z_0)^2\}^{1/2} \end{aligned} \quad (3.43)$$

Comparing eq. (3.43) with eq. (3.31), we find that integrals in eqs. (3.42) are formally quite identical with those in eqs. (3.29). In this case we have only to replace a , b and c in eq. (3.36) with the following variables:

$$a = u, \quad b = r_0, \quad c = H - z_0 \quad (3.44)$$

Differentiation of potentials gives us the magnetic field components

$$\Delta F_k^{(H)} = C_k \int_{u_0}^{\infty} [f_{1k}(u) \cdot g_{1k}^l + f_{2k}(u) \cdot g_{2k}^l] u du \quad (3.45)$$

Again as an example, g_{1x}^x is given by

$$g_{1x}^x = 2r_0 \cos^2 \phi_0 \cdot \Phi_4 - u \cdot (\Phi_8 + \cos 2\phi_0 \cdot \Phi_5) \quad (3.46a)$$

and g_{2x}^x as follows:

$$g_{2x}^x = 3(z_0 - H)[2r_0 \cos^2 \phi_0 \cdot \Phi_7 - u \cdot (\Phi_6 + \cos 2\phi_0 \cdot \Phi_5)] \quad (3.46b)$$

All the g_{ik}^j 's are listed in SASAI (1991), but are not reproduced here. We can numerically calculate integrals in eqs. (3.45) with the aid of DEF. Thus we have managed to evaluate the contribution from an infinite plane boundary with a circular hole.

If the Curie surface does not intersect the demagnetized sphere, we should always evaluate integrals over a plane without a hole, i.e. eq. (3.39) in which $u_0 = 0$. We have already obtained analytic solutions for these particular integrals with the aid of the Fourier transform method. The integral (3.39) must reduce to eqs. (3.9). Actually this is true, which is proved by SASAI (1991). For $|H - D| > b$, we may omit elaborate numerical integrations in eqs. (3.45).

Let us investigate how the surface magnetic field varies with increasing depth of the Curie point isotherm. The behavior of the solution when the source radius decreases is also shown. This gives us a helpful suggestion for the cause of the discrepancy between the type I and type II solutions.

Curie Depth Dependence of the Magnetic Field at the Origin

DAVIS (1976) and SASAI (1979) investigated how the magnetic field at the origin (0, 0, 0) just above the center of dilatation varies with increasing Curie depth H . At this particular point, only two field components, i.e. X_z and Z_z , are non-zero. SUZUKI and OSHIMAN (1990) re-examined DAVIS' numerical calculations by subdividing the medium into sufficiently small elementary volumes. Their model parameters are almost the same as those of DAVIS (1976) for Kilauea Volcano, except for the depth D and the radius b of the source sphere, i.e. $D = 12$ km and $b = 3$ km, respectively. We follow their model parameters here for the sake of comparison.

Fig. 9 shows the Curie depth dependence of X_z and Z_z at the origin. This figure agrees very well with SUZUKI and OSHIMAN's (1990) result (Fig. 7(b) in their paper). This implies that their numerical calculation is very accurate. DAVIS' result is also similar to Fig. 9. As DAVIS (1976) has already pointed out, the piezomagnetic changes become maximum when the Curie depth H is around the source depth D . They decrease to certain values with increasing depth of H . This characteristic is quite different from the type I solution, in which the maximum (absolute) changes are attained at H infinity (SASAI, 1979; See Fig. 15(a) in this

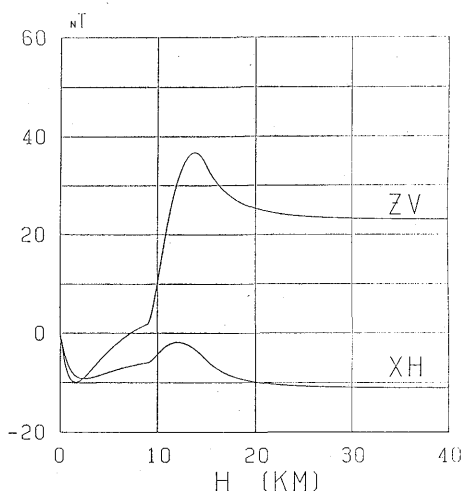


Fig. 9. Two non-zero magnetic components at the origin with increasing depth of H . Model parameters are the same as SUZUKI and OSHIMAN's (1990). XH and ZV indicate X_z and Z_z components, respectively.

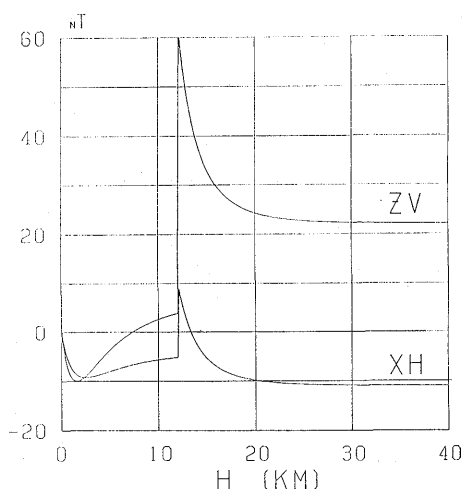


Fig. 10. Curie depth dependence curves of the magnetic components at the origin for $b=30$ m.

paper). Fig. 9 shows that the contribution of the vertical magnetization J_z is much more dominant than that of the horizontal one J_x . This feature was also noticed by DAVIS (1976).

Let us investigate the influence of the source size. Fig. 10 shows the curve of the Curie depth dependence for $b=30$ m. The other model parameters are the same as those in Fig. 9. The special feature of the curve in Fig. 9 is preserved, somewhat exaggerated as b decreases. The peak values of the surface magnetic field around $H=D$ are kept constant for smaller values of b . It never happens that the H dependence curve is drastically converted into that of the type I solution (i.e. Fig. 15(a)).

Surface Distribution of the Magnetic Field on the Earth

Finally we present the surface distribution. Fig. 11 shows total intensity changes we may expect in Kilauea Volcano following Davis' model parameters. DAVIS (1976) gave a numerical result for this model (i.e. Fig. 3 in his paper). Fig. 11 exhibits a slightly different pattern from Davis' results. However, the positions and values of positive and negative peaks roughly coincide with each other. Hence Davis' numerical computations are confirmed again by the present analytic approach. Comparing Fig. 11 with Fig. 7(a) and 7(b), we recognize that the finite spherical source solution obviously resembles the type II solution of the point source problem.

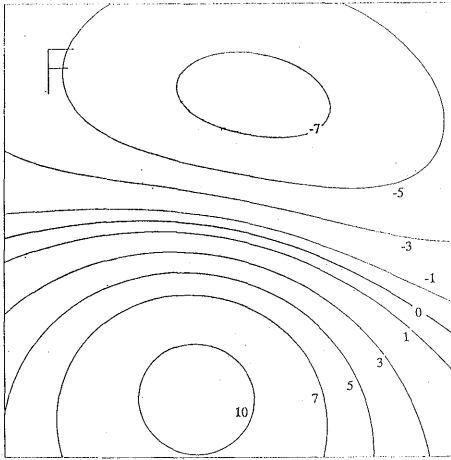


Fig. 11. Surface distribution of total intensity changes for Kilauea Volcano, with the same model parameters as DAVIS' (1979). Unit in nT.

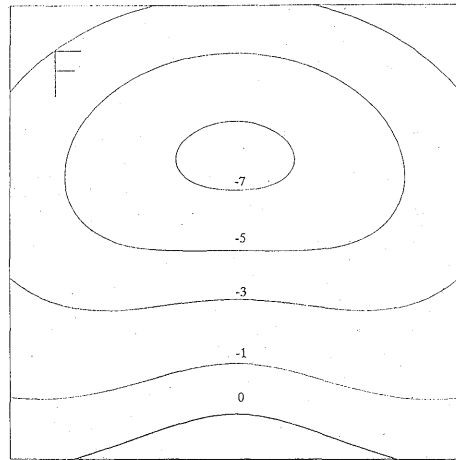


Fig. 12. Total intensity changes for $H=5$ km. Model parameters are SUZUKI and OSHIMAN's (1990). Unit in nT.

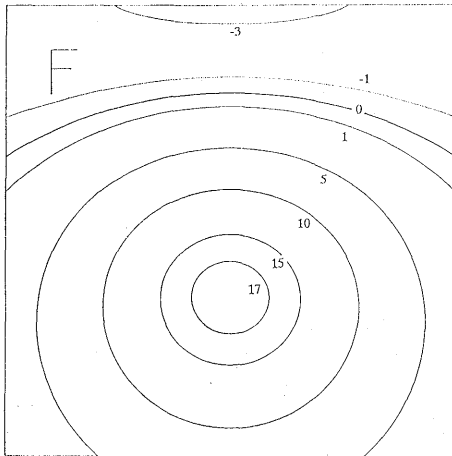


Fig. 13. Total intensity changes for $H=12$ km. Model parameters are SUZUKI and OSHIMAN's (1990). Unit in nT.

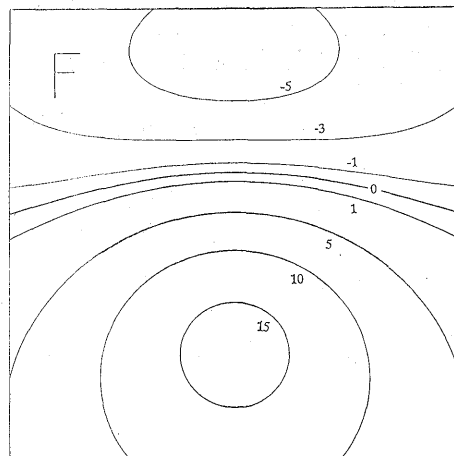


Fig. 14. Total intensity changes for $H=20$ km. Model parameters are SUZUKI and OSHIMAN's (1990). Unit in nT.

Let us investigate the Curie depth dependence of the surface distribution. Coming back again to SUZUKI and OSHIMAN's (1990) parameters, we put $D=12$ km, $b=3$ km, $I_0=45^\circ$, and $D_0=0^\circ$. In Figs. 12, 13 and 14 are shown total intensity changes for $H=5$ km, 12 km and 20 km, respectively. The pattern of piezomagnetic changes is highly dependent on the spatial configuration of the demagnetized sphere and the Curie point

isotherm. In particular, the sign of magnetic field changes reverses depending on whether or not the Curie depth H lies deeper than the source depth D .

3.3 Point Source Solution as a Limiting Case of Finite Spherical Source

In the previous section we found that the general feature of the finite source solution resembles that of type II solution as the source radius diminishes. We will demonstrate here that the type II solution is actually obtained by reducing the source radius b to zero in type III solution. As has been pointed out in section 3.1, the influence of the source sphere is abruptly added as the Curie depth H exceeds the source depth D . Accordingly the magnetic potential varies discontinuously at $H=D$. The transient behavior of the solution around $H=D$ will be presented by investigating the limiting case. The cause of the discrepancy between the type I and type II solutions will be clarified. We find that type II is appropriate for the point source solution.

Let us investigate the integrals over the spherical surface, i.e. eq. (3.27). Among various terms in the integrand, those arising from $u^{(B)}$ are finite at the source point $(0, 0, D)$ and are multiplied by b . They vanish in the limit as b approaches zero. We have only to take account of the contributions from $u^{(A)}$:

$$\frac{2\mu}{C} F_{1x}^{(KA)} = \frac{2(3\lambda + 4\mu)}{3\lambda + 2\mu} \frac{\sin \theta}{b} \quad (3.47a)$$

$$\frac{2\mu}{C} F_{2x}^{(KA)} = \sin \theta \quad (3.47b)$$

$$\frac{2\mu}{C} F_{1z}^{(KA)} = \frac{2(3\lambda + 4\mu)}{(3\lambda + 2\mu)} \frac{\cos \theta}{b} \quad (3.47c)$$

$$\frac{2\mu}{C} F_{2z}^{(KA)} = \cos \theta \quad (3.47d)$$

According to Appendix C, the unit potential functions, G_{1x} etc., have power series representations in k^2 . Expanding them further into a Taylor series in b , we obtain the following:

$$G_{1x} = \pi r_0 \cos \phi_0 \frac{b}{\rho_1^3} \sin \theta \{1 + O(b)\} \quad (3.48a)$$

$$G_{2x} = -\pi r_0 \cos \phi_0 \frac{\sin \theta}{\rho_1^3} \{1 + O(b)\} \quad (3.48b)$$

$$G_{1z} = 2\pi \left\{ \frac{1}{\rho_1} + \frac{b\zeta_0 \cos \theta}{\rho_1^3} + O(b^2) \right\} \quad (3.48c)$$

$$G_{2z} = -2\pi\zeta_0 \frac{\cos \theta}{\rho_1^3} \{1 + O(b)\} \quad (3.48d)$$

Substituting eqs. (3.47) and eqs. (3.48) into eq. (3.27) and integrating by terms, we have

$$\frac{2\mu}{C} W_x^{(KA)} = C_x \frac{3\pi(\lambda+2\mu)}{3\lambda+2\mu} \frac{x_0}{\rho_1^3} \int_0^\pi \sin^3 \theta d\theta + O(b) \quad (3.49a)$$

$$\begin{aligned} \frac{2\mu}{C} W_z^{(KA)} = & C_z \frac{4\pi(3\lambda+4\mu)}{3\lambda+2\mu} \frac{1}{b\rho_1} \int_0^\pi \sin \theta \cos \theta d\theta \\ & + C_z \frac{6\pi(\lambda+2\mu)}{3\lambda+2\mu} \frac{\zeta_0}{\rho_1^3} \int_0^\pi \cos^2 \theta \sin \theta d\theta + O(b) \end{aligned} \quad (3.49b)$$

In case $H > D$, the infinitesimal source sphere is fully included within the magnetized region: we may put $\Theta = 0$. The first term on the right hand side of eq. (3.49b) becomes null. Taking the limit as b approaches zero, we obtain

$$\frac{2\mu}{C} W_x^{(KA)} = C_x \frac{4\pi(\lambda+2\mu)}{3\lambda+2\mu} \frac{x_0}{\rho_1^3} \quad (3.50a)$$

$$\frac{2\mu}{C} W_z^{(KA)} = C_z \frac{4\pi(\lambda+2\mu)}{3\lambda+2\mu} \frac{-D_1}{\rho_1^3} \quad (3.50b)$$

in which we use the relation $\zeta_0 = z_0 - D = -D_1$ (cf. eq. (3.32)). Eqs. (3.50) are coincident with eqs. (3.24). Thus the limit of type III solution as the source radius b decreases is proved to be type II solution.

Next we will investigate the special case in which $H = D$. Since the source surface is a hemisphere, we may put $\Theta = \pi/2$. From eqs. (3.49) we obtain

$$\frac{2\mu}{C} W_x^{(KA)} = C_x \frac{2\pi(\lambda+2\mu)}{3\lambda+2\mu} \frac{x_0}{\rho_1^3} \quad (3.51a)$$

$$\frac{2\mu}{C} W_z^{(KA)} = -C_z \frac{2\pi(3\lambda+4\mu)}{3\lambda+2\mu} \frac{1}{b\rho_1} + C_z \frac{2\pi(\lambda+2\mu)}{3\lambda+2\mu} \frac{-D_1}{\rho_1^3} \quad (3.51b)$$

The first term on the right hand side of eq. (3.51b) diverges as we decrease b to zero. However, a counterpart of this divergent term emerges in the Curie surface integral and they cancel each other. Then only the second term in eq. (3.51b) survives. Notice that the integrals over the

hemispherical surface are just half of those over the entire spherical surface.

We are now to evaluate the Curie surface integral for $H=D$. $f_{1k}^{(B)}$ and $f_{2k}^{(B)}$ have no singularity at $(0,0,D)$. The integral containing them are reduced to elementary functions: i.e. terms having ρ_3 in eqs. (3.9). We should examine integrals involving $f_{1k}^{(A)}$ and $f_{2k}^{(A)}$. Putting $H=D$ in eqs. (3.40a), (3.40c), (3.40e) and (3.40g), we have

$$\frac{2\mu}{C} f_{1x}^{(A)} = 0 \quad (3.52a)$$

$$\frac{2\mu}{C} f_{2x}^{(A)} = \frac{1}{u^2} \quad (3.52b)$$

$$\frac{2\mu}{C} f_{1z}^{(A)} = \frac{3\lambda+4\mu}{3\lambda+2\mu} \frac{1}{u^3} \quad (3.52c)$$

$$\frac{2\mu}{C} f_{2z}^{(A)} = 0 \quad (3.52d)$$

The lower limit of integration u_0 is equal to b . We denote the Curie surface integral contributed from $u^{(A)}$ by superscript (HA). We now seek to obtain the limit of the following integral as we let b approach zero:

$$\frac{2\mu}{C} W_x^{(HA)} = C_z 2(z_0 - D) \cos \phi_0 \int_b^\infty \frac{1}{u} \Phi_4 du \quad (3.53a)$$

$$\frac{2\mu}{C} W_z^{(HA)} = C_z \frac{2(3\lambda+4\mu)}{3\lambda+2\mu} \int_b^\infty \frac{1}{u^2} \Phi_1 du \quad (3.53b)$$

Referring to Appendix C, we substitute Lipschitz-Hankel integrals into Φ_1 and Φ_4 in eqs. (3.53). After some manipulations we find

$$\frac{2\mu}{C} W_x^{(HA)} = -2\pi C_x \cos \phi_0 \frac{r_0}{(r_0^2 + D_1^2)^{3/2}} = -2\pi C_x \frac{x_0}{\rho_1^3} \quad (3.54a)$$

$$\frac{2\mu}{C} W_z^{(HA)} = 2\pi C_z \frac{3\lambda+4\mu}{3\lambda+2\mu} \left\{ -\frac{D_1}{\rho_1^3} + O(b) + \frac{1}{b\rho_1} \right\} \quad (3.54b)$$

Comparing eq. (3.54b) with eq. (3.51b), we find that the divergent term in $W_z^{(KA)}$ is completely canceled out by the divergent one in $W_z^{(HA)}$. Since we always consider the total sum $W_z^{(KA)} + W_z^{(HA)}$, the divergent term disappears. Mathematical details are given in SASAI (1991).

Taking account of eqs. (3.50) and eqs. (3.54), we rewrite the type II solution as given by eqs. (3.25) as follows:

$$\frac{2\mu}{C} W_z = 4\pi C_z \left[\frac{\mu}{3\lambda+2\mu} \left(\frac{x_0}{\rho_1^3} - \frac{x_0}{\rho_3^3} \right) + \frac{6(\lambda+\mu)}{3\lambda+2\mu} H \frac{3x_0 D_3}{\rho_3^5} \right. \\ \left. + \begin{cases} \frac{\lambda+\mu}{3\lambda+2\mu} \left(\frac{x_0}{\rho_1^3} - \frac{3x_0}{\rho_2^3} \right) & (H > D) \\ -\frac{\lambda+\mu}{3\lambda+2\mu} \frac{x_0}{\rho_1^3} & (H = D) \\ 0 & (H < D) \end{cases} \right] \quad (3.55a)$$

$$\frac{2\mu}{C} W_z = 4\pi C_z \left[-\frac{\mu}{3\lambda+2\mu} \left(\frac{D_1}{\rho_1^3} - \frac{D_3}{\rho_3^3} \right) + \frac{6(\lambda+\mu)}{3\lambda+2\mu} H \left(-\frac{1}{\rho_3^3} + \frac{3D_3^2}{\rho_3^5} \right) \right. \\ \left. + \begin{cases} -\frac{\lambda+\mu}{3\lambda+2\mu} \left(\frac{D_1}{\rho_1^3} + \frac{3D_2}{\rho_2^3} \right) & (H > D) \\ -\frac{2(\lambda+\mu)}{3\lambda+2\mu} \frac{D_1}{\rho_1^3} & (H = D) \\ 0 & (H < D) \end{cases} \right] \quad (3.55b)$$

The magnetic potentials has a gap across $H=D$. The potential value at $H=D$ is just the average of the two limiting values for $H=D-0$ and $H=D+0$.

Fig. 15 shows the Curie depth dependence of two magnetic com-

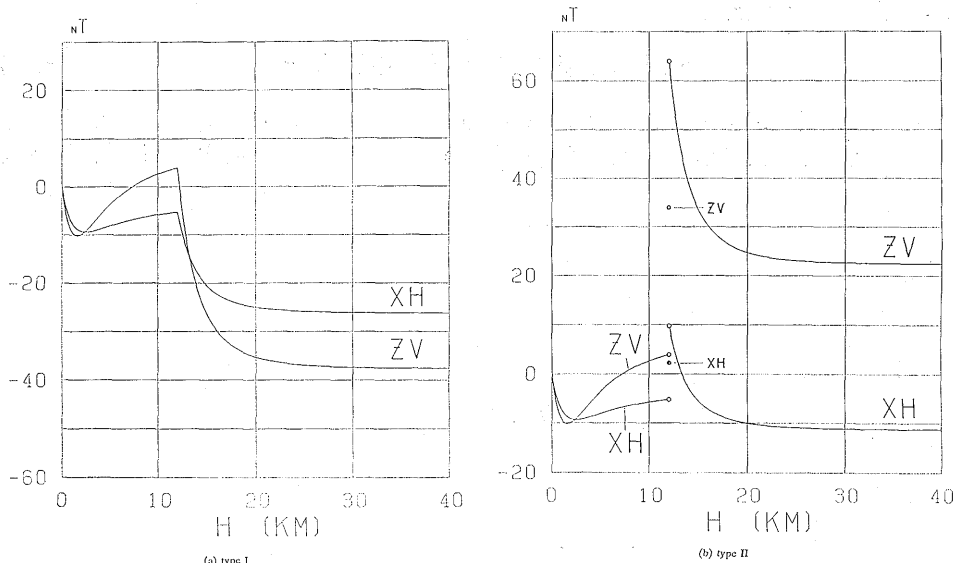


Fig. 15. Curie depth dependence of the two magnetic components at the origin for the point source solution of (a) type I, and (b) type II respectively. Model parameters are SUZUKI and OSHIMA's (1990).

ponents at the origin for (a) type I and (b) type II solutions, respectively. The discontinuity at $H=D$ in type II solution can be recognized as the limit of a steep increase in the magnetic field around $H=D$ for a small value of b as shown in Fig. 10. The nature of the discrepancy between the two types of solutions is now obvious: type I solution is the remainder after subtracting the effect of the source sphere from type II solution. Hence we should naturally suspect the possibility of overlooking part of the piezomagnetic components produced within the whole magnetic body in the type I case.

Now let us recall the definition of the integration area for the two kinds of solutions as depicted in Fig. 5. The magnetic potentials $W_k^{(I)}$ for type I and $W_k^{(II)}$ for type II are given as the sums of surface potentials:

$$W_k^{(I)} = W_k^{(0)} + W_k^{(P)} + W_k^{(H)} \quad (3.56)$$

$$W_k^{(II)} = W_k^{(0)} + W_k^{(K)} + W_k^{(H)} \quad (3.57)$$

where

$$W_k^{(P)} = W_k^{(H=D-\epsilon)} - W_k^{(H=D+\epsilon)} \quad (3.58)$$

Before taking the limit as ϵ approaches zero, we find that disagreement of integration area exists between the two. It is a region surrounded by two horizontal planes $H=D-\epsilon$ and $H=D+\epsilon$ and the source sphere as shown in Fig. 16. We call this area K' . The contribution of K' to the potential is given by

$$W_k^{(K')} = W_k^{(K)} - W_k^{(H=D-\epsilon)} + W_k^{(H=D+\epsilon)} \quad (3.59)$$

In the limit as ϵ approaches zero, the volume of the region K' becomes null. In evaluating type I solution, we implicitly took it for

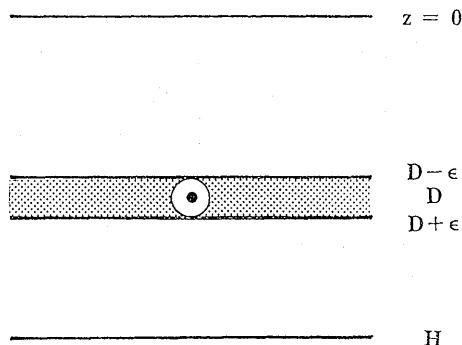


Fig. 16. A schematic representation of the integration area K' (hatched) which is ignored in the type I solution.

granted that the contribution from K' vanishes as well. This is incorrect: the region K' reduces to a thin layer at $H=D$ but produces a finite magnetic field. The relationship among these surface potentials as given by eq. (3.56) through (3.59) holds good even for the limiting case $\epsilon \rightarrow 0$. Then we have

$$W_k^{(I)} + W_k^{(K')} = W_k^{(II)} \quad (3.60)$$

In other words, the jump in the potential values arises from the stress-induced magnetization in a thin layer at $H=D$.

All these considerations imply that type II solution properly evaluates the contributions from all piezomagnetic constituents. Hence we arrive at a final conclusion: *the type II solution is the correct one for the point source problem. The earlier result by SASAI (1979), i.e. the type I solution, should be rejected.* This conclusion compels serious alteration of some earlier works by SASAI. It is because the same way of integration around singular points has been undertaken in constructing Green's functions for tectonomagnetic modeling (i.e. SASAI, 1980; 1986a). We will reexamine all these previous results in the following chapters. However, we will find that in most cases the type I and type II solutions are identical and hence that previous results are still valid.

SASAI (1979) derived the type I solution under the direct suggestion of HAGIWARA's (1977a) work on the gravity change associated with the Mogi model. Hagiwara integrated to obtain the density-related gravity change in the same manner as type I solution. A question arises: is Hagiwara's solution for gravity change erroneous? Since $u^{(A)} = C/2\mu \nabla(R_1^{-1})$, the density change at an arbitrary point due to $u^{(A)}$ is given by

$$\Delta\rho = \rho \operatorname{div} u^{(A)} = \rho \frac{C}{2\mu} \nabla^2(R_1^{-1}) = -4\pi\rho \frac{C}{2\mu} \delta(R_1)$$

Hagiwara put this term equal to zero, because $\nabla^2(R_1^{-1})=0$ everywhere except $R_1=0$. According to the characteristics of Dirac's delta function, the density integral due to $u^{(A)}$ produces a point mass at $(0,0,D)$. Instead he took into account the loss of surrounding mass due to inflation of the source sphere. Recently OKUBO (1991) formulated gravity changes due to point dislocations. He demonstrated that the gravity produced by the delta function is the mass loss due to inflation of the pressure source. Consequently, HAGIWARA's (1977a) result for the gravity change due to the Mogi model is correct.

In our calculation the delta function does not appear explicitly. However, the treatment of the problem in the form of surface integrals is verified with the aid of Green's theorem. Actually the equivalence of $\nabla^2(R_1^{-1})$ to $-4\pi\delta(R_1)$ is also verified through Green's theorem, so that our

derivation of $W_k^{(K)}$ is equivalent to applying the delta function.

However, the physical interpretation of the source term in the gravity change by OKUBO (1991) does not hold as in the case of piezomagnetism. In the Mogi model the source radius expands by $\Delta a = a\Delta P/4\mu$ under an internal pressure ΔP (cf. eq. (2.60)). The magnetic potential corresponding to the vanishing of a magnetized spherical shell of radius a and thickness Δa is given by

$$W_x^{(\Delta a)} = m_x \frac{x_0}{\rho_1^3} \quad (3.61a)$$

$$W_z^{(\Delta a)} = m_z \frac{z_0 - D}{\rho_1^3} \quad (3.61b)$$

where

$$m_k = 4\pi a^2 \Delta a J_k = 2\pi \frac{C}{\mu} J_k \quad (3.62)$$

Comparing eqs. (3.61) with eqs. (3.50), we find

$$W_k^{(K)} = \frac{1}{2} \frac{\lambda + 2\mu}{\lambda + \mu} \beta \mu W_k^{(\Delta a)} \quad (3.63)$$

The source term due to the type II solution is amplified by $\frac{1}{2} \frac{\lambda + 2\mu}{\lambda + \mu} \beta \mu$ times the source expansion effect. This factor amounts to 26.25 for $\beta = 1.0 \times 10^{-4} \text{ bar}^{-1}$, $\lambda = \mu = 3.5 \times 10^5 \text{ bar}$. As we have already seen in section 2.6, the piezomagnetic effect is an order of magnitude or more larger than other causes of magnetic change due to mechanical distortion, i.e. free-air effect, the field produced by upheaved portion of the earth's surface and the source expansion effect. This difference originates from the fundamental nature of piezomagnetism caused by quantum mechanical spin-spin interactions.

Chapter 4. Green's Function Approach to Tectonomagnetic Problems

In this chapter we will develop a unified method to evaluate piezomagnetic field changes associated with various mechanical distortions. We adopt the simplest model of the Earth: i.e. a homogeneous and isotropic elastic half-space having a uniformly magnetized top layer. For such a simplified medium, a variety of tectonic models can be constructed by superposing the displacement field solution of a single force operative

at a point in an elastic half-space. Once the piezomagnetic potential caused by such a force is known, tectonomagnetic changes of these models can be derived from linear combinations of the prescribed potentials. We may call them the fundamental piezomagnetic potentials. The surface integral representation eq. (2.52) will be successfully applied to their derivation process. A Green's function for surface load problems is given simply as a special case of the fundamental potential. The magnetic field produced by a uniform circular load will be calculated as an application example of the present theory.

4.1 Formulation

Let us consider a simple earth model: a homogeneous and isotropic elastic half-space with a uniformly magnetized top layer. We will develop a unified treatment for calculating the piezomagnetic field associated with various types of mechanical deformation within the medium. We take Cartesian coordinates (x_1, x_2, x_3) , in which the semi-infinite elastic medium occupies $x_3 > 0$. The magnetized region is bounded, from the free surface $x_3 = 0$ to the Curie depth $x_3 = H$.

The equation of static equilibrium has already been given before: i.e. eq. (2.20). The displacement field u should satisfy the traction-free boundary condition at $x_3 = 0$:

$$\tau_{31} = \tau_{32} = \tau_{33} = 0. \quad (4.1)$$

The stress field is related to the displacement through Hooke's law: i.e. eq. (2.14).

We begin with the fundamental solution of eq. (2.20) satisfying condition (4.1), i.e., the displacement field caused by a single force operative at a point within an elastic half space. Let G_{ki} be the x_i component of the displacement at $Q(x_1, x_2, x_3)$ produced by a unit single force at $P(\xi_1, \xi_2, \xi_3)$ acting in the x_i direction. We will hereafter refer to the vector representation G_i , together with

$$G_{ki} = G_{ki}(x; \xi) = G_{ki}(x_1, x_2, x_3; \xi_1, \xi_2, \xi_3). \quad (4.2)$$

G_i satisfies the following equation:

$$(\lambda + \mu) \text{grad div } G_i + \mu \nabla^2 G_i + F_i = 0, \quad (4.3)$$

which is the same form as eq. (2.20) except that

$$F_{ii} = \delta_{ii} \delta(x_1 - \xi_1) \delta(x_2 - \xi_2) \delta(x_3 - \xi_3), \quad (4.4)$$

in which δ_{ii} is the Kronecker delta, while $\delta(x)$ is the Dirac delta function. G_i fulfills the boundary condition (4.1), which is rewritten as

$$\begin{aligned}
\mu \left(\frac{\partial G_{3l}}{\partial x_1} + \frac{\partial G_{1l}}{\partial x_3} \right) &= \mu \left(\frac{\partial G_{3l}}{\partial x_2} + \frac{\partial G_{2l}}{\partial x_3} \right) \\
&= \lambda \left(\frac{\partial G_{1l}}{\partial x_1} + \frac{\partial G_{2l}}{\partial x_2} + \frac{\partial G_{3l}}{\partial x_3} \right) + 2\mu \frac{\partial G_{3l}}{\partial x_3} \\
&= 0 \quad \text{at} \quad x_3 = 0.
\end{aligned} \tag{4.5}$$

($l=1, 2, 3$)

Since both the basic equation and the boundary condition are linear, the principle of superposition holds. Then the displacement field u as a linear combination of G_l also satisfies eqs. (2.20) and (4.1):

$$u = \sum_{\alpha} A_{\alpha} G_l(x; \xi^{(k)}) \tag{4.6}$$

in which $\xi^{(k)}$ denotes the k -th discrete source point. This important characteristic of G_l can be extended to a more general class of linear combination, which is expressed by

$$u = L(\xi) G_l(x; \xi). \tag{4.7}$$

The functional $L(\xi)$ is called the integro-differential operator, defined by

$$L(\xi)f = \sum_{\alpha} \left[\int K_{\alpha}(\xi, \xi') D^{\alpha} f(\xi) d\xi' + A_{\alpha} D^{\alpha} f(\xi) \right] \tag{4.8}$$

where D implies the partial differential operator ($D = \partial/\partial \xi_k$) and α is a non-negative integer. Obviously the integral with respect to ξ is a limiting case of the linear combination (4.6). We may also interpret derivatives with respect to ξ as a kind of linear combination, in view of the fact that $\partial G_{kl}/\partial \xi_1$, for example, is by definition

$$\lim_{\Delta \xi_1 \rightarrow 0} \left\{ \frac{1}{\Delta \xi_1} G_{kl}(x; \xi_1 + \Delta \xi_1, \xi_2, \xi_3) - \frac{1}{\Delta \xi_1} G_{kl}(x; \xi_1, \xi_2, \xi_3) \right\}.$$

Hence derivatives of G_{kl} with respect to the parameter ξ as well as their weighted integrals, namely the displacement field given by eq. (4.7), are again the solution of eq. (2.20) under the boundary condition (4.1).

Once the displacement field of a magnetoelastic body is specified, the piezomagnetic potential due to associated stresses is expressible with its displacement as we have seen in the previous chapter. It is given by the following integral, i.e., eq. (2.25):

$$W^m(r) = \iiint_V \Delta M^m(u(x)) \cdot \nabla \left(\frac{1}{\rho} \right) dx \tag{4.9}$$

where

$$\rho = |\mathbf{x} - \mathbf{r}| = \sqrt{(x_1 - x)^2 + (x_2 - y)^2 + (x_3 - z)^2}. \quad (4.10)$$

$\Delta M^m(\mathbf{x})$ is the stress-induced magnetization vector.

Let U_l^m be magnetic potential due to $\Delta M^m(\mathbf{G}_l)$ which is the stress-induced magnetization caused by \mathbf{G}_l operating on \mathbf{J}_m :

$$U_l^m(\mathbf{r}; \boldsymbol{\xi}) = \iiint_V \Delta M^m(\mathbf{G}_l(\mathbf{x}; \boldsymbol{\xi})) \cdot \nabla \left(\frac{1}{\rho} \right) d\mathbf{x}. \quad (4.11)$$

ΔM^m is given by derivatives of \mathbf{u} , in other words, by a linear combination of \mathbf{u} . We now substitute the displacement field (4.7) into (4.9). If we are allowed to interchange the order of operations, i.e., integration with respect to \mathbf{x} and operation of the linear functional $L(\boldsymbol{\xi})$, we obtain

$$\begin{aligned} W^m(\mathbf{r}) &= \iiint_V \Delta M^m(L(\boldsymbol{\xi})\mathbf{G}_l(\mathbf{x}; \boldsymbol{\xi})) \cdot \nabla \left(\frac{1}{\rho} \right) d\mathbf{x} \\ &= L(\boldsymbol{\xi}) \iiint_V \Delta M^m(\mathbf{G}_l(\mathbf{x}; \boldsymbol{\xi})) \cdot \nabla \left(\frac{1}{\rho} \right) d\mathbf{x} = L(\boldsymbol{\xi}) U_l^m(\mathbf{r}; \boldsymbol{\xi}). \end{aligned}$$

However, this interchange is not verified for a particular kind of linear operation. \mathbf{G}_l has a singularity of an order of r^{-1} ($r = |\mathbf{x} - \boldsymbol{\xi}|$) at $\mathbf{x} = \boldsymbol{\xi}$. Then $\Delta M^m(\partial \mathbf{G}_l / \partial \boldsymbol{\xi})$ becomes a function of an order $O(r^{-3})$. In this case the integral in the second identity does not converge as an improper integral. Thus the above relation does not hold good for the differential operator. Dislocation source problems correspond to this case, which will be discussed in detail in Chapter 5.

We meet no such difficulty when the linear operator (4.8) consists only of weighted integrals. We can represent the piezomagnetic potential associated with such mechanical models as follows:

$$W^m(\mathbf{r}) = L_0(\boldsymbol{\xi}) U_l^m(\mathbf{r}; \boldsymbol{\xi}) \quad (4.12)$$

in which we restrict ourselves to deal with only an integral operator:

$$L_0(\boldsymbol{\xi})f = \int K(\boldsymbol{\xi}, \boldsymbol{\xi}') f(\boldsymbol{\xi}') d\boldsymbol{\xi}' \quad (4.8')$$

It is much easier to get at the solution $W^m(\mathbf{r})$ through eq. (4.12) than through eq. (4.9) via eq. (4.7). We may call U_l^m the fundamental piezomagnetic potential.

There are some problems of geophysical interest which can be described in the form of eq. (4.7) and hence eq. (4.12). One is the surface load problem. A typical example is the dam-magnetic effect (DAVIS and STACEY, 1972). The local magnetic change caused by surface load of a man-made lake can be calculated by integrating fundamental potentials

with the weight proportional to the depth topography of the reservoir.

Another application is the volume source problem. A strain which is not associated with stress is called a "stress-free" strain (e.g., ESHELBY, 1957) or an "eigen" strain (MURA, 1982). Eigen strains of geophysical importance are thermal expansion and plastic deformation. Such strains behave as a sort of body force in the elastic equation. Problems containing inelastic inclusions are solved by volumetric integrals of fundamental potentials over the source region.

4.2 Fundamental Piezomagnetic Potentials

In this section we will derive the fundamental solution of the problem, i.e., piezomagnetic potential due to the stress-induced magnetization produced by a single force operative at a point in an elastic half-space, i.e., eq. (4.11). In order to avoid confusion, we discriminate three notations of coordinates for different field quantities: the source point is represented by $\xi(\xi_1, \xi_2, \xi_3)$, and the displacement is a function of $x(x_1, x_2, x_3)$, while the magnetic potential is a function of $r(x, y, z)$. Since the magnetic field is usually measured in free space, z is assumed to be negative in the following calculations.

MINDLIN (1936) obtained the fundamental solution for an isotropic solid with semi-infinite extent. Although Mindlin's solution is given in terms of the Galerkin vector stress function, we find an explicit form of the displacement in a textbook (e.g., MURA, 1982). We may assume a single force acting at a point $(0, 0, \xi_3)$. Replacing x and y by $(x - \xi_1)$ and $(y - \xi_2)$ in the final expressions, we obtain the corresponding results for any arbitrary source position $\xi(\xi_1, \xi_2, \xi_3)$.

The displacement component at $x(x_1, x_2, x_3)$ due to a unit single force at $(0, 0, \xi_3)$ is denoted by g_{ki} , which indicates the x_k component of the displacement produced by a single force in the ξ_i direction. They are given as follows (MURA, 1982, p. 95):

$$g_{ij} = \frac{1}{16\pi\mu(1-\nu)} \left[\frac{3-4\nu}{R_1} \delta_{ij} + \frac{1}{R_2} \delta_{ij} + \frac{x_i x_j}{R_1^3} \right. \\ \left. + (3-4\nu) \frac{x_i x_j}{R_2^3} + \frac{2x_3 \xi_3}{R_2^3} \left\{ \delta_{ij} - \frac{3x_i x_j}{R_2^2} \right\} \right. \\ \left. + \frac{4(1-\nu)(1-2\nu)}{R_2 + x_3 + \xi_3} \left\{ \delta_{ij} - \frac{x_i x_j}{R_2(R_2 + x_3 + \xi_3)} \right\} \right] = g_{ji},$$

$$g_{3j} = \frac{x_j}{16\pi\mu(1-\nu)} \left[\frac{x_3 - \xi_3}{R_1^3} + \frac{(3-4\nu)(x_3 - \xi_3)}{R_2^3} \right. \\ \left. - \frac{6x_3 \xi_3 (x_3 + \xi_3)}{R_2^5} + \frac{4(1-\nu)(1-2\nu)}{R_2(R_2 + x_3 + \xi_3)} \right],$$

$$\begin{aligned}
g_{i3} &= \frac{x_i}{16\pi\mu(1-\nu)} \left[\frac{x_3 - \xi_3}{R_1^3} + \frac{(3-4\nu)(x_3 - \xi_3)}{R_2^3} \right. \\
&\quad \left. + \frac{6x_3\xi_3(x_3 + \xi_3)}{R_2^5} - \frac{4(1-\nu)(1-2\nu)}{R_2(R_2 + x_3 + \xi_3)} \right], \\
g_{33} &= \frac{1}{16\pi\mu(1-\nu)} \left[\frac{3-4\nu}{R_1} + \frac{8(1-\nu)^2 - (3-4\nu)}{R_2} + \frac{(x_3 - \xi_3)^2}{R_1^3} \right. \\
&\quad \left. + \frac{(3-4\nu)(x_3 + \xi_3)^2 - 2x_3\xi_3}{R_2^3} + \frac{6x_3\xi_3(x_3 + \xi_3)^2}{R_2^5} \right], \quad (4.13)
\end{aligned}$$

($i, j = 1, 2$)

where

$$R_1^2 = x_1^2 + x_2^2 + (x_3 - \xi_3)^2 \quad (4.14a)$$

$$R_2^2 = x_1^2 + x_2^2 + (x_3 + \xi_3)^2. \quad (4.14b)$$

We are now to evaluate eq. (4.11). Instead of performing volumetric integrals, we will use an equivalent method of evaluating the piezomagnetic potential through surface integrals, i.e. eq. (2.52). Since there is no body force, the fundamental piezomagnetic potential in free space can be rewritten as follows:

$$U_l^m(\mathbf{r}; \boldsymbol{\xi}) = C_m \iint_S \left[\left\{ -\boldsymbol{\nabla} g_{ml}(\mathbf{x}) + \frac{1}{1+\nu} \Delta \mathbf{m}^{(m)} \right\} \cdot \mathbf{n} \frac{1}{\rho} + \{g_{ml}(\mathbf{x})\} \frac{\partial}{\partial n} \left(\frac{1}{\rho} \right) \right] dS \quad (4.15)$$

where

$$\Delta m_j^{(m)} = \frac{3}{2} \left(\frac{\partial g_{ml}}{\partial x_j} + \frac{\partial g_{jl}}{\partial x_m} \right) - \delta_{mj} \operatorname{div} \mathbf{g}_l \quad (4.16)$$

$$C_m = \frac{1}{2} \beta J_m \mu \frac{3\lambda + 2\mu}{\lambda + \mu} = \beta J_m \mu (1 + \nu) \quad (4.17)$$

We seek to obtain U_l^m 's in the same way as we have obtained the type II solution for the point source problem of the Mogi model. Surfaces surrounding the magnetized medium are the earth's surface $x_3=0$, the Curie point isotherm at $x_3=H$ and a small spherical surface of radius ϵ centered at the point force. If the force acts on the earth's surface or at the Curie point isotherm, we take the sum of a hemispherical surface and an infinite plane with a circular hole.

Thus we have three kinds of surface potentials:

(a) The contribution from an infinite plane surface at depth x_3 ($\neq \xi_3$)

$$v_l^{m(H)}(\mathbf{r}; \xi_3; x_3) = C_m \int_{-\infty}^{\infty} \left\{ f_{ml} \frac{1}{\rho} - g_{ml} \frac{x_3 - z}{\rho^3} \right\} dx_1 dx_2 \quad (4.18)$$

in which the outward normal n is tentatively defined in the downward direction.

(b) The contribution from a plane surface with a circular hole of radius ϵ ($x_3 = \xi_3$)

$$v_l^{m(H')}(\mathbf{r}; \xi_3; \epsilon) = C_m \int_0^{2\pi} d\phi \int_\epsilon^\infty \left\{ f'_{ml} \frac{1}{\rho_u} + g'_{ml} \frac{z - \xi_3}{\rho_u^3} \right\} u du \quad (4.19)$$

in which the outward normal is also taken downward.

(c) The contribution from a spherical surface of radius ϵ

$$v_l^{m(K)}(\mathbf{r}; \xi_3; \epsilon, \theta_1, \theta_2) = C_m \int_0^{2\pi} d\phi \int_{\theta_1}^{\theta_2} \epsilon^2 \left\{ F_{ml}^{(A)} \frac{1}{\rho_\epsilon} + G_{ml}^{(A)} \frac{\epsilon - \rho \cos \gamma}{\rho_\epsilon^3} \right\} \sin \theta d\theta \quad (4.20)$$

f_{ml} , f'_{ml} , $F_{ml}^{(A)}$'s and g_{ml} , g'_{ml} , $G_{ml}^{(A)}$'s are single and double layer distributions, respectively.

There are four typical positions of the single force source. The fundamental piezomagnetic potential can be constructed by summing contributions from these three surfaces.

Case I: when the source point lies at the free surface ($\xi_3 = 0$):

$$U_l^m = \lim_{\epsilon \rightarrow 0} \left\{ -v_l^{m(H')}(\mathbf{r}; 0; \epsilon) + v_l^{m(K)}\left(\mathbf{r}; 0; \epsilon, 0, \frac{\pi}{2}\right) \right\} + v_l^{m(H)}(\mathbf{r}; \xi_3; H) \quad (4.21)$$

Case II: when the source is included in the magnetized region ($0 < \xi_3 < H$):

$$U_l^m = -v_l^{m(H)}(\mathbf{r}; \xi_3; 0) + v_l^{m(H)}(\mathbf{r}; \xi_3; H) + \lim_{\epsilon \rightarrow 0} v_l^{m(K)}(\mathbf{r}; \xi_3, \epsilon, 0, \pi) \quad (4.22)$$

Case III: when the source is at the Curie depth ($\xi_3 = H$):

$$U_l^m = -v_l^{m(H)}(\mathbf{r}; H; 0) + \lim_{\epsilon \rightarrow 0} \left\{ v_l^{m(H')}(\mathbf{r}; H; \epsilon) + v_l^{m(K)}\left(\mathbf{r}; H; \epsilon, \frac{\pi}{2}, \pi\right) \right\} \quad (4.23)$$

Case IV: when the source lies beneath the Curie point isotherm ($\xi_3 > H$):

$$U_l^m = -v_l^{m(H)}(\mathbf{r}; \xi_3; 0) + v_l^{m(H)}(\mathbf{r}; \xi_3; H) \quad (4.24)$$

f_{ml} in eq. (4.18) is given as follows:

$$f_{ml} = -\frac{\partial g_{ml}}{\partial x_3} + \frac{1}{1+\nu} \left\{ \frac{3}{2} \left(\frac{\partial g_{ml}}{\partial x_3} + \frac{\partial g_{3l}}{\partial x_m} \right) - \delta_{m3} \operatorname{div} \mathbf{g}_l \right\} \quad (4.25)$$

The integration can be done by Fourier transform method. This com-

putation has already been done by SASAI (1986), and hence his results are quoted here.

f'_{mi} and g'_{mi} in eq. (4.19) are f_{mi} and g_{mi} in eq. (4.18), rewritten in the cylindrical coordinates (u, ϕ, x_3) as shown in Fig. 8. We separate the displacement field g_i into two parts: the source terms containing R_1 and the surface boundary terms containing R_2 in eqs. (4.13). They are specified with superscripts (A) and (B) respectively. Since contributions from $g_i^{(B)}$ are regular at $u=0$, they can be easily calculated by the Fourier transform method. Only the contributions from $g_i^{(A)}$ are computed according to eq. (4.19).

In the following the common factor $1/16\pi\mu(1-\nu)$ is omitted. This factor will be included only in the final expressions for the solution, i.e. eqs. (4.34) and eqs. (4.35).

$f'_{mi}^{(A)}$ and $g'_{mi}^{(A)}$ at $x_3=\xi_3$ are expressed in the cylindrical coordinates as follows:

$$f'_{x1}^{(A)}=0, \quad g'_{x1}^{(A)}=C_x \left\{ \frac{3-4\nu}{u} + \frac{1}{u} \cos^2 \phi \right\} \quad (4.26a)$$

$$f'_{y1}^{(A)}=0, \quad g'_{y1}^{(A)}=C_y \frac{1}{u} \sin \phi \cos \phi \quad (4.26b)$$

$$f'_{z1}^{(A)}=C_x \frac{4-5\nu}{1+\nu} \frac{1}{u^2} \cos \phi, \quad g'_{z1}^{(A)}=0 \quad (4.26c)$$

$$f'_{x2}^{(A)}=0, \quad g'_{x2}^{(A)}=C_x \frac{1}{u} \sin \phi \cos \phi \quad (4.26d)$$

$$f'_{y2}^{(A)}=0, \quad g'_{y2}^{(A)}=C_y \left\{ \frac{3-4\nu}{u} + \frac{1}{u} \sin^2 \phi \right\} \quad (4.26e)$$

$$f'_{z2}^{(A)}=C_x \frac{4-5\nu}{1+\nu} \frac{1}{u^2} \cos \phi, \quad g'_{z2}^{(A)}=0 \quad (4.26f)$$

$$f'_{x3}^{(A)}=C_x \frac{-4+5\nu}{1+\nu} \frac{1}{u^2} \sin \phi, \quad g'_{x3}^{(A)}=0 \quad (4.26g)$$

$$f'_{y3}^{(A)}=C_y \frac{-4+5\nu}{1+\nu} \frac{1}{u^2} \cos \phi, \quad g'_{y3}^{(A)}=0 \quad (4.26h)$$

$$f'_{z3}^{(A)}=0, \quad g'_{z3}^{(A)}=C_z \frac{3-4\nu}{u} \quad (4.26i)$$

On the other hand, ρ_u in eq. (4.19) is given by

$$\rho_u = \sqrt{u^2 - 2ur_0 \cos(\phi - \phi_0) + r_0^2 + (\xi_3 - z)^2} \quad (4.27)$$

in which (x_1, x_2) and (x, y) are given in the new coordinates (u, ϕ, x_3) as follows:

$$x_1 = u \cos \phi, \quad x_2 = u \sin \phi, \quad x = r_0 \cos \phi_0, \quad y = r_0 \sin \phi_0$$

We first integrate with respect to ϕ in eq. (4.19), which results in the Lipschitz-Hankel type integrals. Then we can obtain the final result by letting ϵ decrease to zero, as we have already done in section 3.3. After some manipulations we find

$$v_1^{x(H)} = 2\pi C_x \left\{ -4(1-\nu) \frac{1}{\rho_1} + \frac{1}{\rho_1 + c_1} - \frac{x^2}{\rho_1(\rho_1 + c_1)^2} \right\} \quad (4.28a)$$

$$v_1^{y(H)} = -2\pi C_y \frac{xy}{\rho_1(\rho_1 + c_1)^2} \quad (4.28b)$$

$$v_1^{z(H)} = 2\pi C_z \frac{4-5\nu}{1+\nu} \frac{x}{\rho_1(\rho_1 + c_1)} \quad (4.28c)$$

$$v_2^{x(H)} = -2\pi C_x \frac{xy}{\rho_1(\rho_1 + c_1)^2} \quad (4.28d)$$

$$v_2^{y(H)} = 2\pi C_y \left\{ -4(1-\nu) \frac{1}{\rho_1} + \frac{1}{\rho_1 + c_1} - \frac{y^2}{\rho_1(\rho_1 + c_1)^2} \right\} \quad (4.28e)$$

$$v_2^{z(H)} = 2\pi C_z \frac{4-5\nu}{1+\nu} \frac{y}{\rho_1(\rho_1 + c_1)} \quad (4.28f)$$

$$v_3^{x(H)} = -2\pi C_x \frac{4-5\nu}{1+\nu} \frac{x}{\rho_1(\rho_1 + c_1)} \quad (4.28g)$$

$$v_3^{y(H)} = -2\pi C_y \frac{4-5\nu}{1+\nu} \frac{y}{\rho_1(\rho_1 + c_1)} \quad (4.28h)$$

$$v_3^{z(H)} = -2\pi C_z (3-4\nu) \frac{1}{\rho_1} \quad (4.28i)$$

$F_{mi}^{(A)}$ and $G_{mi}^{(A)}$ in eq. (4.20) are contributions from $g_i^{(A)}$. Those from $g_i^{(B)}$ are regular at the source point and hence they vanish in the limit $\epsilon \rightarrow 0$. $F_{mi}^{(A)}$ are given as follows:

$$F_{x1}^{(A)} = \frac{C_x}{\epsilon^2} \left\{ \frac{\nu(-5+4\nu)}{1+\nu} + \frac{3(2-\nu)}{1+\nu} \sin^2 \theta \cos^2 \phi \right\} \quad (4.29a)$$

$$F_{y1}^{(A)} = \frac{C_y}{\epsilon^2} \frac{3(2-\nu)}{1+\nu} \sin^2 \theta \sin \phi \cos \phi \quad (4.29b)$$

$$F_{z1}^{(A)} = \frac{C_z}{\epsilon^2} \frac{3(2-\nu)}{1+\nu} \sin \theta \cos \theta \cos \phi \quad (4.29c)$$

$$F_{x2}^{(A)} = \frac{C_x}{\epsilon^2} \frac{3(2-\nu)}{1+\nu} \sin^2 \theta \sin \phi \cos \phi \quad (4.29d)$$

$$F_{y2}^{(A)} = \frac{C_y}{\epsilon^2} \left\{ \frac{\nu(-5+4\nu)}{1+\nu} + \frac{3(2-\nu)}{1+\nu} \sin^2 \theta \sin^2 \phi \right\} \quad (4.29e)$$

$$F_{z2}^{(A)} = \frac{C_z}{\epsilon^2} \frac{3(2-\nu)}{1+\nu} \sin \theta \cos \theta \sin \phi \quad (4.29f)$$

$$F_{x3}^{(A)} = \frac{C_x}{\epsilon^2} \frac{3(2-\nu)}{1+\nu} \sin \theta \cos \theta \cos \phi \quad (4.29g)$$

$$F_{y3}^{(A)} = \frac{C_y}{\epsilon^2} \frac{3(2-\nu)}{1+\nu} \sin \theta \cos \theta \sin \phi \quad (4.29h)$$

$$F_{z3}^{(A)} = \frac{C_z}{\epsilon^2} \left\{ \frac{\nu(-5+4\nu)}{1+\nu} + \frac{3(2-\nu)}{1+\nu} \cos^2 \theta \right\} \quad (4.29i)$$

$G_{mi}^{(A)}$ are given as follows:

$$G_{x1}^{(A)} = \frac{C_x}{\epsilon} \{(3-4\nu) + \sin^2 \theta \cos^2 \phi\} \quad (4.30a)$$

$$G_{y1}^{(A)} = \frac{C_y}{\epsilon} \sin^2 \theta \sin \phi \cos \phi \quad (4.30b)$$

$$G_{z1}^{(A)} = \frac{C_z}{\epsilon} \sin \theta \cos \theta \cos \phi \quad (4.30c)$$

$$G_{x2}^{(A)} = \frac{C_x}{\epsilon} \sin^2 \theta \sin \phi \cos \phi \quad (4.30d)$$

$$G_{y2}^{(A)} = \frac{C_y}{\epsilon} \{(3-4\nu) + \sin^2 \theta \sin^2 \phi\} \quad (4.30e)$$

$$G_{z2}^{(A)} = \frac{C_z}{\epsilon} \sin \theta \cos \theta \sin \phi \quad (4.30f)$$

$$G_{x3}^{(A)} = \frac{C_x}{\epsilon} \sin \theta \cos \theta \cos \phi \quad (4.30g)$$

$$G_{y3}^{(A)} = \frac{C_y}{\epsilon} \sin \theta \cos \theta \sin \phi \quad (4.30h)$$

$$G_{z3}^{(A)} = \frac{C_z}{\epsilon} \{(3-4\nu) + \cos^2\theta\} \quad (4.30i)$$

ρ_ϵ in eq. (4.20) is expressed in polar coordinates (R_1, θ, ϕ) in Fig. 6 as follows:

$$\rho_\epsilon = \sqrt{\epsilon^2 \sin^2\theta - 2r_0\epsilon \sin\theta \cos(\phi - \phi_0) + r_0^2 + (\epsilon \cos\theta + \xi_3 - z)^2} \quad (4.31)$$

As for the integration in eq. (4.20), we apply the same treatment as in section 3.3. We first integrate with respect to ϕ . The Lipschitz-Hankel integrals thus obtained are expanded in a Taylor series in ϵ and then integrated by terms with respect to θ . By taking the limit as ϵ approaches zero, we obtain the final results. Since integrals in the double layer terms $G_{ml}^{(A)}$'s are $O(\epsilon)$, they all vanish in the limit $\epsilon \rightarrow 0$. Moreover, only such single layer terms as $l=m$ have non-zero values. Those with $l \neq m$ disappear because they are also $O(\epsilon)$. Thus we have

$$v_1^{z(K)} = C_z \left\{ 2\pi \frac{\nu(-5+4\nu)}{1+\nu} I_1[\theta_1, \theta_2] + \pi \frac{3(2-\nu)}{1+\nu} I_2[\theta_1, \theta_2] \right\} \quad (4.32a)$$

$$v_2^{y(K)} = C_y \left\{ 2\pi \frac{\nu(-5+4\nu)}{1+\nu} I_1[\theta_1, \theta_2] + \pi \frac{3(2-\nu)}{1+\nu} I_2[\theta_1, \theta_2] \right\} \quad (4.32b)$$

$$v_3^{z(K)} = C_z \left\{ 2\pi \frac{\nu(-5+4\nu)}{1+\nu} I_1[\theta_1, \theta_2] + 2\pi \frac{3(2-\nu)}{1+\nu} I_3[\theta_1, \theta_2] \right\} \quad (4.32c)$$

$$v_l^{m(K)} = 0 \quad (l \neq m) \quad (4.32d)$$

where

$$I_1[\theta_1, \theta_2] = \int_{\theta_1}^{\theta_2} \sin\theta d\theta = \left[-\cos\theta \right]_{\theta_1}^{\theta_2} \quad (4.33a)$$

$$I_2[\theta_1, \theta_2] = \int_{\theta_1}^{\theta_2} \sin^3\theta d\theta = \left[-\cos\theta + \frac{\cos^3\theta}{3} \right]_{\theta_1}^{\theta_2} \quad (4.33b)$$

$$I_3[\theta_1, \theta_2] = \int_{\theta_1}^{\theta_2} \cos^2\theta \sin\theta d\theta = \left[-\frac{\cos^3\theta}{3} \right]_{\theta_1}^{\theta_2} \quad (4.33c)$$

Eq. (4.32d) indicates that all the fundamental piezomagnetic potentials with $l \neq m$ have no contribution from the spherical surface (K) . This implies that the Type II solution coincides with the Type I in those cases. Moreover, in the case of $l=m$ in which a non-zero contribution from (K) emerges, the source term $v_l^{m(K)}$ is completely canceled out by a term equal but of opposite sign, arising from the free surface $v_l^{m(0)}$. However, this situation is valid only for the Stacey-Nagata piezomagnetic solid. A preliminary survey tells us that the source term survives for

the general isotropic piezomagnetic solid with 2 parameters. Anyway, no correction is required for SASAI's (1986a) results for the fundamental piezomagnetic potentials, as far as the Stacey-Nagata solid is concerned.

Finally, following the procedure from eq. (4.22) to eq. (4.24), we obtain fundamental piezomagnetic potential for $\xi_3 > 0$ as follows, in complete agreement with SASAI's (1986a) results.

($l=1$)

$$\begin{aligned} \frac{8}{\beta J_z} U_1^z = & 6 \left[\frac{1}{\rho} \right]_3^1 - \frac{(3-4\nu)(1+\nu)}{1-\nu} \left[\frac{1}{\rho+c} - \frac{x^2}{\rho(\rho+c)^2} \right]_3^1 \\ & + \left\{ 3 \frac{3-4\nu}{1-\nu} H + \frac{1-2\nu}{1-\nu} \xi_3 \right\} \left\{ \frac{1}{\rho_3(\rho_3+c_3)} - \frac{x^2(2\rho_3+c_3)}{\rho_3^3(\rho_3+c_3)^2} \right\} \\ & - \frac{6}{1-\nu} H \xi_3 \left(\frac{1}{\rho_3^3} - \frac{3x^2}{\rho_3^5} \right) \\ & + \left\{ \frac{1-2\nu}{1-\nu} (H-\xi_3) \left\{ \frac{1}{\rho_1(\rho_1+c_1)} - \frac{x^2(2\rho_1+c_1)}{\rho_1^3(\rho_1+c_1)^2} \right\} \right. \quad (H < \xi_3) \\ & \left. + 6 \left[\frac{1}{\rho} \right]_2^1 - \frac{1+\nu}{1-\nu} \left[\frac{1}{\rho+c} - \frac{x^2}{\rho(\rho+c)^2} \right]_2^1 \right. \\ & \left. + \frac{3}{1-\nu} (H-\xi_3) \left\{ \frac{1}{\rho_2(\rho_2+c_2)} - \frac{x^2(2\rho_2+c_2)}{\rho_2^3(\rho_2+c_2)^2} \right\} \right. \quad (H > \xi_3) \end{aligned} \quad (4.34a)$$

$$\begin{aligned} \frac{8}{\beta J_y} U_1^y = & \frac{(3-4\nu)(1+\nu)}{1-\nu} \left[\frac{xy}{\rho(\rho+c)^2} \right]_3^1 + \frac{18}{1-\nu} H \xi_3 \frac{xy}{\rho_3^5} \\ & - \left\{ 3 \frac{3-4\nu}{1-\nu} H + \frac{1-2\nu}{1-\nu} \xi_3 \right\} \frac{xy(2\rho_3+c_3)}{\rho_3^3(\rho_3+c_3)^2} \\ & + \left\{ \begin{aligned} & - \frac{1-2\nu}{1-\nu} (H-\xi_3) \frac{xy(2\rho_1+c_1)}{\rho_1^3(\rho_1+c_1)^2} \quad (H > \xi_3) \\ & + \frac{1+\nu}{1-\nu} \left[\frac{xy}{\rho(\rho+c)^2} \right]_2^1 - \frac{3}{1-\nu} (H-\xi_3) \frac{xy(2\rho_2+c_2)}{\rho_2^3(\rho_2+c_2)^2} \quad (H > \xi_3) \end{aligned} \right. \end{aligned} \quad (4.34b)$$

$$\begin{aligned} \frac{3}{\beta J_z} U_1^z = & - \frac{\nu(5-4\nu)}{1-\nu} \left[\frac{x}{\rho(\rho+c)} \right]_3^1 + \left\{ - \frac{3(3-4\nu)}{1-\nu} H + \frac{1-2\nu}{1-\nu} \xi_3 \right\} \frac{x}{\rho_3^3} \\ & + \frac{18}{1-\nu} H \xi_3 \frac{x}{\rho_3^5} \\ & + \left\{ \begin{aligned} & \frac{1-2\nu}{1-\nu} (H-\xi_3) \frac{x}{\rho_1^3} \quad (H < \xi_3) \\ & - \frac{4-5\nu}{1-\nu} \left[\frac{x}{\rho(\rho+c)} \right]_2^1 - \frac{3}{1-\nu} (H-\xi_3) \frac{x}{\rho_2^3} \quad (H > \xi_3) \end{aligned} \right. \end{aligned} \quad (4.34c)$$

($l=2$)

$$\frac{8}{\beta J_x} U_2^x = \left\{ \frac{8}{\beta J_y} U_1^y \right\} (x \leftrightarrow y) \quad (4.35a)$$

$$\frac{8}{\beta J_y} U_2^y = \left\{ \frac{8}{\beta J_x} U_1^x \right\} (x \leftrightarrow y) \quad (4.35b)$$

$$\frac{8}{\beta J_z} U_2^z = \left\{ \frac{8}{\beta J_z} U_1^z \right\} (x \leftrightarrow y) \quad (4.35c)$$

($l=3$)

$$\begin{aligned} \frac{8}{\beta J_x} U_3^x = & \frac{(5-4\nu)\nu}{1-\nu} \left[\frac{x}{\rho(\rho+c)} \right]_3^1 + \left\{ -\frac{3(3-4\nu)}{1-\nu} H + \frac{1-2\nu}{1-\nu} \xi_3 \right\} \frac{x}{\rho_3^3} \\ & - \frac{18}{1-\nu} H \xi_3 c_3 \frac{x}{\rho_3^5} \\ & + \begin{cases} \frac{1-2\nu}{1-\nu} (H-\xi_3) \frac{x}{\rho_1^3} & (H < \xi_3) \\ \frac{4-5\nu}{1-\nu} \left[\frac{x}{\rho(\rho+c)} \right]_2^1 - \frac{3}{1-\nu} (H-\xi_3) \frac{x}{\rho_2^3} & (H > \xi_3) \end{cases} \end{aligned} \quad (4.36a)$$

$$\frac{8}{\beta J_y} U_3^y = \left\{ \frac{8}{\beta J_x} U_3^x \right\} (x \leftrightarrow y) \quad (4.36b)$$

$$\begin{aligned} \frac{8}{\beta J_z} U_3^z = & \frac{3-5\nu+4\nu^2}{1-\nu} \left[\frac{1}{\rho} \right]_3^1 - \left\{ \frac{3(3-4\nu)}{1-\nu} H + \frac{1-2\nu}{1-\nu} \xi_3 \right\} \frac{c_3}{\rho_3^3} \\ & + \frac{6}{1-\nu} H \xi_3 \left\{ \frac{1}{\rho_3^3} - 3 \frac{c_3^2}{\rho_3^5} \right\} \\ & + \begin{cases} -\frac{1-2\nu}{1-\nu} (H-\xi_3) \frac{c_1}{\rho_1^3} & (H < \xi_3) \\ \frac{5-7\nu}{1-\nu} \left[\frac{1}{\rho} \right]_2^1 - \frac{3}{1-\nu} (H-\xi_3) \frac{c_2}{\rho_2^3} & (H > \xi_3) \end{cases} \end{aligned} \quad (4.36c)$$

where

$$[f(\rho, c)]_k^j = f(\rho_j, c_j) - f(\rho_k, c_k) \quad (4.37a)$$

and

$$\rho_1 = \sqrt{x^2 + y^2 + c_1^2}, \quad c_1 = \xi_3 - z \quad (4.37b)$$

$$\rho_2 = \sqrt{x^2 + y^2 + c_2^2}, \quad c_2 = 2H - \xi_3 - z \quad (4.37c)$$

$$\rho_3 = \sqrt{x^2 + y^2 + c_3^2}, \quad c_3 = 2H + \xi_3 - z \quad (4.37d)$$

In eqs. (4.35), the notation ($x \leftrightarrow y$) implies interchange of x and y .

In particular, when a single force acts at the earth's surface, we have Green's functions for a surface load problem. We denote these potentials by V_i^m . They are given as follows:

($l=1$)

$$\frac{8}{\beta J_x} V_1^x = 12 \left[\frac{1}{\rho} \right]_H^0 - 4(1+\nu) \left[\frac{1}{\rho+c} - \frac{x^2}{\rho(\rho+c)^2} \right]_H^0 + 12H \left\{ \frac{1}{\rho_H(\rho_H+c_H)} - \frac{x^2(2\rho_H+c_H)}{\rho_H^3(\rho_H+c_H)^2} \right\} \quad (4.38a)$$

$$\frac{8}{\beta J_y} V_1^y = 4(1+\nu) \left[\frac{xy}{\rho(\rho+c)^2} \right]_H^0 - 12H \frac{xy(2\rho_H+c_H)}{\rho_H^3(\rho_H+c_H)^2} \quad (4.38b)$$

$$\frac{8}{\beta J_z} V_1^z = -4(1+\nu) \left[\frac{x}{\rho(\rho+c)} \right]_H^0 - 12H \frac{x}{\rho_H^3} \quad (4.38c)$$

($l=2$)

$$\frac{8}{\beta J_x} V_2^x = \left\{ \frac{8}{\beta J_y} V_1^y \right\} (x \leftrightarrow y) \quad (4.39a)$$

$$\frac{8}{\beta J_y} V_2^y = \left\{ \frac{8}{\beta J_x} V_1^x \right\} (x \leftrightarrow y) \quad (4.39b)$$

$$\frac{8}{\beta J_z} V_2^z = \left\{ \frac{8}{\beta J_z} V_1^z \right\} (x \leftrightarrow y) \quad (4.39c)$$

($l=3$)

$$\frac{8}{\beta J_x} V_3^x = 4(1+\nu) \left[\frac{x}{\rho(\rho+c)} \right]_H^0 - 12H \frac{x}{\rho_H^3} \quad (4.40a)$$

$$\frac{8}{\beta J_y} V_3^y = \left\{ \frac{8}{\beta J_x} V_3^x \right\} (x \leftrightarrow y) \quad (4.40b)$$

$$\frac{8}{\beta J_z} V_3^z = -4(2-\nu) \left[\frac{1}{\rho} \right]_H^0 - 12H \frac{c_H}{\rho_H^3} \quad (4.40c)$$

where

$$[f(c)]_H^0 = f(c_0) - f(c_H) \quad (4.41a)$$

$$\rho_j = \sqrt{x^2 + y^2 + c_j^2} \quad (j=0, H) \quad (4.41b)$$

$$c_0 = -z, \quad c_H = 2H - z. \quad (4.41c)$$

4.3 Dam Magnetic Effect

The dam magnetic effect is an interesting subject in tectonomagnetism. The observation of local magnetic changes during the filling of a reservoir is regarded as a large-scale control experiment. Such an effect was observed at Talbingo reservoir in Australia (DAVIS and STACEY, 1972), at Charvak reservoir in the USSR (ABDULLABEKOV *et al.*, 1979), at Miyun reservoir in China (ZHAN, 1989) and so on. A model calculation of the dam magnetic effect was done by DAVIS (1974). He estimated the magnetic change caused by a uniform square-shaped load. The actual man-made lake can be approximated by the sum of squares with normal load proportional to the water-depth.

According to eqs. (4.40), the physical meaning of the piezomagnetic change due to surface load is obvious. In Fig. 17 are shown schematically the equivalent magnetic sources due to the normal load (i.e. Bousinesq problem). The horizontal magnetization J_x produces a line of horizontal dipoles parallel to J_x between the load point ($z=0$) and its mirror image with respect to the Curie depth ($z=2H$). It also produces a quadrupole at the bottom point. The vertical magnetization J_z results in a line of vertical dipoles anti-parallel to J_z and a minor quadrupole term at the bottom. The magnetic field caused by a square load is nearly equal to that of a uniformly magnetized rectangular prism. The quadrupole term at $z=2H$ would have negligible influence on the surface magnetic field. Now we can well understand DAVIS' (1974) results: computed piezomagnetic changes are local magnetic anomaly maps of a prism-shaped magnetic mass.

Fig. 17 also tells us why we always observe decrease in total inten-

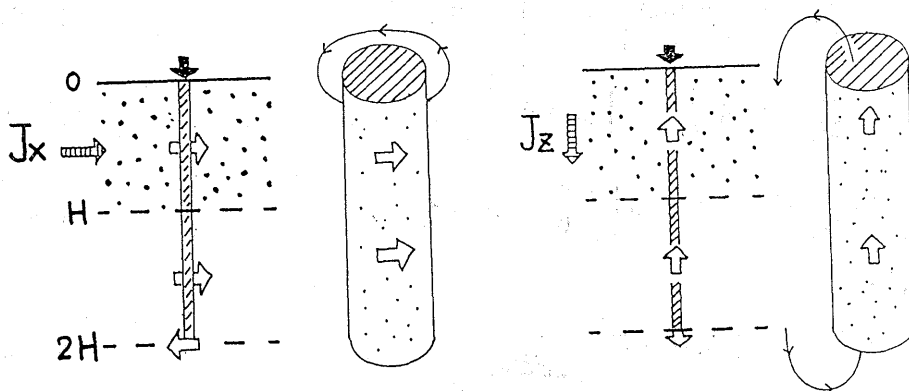


Fig. 17. A schematic representation of the equivalent magnetic sources of the Bousinesq problem. Left: Horizontal magnetization case. Right: Vertical magnetization case.

sity in association with the filling of a man-made lake. One may presume that considerations on the qualitative nature of the piezomagnetic effect would lead us to the same understanding; the normal load produces negative J_z and positive J_x component respectively. It is difficult, however, to imagine the exact features of stress-induced magnetization owing to the complicated stress pattern near the margin of the load.

Let us investigate here local magnetic changes caused by a uniform circular load. The main part of the solution is the field of a uniformly magnetized right circular cylinder. Unlike a prismatic body, the solution is no longer expressible with elementary functions.

We take the x axis in the magnetic north direction. The magnetization is assumed parallel to the ambient field. We replace x with $x - \xi_1$ and y with $y - \xi_2$ in the fundamental potentials V_3^x and V_3^z . We integrate V_3^m over a circle of radius a : $\xi_1^2 + \xi_2^2 = a^2$. With the aid of polar coordinates:

$$x = r \cos \delta, \quad y = r \sin \delta, \quad \xi_1 = \xi \cos \phi, \quad \xi_2 = \xi \sin \phi \quad (4.42)$$

the potentials associated with the uniform load are expressed by

$$\Phi_3^m = W_0 \int_0^a \xi d\xi \int_0^{2\pi} V_3^m(\xi, \phi; r, z) d\phi \quad (m=x, z) \quad (4.43)$$

where W_0 is the load per unit area. To integrate eq. (4.43), we refer to SINGH and SABINA (1978), who obtained an analytic expression for the magnetic field produced by a vertical right circular cylinder.

Eq. (4.43) can be regarded as a convolution of V_3^m with the following function:

$$g(\xi) = W_0 H(a - \xi) \quad (4.44)$$

where $H(a - \xi)$ is the Heaviside step function. Eq. (4.43) is rewritten as

$$\Phi_3^m = \iint_{-\infty}^{\infty} g(\xi_1, \xi_2) V_3^m(x - \xi_1, y - \xi_2) d\xi_1 d\xi_2 \quad (4.45)$$

We denote the Fourier transform of a function by an asterisk. We have already found the Fourier transforms of V_3^m 's during their derivation. Then Φ_3^m is transformed as

$$\Phi_3^{m*} = 2\pi g^* V_3^{m*} = 2\pi a W_0 \frac{J_1(ak)}{k} V_3^{m*} \quad (4.46)$$

The inversion of (4.46) gives rise to

$$\Phi_3^m = 2\pi a W_0 \int_0^{\infty} V_3^{m*} J_1(ak) J_0(kr) dk \quad (4.47)$$

All the terms in V_3^{m*} have a factor e^{-ck} in common, and hence integrals in eq. (4.47) are of the form

$$I[m, n; l; c] = \int_0^\infty J_m(ak) J_n(kr) e^{-ck} k^l dk \quad (4.48)$$

This is the Lipschitz-Hankel type integral, i.e., eq. (3.36), of which parameters are

$$a=a, \quad b=r, \quad c=c_0 \quad \text{or} \quad c_H$$

Finally we have the piezomagnetic potential caused by a uniform circular load:

$$\frac{1}{2\pi W_0 \beta J_z} \Phi_3^x = \frac{x}{r} \left\{ \frac{1+\nu}{2} [I(1, 1; -1; c)]_H^0 - \frac{3}{2} HI(1, 1; 0; c_H) \right\} \quad (4.49a)$$

$$\frac{1}{2\pi W_0 \beta J_z} \Phi_3^z = \frac{2-\nu}{2} [I(1, 0; -1; c)]_H^0 - \frac{3}{2} HI(1, 0; 0; c_H) \quad (4.49b)$$

In deriving Φ_3^x , we use the following relation:

$$\frac{1}{2\pi} \iint_{-\infty}^{\infty} i k_1 f(k_1, k_2) e^{i(k_1 x_1 + k_2 x_2)} dk_1 dk_2 = \int_0^\infty f(k) \frac{\partial J_0(kr)}{\partial x} k dk$$

This is an application of operational rules as described in Appendix B.

The corresponding magnetic field is obtained by differentiation. Differentiation of the Lipschitz-Hankel type integral with respect to its parameters a , b or c is again reduced to the same type of integral of different m , n or l . All the necessary functions are given in Appendix C. Formulas for the magnetic field are obtained from SASAI (1986a).

In Fig. 18 are shown horizontal and vertical component changes produced by horizontal magnetization (ΔX^x and ΔZ^x) and those by vertical magnetization (ΔX^z and ΔZ^z) along the N-S meridian. Putting $\nu=0.25$ and $H=15$ km, we computed field components for $a=1$ km and sensor height $-z=2.5$ m. Unit of the vertical axis is $\beta J W_0$. Numerals along the axis are given in units of nT if we assume $\beta=2.0 \times 10^{-4} \text{ bar}^{-1}$, $J=5.0$ A/m and $W_0=10$ bar (load by 100 m water depth) after DAVIS (1974). The ΔZ^x and ΔX^z components become divergent at $r=a$ for $z=0$. The peak values at $r=a$ are highly dependent on the ratio z/a for small z . At distances several times as much as z from the edge, however, either ΔZ^x or ΔX^z has nearly the same values for different values of z/a . In other words the local edge effect rapidly diminishes as we leave the periphery of the load.

Fig. 19 shows changes in the F component for $W_0=14$ bars with the magnetic dip $I=55^\circ$, which are specified for the Talbingo reservoir case

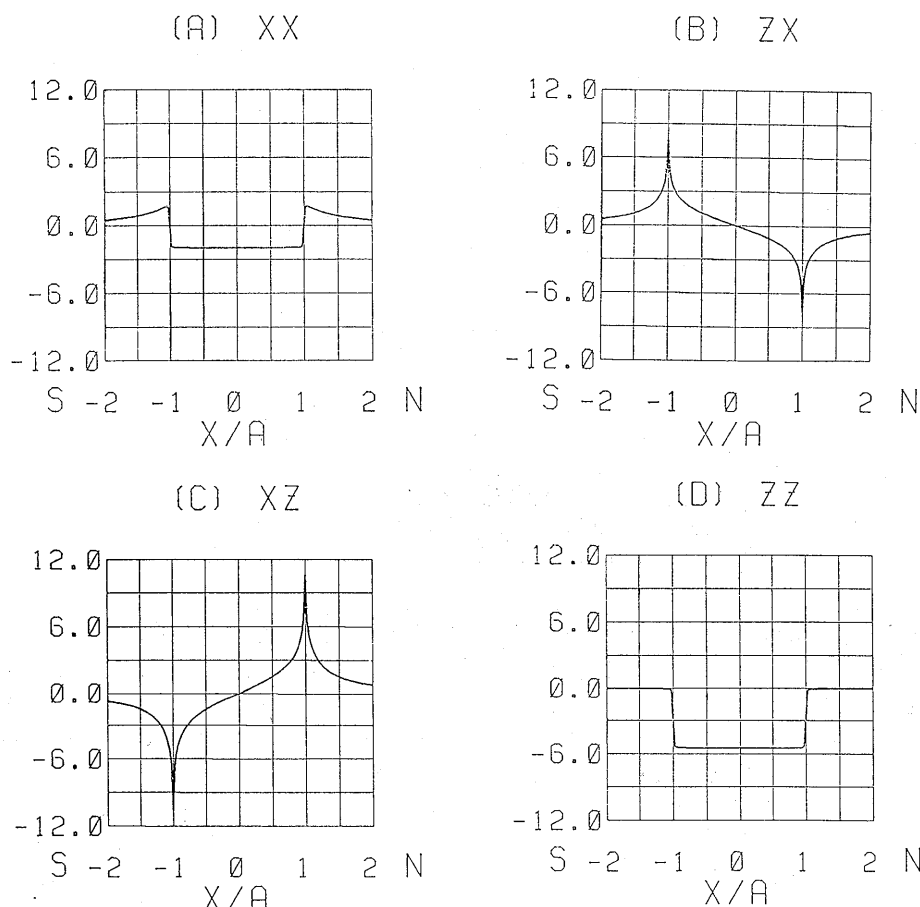


Fig. 18. Magnetic field elements due to a uniform circular load along a line passing through the center from magnetic North to South: (A) ΔX^z , (B) ΔZ^z , (C) ΔX^z and (D) ΔZ^z component.

by DAVIS (1974). These are reasonably expected from the schematic illustration in Fig. 17. Although the shape of the load is different, numerical values are in good agreement with Davis' result for a square-shaped lake. According to these model studies, we are obliged to assume $\beta J \approx 0.1$ nT/bar in order to attain several nT changes against 10 bars load. This parameter is an order of magnitude larger than the ordinary one $\beta J \approx 0.01$ nT/bar (e.g. $\beta = 1.0 \times 10^{-4} \text{ bar}^{-1}$, $J = 1.0$ A/m).

DAVIS and STACEY (1972) detected an average local change in the geomagnetic total intensity of 5.3 nT in the vicinity of Talbingo reservoir, coinciding with the filling of the lake. DAVIS (1974) assumed an intense magnetization of 5 A/m at depth beneath the Talbingo reservoir, based on geological evidence. Recently ZHAN (1989) compiled observations of

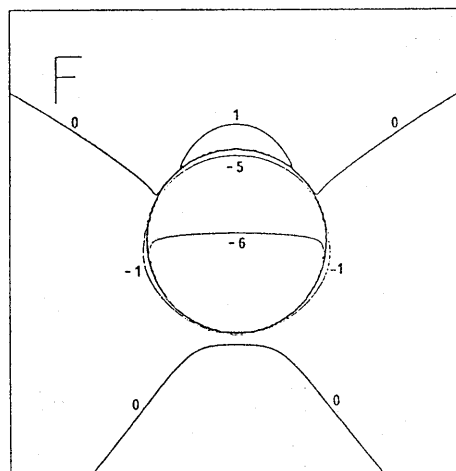


Fig. 19. The total intensity anomaly caused by a uniform circular load. Unit in nT. The thick centered circle indicates the location of the load.

the dam magnetic effect. According to his collected examples, the geomagnetic change rate against water level ranges from 0.025 to 0.28 nT/m. The Talbingo reservoir case gives the smallest value for the change rate. Then a question arises: Are all the reservoirs in the world located on an intense magnetization of 5 A/m or much more?

HAMANO (1983) conducted uniaxial compression experiments on natural remanent magnetization (NRM) of various rocks. He found that some porous rocks show several to more than 10% decrease in the NRM under the pressure of 100 bars. Some samples exhibited irreversible changes, though. Stress sensitivity of susceptibility was also measured for the same rocks by HAMANO *et al.* (1989). The susceptibility changes were in most cases reversible. They found that some mechanically weak rocks such as tuff have stress sensitivity of $1.0 \times 10^{-8} \text{ bar}^{-1}$. HAMANO (1983) concluded that the stress sensitivity increases with porosity due to stress intensification multiplying local stress within the sample. Then we may naturally presume that the same condition holds as a whole in the upper crust: the *in situ* stress sensitivity of the upper crust might be on the order of 10^{-8} bar^{-1} . Further investigation of the dam magnetic effect is needed to verify such a presumption. The formulas (4.38) through (4.40) can be a powerful tool for calculating piezomagnetic changes due to surface load with any shape of the actual reservoir.

Chapter 5. Dislocation Source Problems

In this chapter, we will systematically develop a method of calculating piezomagnetic changes accompanying dislocation models. The mathematical treatment is quite similar to that in the previous chapter. When the dislocation, i.e. the discontinuity in the displacement, exists along a surface in a homogeneous and isotropic semi-infinite medium, its elastic field can be given by the Volterra formula (STEKETEE, 1958a, b; MARUYAMA, 1964). This formula consists of an integral of certain strain nuclei over the dislocation surface: the nuclei are called elementary dislocations. Now we consider the piezomagnetic potentials produced by elementary dislocations. We call them the elementary piezomagnetic potentials. It is shown that the piezomagnetic change associated with any dislocation model can be obtained by integrating elementary piezomagnetic potentials over the dislocation surface with weight of displacement discontinuity. We call this equation Volterra's formula for a piezomagnetic field.

In evaluating elementary piezomagnetic potentials, we follow here a modified version of SASAI's (1980) method. The volumetric integrals in SASAI (1980) are converted into surface integrals by virtue of the representation theorem. However, operational calculus based on the Fourier transform will be extensively used as before. It is convenient to deal with convolution integrals of complicated secondary terms arising from the traction-free boundary conditions. The only difference from SASAI (1980) is that we seek to obtain a type II solution around a point dislocation. The shape of the closed surface surrounding the source point is assumed to be a thin disk. Unlike the single force problems described in Chapter 4, we are required to correct some previous results (SAI, 1980). Although the corrections are simple, they seriously affect overall features of piezomagnetic changes due to dislocation sources.

One important application is the multiple tension-crack model. SASAI (1986b) extended HAGIWARA's (1977b) multiple Mogi model. The multiple tension-crack model is the Gaussian distribution of a number of small tensile cracks in an elastic half-space: formulas for surface displacement, gravity and magnetic change are presented (SAI, 1986b; 1988). In the formulation, we need Fourier transforms of elementary piezomagnetic potentials, which is another reason why we follow the Fourier transform method.

Finally, we consider a vertical rectangular fault. Both strike-slip and tensile faulting are considered. The piezomagnetic field associated with such a fault, or the seismomagnetic effect, can be obtained by integrating elementary piezomagnetic potentials over the fault. Formulas based on type I solutions have already been given by SASAI (1980) and

SASAI (1984); they are corrected here according to a new version of the elementary piezomagnetic potentials.

5.1 Volterra's Formula for the Piezomagnetic Field

The elasticity theory of dislocations was originally introduced into geophysics by STEKETEE (1958a, b). He developed a Green's function method to include the effect of a stress-free plane boundary, and formulated displacement and stress field in a semi-infinite elastic medium. A dislocation surface, across which the displacement discontinuity exists, is equivalent to a distribution of strain nuclei. There are six sets of such strain nuclei to describe any type of dislocation. The analytical expressions for all these Green's functions were obtained by MARUYAMA (1964). PRESS (1965) showed that we can derive the same results by combining MINDLIN and CHENG's (1950) solutions for various strain nuclei in the semi-infinite solid.

We take Cartesian coordinates (x_1, x_2, x_3) as before; the x_3 axis is positive downward. A semi-infinite elastic medium occupies $x_3 > 0$. It is also assumed that the top layer from the plane surface boundary $x_3 = 0$ to the Curie depth $x_3 = H$ is uniformly magnetized, the stress sensitivity β being constant within the layer.

Let us consider a dislocation surface Σ in the semi-infinite elastic medium. A Somigliana dislocation is defined as a discontinuity in displacements across the surface Σ , $\Delta u_k = u_k^+ - u_k^-$, which may have any form as long as the tractions to maintain the dislocation satisfy continuity conditions across Σ : $\tau_{kl}^+ \nu_l - \tau_{kl}^- \nu_l = 0$. A point on the dislocation surface is designated by $\xi(\xi_1, \xi_2, \xi_3)$. The displacement field produced by the dislocation $\Delta u_k(\xi)$ at an arbitrary point $x(x_1, x_2, x_3)$ in the elastic medium can be given by the following Volterra's formula:

$$u_n(x) = \iint_{\Sigma} \Delta u_k(\xi) T_{kl}^n(\xi, x) \nu_l(\xi) d\Sigma(\xi) \quad (5.1)$$

$$k, l = 1, 2, 3. \quad n = x, y, z.$$

where $\nu_l(\xi)$ denotes the l -th component of a unit vector outward normal to the surface element $d\Sigma$. Einstein's summation convention applies with respect to k and l . The third rank tensor T_{kl}^n indicates the n -th component of displacement at x produced by a certain strain nucleus at ξ , which is called an elementary dislocation. Suffixes k and l specify the type and orientation of the elementary dislocation. Strain nuclei with $k=l$ represent relative movement normal to the dislocation surface Σ , while those with $k \neq l$ describe parallel ones along Σ . STEKETEE (1958b) called the former A nuclei and the latter B nuclei. They can be ex-

pressed by combinations of double forces as shown schematically in Fig. 20.

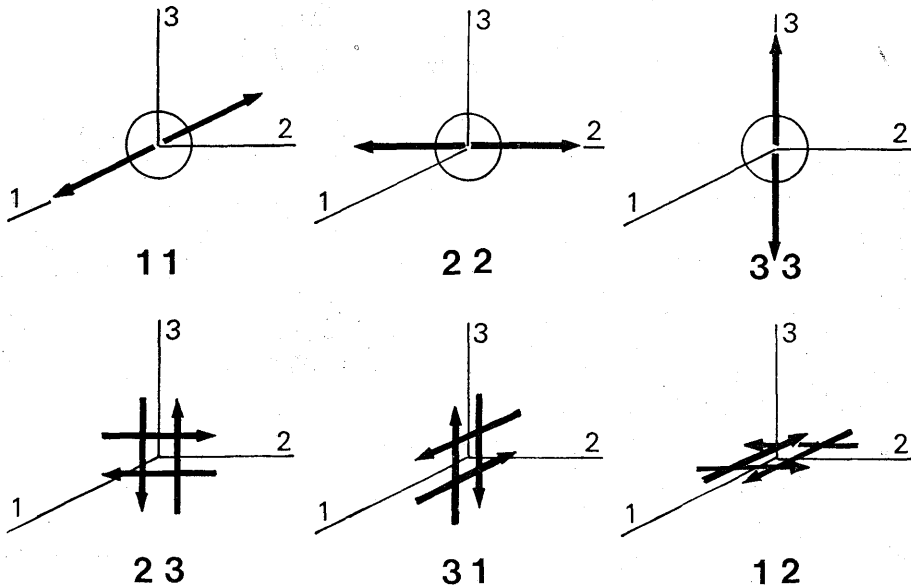


Fig. 20. A schematic representation of elementary dislocations (after MARUYAMA, 1964). The A nuclei, (11), (22) and (33), correspond to the crack-forming movement, represented by the center of dilatation (circle) and the double force without moment (arrows). The B nuclei, (23), (31) and (12), can describe the shearing offset of the dislocation surface, represented by two co-planar, mutually perpendicular double forces with moment.

We are now to obtain the piezomagnetic potential due to the displacement field given by eq. (5.1). Substituting eq. (5.1) into eq. (2.53) we obtain the stress-induced magnetization:

$$\Delta M_n^{(m)}(x) = C_m \iint_{\Sigma} \Delta u_k(\xi) S_{kl}^{mn}(\xi, x) \nu_l(\xi) d\Sigma \quad (5.2)$$

where

$$S_{kl}^{mn} = \frac{3}{2} \left(\frac{\partial T_{kl}^m}{\partial x_n} + \frac{\partial T_{kl}^n}{\partial x_m} \right) - \delta_{mn} \operatorname{div} T_{kl} \quad (5.3)$$

The piezomagnetic potential is given by the dipole law of force:

$$W^m(r) = \iint_V \Delta M^{(m)}(x) \cdot \nabla \left(\frac{1}{\rho} \right) dx \quad (5.4)$$

where $\rho = |x - r|$. Substituting eq. (5.2) into eq. (5.4) and interchanging the order of intergrations with respect to x and ξ , we obtain the following formula.

$$W^m(\mathbf{r}) = \iint_{\Sigma} \Delta u_k(\xi) w_{kl}^m(\xi, \mathbf{r}) \nu_l(\xi) d\Sigma(\xi) \quad (5.5)$$

where

$$w_{kl}^m(\xi, \mathbf{r}) = C_m \iiint_V S_{kl}^{(m)} \cdot \nabla \left(\frac{1}{\rho} \right) dx \quad (5.6)$$

$S_{kl}^{(m)}$ is the stress-induced magnetization vector, the n -th component of which is defined by eq. (5.3). Since eq. (5.5) has the same form as eq. (5.1), we may call it Volterra's formula for the piezomagnetic potential. Eq. (5.5) was first derived by SASAI (1980). w_{kl}^m is the piezomagnetic potential produced by a point dislocation of the type (kl) . We may call it the elementary piezomagnetic potential.

In deriving eq. (5.5) from eq. (5.4), we define the integration area as shown in Fig. 21. It is a magnetized region surrounded by the free surface $x_3=0$, the Curie point isotherm $x_3=H$ and a thin closed surface S' including the dislocation surface Σ in it. Within this volume, the order of integration is allowed to interchange, because all the singular points are excluded. The formula (5.5) is obtained in the limit as the closed surface S' approaches the dislocation surface Σ . Hence we should choose an appropriate shape of the closed surface in evaluating the type II solution for the elementary piezomagnetic potential. In other words, the orientation of the dislocation surface should be properly taken into account.

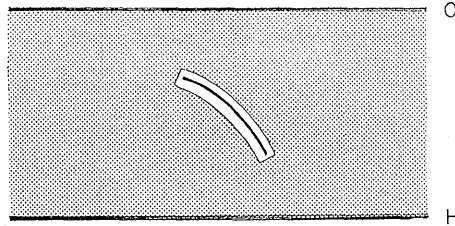


Fig. 21. The integration area for the piezomagnetic calculation of dislocation problems.

5.2 Elementary Piezomagnetic Potentials

Let us consider the piezomagnetic potential produced by a point dislocation. The situation is very similar to the case when we obtained the fundamental piezomagnetic potentials in the previous chapter. However, we must be careful about the shape of the "point" dislocation source in evaluating the type II solution. Recently, this problem was discussed by OKUBO (1991), who formulated gravity change due to dislo-

cation sources. He pointed out that the infinitesimal volume surrounding a point dislocation should have surfaces parallel to the (infinitesimal) dislocation surface. According to his arguments, we should adopt a small circular disk rather than a sphere.

This is because even the "point" dislocation is also defined as the displacement discontinuity across an infinitesimal plane surface. We specify the orientation of the disk parallel to the dislocation plane. We first pass a limit by decreasing the thickness of the disk $2\epsilon_z$ indefinitely and then letting the radius ϵ_r approach zero. Surface potential arising from the cylindrical side of the disk should vanish when ϵ_z diminishes. This is actually true, as will be proved later in this section. The contributions from the circular surfaces of the disk remain finite as the radius decreases. Thus we can construct the closed surface S' enveloping Σ with such disks distributed along Σ .

SASAI (1980) obtained type I solutions for elementary piezomagnetic potentials. To convert those to type II ones, we should add the contribution from the K' region for the case of the Mogi model as depicted in Fig. 16. The K' region is defined as an infinite horizontal plate of thickness 2ϵ from which a disk-shaped area including the small dislocation surface is excavated. The disk lies horizontally for elementary dislocations of type $(kl)=33, 13$ and 23 , vertically for those of type $(kl)=11, 22, 21, 12, 31$ and 32 , depending on the orientation of the infinitesimal dislocation surface (see Fig. 20 and Fig. 22).

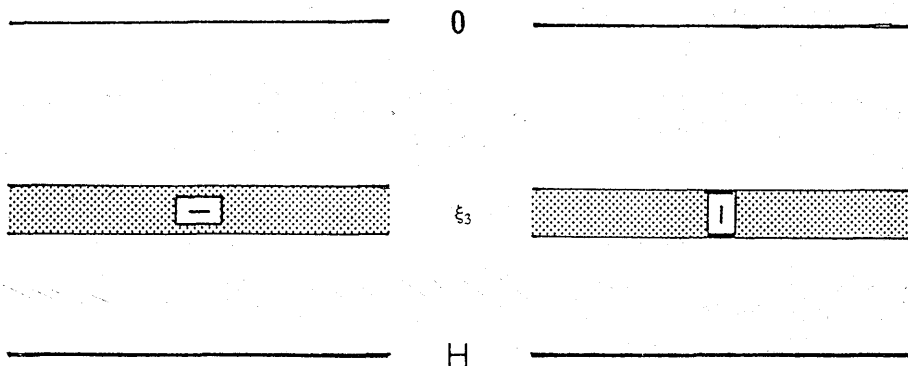


Fig. 22. The K' region (hatched) defined for strain nuclei $(kl)=33, 13, 23$ (left) and $(kl)=11, 22, 12$ (right) respectively. The small rectangle indicates the cross section of a disk including the point dislocation.

We assume that the elementary dislocation is located at $(0, 0, \xi_3)$. Replacing x and y with $(x-\xi_1)$ and $(y-\xi_2)$ in the final expressions, we can arrive at corresponding results for any arbitrary point $\xi(\xi_1, \xi_2, \xi_3)$.

Now we apply the representation theorem (2.52) to obtain the type II solutions of the elementary piezomagnetic potentials. Each potential for the particular type of strain nucleus (kl) consists of three parts: i.e.

$$w_{kl}^m = w_{kl}^{m(0)} + w_{kl}^{m(H)} + w_{kl}^{m(K)} \quad (5.7)$$

$w_{kl}^{m(0)}$ and $w_{kl}^{m(H)}$ are contributions from the free surface (0) and the Curie surface (H) respectively. $w_{kl}^{m(K)}$ arises from the surfaces of the disk, where the outward normal is defined toward the inside. This term vanishes if the point dislocation lies beneath the Curie depth ($\xi_3 < H$).

First we seek to obtain $w_{kl}^{m(H)}$'s. Taking a horizontal plane $x_3 = H$ as the surface S and putting the direction of outward normal $\mathbf{n} = \mathbf{e}_{x_3}$, we can represent the surface potential as follows:

$$w_{kl}^{m(H)} = C_m \iint_{-\infty}^{\infty} \left[S_{kl}^{mz} \frac{1}{\rho_H} + D_{kl}^{(m)} \frac{H-z}{\rho_H^3} \right]_{(x_3=H)} dx_1 dx_2 \quad (5.8)$$

where

$$S_{kl}^{mn} = -\frac{\partial T_{kl}^m}{\partial x_n} + \frac{2\alpha}{4\alpha-1} \left\{ \frac{3}{2} \left(\frac{\partial T_{kl}^m}{\partial x_n} + \frac{\partial T_{kl}^n}{\partial x_m} \right) - \delta_{mn} \nabla \cdot \mathbf{T}_{kl} \right\} \quad (5.9a)$$

$$D_{kl}^{(m)} = T_{kl}^m \quad (5.9b)$$

and $\rho_H = \sqrt{(x-x_1)^2 + (y-x_2)^2 + (z-H)^2}$. S_{kl}^{mn} is the n -th component of the vector $S_{kl}^{(m)}$, while T_{kl}^m the m -th component of the displacement due to a strain nucleus of the type (kl). According to MARUYAMA (1964), the displacement field \mathbf{T}_{kl} is derived from a Galerkin vector \mathbf{F}_{kl} as

$$\mathbf{T}_{kl} = (\nabla^2 - \alpha \operatorname{grad} \operatorname{div}) \mathbf{F}_{kl} \quad (5.10a)$$

where

$$\mathbf{F}_{kl} = (F_{kl}^1, F_{kl}^2, F_{kl}^3) + (0, 0, F_{kl}) \quad (5.10b)$$

and $\alpha = (\lambda + \mu)/(\lambda + 2\mu)$. The first term on the right hand side of eq. (5.10b) represents the effect of strain nuclei at $(0, 0, \xi_3)$ and at its mirror image $(0, 0, -\xi_3)$, while the second term, the Boussinesq solution, cancels the resultant normal force due to the first term.

By taking Fourier transforms of both sides of eq. (5.8), we have

$$w_{kl}^{m(H)*} = 2\pi C_m \left\{ S_{kl}^{mz*} \frac{e^{-k\zeta}}{k} - D_{kl}^{(m)*} e^{-k\zeta} \right\} \quad (5.11)$$

where $\zeta = H - z$. All the Fourier transforms S_{kl}^{mz*} 's and $D_{kl}^{(m)*}$'s are calculated systematically by the method developed in Appendix B. Such calculations are briefly described in Appendix D1. The inverse Fourier transformation of eq. (5.11) leads us to $w_{kl}^{m(H)}$'s, which are expressed with

elementary functions.

Obviously, $w_{kl}^{m(0)}$ is defined by

$$w_{kl}^{m(0)} = -w_{kl}^{m(H=0)} \quad (5.12)$$

$w_{kl}^{m(0)}$'s thus obtained are listed in Appendix D2.

Finally we will obtain $w_{kl}^{(K)}$. The displacement field due to a point dislocation can be divided into two constituents: i.e. $u^{(A)}$ arising from the source point and $u^{(B)}$ from the traction-free boundary conditions. Since $u^{(B)}$ is regular at $(0, 0, \xi_3)$, the contribution from this component vanishes through limiting operations as the K region becomes smaller. Thus we have only to take into account $u^{(A)}$. The displacement components due to a point dislocation of the type (kl) in an *infinite* medium, or $u^{(A)}$, are given as follows (MARUYAMA, 1964):

$$T_{kl}^m = \frac{1}{4\pi} \left\{ (1-\alpha) \left(\delta_{kl} \frac{r_m}{R_1^3} + \delta_{mk} \frac{r_l}{R_1^3} + \delta_{lm} \frac{r_k}{R_1^3} \right) + 3\alpha \frac{r_k r_l r_m}{R_1^5} \right\} \quad (5.13)$$

where

$$R_1 = \sqrt{x_1^2 + x_2^2 + (x_3 - \xi_3)^2} \quad (5.14a)$$

$$r_k = x_k - \xi_k \quad (5.14b)$$

and $\xi_1 = \xi_2 = 0$, $\xi_3 \neq 0$ in this case. We find that all the strain nuclei in infinite medium are axially symmetric with respect to their normal axes to the dislocation surface. By symmetry considerations, we can easily obtain $w_{11}^{m(K)}$'s and $w_{22}^{m(K)}$'s, once we know $w_{33}^{m(K)}$'s. Similarly, $w_{12}^{m(K)}$'s and $w_{23}^{m(K)}$'s are obtained if $w_{31}^{m(K)}$'s are known.

We consider a disk of radius ϵ_r and thickness $2\epsilon_z$ as shown in Fig. 23. The circular surfaces of the disk are parallel to an infinitesimal dislocation surface, which is included within the disk. We calculate potentials arising from surfaces of the disk for strain nuclei of the type $(kl) = (33)$, and $(kl) = (13)$. The latter is equivalent to that of $(kl) = (31)$. We take the cylindrical coordinates (r, θ, z) whose origin is at the source point $(0, 0, \xi_3)$ and whose polar axis is the x_3 axis, positive downward. The moving point $P(x_1, x_2, x_3)$ on the disk and the observation point $Q(x_0, y_0, z_0)$ are expressed by the new coordinates as

$$x_1 = r \cos \theta, \quad x_2 = r \sin \theta, \quad x_3 = z$$

$$x_0 = r_0 \cos \theta_0, \quad y_0 = r_0 \sin \theta_0, \quad z_0 = z_0$$

We specify the bottom surface of the disk with $B+$, the top surface with $B-$ and the cylindrical side with C respectively. See Fig. 23. $w_{33}^{m(K)}$ consists of three parts:

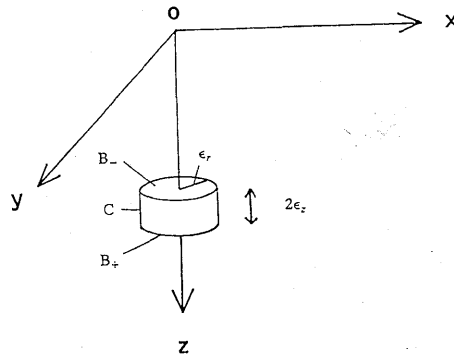


Fig. 23. A closeup of the disk enveloping the point dislocation of the type $(kl)=33, 13, 23$. A small dislocation surface lies horizontally at the center $(0, 0, \xi_3)$ within the disk.

$$w_{33}^{m(K)} = w_{33}^{m(B+)} + w_{33}^{m(B-)} + w_{33}^{m(C)} \quad (5.15)$$

Let us calculate $w_{33}^{x(K)}$ as an example. Potentials from three surfaces B_+ , B_- and C are given by

$$\frac{4\pi}{C_x} w_{33}^{x(B+)} = \int_0^{\epsilon_r} r dr \left[S^+(r) \int_0^{2\pi} \frac{\cos \theta}{\rho_+} d\theta + \zeta^+ D^+(r) \int_0^{2\pi} \frac{\cos \theta}{\rho_+^3} d\theta \right] \quad (5.16a)$$

$$\frac{4\pi}{C_x} w_{33}^{x(B-)} = \int_0^{\epsilon_r} r dr \left[S^-(r) \int_0^{2\pi} \frac{\cos \theta}{\rho_-} d\theta + \zeta^- D^-(r) \int_0^{2\pi} \frac{\cos \theta}{\rho_-^3} d\theta \right] \quad (5.16b)$$

$$\begin{aligned} \frac{4\pi}{C_x} w_{33}^{x(C)} = & \int_{-\epsilon_z}^{\epsilon_z} dz \epsilon_r \left[S^C(z) \int_0^{2\pi} \frac{\cos \theta}{\rho_C} d\theta \right. \\ & \left. + D^C(z) \left\{ \epsilon_r \int_0^{2\pi} \frac{\cos \theta}{\rho_C^3} d\theta - r_0 \int_0^{2\pi} \frac{\cos \theta \cos(\theta - \theta_0)}{\rho_C^3} d\theta \right\} \right] \quad (5.16c) \end{aligned}$$

where

$$S^+(r) = -3 \frac{(1-\alpha)(1-2\alpha)}{4\alpha-1} \frac{\epsilon_z r}{(r^2 + \epsilon_z^2)^{5/2}} + 15\alpha \frac{1+2\alpha}{4\alpha-1} \frac{\epsilon_z^3 r}{(r^2 + \epsilon_z^2)^{7/2}} \quad (5.17a)$$

$$D^+(r) = -(1-\alpha) \frac{r}{(r^2 + \epsilon_z^2)^{3/2}} + 3\alpha \frac{\epsilon_z^2 r}{(r^2 + \epsilon_z^2)^{5/2}} \quad (5.17b)$$

$$S^-(r) = S^+(r) \quad (5.17c)$$

$$D^-(r) = -D^+(r) \quad (5.17d)$$

$$S^C(z) = \frac{(1+6\alpha)(1-\alpha)}{4\alpha-1} \frac{1}{(z^2 + \epsilon_r^2)^{3/2}} - 3 \frac{(1-\alpha)(1+2\alpha)}{4\alpha-1} \frac{\epsilon_r^2}{(z^2 + \epsilon_r^2)^{5/2}}$$

$$+ \frac{3\alpha(2\alpha-5)}{4\alpha-1} \frac{z^2}{(z^2+\varepsilon_r^2)^{5/2}} + \frac{15\alpha(1+2\alpha)}{4\alpha-1} \frac{\varepsilon_r^2 z^2}{(z^2+\varepsilon_r^2)^{7/2}} \quad (5.17e)$$

$$D^C(z) = -(1-\alpha) \frac{\varepsilon_r}{(z^2+\varepsilon_r^2)^{3/2}} + 3\alpha \frac{\varepsilon_r z^2}{(z^2+\varepsilon_r^2)^{5/2}} \quad (5.17f)$$

and

$$\rho_+ = \sqrt{r^2 - 2rr_0 \cos(\theta - \theta_0) + r_0^2 + (\zeta^+)^2}, \quad \zeta^+ = \xi_3 - z_0 + \varepsilon_z \quad (5.18a)$$

$$\rho_- = \sqrt{r^2 - 2rr_0 \cos(\theta - \theta_0) + r_0^2 + (\zeta^-)^2}, \quad \zeta^- = \xi_3 - z_0 - \varepsilon_z \quad (5.18b)$$

$$\rho_C = \sqrt{\varepsilon_r^2 - 2\varepsilon_r r_0 \cos(\theta - \theta_0) + r_0^2 + (\xi_3 - z_0 + z)^2} \quad (5.18c)$$

Integrals with respect to θ can be reduced to the Lipschitz-Hankel type ones. Referring to Appendix C, we have the following series expansions for small values of r and/or z .

$$\int_0^{2\pi} \frac{\cos \theta}{\rho_{\pm}} d\theta = 2 \cos \theta_0 \Phi_2 = \pi \cos \theta_0 \frac{rr_0}{\rho_1^3} \{1 + O(r)\} \quad (5.19a)$$

$$\int_0^{2\pi} \frac{\cos \theta}{\rho_{\pm}^3} d\theta = 2 \cos \theta_0 \Phi_4 = 3\pi \cos \theta_0 \frac{rr_0}{\rho_1^5} \{1 + O(r)\} \quad (5.19b)$$

$$\int_0^{2\pi} \frac{\cos \theta}{\rho_C} d\theta = 2 \cos \theta_0 \Phi_2 = \pi \cos \theta_0 \frac{\varepsilon_r r_0}{\rho_1^3} \left\{ 1 - 3 \frac{c_1 z}{\rho_1^2} + \dots \right\} \quad (5.19c)$$

$$\int_0^{2\pi} \frac{\cos \theta}{\rho_C^3} d\theta = 2 \cos \theta_0 \Phi_4 = 3\pi \cos \theta_0 \frac{\varepsilon_r r_0}{\rho_1^5} \left\{ 1 - 5 \frac{c_1 z}{\rho_1^2} + \dots \right\} \quad (5.19d)$$

$$\int_0^{2\pi} \frac{\cos \theta \cos(\theta - \theta_0)}{\rho_C^3} d\theta = \cos \theta_0 (\Phi_3 + \Phi_5) = \frac{\pi \cos \theta_0}{\rho_1^3} \left\{ 1 - 3 \frac{c_1 z}{\rho_1^2} + \dots \right\} \quad (5.19e)$$

where

$$\rho_1 = \sqrt{r_0^2 + c_1^2}, \quad c_1 = \xi_3 - z_0 \quad (5.19f)$$

Since the infinite series in eqs. (5.19) are uniformly convergent, we may substitute them into eqs. (5.16) and integrate by terms with respect to r or z . However, we may neglect the effect of higher order terms of r and z , because they ultimately vanish as we approach a limit by decreasing ε_z and ε_r .

Thus we obtain the following:

$$\begin{aligned} \frac{4\pi}{C_x} \omega_{33}^{x(B+)} = \pi \left[\left\{ -3 \frac{(1-\alpha)(1-2\alpha)}{4\alpha-1} \varepsilon_z K_2 + \frac{15\alpha(1+2\alpha)}{4\alpha-1} \varepsilon_z^3 K_3 \right\} \frac{x_0}{\rho_1^3} \right. \\ \left. + 3 \left\{ -(1-\alpha) K_1 + 3\alpha \varepsilon_z^2 K_2 \right\} \frac{x_0}{\rho_1^5} \right] \quad (5.20a) \end{aligned}$$

$$\frac{4\pi}{C_x} \omega_{33}^{x(B-)} = \pi \left[\left\{ -3 \frac{(1-\alpha)(1-2\alpha)}{4\alpha-1} \varepsilon_z K_2 + \frac{15\alpha(1+2\alpha)}{4\alpha-1} \varepsilon_z^3 K_3 \right\} \frac{x_0}{\rho_1^3} \right. \\ \left. + 3 \left\{ (1-\alpha) K_1 - 3\alpha \varepsilon_z^2 K_2 \right\} \frac{x_0}{\rho_1^5} \right] \quad (5.20b)$$

$$\frac{4\pi}{C_x} \omega_{33}^{x(C)} = \pi \left[\left\{ \frac{(1-\alpha)(1+6\alpha)}{4\alpha-1} \varepsilon_r^2 K_4 - 3 \frac{(1-\alpha)(1+2\alpha)}{4\alpha-1} \varepsilon_r^4 K_5 \right. \right. \\ \left. \left. + \frac{3\alpha(2\alpha-5)}{4\alpha-1} \varepsilon_r^2 K_6 + \frac{15\alpha(1+2\alpha)}{4\alpha-1} \varepsilon_r^4 K_7 \right\} \frac{x_0}{\rho_1^3} \right. \\ \left. + \left\{ -3(1-\alpha) \varepsilon_r^3 K_4 + 9\alpha \varepsilon_r^3 K_6 \right\} \frac{x_0}{\rho_1^5} + \left\{ (1-\alpha) \varepsilon_r^2 K_4 - 3\alpha \varepsilon_r^2 K_6 \right\} \frac{x_0}{\rho_1^3} \right. \\ \left. + \frac{15}{8} \varepsilon_r^4 \left\{ (1-\alpha) K_4 - 3\alpha K_6 \right\} \frac{r_0 x_0}{\rho_1^7} \right] \quad (5.20c)$$

where

$$K_1 = \int_0^{\varepsilon_r} \frac{r^3 dr}{(r^2 + \varepsilon_z^2)^{3/2}} = \frac{\varepsilon_r^2 + 2\varepsilon_z^2}{\sqrt{\varepsilon_r^2 + \varepsilon_z^2}} - 2\varepsilon_z \quad (5.21a)$$

$$\varepsilon_z K_2 = \varepsilon_z \int_0^{\varepsilon_r} \frac{r^3 dr}{(r^2 + \varepsilon_z^2)^{5/2}} = -\frac{\varepsilon_z(\varepsilon_r^2 + 2/3\varepsilon_z^2)}{(\varepsilon_r^2 + \varepsilon_z^2)^{3/2}} - \frac{2}{3} \quad (5.21b)$$

$$\varepsilon_z^3 K_3 = \varepsilon_z^3 \int_0^{\varepsilon_r} \frac{r^3 dr}{(r^2 + \varepsilon_z^2)^{7/2}} = -\frac{1}{3} \frac{\varepsilon_z^3}{(\varepsilon_r^2 + \varepsilon_z^2)^{3/2}} + \frac{1}{5} \frac{\varepsilon_z^5}{(\varepsilon_r^2 + \varepsilon_z^2)^{5/2}} - \frac{2}{15} \quad (5.21c)$$

$$\varepsilon_r^2 K_4 = \varepsilon_r^2 \int_{-\varepsilon_z}^{\varepsilon_z} \frac{dz}{(z^2 + \varepsilon_r^2)^{3/2}} = \frac{2\varepsilon_z}{\sqrt{\varepsilon_r^2 + \varepsilon_z^2}} - 2\varepsilon_z \quad (5.21d)$$

$$\varepsilon_r^4 K_5 = \varepsilon_r^4 \int_{-\varepsilon_z}^{\varepsilon_z} \frac{dz}{(z^2 + \varepsilon_r^2)^{5/2}} = \frac{2\varepsilon_z}{\sqrt{\varepsilon_r^2 + \varepsilon_z^2}} - \frac{2}{3} \frac{\varepsilon_z^3}{(\varepsilon_r^2 + \varepsilon_z^2)^{3/2}} \quad (5.21e)$$

$$\varepsilon_r^2 K_6 = \varepsilon_r^2 \int_{-\varepsilon_z}^{\varepsilon_z} \frac{z^2 dz}{(z^2 + \varepsilon_r^2)^{5/2}} = \frac{2}{3} \frac{\varepsilon_z^3}{(\varepsilon_r^2 + \varepsilon_z^2)^{3/2}} \quad (5.21f)$$

$$\varepsilon_r^4 K_7 = \varepsilon_r^4 \int_{-\varepsilon_z}^{\varepsilon_z} \frac{z^2 dz}{(z^2 + \varepsilon_r^2)^{7/2}} = \frac{2}{3} \frac{\varepsilon_z^3}{(\varepsilon_r^2 + \varepsilon_z^2)^{3/2}} - \frac{2}{5} \frac{\varepsilon_z^5}{(\varepsilon_r^2 + \varepsilon_z^2)^{5/2}} \quad (5.21g)$$

According to eqs. (5.21), we find that the limit values are different depending on whether ε_r or ε_z is first decreased. This implies that the solutions depend on the shape or aspect ratio of the closed surface surrounding the point dislocation. As we have discussed in the beginning of this section, we first decrease the thickness of the disk to zero ($\varepsilon_z \rightarrow 0$) and then shrink the area of the disk ($\varepsilon_r \rightarrow 0$). We denote such a limiting operation by ($\varepsilon_z \rightarrow 0, \varepsilon_r \rightarrow 0$). Then we obtain the final results as follows:

$$\frac{4\pi}{C_x} w_{33}^{x(K)} = \lim_{(\varepsilon_z \rightarrow 0, \varepsilon_r \rightarrow 0)} \{w_{33}^{x(B+)} + w_{33}^{x(B-)} + w_{33}^{x(C)}\} = 4\pi \frac{x_0}{\rho_1^3} \quad (5.22a)$$

Similarly we have

$$w_{33}^{y(K)} = C_y \frac{y_0}{\rho_1^3} \quad (5.22b)$$

$$w_{33}^{z(K)} = C_z \frac{c_1}{\rho_1^3} \quad (5.22c)$$

Similarly deriving eqs. (5.22) from eqs. (5.16) leads us to $w_{31}^{m(K)}$'s:

$$w_{31}^{x(K)} = C_x \frac{c_1}{\rho_1^3} \quad (5.23a)$$

$$w_{31}^{y(K)} = 0 \quad (5.23b)$$

$$w_{31}^{z(K)} = -C_z \frac{x_0}{\rho_1^3} \quad (5.23c)$$

We notice that $w_{kl}^{m(C)}$'s vanish by first setting ε_z equal to zero (see eqs. (5.21d) through (5.21g)). $w_{33}^{m(K)}$ and $w_{31}^{m(K)}$ are elementary piezomagnetic potentials due to the *A* and *B* nuclei respectively. By symmetry considerations, other $w_{kl}^{m(K)}$'s are easily obtained; they are summarized in Appendix D3.

Finally we can construct type II solutions for elementary piezomagnetic potentials via eq. (5.7). They are given as follows:

($kl=11$)

$$\begin{aligned} \frac{2}{C_x} w_{11}^x = & -\frac{3\alpha}{4\alpha-1} \left[-\frac{x}{\rho^3} \right]_3^1 - (2-\alpha) \left[-\frac{1}{4} \frac{x}{\rho^3} + \frac{1}{4} \frac{x(3y^2-x^2)(3\rho+c)}{\rho^3(\rho+c)^3} \right]_3^1 \\ & + \frac{2\alpha(1-\alpha)}{4\alpha-1} \xi_3 \left[-\frac{3x(2\rho+c)}{\rho^3(\rho+c)^2} + \frac{2x^3}{\rho^3(\rho+c)^3} + \frac{3x^3(2\rho+c)}{\rho^5(\rho+c)^2} \right]_3^1 \\ & - \frac{18\alpha^2}{4\alpha-1} H \left\{ -\frac{3x(2\rho_3+c_3)}{\rho_3^3(\rho_3+c_3)^2} + \frac{2x^3}{\rho_3^3(\rho_3+c_3)^3} + \frac{3x^3(2\rho_3+c_3)}{\rho_3^5(\rho_3+c_3)^2} \right\} \\ & + \frac{12\alpha(1-2\alpha)}{4\alpha-1} H \left\{ -\frac{x(2\rho_3+c_3)}{\rho_3^3(\rho_3+c_3)^2} + \frac{2xy^2}{\rho_3^3(\rho_3+c_3)^3} + \frac{3xy^2(2\rho_3+c_3)}{\rho_3^5(\rho_3+c_3)^2} \right\} \\ & + \frac{12\alpha^2}{4\alpha-1} H \xi_3 \left\{ -\frac{9x}{\rho_3^5} + \frac{15x^3}{\rho_3^7} \right\} \\ & + \left\{ -\frac{2\alpha(1-\alpha)}{4\alpha-1} H \left\{ -\frac{3x(2\rho_1+c_1)}{\rho_1^3(\rho_1+c_1)^2} + \frac{2x^3}{\rho_1^3(\rho_1+c_1)^3} + \frac{3x^3(2\rho_1+c_1)}{\rho_1^5(\rho_1+c_1)^2} \right\} (H < \xi_3) \right. \\ & \left. + \left[-\frac{3\alpha}{4\alpha-1} \left[-\frac{x}{\rho^3} \right]_2^1 + \frac{4\alpha(1+2\alpha)}{4\alpha-1} \left\{ -\frac{x}{\rho_2^3} \right\} \right] \right\} \end{aligned}$$

$$\begin{aligned}
& -\alpha \left[-\frac{1}{4} \frac{x}{\rho^3} + \frac{1}{4} \frac{x(3y^2 - x^2)(3\rho + c)}{\rho^3(\rho + c)^3} \right]_2^1 \\
& - \frac{2\alpha(1-\alpha)}{4\alpha-1} \xi_3 \left\{ -\frac{3x(2\rho_1 + c_1)}{\rho_1^3(\rho_1 + c_1)^2} + \frac{2x^3}{\rho_1^3(\rho_1 + c_1)^3} + \frac{3x^3(2\rho_1 + c_1)}{\rho_1^5(\rho_1 + c_1)^2} \right\} \\
& - \frac{6\alpha^2}{4\alpha-1} (H - \xi_3) \left\{ -\frac{3x(2\rho_2 + c_2)}{\rho_2^3(\rho_2 + c_2)^2} + \frac{2x^3}{\rho_2^3(\rho_2 + c_2)^3} + \frac{3x^3(2\rho_2 + c_2)}{\rho_2^5(\rho_2 + c_2)^2} \right\} (H > \xi_3)
\end{aligned} \tag{5.24a}$$

$$\begin{aligned}
\frac{2}{C_y} w_{11}^y = & \frac{2(1-2\alpha)(1-\alpha)}{4\alpha-1} \left[-\frac{y}{\rho^3} \right]_3^1 \\
& + (2-\alpha) \left[-\frac{1}{4} \frac{y}{\rho^3} + \frac{1}{4} \frac{y(3x^2 - y^2)(3\rho + c)}{\rho^3(\rho + c)^3} \right]_3^1 \\
& + \frac{2\alpha(1-\alpha)}{4\alpha-1} \xi_3 \left[-\frac{y(2\rho + c)}{\rho^3(\rho + c)^2} + \frac{2x^2 y}{\rho^3(\rho + c)^3} + \frac{3x^2 y(2\rho + c)}{\rho^5(\rho + c)^2} \right]_3^1 \\
& - \frac{18\alpha^2}{4\alpha-1} H \left\{ -\frac{y(2\rho_3 + c_3)}{\rho_3^3(\rho_3 + c_3)^2} + \frac{2x^2 y}{\rho_3^3(\rho_3 + c_3)^3} + \frac{3x^2 y(2\rho_3 + c_3)}{\rho_3^5(\rho_3 + c_3)^2} \right\} \\
& + \frac{12\alpha(1-2\alpha)}{4\alpha-1} H \left\{ -\frac{3y(2\rho_3 + c_3)}{\rho_3^3(\rho_3 + c_3)^2} + \frac{2y^3}{\rho_3^3(\rho_3 + c_3)^3} + \frac{3y^3(2\rho_3 + c_3)}{\rho_3^5(\rho_3 + c_3)^2} \right\} \\
& + \frac{12\alpha^2}{4\alpha-1} H \xi_3 \left\{ -\frac{3y}{\rho_3^5} + \frac{15x^2 y}{\rho_3^7} \right\} \\
& + \left\{ -\frac{2\alpha(1-\alpha)}{4\alpha-1} H \left\{ -\frac{y(2\rho_1 + c_1)}{\rho_1^3(\rho_1 + c_1)^2} + \frac{2x^2 y}{\rho_1^3(\rho_1 + c_1)^3} + \frac{3x^2 y(2\rho_1 + c_1)}{\rho_1^5(\rho_1 + c_1)^2} \right\} \right. \\
& \left. - \frac{2\alpha(1+2\alpha)}{4\alpha-1} \left[-\frac{y}{\rho^3} \right]_2^1 - \frac{8\alpha(1-\alpha)}{4\alpha-1} \left\{ -\frac{y}{\rho_2^3} \right\} \right. \\
& \left. + \alpha \left[-\frac{1}{4} \frac{y}{\rho^3} + \frac{1}{4} \frac{y(3x^2 - y^2)(3\rho + c)}{\rho^3(\rho + c)^3} \right]_2^1 \right. \\
& \left. - \frac{2\alpha(1-\alpha)}{4\alpha-1} \xi_3 \left\{ -\frac{y(2\rho_1 + c_1)}{\rho_1^3(\rho_1 + c_1)^2} + \frac{2x^2 y}{\rho_1^3(\rho_1 + c_1)^3} + \frac{3x^2 y(2\rho_1 + c_1)}{\rho_1^5(\rho_1 + c_1)^2} \right\} \right. \\
& \left. - \frac{6\alpha^2}{4\alpha-1} (H - \xi_3) \left\{ -\frac{y(2\rho_2 + c_2)}{\rho_2^3(\rho_2 + c_2)^2} + \frac{2x^2 y}{\rho_2^3(\rho_2 + c_2)^3} + \frac{3x^2 y(2\rho_2 + c_2)}{\rho_2^5(\rho_2 + c_2)^2} \right\} \right\} (H < \xi_3) \\
& + \left\{ -\frac{2\alpha(1-\alpha)}{4\alpha-1} \xi_3 \left\{ -\frac{y(2\rho_1 + c_1)}{\rho_1^3(\rho_1 + c_1)^2} + \frac{2x^2 y}{\rho_1^3(\rho_1 + c_1)^3} + \frac{3x^2 y(2\rho_1 + c_1)}{\rho_1^5(\rho_1 + c_1)^2} \right\} \right. \\
& \left. - \frac{6\alpha^2}{4\alpha-1} (H - \xi_3) \left\{ -\frac{y(2\rho_2 + c_2)}{\rho_2^3(\rho_2 + c_2)^2} + \frac{2x^2 y}{\rho_2^3(\rho_2 + c_2)^3} + \frac{3x^2 y(2\rho_2 + c_2)}{\rho_2^5(\rho_2 + c_2)^2} \right\} \right\} (H > \xi_3)
\end{aligned} \tag{5.24b}$$

$$\begin{aligned}
\frac{2}{C_z} w_{11}^z = & -\frac{(1-2\alpha)(2+\alpha)}{4\alpha-1} \left[\frac{1}{\rho(\rho + c)} - \frac{x^2(2\rho + c)}{\rho^3(\rho + c)^2} \right]_3^1 \\
& + \frac{2(1-2\alpha)(1-\alpha)}{4\alpha-1} \left[\frac{c}{\rho^3} \right]_3^1 + \frac{2\alpha(1-\alpha)}{4\alpha-1} \xi_3 \left[\frac{1}{\rho^3} - \frac{3x^2}{\rho^5} \right]_3^1 \\
& + \frac{18\alpha^2}{4\alpha-1} H \left\{ \frac{1}{\rho_3^3} - \frac{3x^2}{\rho_3^5} \right\} - \frac{12\alpha(1-2\alpha)}{4\alpha-1} H \left\{ \frac{1}{\rho_3^3} - \frac{3y^2}{\rho_3^5} \right\}
\end{aligned}$$

$$\begin{aligned}
& -\frac{12\alpha^2}{4\alpha-1} H\tilde{\xi}_3 \left\{ \frac{3c_3}{\rho_3^5} - \frac{15c_3x^2}{\rho_3^7} \right\} \\
& + \left\{ -\frac{2\alpha(1-\alpha)}{4\alpha-1} H \left\{ \frac{1}{\rho_1^3} - \frac{3x^2}{\rho_1^5} \right\} \right. \quad (H < \tilde{\xi}_3) \\
& \quad -\frac{2\alpha(1+2\alpha)}{4\alpha-1} \left[\frac{c}{\rho^3} \right]_2^1 - 4\alpha \left\{ \frac{c_2}{\rho_2^3} \right\} \\
& \quad -\frac{\alpha(2\alpha-5)}{4\alpha-1} \left[\frac{1}{\rho(\rho+c)} - \frac{x^2(2\rho+c)}{\rho^3(\rho+c)^2} \right]_2^1 \\
& \quad \left. -\frac{2\alpha(1-\alpha)}{4\alpha-1} \tilde{\xi}_3 \left\{ \frac{1}{\rho_1^3} - \frac{3x^2}{\rho_1^5} \right\} + \frac{6\alpha^2}{4\alpha-1} (H-\tilde{\xi}_3) \left\{ \frac{1}{\rho_2^3} - \frac{3x^2}{\rho_2^5} \right\} \right. \quad (H > \tilde{\xi}_3) \\
& \quad \left. \right\} \quad (5.24c)
\end{aligned}$$

(kl=22)

$$w_{22}^x(x, y) = w_{11}^y(y, x) \quad (5.25a)$$

$$w_{22}^y(x, y) = w_{11}^x(y, x) \quad (5.25b)$$

$$w_{22}^z(x, y) = w_{11}^z(y, x) \quad (5.25c)$$

(kl=33)

$$\begin{aligned}
\frac{2}{C_z} w_{33}^x &= \alpha \left[-\frac{x}{\rho^3} \right]_3^1 - \frac{2\alpha(1-\alpha)}{4\alpha-1} \tilde{\xi}_3 \left[-\frac{3cx}{\rho^5} \right]_3^1 \\
& -\frac{6\alpha^2}{4\alpha-1} H \left\{ -\frac{3c_3x}{\rho_3^5} \right\} - \frac{12\alpha^2}{4\alpha-1} H\tilde{\xi}_3 \left\{ \frac{3x}{\rho_3^5} - \frac{15c_3^2x}{\rho_3^7} \right\} \\
& + \left\{ \frac{2\alpha(1-\alpha)}{4\alpha-1} H \left\{ -\frac{3c_1x}{\rho_1^5} \right\} \right. \quad (H < \tilde{\xi}_3) \\
& \quad -\alpha \left[-\frac{x}{\rho^3} \right]_2^1 + \frac{2\alpha(1-\alpha)}{4\alpha-1} \tilde{\xi}_3 \left\{ -\frac{3c_1x}{\rho_1^5} \right\} \\
& \quad \left. + \frac{6\alpha^2}{4\alpha-1} (H-\tilde{\xi}_3) \left\{ -\frac{3c_2x}{\rho_2^5} \right\} \right. \quad (H > \tilde{\xi}_3) \\
& \quad \left. \right\} \quad (5.26a)
\end{aligned}$$

$$w_{33}^y(x, y) = w_{33}^x(y, x) \quad (5.26b)$$

$$\begin{aligned}
\frac{2}{C_z} w_{33}^z &= -\frac{\alpha(1+2\alpha)}{4\alpha-1} \left[\frac{c}{\rho^3} \right]_3^1 - \frac{2\alpha(1-\alpha)}{4\alpha-1} \tilde{\xi}_3 \left[-\frac{1}{\rho^3} + \frac{3c^2}{\rho^5} \right]_3^1 \\
& + \frac{6\alpha^2}{4\alpha-1} H \left\{ -\frac{1}{\rho_3^3} + \frac{3c_3^2}{\rho_3^5} \right\} + \frac{12\alpha^2}{4\alpha-1} H\tilde{\xi}_3 \left\{ -\frac{9c_3}{\rho_3^5} + \frac{15c_3^3}{\rho_3^7} \right\} \\
& + \left\{ \frac{2\alpha(1-\alpha)}{4\alpha-1} H \left\{ -\frac{1}{\rho_1^3} + \frac{3c_1^2}{\rho_1^5} \right\} \right. \quad (H < \tilde{\xi}_3) \\
& \quad \left. + \frac{\alpha(1+2\alpha)}{4\alpha-1} \left[\frac{c}{\rho^3} \right]_2^1 + \frac{2\alpha(1-\alpha)}{4\alpha-1} \tilde{\xi}_3 \left\{ -\frac{1}{\rho_1^3} + \frac{3c_1^2}{\rho_1^5} \right\} \right. \\
& \quad \left. \right\}
\end{aligned}$$

$$-\frac{6\alpha^2}{4\alpha-1}(H-\xi_3)\left\{-\frac{1}{\rho_2^3}+\frac{3c_2^2}{\rho_2^5}\right\} \quad (H>\xi_3) \quad (5.26c)$$

(kl=23)

$$\begin{aligned} \frac{2}{C_x}w_{23}^x &= \frac{2\alpha(1-\alpha)}{4\alpha-1}\left[-\frac{xy(2\rho+c)}{\rho^3(\rho+c)^2}\right]_3^1 + \frac{2\alpha(1-\alpha)}{4\alpha-1}\xi_3\left[-\frac{3xy}{\rho^5}\right]_3^1 \\ &\quad - \frac{6\alpha^2}{4\alpha-1}H\left\{-\frac{3xy}{\rho_3^5}\right\} + \frac{12\alpha^2}{4\alpha-1}H\xi_3\left\{-\frac{15c_3xy}{\rho_3^7}\right\} \\ &\quad + \begin{cases} -\frac{2\alpha(1-\alpha)}{4\alpha-1}H\left\{-\frac{3xy}{\rho_1^5}\right\} & (H<\xi_3) \\ -\frac{2\alpha(1-\alpha)}{4\alpha-1}\left[-\frac{xy(2\rho+c)}{\rho^3(\rho+c)^2}\right]_2^1 - \frac{2\alpha(1-\alpha)}{4\alpha-1}\xi_3\left\{-\frac{3xy}{\rho_1^5}\right\} \\ + \frac{6\alpha^2}{4\alpha-1}(H-\xi_3)\left\{-\frac{3xy}{\rho_2^5}\right\} & (H>\xi_3) \end{cases} \end{aligned} \quad (5.27a)$$

$$\begin{aligned} \frac{2}{C_y}w_{23}^y &= -\frac{3\alpha}{4\alpha-1}\left[\frac{c}{\rho^3}\right]_3^1 + \frac{2\alpha(1-\alpha)}{4\alpha-1}\left[\frac{1}{\rho(\rho+c)} - \frac{y^2(2\rho+c)}{\rho^3(\rho+c)^2}\right]_3^1 \\ &\quad + \frac{2\alpha(1-\alpha)}{4\alpha-1}\xi_3\left[\frac{1}{\rho^3} - \frac{3y^2}{\rho^5}\right]_3^1 \\ &\quad - \frac{6\alpha^2}{4\alpha-1}H\left\{\frac{1}{\rho_3^3} - \frac{3y^2}{\rho_3^5}\right\} + \frac{12\alpha^2}{4\alpha-1}H\xi_3\left\{\frac{3c_3}{\rho_3^5} - \frac{15c_3y^2}{\rho_3^7}\right\} \\ &\quad + \begin{cases} -\frac{2\alpha(1-\alpha)}{4\alpha-1}H\left\{\frac{1}{\rho_1^3} - \frac{3y^2}{\rho_1^5}\right\} & (H<\xi_3) \\ \frac{3\alpha}{4\alpha-1}\left[\frac{c}{\rho^3}\right]_2^1 - \frac{2\alpha(1-\alpha)}{4\alpha-1}\left[\frac{1}{\rho(\rho+c)} - \frac{y^2(2\rho+c)}{\rho^3(\rho+c)^2}\right]_2^1 \\ - \frac{2\alpha(1-\alpha)}{4\alpha-1}\xi_3\left\{\frac{1}{\rho_1^3} - \frac{3y^2}{\rho_1^5}\right\} + \frac{6\alpha^2}{4\alpha-1}(H-\xi_3)\left\{\frac{1}{\rho_2^3} - \frac{3y^2}{\rho_2^5}\right\} & (H>\xi_3) \end{cases} \end{aligned} \quad (5.27b)$$

$$\begin{aligned} \frac{2}{C_z}w_{23}^z &= -\alpha\left[-\frac{y}{\rho^3}\right]_3^1 - \frac{2\alpha(1-\alpha)}{4\alpha-1}\xi_3\left[-\frac{3cy}{\rho^5}\right]_3^1 \\ &\quad - \frac{6\alpha^2}{4\alpha-1}H\left\{-\frac{3c_3y}{\rho_3^5}\right\} + \frac{12\alpha^2}{4\alpha-1}\xi_3H\left\{\frac{3y}{\rho_3^5} - \frac{15c_3^2y}{\rho_3^7}\right\} \\ &\quad + \begin{cases} \frac{2\alpha(1-\alpha)}{4\alpha-1}H\left\{-\frac{3c_1y}{\rho_1^5}\right\} & (H<\xi_3) \\ \alpha\left[-\frac{y}{\rho^3}\right]_2^1 + \frac{2\alpha(1-\alpha)}{4\alpha-1}\xi_3\left\{-\frac{3c_1y}{\rho_1^5}\right\} \\ + \frac{6\alpha^2}{4\alpha-1}(H-\xi_3)\left\{-\frac{3c_2y}{\rho_2^5}\right\} & (H>\xi_3) \end{cases} \end{aligned} \quad (5.27c)$$

$(kl=31)$

$$w_{31}^x(x, y) = w_{23}^y(y, x) \quad (5.28a)$$

$$w_{31}^y(x, y) = w_{23}^x(y, x) \quad (5.28b)$$

$$w_{31}^z(x, y) = w_{23}^z(y, x) \quad (5.28c)$$

 $(kl=12)$

$$\begin{aligned} \frac{2}{C_z} w_{12}^x = & -\frac{3\alpha}{4\alpha-1} \left[-\frac{y}{\rho^3} \right]_3^1 + (2-\alpha) \left[-\frac{1}{4} \frac{y}{\rho^3} + \frac{1}{4} \frac{y(3x^2-y^2)(3\rho+c)}{\rho^3(\rho+c)^3} \right]_3^1 \\ & + \frac{2\alpha(1-\alpha)}{4\alpha-1} \xi_3 \left[-\frac{y(2\rho+c)}{\rho^3(\rho+c)^2} + \frac{2x^2y}{\rho^3(\rho+c)^3} + \frac{3x^2y(2\rho+c)}{\rho^5(\rho+c)^2} \right]_3^1 \\ & - \frac{6\alpha(2-\alpha)}{4\alpha-1} H \left\{ -\frac{y(2\rho_3+c_3)}{\rho_3^3(\rho_3+c_3)^2} + \frac{2x^2y}{\rho_3^3(\rho_3+c_3)^3} + \frac{3x^2y(2\rho_3+c_3)}{\rho_3^5(\rho_3+c_3)^2} \right\} \\ & + \frac{12\alpha^2}{4\alpha-1} H \xi_3 \left\{ -\frac{3y}{\rho_3^5} + \frac{15x^2y}{\rho_3^7} \right\} \\ & + \left\{ -\frac{2\alpha(1-\alpha)}{4\alpha-1} H \left\{ -\frac{y(2\rho_1+c_1)}{\rho_1^3(\rho_1+c_1)^2} + \frac{2x^2y}{\rho_1^3(\rho_1+c_1)^3} + \frac{3x^2y(2\rho_1+c_1)}{\rho_1^5(\rho_1+c_1)^2} \right\} \right. \\ & \left. + \left[-\frac{3\alpha}{4\alpha-1} \left[-\frac{y}{\rho^3} \right]_2^1 + \frac{6\alpha}{4\alpha-1} \left\{ -\frac{y}{\rho_2^3} \right\} \right. \right. \\ & \left. + \alpha \left[-\frac{1}{4} \frac{y}{\rho^3} + \frac{1}{4} \frac{y(3x^2-y^2)(3\rho+c)}{\rho^3(\rho+c)^3} \right]_2^1 \right. \\ & \left. - \frac{2\alpha(1-\alpha)}{4\alpha-1} \xi_3 \left\{ -\frac{y(2\rho_1+c_1)}{\rho_1^3(\rho_1+c_1)^2} + \frac{2x^2y}{\rho_1^3(\rho_1+c_1)^3} + \frac{3x^2y(2\rho_1+c_1)}{\rho_1^5(\rho_1+c_1)^2} \right\} \right. \\ & \left. - \frac{6\alpha^2}{4\alpha-1} (H-\xi_3) \left\{ -\frac{y(2\rho_2+c_2)}{\rho_2^3(\rho_2+c_2)^2} + \frac{2x^2y}{\rho_2^3(\rho_2+c_2)^3} + \frac{3x^2y(2\rho_2+c_2)}{\rho_2^5(\rho_2+c_2)^2} \right\} \right\} \\ & \quad (H > \xi_3) \quad (5.29a) \end{aligned}$$

$$w_{12}^y(x, y) = w_{12}^x(y, x) \quad (5.29b)$$

$$\begin{aligned} \frac{2}{C_z} w_{12}^z = & \frac{(2\alpha-1)(\alpha+2)}{4\alpha-1} \left[-\frac{xy(2\rho+c)}{\rho^3(\rho+c)^2} \right]_3^1 + \frac{2\alpha(1-\alpha)}{4\alpha-1} \xi_3 \left[-\frac{3xy}{\rho^5} \right]_3^1 \\ & + \frac{6\alpha(2-\alpha)}{4\alpha-1} H \left\{ -\frac{3xy}{\rho_3^5} \right\} - \frac{12\alpha^2}{4\alpha-1} H \xi_3 \left\{ -\frac{15c_3xy}{\rho_3^7} \right\} \\ & + \left\{ -\frac{2\alpha(1-\alpha)}{4\alpha-1} H \left\{ -\frac{3xy}{\rho_1^5} \right\} \right. \\ & \left. + \left[-\frac{\alpha(2\alpha-5)}{4\alpha-1} \left[-\frac{xy(2\rho+c)}{\rho^3(\rho+c)^2} \right]_2^1 - \frac{2\alpha(1-\alpha)}{4\alpha-1} \xi_3 \left\{ -\frac{3xy}{\rho_1^5} \right\} \right. \right. \\ & \left. \left. + \frac{6\alpha^2}{4\alpha-1} (H-\xi_3) \left\{ -\frac{3xy}{\rho_2^5} \right\} \right\} \right. \\ & \quad (H > \xi_3) \quad (5.29c) \end{aligned}$$

where

$$[f(\rho, c)]_i = f(\rho_i, c_i) - f(\rho_j, c_j)$$

and

$$\begin{aligned}\rho_1 &= \sqrt{x^2 + y^2 + c_1^2}, & c_1 &= \xi_3 - z \\ \rho_2 &= \sqrt{x^2 + y^2 + c_2^2}, & c_2 &= 2H - \xi_3 - z \\ \rho_3 &= \sqrt{x^2 + y^2 + c_3^2}, & c_3 &= 2H + \xi_3 - z\end{aligned}$$

which already appeared in eqs. (4.37).

On the other hand, we can construct type I solutions of elementary piezomagnetic potentials by combining $w_{kl}^{m(H)}$'s as follows:

$$w_{kl}^{(I)} = w_{kl}^{m(0)} + w_{kl}^{m(P)} + w_{kl}^{m(H)}$$

in which

$$w_{kl}^{m(P)} = \lim_{\varepsilon \rightarrow 0} \{w_{kl}^{m(H=\xi_3-\varepsilon)} - w_{kl}^{m(H=\xi_3+\varepsilon)}\}$$

This procedure is the same as that by which we obtained the type I solution for the Mogi model in Chapter 3. Actually, results thus obtained were compared with those given by SASAI (1980), which confirmed the validity of previous calculations.

Now we find that type I and type II solutions are identical for strain nuclei of $(kl) = (33)$, (23) and (31) . However, those for $(kl) = (11)$, (22) and (12) are different. All the terms arising from $w_{kl}^{m(H)}$'s remain unchanged even for these inconsistent solutions, but they can produce only a weak magnetic field on the earth. On the contrary, the corrected terms are equivalent dipoles at a position of point dislocation, and make important contribution.

$w_{kl}^{m(K)}$ indicates the equivalent dipole bearing the seismomagnetic moment as has been discussed in Chapter 2. Comparing Appendices D2 and D3, we notice that $w_{kl}^{m(0)}$ almost, or in some cases completely, cancels $w_{kl}^{m(K)}$. This implies that the concept of the seismomagnetic moment does not work well in such a simple homogeneous earth model. In the case of particular kinds of dislocations, i.e. $(kl) = (33)$, (23) and (31) , magnetic source equivalents do not appear at the fault position, but only at mirror points far deeper below the Curie point isotherm. Even in the case of the nuclei $(kl) = (11)$, (22) and (12) , the intensity of source equivalents is different from that expected from the seismomagnetic moment. We will briefly discuss in section 5.4 what kind of fault motion can produce surface magnetic changes effectively.

5.3 Multiple Tension-Crack Model

A multiple tension-crack model was proposed by SASAI (1986b) as an extended version of HAGIWARA's (1977b) multiple Mogi model. The

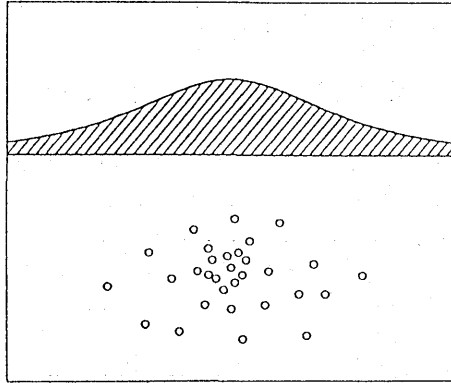


Fig. 24. A schematic view of the multiple tension-crack model.

multiple tension-crack model can explain surface deformations and related gravity and magnetic changes accompanying the injection of fluid materials such as magma, volcanic gas and pressurized water into a shallow portion of the earth's crust. In evaluating piezomagnetic changes, SASAI (1986b) used the type I solutions. Moreover, some results on the gravity changes should be reexamined, according to OKUBO (1991). All these corrections will be completed elsewhere. In this section, we will present the basic concept of the model, and will derive the magnetic change associated with the multiple Mogi model.

Suppose there is a Gaussian distribution of microcracks centered at $(0, 0, D)$ (see Fig. 24). We assume that the variance σ_r^2 in the horizontal distribution is isotropic and the vertical variance σ_z^2 differs from σ_r^2 . The distribution function is given by

$$p(x, y) = \frac{1}{2\pi\sigma_r^2} \exp\left(-\frac{x^2 + y^2}{2\sigma_r^2}\right) \quad (5.30a)$$

$$q(z) = \frac{1}{\sqrt{2\pi}\sigma_z} \exp\left\{-\frac{(D-z)^2}{2\sigma_z^2}\right\} \quad (5.30b)$$

Quantities related to the mechanical distortion are given by the displacement field itself due to appropriate strain nuclei and/or its derivatives. Let us assume such an influence function $f(x, y, z, z')$, which represents the effect of a single crack placed at $(0, 0, z')$. The total effect of cracks under the distribution (5.30) is given by

$$g(x, y, z) = \int_0^\infty q(z') F(x, y, z, z') dz' \quad (5.31)$$

where

$$F(x, y, z, z') = \iint_{-\infty}^{\infty} f(x-x', y-y', z, z') p(x', y') dx' dy' \quad (5.32)$$

The convolution integral (5.32) can be evaluated by the Fourier transform method.

Let us first derive an expression for the surface uplift due to the multiple Mogi model. It forms a prototype for obtaining all the other formulas. We already have the displacement field associated with the Mogi model. When a small sphere at (x', y', z') expands hydrostatically, the uplift Δh_p at a surface point $(x, y, 0)$ is given by

$$\Delta h_p(x, y) = -\frac{\lambda+2\mu}{2\mu(\lambda+\mu)} a^3 \Delta P \frac{z'}{\{(x-x')^2 + (y-y')^2 + z'^2\}^{3/2}} \quad (5.33)$$

Substituting eq. (5.33) into f in eq. (5.32), we obtain the resultant uplift $\Delta H_{00}(x, y)$ as follows:

$$\Delta H_{00}(x, y) = -\frac{\lambda+2\mu}{2\mu(\lambda+\mu)} a^3 \Delta P \int_0^{\infty} q(z') F(x, y, z') dz' \quad (5.34)$$

where

$$F(x, y, z') = \iint_{-\infty}^{\infty} \frac{z'}{\{(x-x')^2 + (y-y')^2 + z'^2\}^{3/2}} p(x', y') dx' dy' \quad (5.35)$$

Since

$$p^*(k_1, k_2) = \frac{1}{2\pi} \exp\left(-\frac{1}{2} \sigma_r^2 k^2\right) \quad (5.36a)$$

$$\Delta h_p^*(k_1, k_2) = -\frac{\lambda+2\mu}{2\mu(\lambda+\mu)} a^3 \Delta P e^{-kz'} \quad (5.36b)$$

we obtain

$$\begin{aligned} \Delta H_{00}^*(k_1, k_2) &= -\frac{\lambda+2\mu}{2\mu(\lambda+\mu)} a^3 \Delta P \int_0^{\infty} q(z') e^{-kz'} \exp\left(-\frac{1}{2} \sigma_r^2 k^2\right) dz' \\ &= -\frac{\lambda+2\mu}{2\mu(\lambda+\mu)} a^3 \Delta P \exp\left\{-\frac{1}{2} (\sigma_r^2 - \sigma_z^2) k^2\right\} \Phi\left(\frac{-D + \sigma_z^2 k}{\sqrt{2} \sigma_z}\right) \end{aligned} \quad (5.37)$$

$\Phi(x)$ is defined as

$$\Phi(x) = \frac{1}{\sqrt{\pi}} \int_x^{\infty} e^{-t^2} dt = \begin{cases} \frac{1}{2} \operatorname{erfc}(x) & (x \geq 0) \\ \frac{1}{2} \{1 + \operatorname{erf}(|x|)\} & (x < 0) \end{cases} \quad (5.38)$$

in which $\operatorname{erf}(x)$ and $\operatorname{erfc}(x)$ are Gauss' error and complementary error functions.

The inverse Fourier transform of eq. (5.37) gives rise to

$$\Delta H_{00}(r) = \int_0^\infty \Delta H_{00}^*(k) J_0(kr) k dk \quad (5.39)$$

Δh_0 , the value of ΔH_{00} at $r=0$, gives the maximum uplift:

$$\Delta h_0 = -\frac{\lambda + 2\mu}{2\mu(\lambda + \mu)} a^3 \Delta P h_{00} \quad (5.40)$$

where

$$h_{00} = \int_0^\infty \exp\left\{-\frac{1}{2}(\sigma_r^2 - \sigma_z^2)k^2\right\} e^{-kD} \Phi\left(\frac{-D + \sigma_z^2 k}{\sqrt{2}\sigma_z}\right) k dk \quad (5.41)$$

h_{00} is a constant peculiar to the model specified by parameters $\{\sigma_r, \sigma_z, D\}$. All the distortion-related quantities are proportional to the moment of source spheres, i.e. $\frac{\lambda + 2\mu}{2\mu(\lambda + \mu)} a^3 \Delta P$ in eq. (5.40). This parameter is not, however, observable. Instead we may give the maximum uplift Δh_0 as a measure of the moment intensity. Eq. (5.39) is rewritten as

$$\Delta H_{00}(x, y) = \frac{\Delta h_0}{h_{00}} \int_0^\infty Q_1(k) e^{-kD} J_0(kr) k dk \quad (5.42)$$

where

$$Q_1(k) = \exp\left\{-\frac{1}{2}(\sigma_r^2 - \sigma_z^2)k^2\right\} \Phi\left(\frac{-D + \sigma_z^2 k}{\sqrt{2}\sigma_z}\right) \quad (5.43)$$

Eq. (5.42) is the rigorous solution for the surface uplift caused by the multiple Mogi model. HAGIWARA (1977b) gave merely an approximate solution for the uplift, which was expressed with elementary functions. It is valid only in a limited case $D \gg \sigma_r \geq \sigma_z$. The present solution (5.42) is no longer expressible with elementary functions. The error and Bessel functions are originally defined in integral forms. In other words, eq. (5.42) is a formal reduction to a one dimensional integral from the volumetric one in eq. (5.34). We have, however, useful mini-max approximation formulas for error and Bessel functions (e.g. HASTING, 1955) to compute numerical values with sufficient accuracy and speed. The double exponential formula (TAKAHASI and MORI, 1974) is again applied to numerically integrate eq. (5.42).

The horizontal displacements in the x and y directions are obtained in a similar manner as follows:

$$\Delta X_{00}(x, y) = \frac{\Delta h_0}{h_{00}} \frac{x}{r} \int_0^\infty Q_1(k) e^{-kD} J_1(kr) k dk \quad (5.44a)$$

$$\Delta Y_{00}(x, y) = \frac{\Delta h_0}{h_{00}} \frac{y}{r} \int_0^\infty Q_1(k) e^{-kD} J_1(kr) k dk \quad (5.44b)$$

The gravity change is simply proportional to the uplift at the observation site, which is given by

$$\delta G_{00} = \left\{ -\gamma + \frac{2\pi G \rho_0 (\lambda + \mu)}{\lambda + 2\mu} \right\} \Delta H_{00} \quad (5.45)$$

where γ is the free-air gravity change rate ($\gamma = 0.3086$ mgal/m), G the gravitational constant and ρ_0 the material density filling the source sphere.

Now let us investigate the piezomagnetic change. We already have a point source solution for the piezomagnetic change associated with the Mogi model, i.e. eqs. (3.55). We may use them as the influence functions f in eq. (5.32). Exchanging x_0 , y_0 and D for $x-x'$, $y-y'$ and z' , we rewrite W_x and W_z as w_{00}^x and w_{00}^z . Fourier transforms of w_{00}^x and w_{00}^z are given by

$$\begin{aligned} \frac{w_{00}^{x*}}{C_{00}^x} = & -\frac{\mu}{3\lambda + 2\mu} \frac{ik_1}{k} (e^{-kz_1} - e^{-kz_3}) - \frac{6(\lambda + \mu)}{2\lambda + 2\mu} H ik_1 e^{-kz_3} \\ & + \begin{cases} -\frac{\lambda + \mu}{3\lambda + 2\mu} \frac{ik_1}{k} (e^{-kz_1} - 3e^{-kz_2}) & (H > z') \\ 0 & (H < z') \end{cases} \end{aligned} \quad (5.46a)$$

$$\begin{aligned} \frac{w_{00}^{z*}}{C_{00}^z} = & -\frac{\mu}{3\lambda + 2\mu} (e^{-kz_1} - e^{-kz_3}) - \frac{6(\lambda + \mu)}{3\lambda + 2\mu} H k e^{-kz_3} \\ & + \begin{cases} -\frac{\lambda + \mu}{3\lambda + 2\mu} (e^{-kz_1} + 3e^{-kz_2}) & (H > z') \\ 0 & (H < z') \end{cases} \end{aligned} \quad (5.46b)$$

where

$$C_{00}^m = \pi \beta J_m C \frac{3\lambda + 2\mu}{\lambda + \mu} \quad (5.47a)$$

$$z_1 = z' - z, \quad z_2 = 2H - z' - z, \quad z_3 = 2H + z' - z. \quad (5.47b)$$

Combining eqs. (5.46) with eq. (5.36a), integrating with respect to z' and conducting inverse Fourier transformation, we find piezomagnetic potentials due to the multiple Mogi model as follows:

$$W_{00}^x / C_{00}^x = -\frac{x}{r} \int_0^\infty U_{00}^x(k, z) J_1(kr) k^2 dk \quad (5.48a)$$

$$W_{00}^z / C_{00}^z = \int_0^\infty U_{00}^z(k, z) J_0(kr) k dk \quad (5.48b)$$

where

$$U_{00}^z(k, z) = -\frac{\mu}{3\lambda+2\mu} \frac{1}{k} Q_1(k) (e^{-kD_1} - e^{-kD_3}) - \frac{6(\lambda+\mu)}{3\lambda+2\mu} H Q_1(k) e^{-kD_3} \\ - \frac{\lambda+\mu}{3\lambda+2\mu} \frac{1}{k} \left[\{Q_1(k) - Q_2(k)\} e^{-kD_1} - 3\{Q_3(k) - Q_4(k)\} e^{-kD_2} \right] \quad (5.49a)$$

$$U_{00}^z(k, z) = -\frac{\mu}{3\lambda+2\mu} Q_1(k) (e^{-kD_1} - e^{-kD_3}) + \frac{6(\lambda+\mu)}{3\lambda+2\mu} H k Q_1(k) e^{-kD_3} \\ - \frac{\lambda+\mu}{3\lambda+2\mu} \left[\{Q_1(k) - Q_2(k)\} e^{-kD_1} + 3\{Q_3(k) - Q_4(k)\} e^{-kD_2} \right] \quad (5.49b)$$

and

$$|Q_n(k) = \exp\left\{-\frac{1}{2}(\sigma_r^2 - \sigma_z^2)k^2\right\} \Phi(x_n) \quad (5.50)$$

$$x_1 = \frac{-D + \sigma_z^2 k}{\sqrt{2} \sigma_z}, \quad x_2 = \frac{H - D + \sigma_z^2 k}{\sqrt{2} \sigma_z}, \quad (5.51a)$$

$$x_3 = \frac{-D - \sigma_z^2 k}{\sqrt{2} \sigma_z}, \quad x_4 = \frac{H - D - \sigma_z^2 k}{\sqrt{2} \sigma_z}. \quad (5.51b)$$

$$D_1 = D - z, \quad D_2 = 2H - D - z, \quad D_3 = 2H + D - z \quad (5.51c)$$

With the aid of the relationship (5.40), C_{00}^m 's ($m=x, z$) in eq. (5.47a) are reduced to

$$C_{00}^m = \pi \beta J_m \frac{\mu(3\lambda+2\mu)}{\lambda+2\mu} \frac{\Delta h_0}{h_{00}} \quad (5.52)$$

The magnetic field is given by differentiation of potentials (5.48). We denote three components of the magnetic field in association with J_x and J_z as (x_H, y_H, z_H) and (x_V, y_V, z_V) respectively. They are represented by

$$x_H = A + \frac{x^2}{r^2} (B - 2A), \quad y_H = \frac{xy}{r^2} (B - 2A), \quad z_H = C x \quad (5.53a)$$

$$x_V = Dx, \quad y_V = Dy, \quad z_V = -E \quad (5.53b)$$

where

$$A(r, z) = \int_0^\infty U_{00}^z(k, z) \frac{J_1(kr)}{r} k^2 dk \quad (5.54a)$$

$$B(r, z) = \int_0^\infty U_{00}^x(k, z) J_0(kr) k^3 dk \quad (5.54b)$$

$$C(r, z) = \int_0^\infty U_{00}^z(k, z) \frac{J_1(kr)}{r} k^3 dk \quad (5.54c)$$

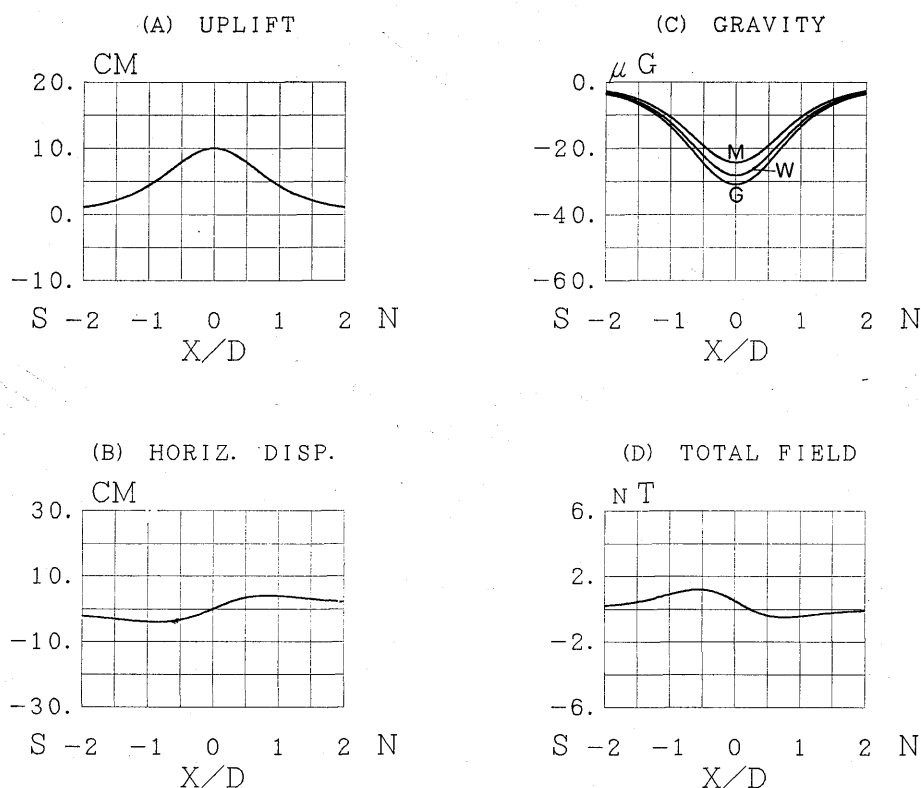


Fig. 25. Results along the N-S meridian for the multiple Mogi model with $D=1.0$ km, $\sigma_r=\sigma_z=0.5$ km and $\Delta h_0=10$ cm. (A) Uplift, (B) Horizontal displacement, (C) Gravity change: three curves indicate different kinds of crack-filling materials i.e. gas (G), water (W) and magma (M), and (D) Magnetic total intensity.

$$D(r, z) = \int_0^\infty U_{00}^z(k, z) \frac{J_1(kr)}{r} k^2 dk \quad (5.54d)$$

$$E(r, z) = \int_0^\infty U_{00}^z(k, z) J_0(kr) k^2 dk \quad (5.54e)$$

Some of eqs. (5.53) and eqs. (5.54) look apparently indefinite at $r=0$. Taking into account the characteristics of Bessel functions

$$\lim_{r \rightarrow 0} J_1(kr)/r = \frac{1}{2} k, \quad \lim_{r \rightarrow 0} J_0(kr) = 1,$$

we find that all of them converge at $r=0$. In particular, $B=2A$ at $r=0$; hence, we have:

$$x_H = A(r=0), \quad y_H = 0 \quad (5.55)$$

We will present an example. In Fig. 25 are shown (a) uplift, (b)

Table 1. Material properties of the elastomagnetic medium and parameters of the geomagnetic field.

Rigidity	μ	3.5×10^{11}	cgs
Poisson's ratio	ν	0.25	
Density	ρ	2.65	g/cc
Density of crack-filling materials	ρ_0		
Gas		0.0	g/cc
Water		1.0	g/cc
Magma		2.35	g/cc
Average magnetization	J	1.0	A/m
Stress sensitivity	β	1.0×10^{-4}	bar $^{-1}$
Curie depth	H	15	km
Average magnetic dip	I_0	45°	

horizontal displacement, (c) gravity and (d) magnetic total intensity changes associated with the multiple Mogi model for $D=1$ km, $\sigma_r=\sigma_z=0.5$ km and $\Delta h_0=10$ cm. These are profiles along the N-S meridian. Material properties of the medium and parameters of the ambient geomagnetic field are summarized in Table 1. Three curves in the gravity change correspond to three different materials filling cracks, i.e. gas (G), water (W) and magma (M).

5.4 Magnetic Change due to Vertical Strike-Slip and Tensile Faults

Finally we will derive some formulas for piezomagnetic changes associated with faulting. SASAI (1980) obtained the piezomagnetic field due to a vertical rectangular strike-slip fault. He also formulated the magnetic changes caused by intrusion of a vertical dyke (SASAI, 1984). Both the formulas should be corrected because of a new version of elementary piezomagnetic potentials.

Fig. 26 shows the geometry of a vertical strike-slip fault. According to Volterra's formula, eq. (5.5), the piezomagnetic potential due to such faulting can be given by the following integral:

$$W^{m(S)}(x, y, z) = \Delta U \int_a^D d\xi_3 \int_{-L}^{+L} w_{12}^m(x - \xi_1, y, z, \xi_3) d\xi_1 \quad (5.56)$$

Integrals with respect to ξ_1 can be easily done with the aid of a property of Fourier transforms, as described in Appendix B. Final results for integrations of eq. (5.56) are summarized in Appendix E1.

Some typical examples are computed. Model parameters are given in Table 2. In Figs. 27 are shown magnetic changes accompanied by a magnetic N-S oriented fault. They are (a) horizontal (northward), (b) declination (eastward), (c) vertical (downward) and (d) total intensity,

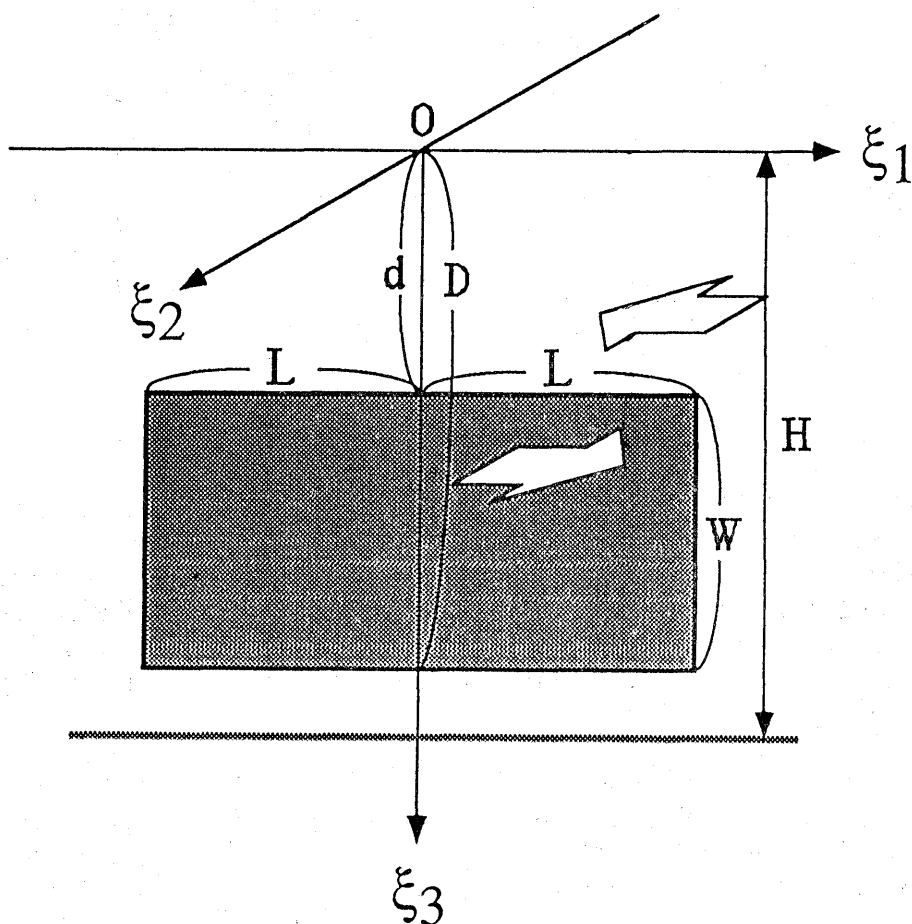


Fig. 26. The geometry of a vertical rectangular strike-slip fault.

respectively. Similarly, results for a NW-SE oriented and an E-W oriented fault are shown in Figs. 28 and Figs. 29 respectively. Unlike the previous results (SASAI 1980), relatively intense magnetic changes are seen only around both tips of the fault. This arises from a characteristic of w_{12}^m that no dipole term appears along the fault surface. Integration of higher-order magnetic sources over a fault plane results in having the outlets of magnetic lines of force only along both edges of the fault.

Fig. 30 shows a schematic view of a vertical rectangular dyke. The piezomagnetic potential due to a vertical tensile fault $W^{m(T)}$ is represented by

$$W^{m(T)}(x, y, z) = \Delta U \int_a^D d\xi_3 \int_{-L}^{+L} w_{22}^m(x - \xi_1, y, z, \xi_3) d\xi_1 \quad (5.57)$$

Table 2. Parameters of a vertical rectangular fault.

Fault length	$2L$	10	km
Fault width	W	5	km
Depth of burial	d	0.5	km
Dislocation	ΔU	1	m
Rigidity	μ	3.5×10^{11}	cgcs
Poisson's ratio	ν	0.25	
Average magnetization	J	1.0	A/m
Stress sensitivity	β	1.0×10^{-4}	bar $^{-1}$
Curie depth	H	15	km
Average magnetic dip	I_0	45°	

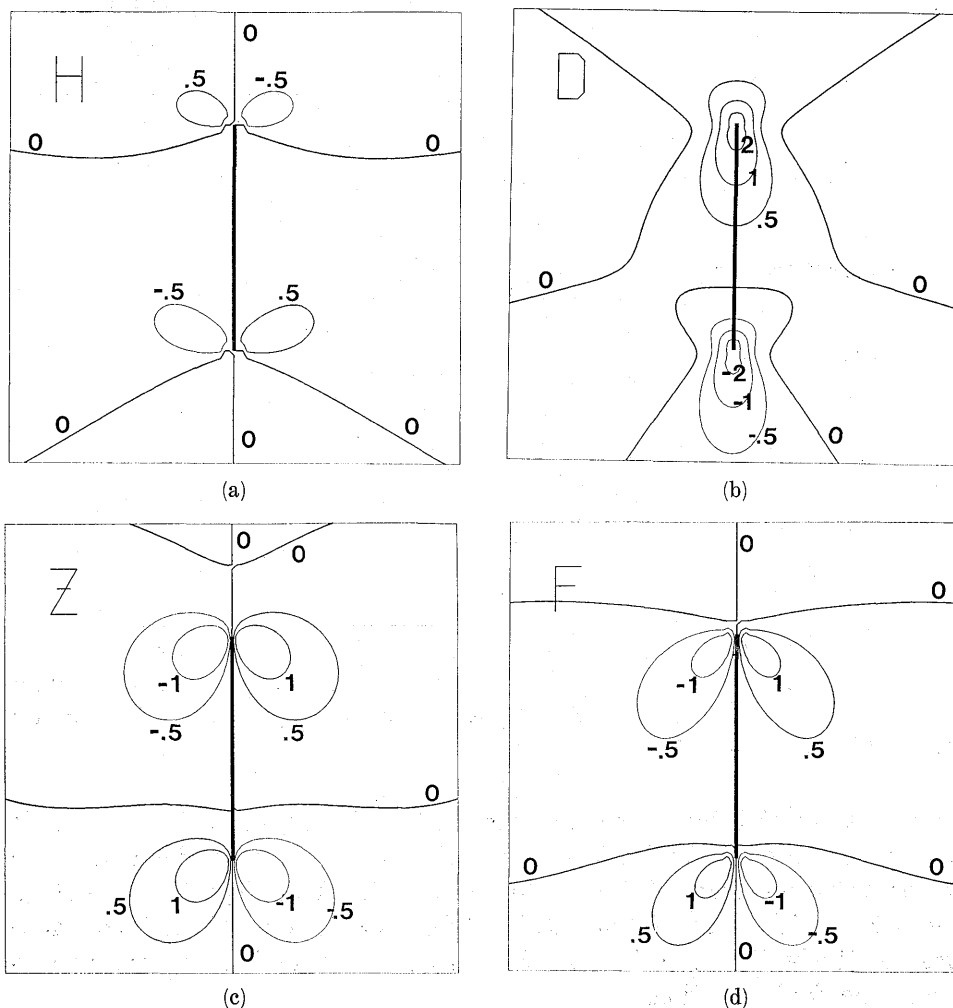


Fig. 27. The magnetic field accompanying left-lateral strike-slip faulting of a north-south oriented fault. (a) Northward (H), (b) eastward (D), (c) vertical (Z) and (d) total intensity (F) respectively. Unit in nT.

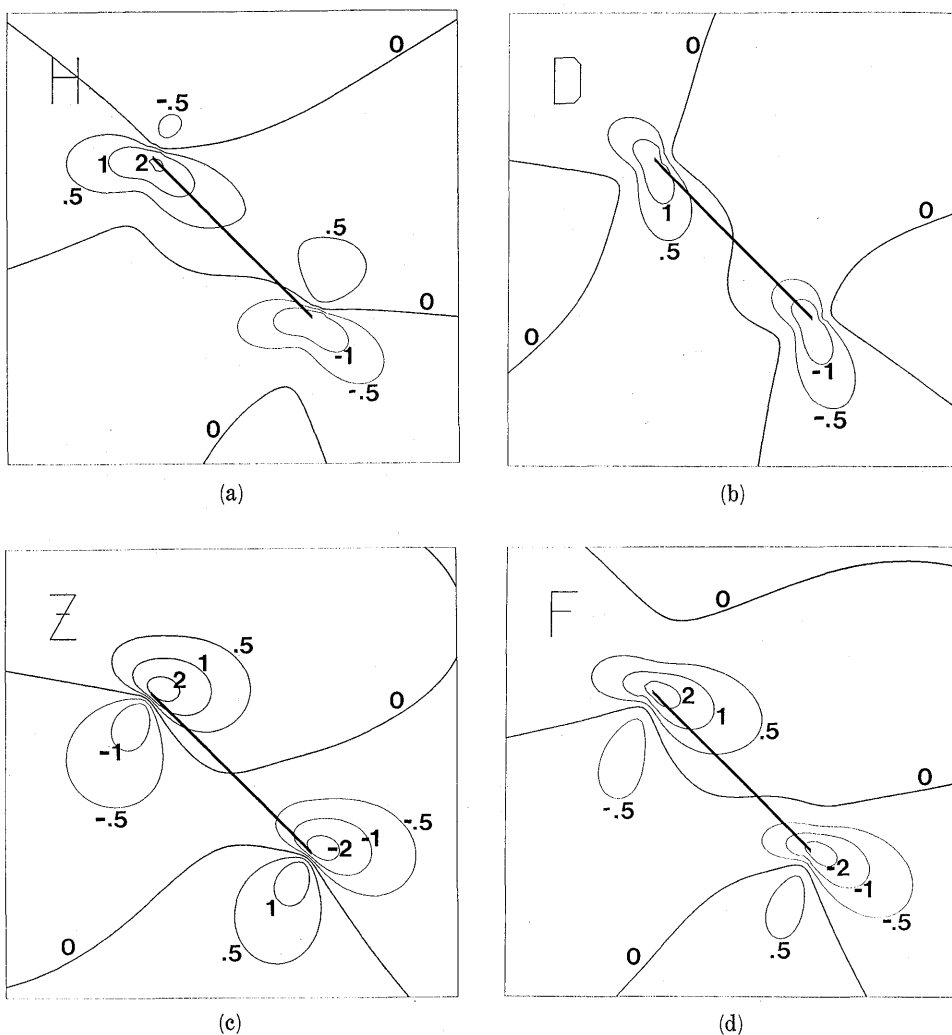


Fig. 28. The magnetic field accompanying left-lateral strike-slip faulting of a NW-SE oriented fault. (a) Northward (H), (b) eastward (D), (c) vertical (Z) and (d) total intensity (F) respectively. Unit in nT.

Final results of integrations are summarized in Appendix E2. Magnetic changes are computed with the same model parameters as given in Table 2, for crack openings of 1 m. They are depicted in Figs. 31, 32 and 33 for N-S, NW-SE and E-W oriented dykes, respectively. Magnetic changes are relatively large, owing to the effect of equivalent source dipoles along the fault position.

Now let us investigate what kind of faulting can generate piezo-magnetic changes effectively. We consider a fault as shown in Fig. 34.

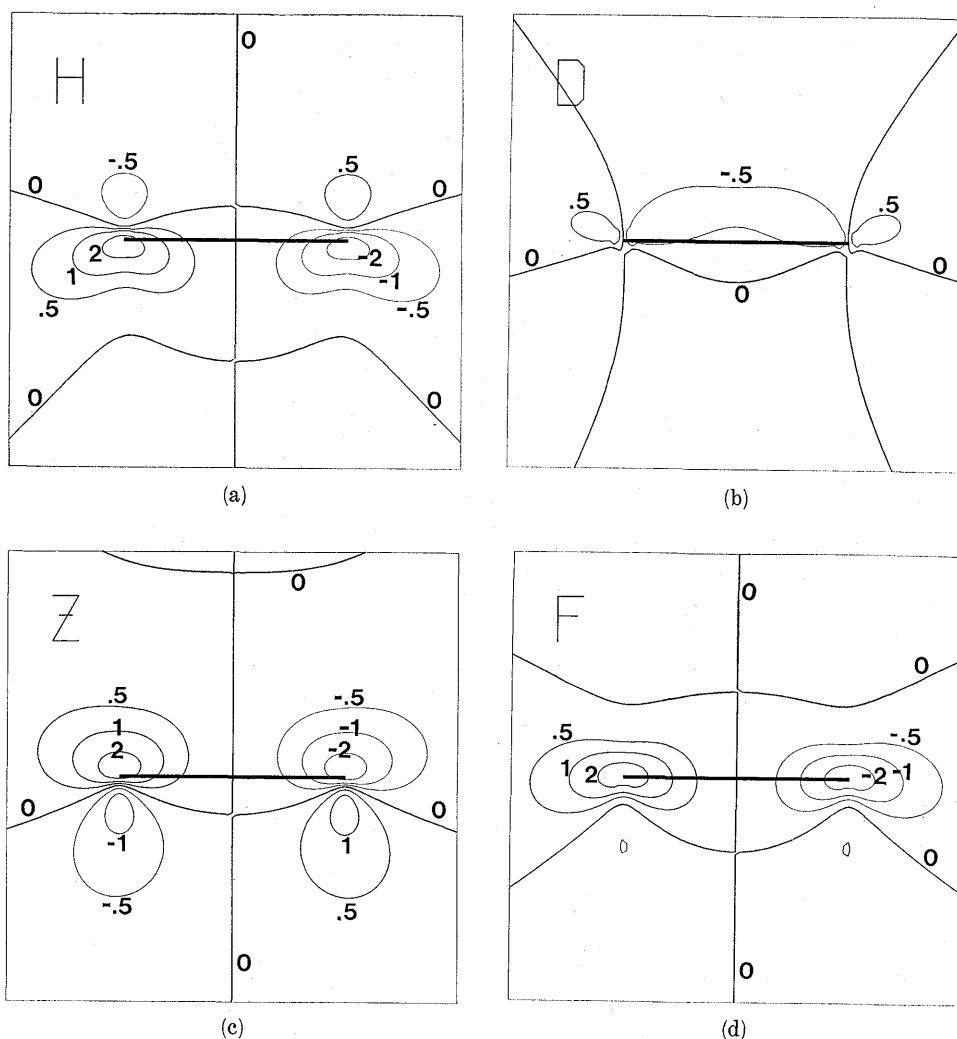


Fig. 29. The magnetic field accompanying left-lateral strike-slip faulting of an E-W oriented fault. (a) Northward (H), (b) eastward (D), (c) vertical (Z) and (d) total intensity (F) respectively. Unit in nT.

Arrows indicate the movement of hanging-wall side block relative to foot-wall side one. We define positive U_1 as left-lateral movement; positive U_2 as thrust motion for $\sin 2\delta > 0$, but as normal faulting for $\sin 2\delta < 0$; and positive U_3 as the crack-opening movement. We introduce the coordinate ξ , measured positive down the fault dip as shown in Fig. 34.

We apply Volterra's formula, eq. (5.5), to such a fault. Piezomagnetic potentials for three kinds of faulting are represented by the follow-

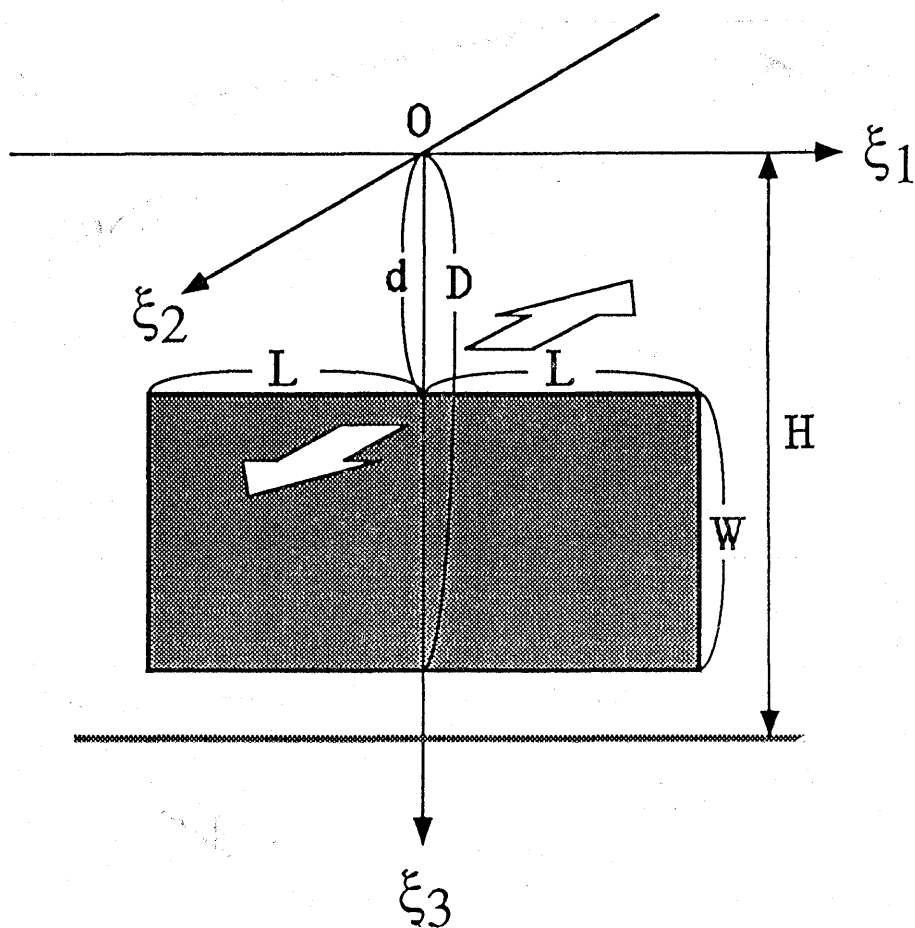


Fig. 30. The geometry of a vertical rectangular tensile fault.

ing integrals:

(i) Strike-slip fault

$$W_s^m = U_1 \int_0^W d\xi \int_{-L}^L \{w_{12}^m \sin \delta - w_{13}^m \cos \delta\} d\xi_1 \quad (5.58)$$

(ii) Dip-slip fault

$$W_D^m = U_2 \int_0^W d\xi \int_{-L}^L \left\{ \frac{1}{2} (w_{33}^m - w_{22}^m) \sin 2\delta + w_{12}^m \cos 2\delta \right\} d\xi_1 \quad (5.59)$$

(iii) Tensile fault

$$W_T^m = U_3 \int_0^W d\xi \int_{-L}^L \{w_{22}^m \sin^2 \delta - w_{23}^m \sin 2\delta + w_{33}^m \cos^2 \delta\} d\xi_1 \quad (5.60)$$

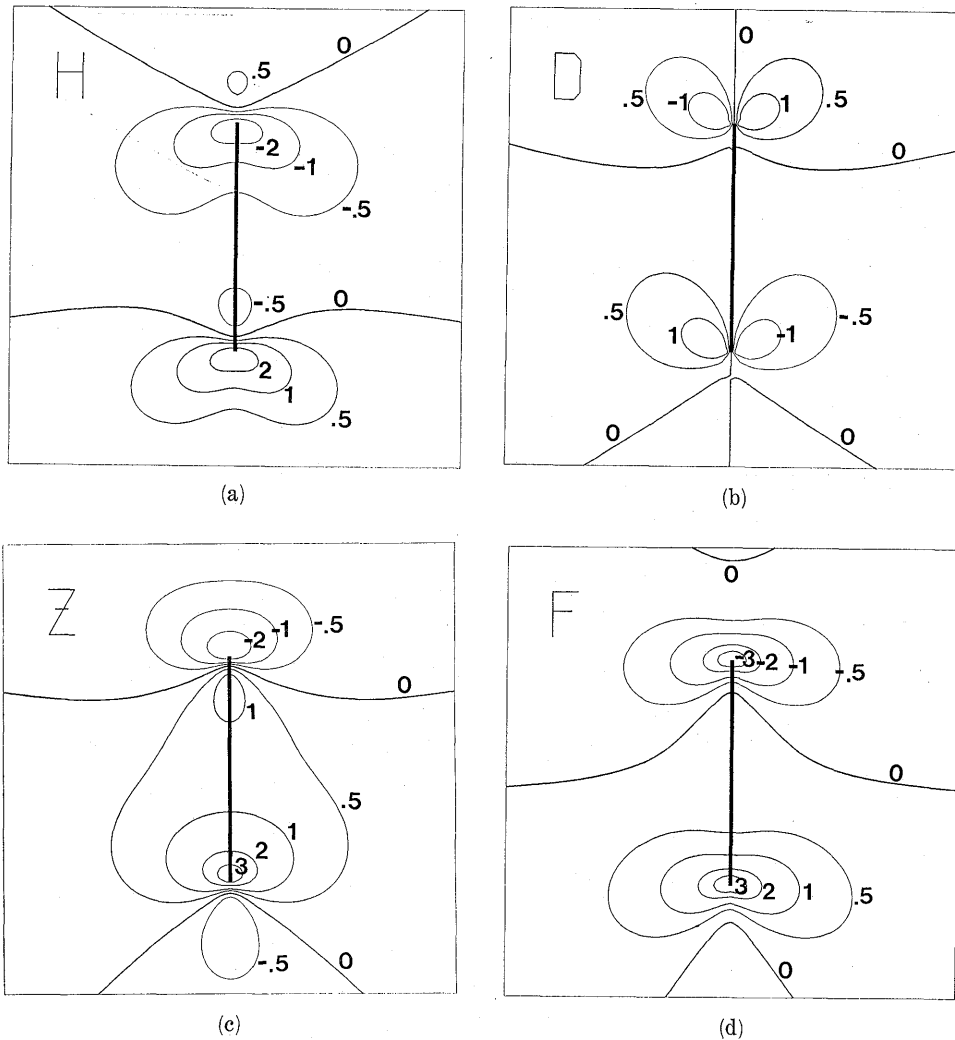


Fig. 31. The magnetic field caused by intrusion of a north-south oriented dyke. (a) Northward (H), (b) eastward (D), (c) vertical (Z) and (d) total intensity (F) respectively. Unit in nT.

In the above equations, $w_{kl}^m = w_{kl}^m(x - \xi_1, y - \xi_2, z, \xi_3)$.

We have already found in section 5.2 that two types of strain nuclei exist: those which produce magnetic source equivalents at the fault position and the remainder which do not. Actually we have only to notice elementary potentials of w_{22}^m and w_{12}^m , which have magnetic sources at the fault position. Consequently we can clearly discriminate what kind of fault motion can generate magnetic field changes most effectively. They are (i) vertical strike-slip fault, (ii) normal or thrust fault inclined

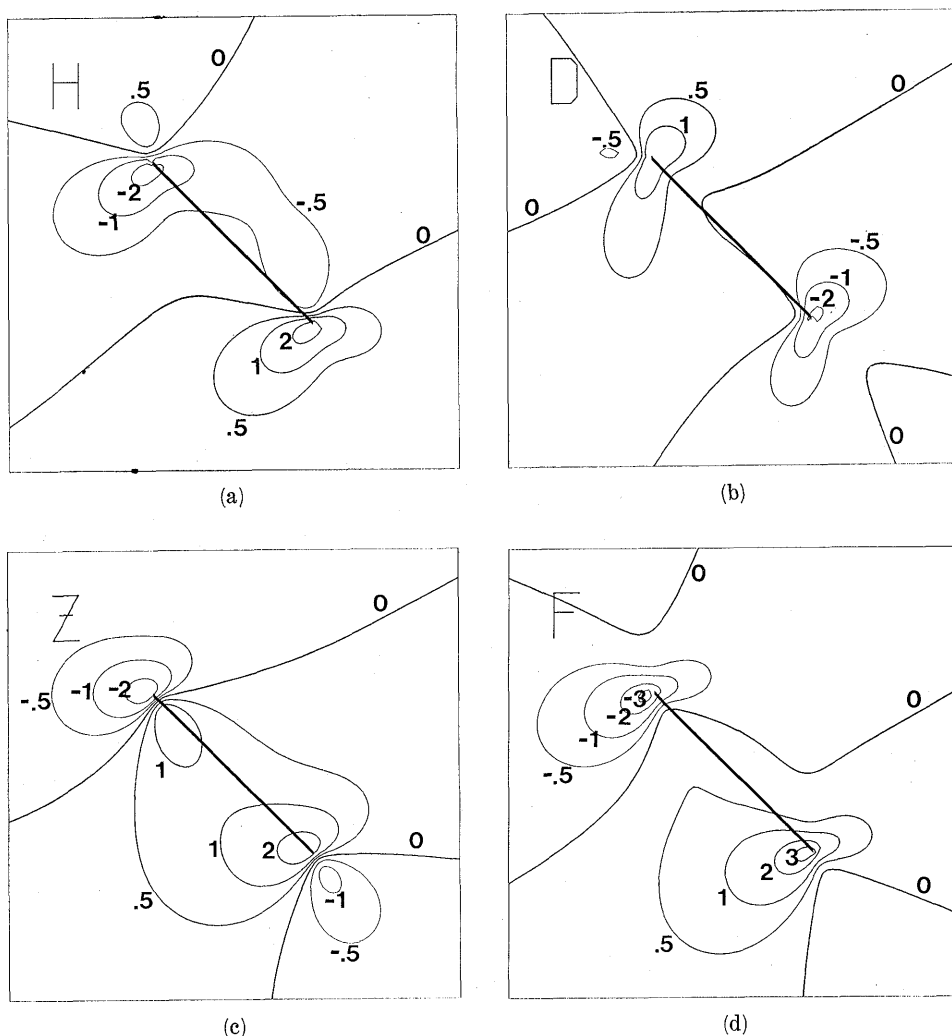


Fig. 32. The magnetic field caused by intrusion of a NW-SE oriented dyke. (a) Northward (H), (b) eastward (D), (c) vertical (Z) and (d) total intensity (F) respectively. Unit in nT.

by 45° , and (iii) vertical tensile fault. Results of integrations in eqs. (5.58) through (5.60) as well as some case studies will be reported elsewhere.

Further Subjects of Tectonomagnetic Modeling

We have so far developed the Green's function method for tectonomagnetic modeling. As has been stated in the Introduction, the traditional volume element method compelled us to do elaborate computer

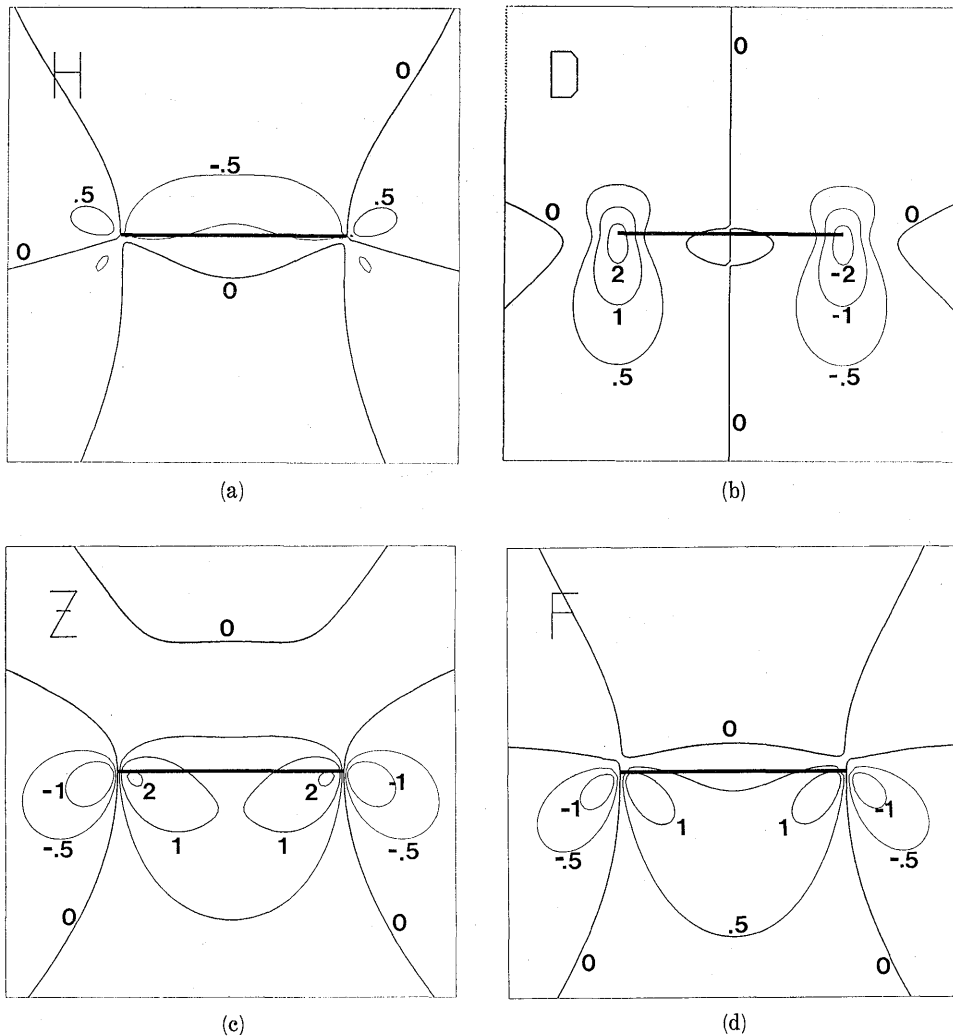


Fig. 33. The magnetic field caused by intrusion of an E-W oriented dyke. (a) Northward (H), (b) eastward (D), (c) vertical (Z) and (d) total intensity (F) respectively. Unit in nT.

work. According to the Green's function method, we no longer need to calculate the stress-induced magnetization itself, but only specify the shape and slippage of the fault. This simplification involves, however, serious defects. In the simplest Volterra dislocations, there exists stress singularity along the fault edge. The Green's function method implicitly builds in such locally divergent stresses. The approximate formula for the linear piezomagnetic effect does not work at a high stress level.

This is the very point on which HAO *et al.* (1982) criticized SASAI's

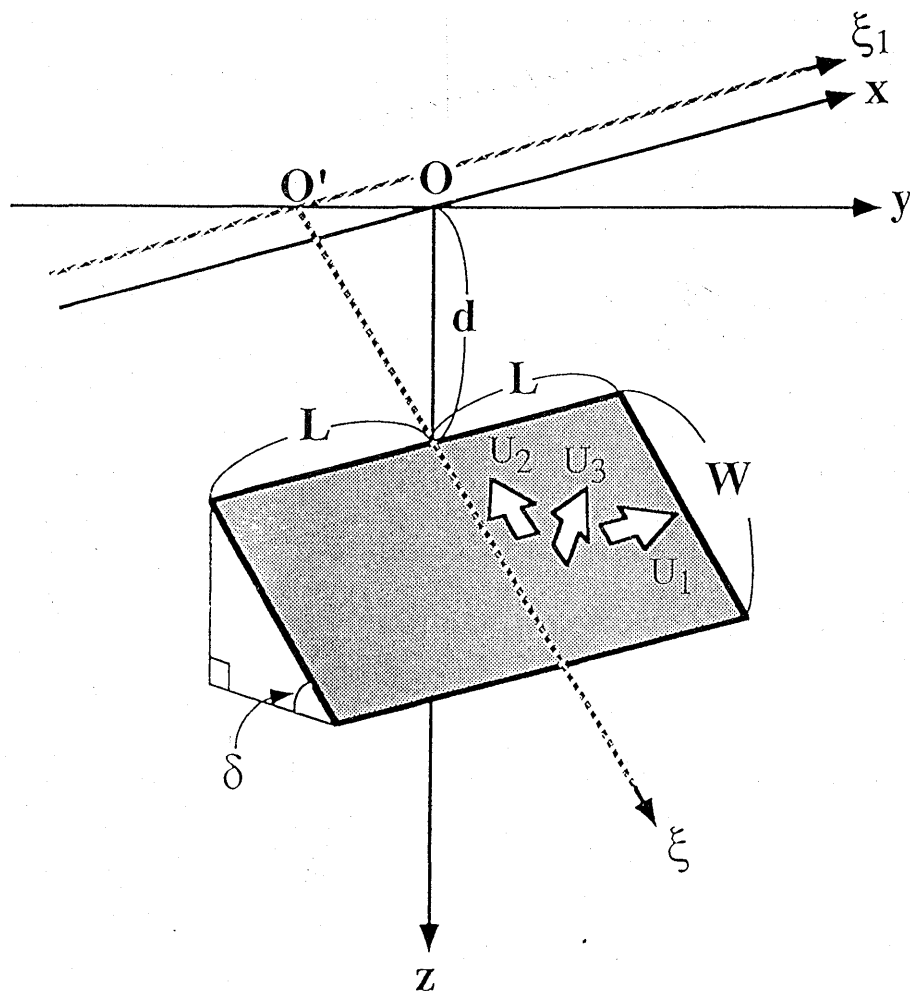


Fig. 34. The geometry of an inclined rectangular fault.

(1980) result. They revived the volume element method and showed that the magnetic field change became smaller for a fault model with the slip discontinuity decreasing step-wise to zero at the edge. ZLOTNICKI and CORNET (1986) investigated such fault and dyke models that had no stress singularities.

Recently, some authors have noticed the enhancement effect of tectonomagnetic signals due to inhomogeneous magnetization of the crust (e.g. UHRENBACHER, 1988; OSHIMAN, 1990). In fact, STACEY (1964) had already discussed this problem in his first seismomagnetic calculations. He estimated the seismomagnetic changes in the case in which one side across a fault is non-magnetic and showed that coseismic changes were

much enhanced. In other words, according to the representation theorem, a magnetic source layer appears along the surface of a strained magnetoelastic body: magnetic lines of force concentrate at the boundaries of magnetic blocks, where the signal enhancement occurs. This gives an effective guide for selecting the most sensitive observation sites in such a case (UHRENBACHER, 1988).

Since we have little knowledge of such tectonomagnetic changes as due to local inhomogeneity of magnetization, we should systematically promote such studies. For that purpose we should develop a hybrid method combining the volume element and the surface integral methods. As we have seen throughout the present study, piezomagnetic modeling is simply analyses of the stress field. The analysis around the singular point we have developed in this study would be useful for further investigation of magnetic changes based on more realistic models of earthquake faulting.

Acknowledgements

I would like to express my sincere gratitude to Emeritus Professor Tsuneji Rikitake, who introduced and guided me into this field of study. My hearty thanks are also due to Professors Takesi Yukutake, Yukio Hagiwara, Takuo Maruyama, Ichiro Murata, Hajimu Kinoshita and Hidefumi Watanabe, who encouraged me during the course of study. Discussions on various aspects of the problem with Hisashi Utada, Naoto Oshiman, Yozo Hamano, Shuhei Okubo, Ichiro Nakagawa, Yasunori Nishida, Yoshikazu Tanaka, Norihiko Sumitomo, Yoshimori Honkura and Toshio Mori were very helpful. I am greatly indebted to Munehisa Sawada, Tsutomu Miyazaki and Yoshinobu Ishikawa for their encouragement and kind help in preparing the present paper.

Appendix A: Derivation of the Isotropic Piezomagnetic Law

Eq. (2.11) is reproduced here:

$$\Delta J_i e_i = J_i \{ \beta_2 (\sigma_j + \sigma_k) + \beta_1 \sigma_i \} e_i \quad (\text{A.1})$$

We may write the stress tensor in Cartesian coordinates as

$$T = \begin{bmatrix} \tau_{xx} & \tau_{yx} & \tau_{zx} \\ \tau_{xy} & \tau_{yy} & \tau_{zy} \\ \tau_{xz} & \tau_{yz} & \tau_{zz} \end{bmatrix} \quad (\text{A.2})$$

$$P^{-1} \cdot T \cdot P = \begin{bmatrix} \sigma_1 & 0 & 0 \\ 0 & \sigma_2 & 0 \\ 0 & 0 & \sigma_3 \end{bmatrix} \quad (\text{A.3})$$

Components of P and P^{-1} are given by

$$P = \begin{bmatrix} \lambda_1 & \lambda_2 & \lambda_3 \\ \mu_1 & \mu_2 & \mu_3 \\ \nu_1 & \nu_2 & \nu_3 \end{bmatrix}, \quad P^{-1} = \begin{bmatrix} \lambda_1 & \mu_1 & \nu_1 \\ \lambda_2 & \mu_2 & \nu_2 \\ \lambda_3 & \mu_3 & \nu_3 \end{bmatrix} \quad (\text{A.4})$$

Let us first investigate the changes in the J_x component: i.e. $J_x = (J_x, 0, 0)^t$. The superscript t denotes the transpose matrix. Substituting $(J_1, J_2, J_3)^t = P^{-1} \cdot (J_x, 0, 0)^t$ into (A.1), we have

$$\Delta J_i = \lambda_i T_i J_x \quad (\text{A.5})$$

where

$$T_i = \beta_2 \Theta + (\beta_1 + \beta_2) \sigma_i \quad (\text{A.6})$$

and

$$\Theta = \sigma_1 + \sigma_2 + \sigma_3 = \tau_{xx} + \tau_{yy} + \tau_{zz} \quad (\text{A.7})$$

On the other hand, the set of unit vectors $\{e_1, e_2, e_3\}$ is related to the original set $\{e_x, e_y, e_z\}$ as follows:

$$\left. \begin{aligned} e_1 &= \lambda_1 e_x + \lambda_2 e_y + \lambda_3 e_z \\ e_2 &= \mu_1 e_x + \mu_2 e_y + \mu_3 e_z \\ e_3 &= \nu_1 e_x + \nu_2 e_y + \nu_3 e_z \end{aligned} \right\} \quad (\text{A.8})$$

We may represent the total magnetization change produced by J_x as ΔJ_x :

$$\begin{aligned} \Delta J_x &= \Delta J_1 e_1 + \Delta J_2 e_2 + \Delta J_3 e_3 \\ &= (S_{xx} e_x + S_{xy} e_y + S_{xz} e_z) \end{aligned} \quad (\text{A.9})$$

where

$$S_{xx} = \lambda_1^2 T_1 + \lambda_2^2 T_2 + \lambda_3^2 T_3 \quad (\text{A.10a})$$

$$S_{xy} = \lambda_1 \mu_1 T_1 + \lambda_2 \mu_2 T_2 + \lambda_3 \mu_3 T_3 \quad (\text{A.10b})$$

$$S_{xz} = \lambda_1 \nu_1 T_1 + \lambda_2 \nu_2 T_2 + \lambda_3 \nu_3 T_3 \quad (\text{A.10c})$$

Multiplying P on both sides of eq. (A.3), we have the following relations:

$$\left. \begin{aligned} \lambda_1 \tau_{xx} + \mu_1 \tau_{xy} + \nu_1 \tau_{xz} &= \lambda_1 \sigma_1 \\ \lambda_2 \tau_{xx} + \mu_2 \tau_{xy} + \nu_2 \tau_{xz} &= \lambda_2 \sigma_2 \\ \lambda_3 \tau_{xx} + \mu_3 \tau_{xy} + \nu_3 \tau_{xz} &= \lambda_3 \sigma_3 \end{aligned} \right\} \quad (\text{A.11})$$

Then we have simply

$$\lambda_1^2 \sigma_1 + \lambda_2^2 \sigma_2 + \lambda_3^2 \sigma_3 = \tau_{xx} \quad (\text{A.12})$$

in which we used the following properties of the modal matrix:

$$\lambda_1^2 + \lambda_2^2 + \lambda_3^2 = 1, \quad \lambda_1\mu_1 + \lambda_2\mu_2 + \lambda_3\mu_3 = 0, \text{ etc.} \quad (\text{A.13})$$

Finally we obtain

$$\begin{aligned} S_{xx} &= \beta_2(\lambda_1^2 + \lambda_2^2 + \lambda_3^2)\Theta + (\beta_1 - \beta_2)(\lambda_1^2\sigma_1 + \lambda_2^2\sigma_2 + \lambda_3^2\sigma_3) \\ &= \beta_2\Theta + (\beta_1 - \beta_2)\tau_{xx} \end{aligned} \quad (\text{A.14a})$$

Similarly we have

$$S_{xy} = (\beta_1 - \beta_2)\tau_{xy} \quad (\text{A.14b})$$

$$S_{xz} = (\beta_1 - \beta_2)\tau_{xz} \quad (\text{A.14c})$$

In the same manner we can obtain the incremental magnetization due to $J_y = (0, J_y, 0)^t$ as

$$S_{yx} = (\beta_1 - \beta_2)\tau_{yx} \quad (\text{A.15a})$$

$$S_{yy} = \beta_2\Theta + (\beta_1 - \beta_2)\tau_{yy} \quad (\text{A.15b})$$

$$S_{yz} = (\beta_1 - \beta_2)\tau_{yz} \quad (\text{A.15c})$$

and the incremental magnetization due to $J_z = (0, 0, J_z)^t$ as

$$S_{zx} = (\beta_1 - \beta_2)\tau_{zx} \quad (\text{A.16a})$$

$$S_{zy} = (\beta_1 - \beta_2)\tau_{zy} \quad (\text{A.16b})$$

$$S_{zz} = \beta_2\Theta + (\beta_1 - \beta_2)\tau_{zz} \quad (\text{A.16c})$$

Summarizing eqs. (A.14), (A.15) and (A.16), we have

$$\Delta J = \begin{bmatrix} S_{xx} & S_{xy} & S_{xz} \\ S_{yx} & S_{yy} & S_{yz} \\ S_{zx} & S_{zy} & S_{zz} \end{bmatrix} \cdot \begin{bmatrix} J_x \\ J_y \\ J_z \end{bmatrix} = S \cdot J \quad (\text{A.17})$$

$$S = \beta_2\Theta + (\beta_1 - \beta_2)T = (\beta_1 + 2\beta_2)\sigma_0 + (\beta_1 - \beta_2)T' \quad (\text{A.18})$$

This is nothing but eq. (2.12) in Chapter 2.

Appendix B: The Double Fourier Transforms

In this paper we define the double Fourier transform and its inverse as follows:

$$f^*(k_1, k_2) = \frac{1}{2\pi} \int_{-\infty}^{\infty} \int_{-\infty}^{\infty} f(x_1, x_2) e^{-i(k_1x_1 + k_2x_2)} dx_1 dx_2 \quad (\text{B.1})$$

$$f(x_1, x_2) = \frac{1}{2\pi} \int_{-\infty}^{\infty} \int_{-\infty}^{\infty} f^*(k_1, k_2) e^{i(k_1x_1 + k_2x_2)} dk_1 dk_2 \quad (\text{B.2})$$

The convolution of two functions $f(x_1, x_2)$ and $g(x_1, x_2)$ is defined by

$$\begin{aligned} h(x_1, x_2) &= \iint_{-\infty}^{\infty} f(x'_1, x'_2) g(x_1 - x'_1, x_2 - x'_2) dx'_1 dx'_2 \\ &= \iint_{-\infty}^{\infty} g(x'_1, x'_2) f(x_1 - x'_1, x_2 - x'_2) dx'_1 dx'_2 \end{aligned} \quad (\text{B.3})$$

It is easily proved that the Fourier transform of $h(x_1, x_2)$ is given by

$$h^*(k_1, k_2) = 2\pi f^*(k_1, k_2) g^*(k_1, k_2) \quad (\text{B.4})$$

We can evaluate the convolution integrals with the aid of eq. (B.4).

All the Fourier transforms required in this study are those of derivatives of the following function:

$$f_1(x_1, x_2) = \frac{1}{\sqrt{x_1^2 + x_2^2 + \zeta^2}} \quad (\zeta > 0) \quad (\text{B.5})$$

Now let us obtain $f_1^*(k_1, k_2)$: i.e.

$$f_1^*(k_1, k_2) = \frac{1}{2\pi} \iint_{-\infty}^{\infty} \frac{1}{\sqrt{x_1^2 + x_2^2 + \zeta^2}} e^{-i(k_1 x_1 + k_2 x_2)} dx_1 dx_2 \quad (\text{B.6})$$

Substituting

$$x_1 = r \cos \theta, \quad x_2 = r \sin \theta, \quad k_1 = k \cos \phi, \quad k_2 = k \sin \phi, \quad (\text{B.7})$$

eq. (B.6) is reduced to

$$f_1^*(k_1, k_2) = \int_0^{\infty} \frac{1}{\sqrt{r^2 + \zeta^2}} J_0(kr) r dr \quad (\text{B.8})$$

in which we use Hansen's integral representation of the Bessel function $J_n(kr)$:

$$J_n(kr) = \frac{(-i)^n}{2\pi} \int_0^{2\pi} e^{ikr \cos \phi} \cos n\phi d\phi \quad (\text{B.9})$$

Multiplying eq. (B.9) for $n=0$ by $e^{-k\zeta}$ and integrating it with respect to k , we obtain the following (WATSON, 1922),

$$\int_0^{\infty} e^{-k\zeta} J_0(kr) dk = \frac{1}{\sqrt{r^2 + \zeta^2}} \quad (\zeta > 0) \quad (\text{B.10})$$

Hankel's inversion theorem is applied to eq. (B.10), which leads to

$$\frac{1}{2\pi} \iint_{-\infty}^{\infty} \frac{1}{\sqrt{x_1^2 + x_2^2 + \zeta^2}} e^{-i(k_1 x_1 + k_2 x_2)} dx_1 dx_2 = \int_0^{\infty} \frac{1}{\sqrt{r^2 + \zeta^2}} J_0(kr) r dr = \frac{e^{-k\zeta}}{k} \quad (\text{B.11})$$

Differentiating eq. (B.11) with respect to ζ , we have the following formula:

$$\frac{1}{2\pi} \iint_{-\infty}^{\infty} \frac{1}{(x_1^2 + x_2^2 + \zeta^2)^{3/2}} e^{-i(k_1 x_1 + k_2 x_2)} dx_1 dx_2 = \frac{e^{-k\zeta}}{\zeta} \quad (\text{B.12})$$

Thus we obtain the Fourier transform of a function which is the derivative of $f_1(x_1, x_2)$ with respect to ζ . Differentiating both sides of eq. (B.2), we have

$$\left\{ \frac{\partial f}{\partial x_1} \right\}^* = i k_1 f^*(k_1, k_2) \quad (\text{B.13})$$

This formula gives the Fourier transform of a function which is the derivative of $f_1(x_1, x_2)$ with respect to x_1 .

Eq. (B.13) implies that differentiation in the space domain is converted simply into a multiplication in the wave number domain. By utilizing this property, we can deal with complicated derivatives; this is called operational calculus. This technique is systematically used in evaluating fundamental piezomagnetic potentials (section 4.2) as well as elementary piezomagnetic potentials (section 5.2). The operational calculus based on eq. (B.13) sometimes does not work as it is, because the (inverse) Fourier transform of $i k_1 f^*(k_1, k_2)$ does not always exist even if $f^*(k_1, k_2)$ itself exists. In such cases, we must take into account the Fourier transform in the sense of *distribution* or *generalized function* (VLADIMIROV, 1971). Such a generalized Fourier transform was actually used by SASAI (1980). Details are given in Appendix A of SASAI (1980).

Besides, eq. (B.13) implies the following useful relation. Once the Fourier transform of a function $g(x_1, x_2)$ is known, $(i k_1)^{-1} g^*(k_1, k_2)$ gives the Fourier transform of a function G , which is an indefinite integral of $g(x_1, x_2)$ with respect to x_1 : $G = \int g(x_1, x_2) dx_1$. With the help of this property, integrations with respect to ξ_1 in the fault models can be easily achieved (see section 5.4).

Looking back to the derivation of eq. (B.8), we find that the following expressions hold good in general:

$$f^*(k_1, k_2) = \int_0^\infty f(x_1, x_2) J_0(kr) r dr \quad (\text{B.14a})$$

$$f(x_1, x_2) = \int_0^\infty f^*(k_1, k_2) J_0(kr) k dk \quad (\text{B.14b})$$

Eqs. (B.14) are called the Hankel transform. Differentiating both sides of eq. (B.14b) with respect to x_1 , we have

$$\frac{\partial f}{\partial x_1} = \int_0^\infty f^*(k_1, k_2) \frac{\partial J_0(kr)}{\partial x_1} k dk = - \frac{x_1}{r} \int_0^\infty f^*(k_1, k_2) J_1(kr) k^2 dk \quad (\text{B.15})$$

This relation is frequently used in obtaining the piezomagnetic field due to a circular load (section 4.3) and in the formulation of the multiple tension-crack model (section 5.3).

Appendix C: The Integrals of Lipschitz-Hankel Type

Reduction of Φ_n functions to Lipschitz-Hankel type integrals

The integral of Lipschitz-Hankel type is defined by EASON *et al.* (1955) as

$$I(\mu, \nu; \lambda) = \int_0^\infty J_\mu(at) J_\nu(bt) e^{-c^2 t^2} dt \quad (c > 0) \quad (C.1)$$

We consider here only the case in which λ , μ and ν are integers; hence we replace these letters with l , m and n . The problem is to reduce the following integral into the form of eq. (C.1).

$$\Phi = \int_0^\pi \frac{\cos(j\phi)}{\{\rho_\phi\}^k} d\phi \quad (C.2)$$

in which j and k are non-negative integers. ρ_ϕ is given by

$$\rho_\phi = \sqrt{R^2 + c^2} \quad (c > 0) \quad (C.3)$$

where

$$R^2 = a^2 - 2ab \cos \phi + b^2 \quad (C.4)$$

Such a simple form of integral cannot be expressed with elementary functions. This sort of integral inevitably appears in any potential problem with axial symmetry.

Let us first investigate

$$\Phi_1 = \int_0^\pi \frac{1}{\rho_\phi} d\phi \quad (C.5)$$

We start from the Lipschitz integral (WATSON, 1922):

$$\int_0^\infty e^{-ct} J_0(Rt) dt = \frac{1}{\sqrt{R^2 + c^2}} \quad (C.6)$$

Substituting eq. (C.6) into eq. (C.5) and changing the order of integrations with respect to t and ϕ , we obtain

$$\Phi_1 = \int_0^\infty e^{-ct} dt \int_0^\pi J_0(Rt) d\phi \quad (C.7)$$

We recall Gegenbauer's addition theorem (WATSON, 1922):

$$J_0(Rt) = J_0(at) J_0(bt) + 2 \sum_{m=1}^\infty J_m(at) J_m(bt) \cdot \cos m\phi \quad (C.8)$$

Integrating both sides of eq. (C.8) with respect to ϕ from 0 to π , we find

$$\int_0^\pi J_0(Rt) d\phi = \pi J_0(at) J_0(bt) \quad (\text{C.9})$$

which is put into (C.7) to obtain

$$\Phi_1 = \pi \int_0^\infty J_0(at) J_0(bt) e^{-ct} dt = \pi I(0, 0; 0) \quad (\text{C.10})$$

Differentiating (C.5) with respect to c and taking eq. (C.10) into account, we find

$$\Phi_3 = -\frac{1}{c} \frac{\partial \Phi_1}{\partial c} = \frac{\pi}{c} I(0, 0; 1) \quad (\text{C.11})$$

The procedure to obtain eq. (C.10) and eq. (C.11) is the fundamental technique to reduce Φ_n functions to Lipschitz-Hankel type integrals. We summarize only the results in the following.

$$\Phi_2 = \pi I(1, 1; 0) \quad (\text{C.12a})$$

$$\Phi_4 = \frac{\pi}{c} I(1, 1; 1) \quad (\text{C.12b})$$

$$\Phi_5 = \frac{\pi}{c} I(2, 2; 1) \quad (\text{C.12c})$$

$$\Phi_6 = \frac{\pi}{3c^3} \{cI(0, 0; 2) + I(0, 0; 1)\} \quad (\text{C.12d})$$

$$\Phi_7 = \frac{\pi}{3c^3} \{cI(1, 1; 2) + I(1, 1; 1)\} \quad (\text{C.12e})$$

$$\Phi_8 = \frac{\pi}{3c^3} \{cI(2, 2; 2) + I(2, 2; 1)\} \quad (\text{C.12f})$$

$$\Phi_9 = \frac{\pi}{3c^3} \{cI(3, 3; 2) + I(3, 3; 1)\} \quad (\text{C.12g})$$

The reason why we use a more complicated expression of the Lipschitz-Hankel type is obvious: differentials of these functions (C.1) with respect to a , b or c reduce again to the same type of integrals with different m , n or l . In the following we will find that these functions are expressible as complete elliptic integrals. To directly differentiate complete elliptic integrals is, however, a mathematical mess.

Lipschitz-Hankel Integrals as Expressed by Complete Elliptic Integrals

Some of the integrals (C.1) have already been given as combinations of complete elliptic integrals by EASON *et al.* (1955). We follow their notations. They define complete elliptic integrals of the first and the second kind multiplied by $2/\pi$ as follows.

$$F_0(k) = \frac{2}{\pi} \int_0^{\pi/2} \frac{d\phi}{\sqrt{1-k^2 \sin^2 \phi}} \quad (\text{C.13})$$

$$E_0(k) = \frac{2}{\pi} \int_0^{\pi/2} \sqrt{1-k^2 \sin^2 \phi} d\phi \quad (\text{C.14})$$

where

$$k^2 = \frac{4ab}{(a+b)^2 + c^2} \quad (\text{C.15})$$

a , b and c are parameters in the integral (C.1). We need $I(0, 0; 0)$, $I(1, 1; 0)$, $I(0, 0; 1)$, $I(1, 1; 1)$, $I(0, 0; 2)$, $I(1, 1; 2)$, $I(2, 2; 1)$, $I(2, 2; 2)$, $I(3, 3; 1)$, and $I(3, 3; 2)$. The first four functions are found in EASON *et al.*'s (1955) table, and are reproduced here:

$$I(0, 0; 0) = \frac{k}{2\sqrt{ab}} F_0(k) \quad (\text{C.16a})$$

$$I(1, 1; 0) = \frac{1}{k\sqrt{ab}} \left\{ \left(1 - \frac{1}{2} k^2 \right) F_0(k) - E_0(k) \right\} \quad (\text{C.16b})$$

$$I(0, 0; 1) = \frac{ck^3}{8k'^2(ab)^{3/2}} E_0(k) \quad (\text{C.16c})$$

$$I(1, 1; 1) = \frac{ck}{4(ab)^{3/2}} \left\{ \left(1 - \frac{1}{2} k^2 \right) k'^{-2} E_0(k) - F_0(k) \right\} \quad (\text{C.16d})$$

where $k'^2 = 1 - k^2$.

The remaining six functions have the form of either $I(n, n; 1)$, or $I(n, n; 2)$. EASON *et al.* (1955) gave the formula:

$$I(n, n; 1) = \frac{(-1)^n ck^3}{4\pi(ab)^{3/2}} \int_0^{\pi/2} \frac{\cos(2n\phi) d\phi}{(1-k^2 \sin^2 \phi)^{3/2}} \quad (\text{C.17})$$

Differentiating (C.17) with respect to c , we have

$$I(n, n; 2) = -\frac{\partial}{\partial c} I(n, n; 1)$$

$$= \frac{(-1)^n k^3}{4\pi(ab)^{3/2}} \left\{ - \int_0^{\pi/2} \frac{\cos 2n\phi}{(1-k^2 \sin^2 \phi)^{3/2}} d\phi + \frac{3c^2 k^2}{4ab} \int_0^{\pi/2} \frac{\cos 2n\phi}{(1-k^2 \sin^2 \phi)^{5/2}} d\phi \right\} \quad (\text{C.18})$$

Some additional formulas are necessary for further calculations:

$$\int_0^{\pi/2} \frac{d\phi}{(1-k^2 \sin^2 \phi)^{3/2}} = \frac{1}{k'^2} E(k) \quad (\text{C.19a})$$

$$\int_0^{\pi/2} \frac{d\phi}{(1-k^2 \sin^2 \phi)^{5/2}} = -\frac{1}{3k'^2} F(k) + \frac{2(k'^2+1)}{3k'^4} E(k) \quad (\text{C.19b})$$

$$\int_0^{\pi/2} (1-k^2 \sin^2 \phi)^{3/2} d\phi = \frac{2}{3} (1+k'^2) E(k) - \frac{k'^2}{3} F(k) \quad (\text{C.19c})$$

(Eq. (C.19b) corresponds to eq. (3.7) in EASON *et al.* (1955). The latter is incorrect, probably owing to a misprint.)

Putting $n=0$ through 3 in eq. (C.17) and (C.18), we can obtain the following:

$$I(0, 0; 2) = \frac{k^3}{8(ab)^{3/2} k'^2} \left[-E_0(k) + \frac{c^2 k^2}{4ab} \left\{ -F_0(k) + \frac{2(1+k'^2)}{k'^2} E_0(k) \right\} \right] \quad (\text{C.20a})$$

$$I(1, 1; 2) = \frac{k}{8(ab)^{3/2} k'^2} \left[2k'^2 F_0(k) - (1+k'^2) E_0(k) - \frac{c^2 k^2}{4ab} \left\{ (1+k'^2) F_0(k) - \frac{2(1-k^2+k^4)}{k'^2} E_0(k) \right\} \right] \quad (\text{C.20b})$$

$$I(2, 2; 1) = \frac{c}{8(ab)^{3/2} k} \left\{ -8(2-k^2) F_0(k) + \frac{k^4-16k^2+16}{k'^2} E_0(k) \right\} \quad (\text{C.20c})$$

$$I(2, 2; 2) = \frac{1}{8(ab)^{3/2} k} \left[8(2-k^2) F_0(k) - \frac{k^4-16k^2+16}{k'^2} E_0(k) + \frac{c^2 k^2}{4abk'^2} \left\{ (16-16k^2-k^4) F_0(k) - \frac{2(2-k^2)(4-4k^2-k^4)}{k'^2} E_0(k) \right\} \right] \quad (\text{C.20d})$$

$$I(3, 3; 1) = \frac{c}{8(ab)^{3/2} k^3} \left[(2-k^2) \left\{ \frac{k^4-16k^2+16}{k'^2} + \frac{80}{3} \right\} E_0(k) - \left\{ 6(3k^4-16k^2+16) - \frac{32}{3} k'^2 \right\} F_0(k) \right] \quad (\text{C.20e})$$

$$I(3, 3; 2) = \frac{1}{8(ab)^{3/2} k^3} \left[-(2-k^2) \left\{ \frac{k^4-16k^2+16}{k'^2} + \frac{80}{3} \right\} E_0(k) \right]$$

$$\begin{aligned}
& + \left\{ 6(3k^4 - 16k^2 + 16) - \frac{32}{3}k'^2 \right\} F_0(k) \\
& - \frac{3c^2k^2}{4abk'^2} \left\{ 2 \left(9k^4 - 64k^2 + 64 - \frac{(k^2 - 2)^2(k^4 - 16k^2 + 16)}{3k'^2} \right) E_0(k) \right. \\
& \left. + (k^2 - 2) \left(48k'^2 - \frac{k^4 - 16k^2 + 16}{3} \right) F_0(k) \right\} \quad (C.20f)
\end{aligned}$$

All these functions have ab and k in the denominators, which cause numerical instability when a or b approaches zero. For small values of a , b and k , we have power series expansions with respect to k with the aid of series representations for $F_0(k)$ and $E_0(k)$. They are summarized in SASAI (1991). Only five formulas are listed here, which are required in section 3.4.

$$I(0, 0; 0) = \frac{1}{\sqrt{(a+b)^2 + c^2}} \left\{ 1 + \frac{1}{4}k^2 + \frac{9}{64}k^4 + \dots \right\} \quad (C.21a)$$

$$I(1, 1; 0) = \frac{1}{8} \frac{k^2}{\sqrt{(a+b)^2 + c^2}} \left\{ 1 + \frac{3}{4}k^2 + \frac{75}{128}k^4 + \dots \right\} \quad (C.21b)$$

$$I(0, 0; 1) = \frac{c}{\{(a+b)^2 + c^2\}^{3/2}} \left\{ 1 + \frac{3}{4}k^2 + \frac{45}{64}k^4 + \dots \right\} \quad (C.21c)$$

$$I(1, 1; 1) = \frac{3}{8} \frac{ck^2}{\{(a+b)^2 + c^2\}^{3/2}} \left\{ 1 + \frac{5}{4}k^2 + \frac{175}{128}k^4 + \dots \right\} \quad (C.21d)$$

$$I(2, 2; 1) = \frac{15}{128} \frac{ck^4}{\{(a+b)^2 + c^2\}^{3/2}} \left\{ 1 + \frac{7}{4}k^2 + \dots \right\} \quad (C.21e)$$

Other Important Integrals Required in Chapter 4

We need some other kind of integrals to compute the piezomagnetic field due to a circular load. They are given as follows (EASON *et al.*, 1955):

$$\begin{aligned}
I(1, 1; -1) = & \begin{cases} \frac{cE_0(k)}{2k\sqrt{ab}} - \frac{kc}{4ab\sqrt{ab}} \left(a^2 + b^2 + \frac{1}{2}c^2 \right) F_0(k) + \frac{a^2 - b^2}{4ab} A_0 + \frac{b}{2a} & (a > b) \\ \frac{c}{2ka} E_0(k) - \frac{kc}{4a^3} \left(2a^2 + \frac{1}{2}c^2 \right) F_0(k) + \frac{1}{2} & (a = b) \\ \frac{cE_0(k)}{2k\sqrt{ab}} - \frac{kc}{4ab\sqrt{ab}} \left(a^2 + b^2 + \frac{1}{2}c^2 \right) F_0(k) + \frac{b^2 - a^2}{4ab} A_0 + \frac{a}{2b} & (a < b) \end{cases} \quad (C.22a)
\end{aligned}$$

$$I(1, 0; 0) = \begin{cases} \frac{kc}{4a\sqrt{ab}}F_0(k) - \frac{1}{2a}A_0 + \frac{1}{a} & (a > b) \\ -\frac{kc}{4a^2}F_0(k) + \frac{1}{2a} & (a = b) \\ -\frac{kc}{4a\sqrt{ab}}F_0(k) + \frac{1}{2a}A_0 & (a < b) \end{cases} \quad (\text{C.22b})$$

$$I(1, 0; 1) = \frac{k^3(a^2 - b^2 - c^2)}{16ak'^2(ab)^{3/2}}E_0(k) + \frac{k}{4a\sqrt{ab}}F_0(k) \quad (\text{C.22c})$$

where A_0 is Heuman's lambda function multiplied by $2/\pi$. A_0 is related to the complete elliptic integral of the third kind as

$$A_0 = \frac{2}{\pi}(1-p)^{1/2}(1-k^2/p)^{1/2} \int_0^{\pi/2} \frac{d\phi}{(1-p\sin^2\phi)\sqrt{1-k^2\sin^2\phi}} \quad (\text{C.23})$$

where

$$p = \frac{4ab}{(a+b)^2} \quad (\text{C.24})$$

Heuman's lambda function can be effectively estimated by NAGY's (1965) method, while complete integrals of the first and second kind are computed with HASTING's (1955) formulas.

Appendix D: Three Constituents of the Elementary Piezomagnetic Potentials

D1: Fourier transforms of the contribution from the Curie surface

We briefly summarize the procedure to calculate Fourier transforms as given by eq. (5.11). This is quite similar to the method developed by SASAI (1980) in obtaining the type I solution of elementary piezomagnetic potentials. As shown by eq. (5.10), the displacement due to an elementary dislocation can be derived from differentiation of the Galerkin vector. By virtue of the property of the Fourier transform, i.e. eq. (B.13) in Appendix B, the Fourier transforms of the displacement field can be expressed with transforms of the Galerkin vector multiplied by (for example) ik_i . Actually the Fourier transforms of the displacement T_{kl}^m are given as follows:

$$T_{kl}^{1*} = (\alpha k_1^2 - k^2 + p^2)\Gamma_{kl}^{1*} + \alpha k_1 k_2 \Gamma_{kl}^{2*} - \alpha i k_1 p (\Gamma_{kl}^{3*} + \Gamma_{kl}^{*}) \quad (\text{D.1a})$$

$$T_{kl}^{2*} = \alpha k_1 k_2 \Gamma_{kl}^{1*} + (\alpha k_2^2 - k^2 + p^2)\Gamma_{kl}^{2*} - \alpha i k_2 p (\Gamma_{kl}^{3*} + \Gamma_{kl}^{*}) \quad (\text{D.1b})$$

$$T_{kl}^{3*} = -\alpha i k_1 p \Gamma_{kl}^{1*} - \alpha i k_2 p \Gamma_{kl}^{2*} + (-k^2 + (1-\alpha)p^2)(\Gamma_{kl}^{3*} + \Gamma_{kl}^{*}) \quad (\text{D.1c})$$

in which p is a differential operator:

$$p = \frac{\partial}{\partial x_3} \quad (\text{D.2})$$

Utilizing the same property, we obtain the Fourier transforms of S_{kl}^{mz} 's as

$$\begin{aligned} (4\alpha-1)S_{kl}^{1z*} = & \{(1-\alpha)p^3 - (1-\alpha)k^2p + \alpha(2\alpha+1)k_1^2p\}\Gamma_{kl}^{1*} \\ & + \alpha(2\alpha+1)k_1k_2p\Gamma_{kl}^{2*} \\ & + \{-3\alpha ik_1k^2 + 2\alpha(1-\alpha)ik_1p^2\}(\Gamma_{kl}^{3*} + \Gamma_{kl}^{*}) \end{aligned} \quad (\text{D.3a})$$

$$\begin{aligned} (4\alpha-1)S_{kl}^{2z*} = & \alpha(2\alpha+1)k_1k_2p\Gamma_{kl}^{1*} \\ & + \{(1-\alpha)p^3 - (1-\alpha)k^2p + \alpha(2\alpha+1)k_2^2p\}\Gamma_{kl}^{2*} \\ & + \{-3\alpha ik_2k^2 + 2\alpha(1-\alpha)ik_2p^2\}(\Gamma_{kl}^{3*} + \Gamma_{kl}^{*}) \end{aligned} \quad (\text{D.3b})$$

$$\begin{aligned} (4\alpha-1)S_{kl}^{3z*} = & \{-3\alpha ik_1p^2 + 2\alpha(1-\alpha)ik_1k^2\}\Gamma_{kl}^{1*} \\ & + \{-3\alpha ik_2p^2 + 2\alpha(1-\alpha)ik_2k^2\}\Gamma_{kl}^{2*} \\ & + \{-(1+2\alpha^2)k^2p + (1-\alpha)p^3\}(\Gamma_{kl}^{3*} + \Gamma_{kl}^{*}) \end{aligned} \quad (\text{D.3c})$$

Fourier transforms of all the Galerkin vectors are explicitly given by SASAI (1980). Eqs. (D.1) and (D.3) can be calculated with his results. Substituting S_{kl}^{mz} 's and T_{kl}^{mz} 's into eq. (5.11), we arrive at Fourier transforms of $w_{kl}^{m(H)}$'s. They are given as follows.

$$(kl) = (11)$$

$$\begin{aligned} \frac{2}{C_x} w_{11}^{x(H)*} = & \left[\frac{3\alpha}{4\alpha-1} \frac{ik_1}{k} + (2-\alpha) \frac{ik_1k_2^2}{k^3} + \frac{2\alpha(\alpha-1)}{4\alpha-1} \xi_3 \frac{ik_1^3}{k^2} \right. \\ & + \left\{ -\frac{18\alpha^2}{4\alpha-1} \frac{ik_1^3}{k^2} + \frac{6\alpha(1-2\alpha)}{4\alpha-1} \frac{ik_1k_2^2}{k^2} + \frac{6\alpha^2}{4\alpha-1} \xi_3 \frac{ik_1^3}{k} \right\} H \Big] e^{-kC_3} \\ & + \left\{ \left[\frac{5\alpha-2}{4\alpha-1} \frac{ik_1}{k} + \alpha \frac{ik_1k_2^2}{k^3} + \frac{2\alpha(1-\alpha)}{4\alpha-1} (\xi_3 - H) \frac{ik_1^3}{k^2} \right] e^{-kC_1} \quad (H < \xi_3) \right. \\ & + \left. \left[\frac{\alpha(1+8\alpha)}{4\alpha-1} \frac{ik_1}{k} + \alpha \frac{ik_1k_2^2}{k^3} - \frac{6\alpha^2}{4\alpha-1} (H - \xi_3) \frac{ik_1^3}{k^2} \right] e^{-kC_2} \quad (H > \xi_3) \right\} \end{aligned} \quad (\text{D.4a})$$

$$\begin{aligned} \frac{2}{C_y} w_{11}^{y(H)*} = & \left[-\frac{2(1-2\alpha)(1-\alpha)}{4\alpha-1} \frac{ik_2}{k} + (\alpha-2) \frac{ik_1^2k_2}{k^3} - \frac{2\alpha(1-\alpha)}{4\alpha-1} \xi_3 \frac{ik_1^2k_2}{k^2} \right. \\ & + \left\{ -\frac{18\alpha^2}{4\alpha-1} \frac{ik_1^2k_2}{k^2} - \frac{12\alpha(2\alpha-1)}{4\alpha-1} \frac{ik_2^3}{k^2} + \frac{12\alpha^2}{4\alpha-1} \xi_3 \frac{ik_1^2k_2}{k} \right\} H \Big] e^{-kC_3} \end{aligned}$$

$$+ \begin{cases} \left[\frac{2(1-2\alpha)(1-\alpha)}{4\alpha-1} \frac{ik_2}{k} - \alpha \frac{ik_1^2 k_2}{k^3} + \frac{2\alpha(1-\alpha)}{4\alpha-1} (\xi_3 - H) \frac{ik_1^2 k_2}{k^2} \right] e^{-kC_1} & (H < \xi_3) \\ \left[-\frac{6\alpha(1-2\alpha)}{4\alpha-1} \frac{ik_2}{k} - \alpha \frac{ik_1^2 k_2}{k^3} - \frac{6\alpha^2}{4\alpha-1} (H - \xi_3) \frac{ik_1^2 k_2}{k^2} \right] e^{-kC_2} & (H > \xi_3) \end{cases} \quad (D.4b)$$

$$\begin{aligned} \frac{2}{C_z} w_{11}^{z(H)*} = & \left[\frac{(1-2\alpha)(2+\alpha)}{4\alpha-1} \frac{k_1^2}{k^2} - \frac{2(1-2\alpha)(1-\alpha)}{4\alpha-1} - \frac{2\alpha(1-\alpha)}{4\alpha-1} \xi_3 \frac{k_1^2}{k} \right. \\ & \left. + \left\{ \frac{6\alpha(2-\alpha)}{4\alpha-1} \frac{k_1^2}{k} + \frac{12\alpha(2\alpha-1)}{4\alpha-1} k - \frac{12\alpha^2}{4\alpha-1} \xi_3 k_1^2 \right\} H \right] e^{-kC_3} \\ & + \begin{cases} \left[\frac{\alpha(2\alpha-5)}{4\alpha-1} \frac{k_1^2}{k^2} + \frac{2(1-2\alpha)(1-\alpha)}{4\alpha-1} + \frac{2\alpha(1-\alpha)}{4\alpha-1} (\xi_3 - H) \frac{k_1^2}{k} \right] e^{-kC_1} & (H < \xi_3) \\ \left[\frac{\alpha(2\alpha-5)}{4\alpha-1} \frac{k_1^2}{k^2} + \frac{6\alpha(1-2\alpha)}{4\alpha-1} + \frac{6\alpha^2}{4\alpha-1} (H - \xi_3) \frac{k_1^2}{k} \right] e^{-kC_2} & (H > \xi_3) \end{cases} \end{aligned} \quad (D.4c)$$

(kl) = (22)

$$w_{22}^{x(H)*}(k_1, k_2) = w_{11}^{y(H)*}(k_2, k_1) \quad (D.5a)$$

$$w_{22}^{y(H)*}(k_1, k_2) = w_{11}^{x(H)*}(k_2, k_1) \quad (D.5b)$$

$$w_{22}^{z(H)*}(k_1, k_2) = w_{11}^{z(H)*}(k_2, k_1) \quad (D.5c)$$

(kl) = (33)

$$\begin{aligned} \frac{2}{C_z} w_{33}^{x(H)*} = & \left[-\alpha \frac{ik_1}{k} + \frac{2\alpha(1-\alpha)}{4\alpha-1} \xi_3 ik_1 \right. \\ & \left. + \left\{ -\frac{6\alpha^2}{4\alpha-1} ik_1 - \frac{12\alpha^2}{4\alpha-1} \xi_3 ik_1 k \right\} H \right] e^{-kC_3} \\ & + \begin{cases} \left[(\alpha-2) \frac{ik_1}{k} - \frac{2\alpha(1-\alpha)}{4\alpha-1} (\xi_3 - H) ik_1 \right] e^{-kC_1} & (H < \xi_3) \\ \left[\alpha \frac{ik_1}{k} + \frac{6\alpha^2}{4\alpha-1} (H - \xi_3) ik_1 \right] e^{-kC_2} & (H > \xi_3) \end{cases} \end{aligned} \quad (D.6a)$$

$$w_{33}^{y(H)*}(k_1, k_2) = w_{33}^{x(H)*}(k_2, k_1) \quad (D.6b)$$

$$\begin{aligned} \frac{2}{C_z} w_{33}^{z(H)*} = & \left[\frac{\alpha(1+2\alpha)}{4\alpha-1} + \frac{2\alpha(1-\alpha)}{4\alpha-1} \xi_3 k + \left\{ \frac{6\alpha^2}{4\alpha-1} k + \frac{12\alpha^2}{4\alpha-1} \xi_3 k^2 \right\} H \right] e^{-kC_3} \\ & + \begin{cases} \left[\frac{-2\alpha^2+7\alpha-2}{4\alpha-1} - \frac{2\alpha(1-\alpha)}{4\alpha-1} (\xi_3 - H) k \right] e^{-kC_1} & (H < \xi_3) \\ \left[-\frac{\alpha(1+2\alpha)}{4\alpha-1} - \frac{6\alpha^2}{4\alpha-1} (H - \xi_3) k \right] e^{-kC_2} & (H > \xi_3) \end{cases} \end{aligned} \quad (D.6c)$$

(kl) = (23)

$$\begin{aligned}
\frac{2}{C_x} w_{23}^{x(H)*} = & \left[-\frac{2\alpha(1-\alpha)}{4\alpha-1} \frac{k_1 k_2}{k^2} - \frac{2\alpha(1-\alpha)}{4\alpha-1} \xi_3 \frac{k_1 k_2}{k} \right. \\
& + \left. \left\{ -\frac{6\alpha^2}{4\alpha-1} \frac{k_1 k_2}{k} + \frac{12\alpha^2}{4\alpha-1} \xi_3 k_1 k_2 \right\} H \right] e^{-kC_3} \\
& + \begin{cases} \left[\frac{2\alpha(1-\alpha)}{4\alpha-1} \frac{k_1 k_2}{k^2} + \frac{2\alpha(1-\alpha)}{4\alpha-1} (\xi_3 - H) \frac{k_1 k_2}{k} \right] e^{-kC_1} & (H < \xi_3) \\ \left[\frac{2\alpha(1-\alpha)}{4\alpha-1} \frac{k_1 k_2}{k^2} + \frac{6\alpha^2}{4\alpha-1} (H - \xi_3) \frac{k_1 k_2}{k} \right] e^{-kC_2} & (H > \xi_3) \end{cases} \quad (D.7a)
\end{aligned}$$

$$\begin{aligned}
\frac{2}{C_y} w_{23}^{y(H)*} = & \left[\frac{3\alpha}{4\alpha-1} - \frac{2\alpha(1-\alpha)}{4\alpha-1} \frac{k_2^2}{k^2} - \frac{2\alpha(1-\alpha)}{4\alpha-1} \xi_3 \frac{k_2^2}{k} \right. \\
& + \left. \left\{ -\frac{6\alpha^2}{4\alpha-1} \frac{k_2^2}{k^2} + \frac{12\alpha^2}{4\alpha-1} \xi_3 \frac{k_2^2}{k} \right\} H \right] e^{-kC_3} \\
& + \begin{cases} \left[\frac{5\alpha-2}{4\alpha-1} + \frac{2\alpha(1-\alpha)}{4\alpha-1} \frac{k_2^2}{k^2} + \frac{2\alpha(1-\alpha)}{4\alpha-1} (\xi_3 - H) \frac{k_2^2}{k} \right] e^{-kC_1} & (H < \xi_3) \\ \left[-\frac{3\alpha}{4\alpha-1} + \frac{2\alpha(1-\alpha)}{4\alpha-1} \frac{k_2^2}{k^2} + \frac{6\alpha^2}{4\alpha-1} (H - \xi_3) \frac{k_2^2}{k} \right] e^{-kC_2} & (H > \xi_3) \end{cases} \quad (D.7b)
\end{aligned}$$

$$\begin{aligned}
\frac{2}{C_z} w_{23}^{z(H)*} = & \left[\alpha \frac{ik_2}{k} + \frac{2\alpha(1-\alpha)}{4\alpha-1} \xi_3 ik_2 \right. \\
& + \left. \left\{ -\frac{6\alpha^2}{4\alpha-1} ik_2 + \frac{12\alpha^2}{4\alpha-1} \xi_3 ik_2 k \right\} H \right] e^{-kC_3} \\
& + \begin{cases} \left[(2-\alpha) \frac{ik_2}{k} - \frac{2\alpha(1-\alpha)}{4\alpha-1} (\xi_3 - H) ik_2 \right] e^{-kC_1} & (H < \xi_3) \\ \left[-\alpha \frac{ik_2}{k} + \frac{6\alpha^2}{4\alpha-1} (H - \xi_3) ik_2 \right] e^{-kC_2} & (H > \xi_3) \end{cases} \quad (D.7c)
\end{aligned}$$

(kl) = 31

$$w_{31}^{x(H)*}(k_1, k_2) = w_{23}^{y(H)*}(k_2, k_1) \quad (D.8a)$$

$$w_{31}^{y(H)*}(k_1, k_2) = w_{23}^{x(H)*}(k_2, k_1) \quad (D.8b)$$

$$w_{31}^{z(H)*}(k_1, k_2) = w_{23}^{z(H)*}(k_2, k_1) \quad (D.8c)$$

(kl) = (12)

$$\begin{aligned}
\frac{2}{C_x} w_{12}^{x(H)*} = & \left[\frac{3\alpha}{4\alpha-1} \frac{ik_2}{k} - (2-\alpha) \frac{ik_1^2 k_2}{k^3} - \frac{2\alpha(1-\alpha)}{4\alpha-1} \xi_3 \frac{ik_1^2 k_2}{k^2} \right. \\
& + \left. \left\{ \frac{6\alpha(\alpha-2)}{4\alpha-1} \frac{ik_1^2 k_2}{k^2} + \frac{12\alpha^2}{4\alpha-1} \xi_3 \frac{ik_1^2 k_2}{k} \right\} H \right] e^{-kC_3}
\end{aligned}$$

$$\begin{aligned}
& + \left\{ \left[\frac{(5\alpha-2)}{4\alpha-1} \frac{ik_2}{k} - \alpha \frac{ik_1^2 k_2}{k^3} + \frac{2\alpha(1-\alpha)}{4\alpha-1} (\xi_3 - H) \frac{ik_1^2 k_2}{k^2} \right] e^{-kC_1} \quad (H < \xi_3) \right. \\
& \left. + \left[\frac{3\alpha}{4\alpha-1} \frac{ik_2}{k} - \alpha \frac{ik_1^2 k_2}{k^3} - \frac{6\alpha^2}{4\alpha-1} (H - \xi_3) \frac{ik_1^2 k_2}{k^2} \right] e^{-kC_2} \quad (H > \xi_3) \right\}
\end{aligned} \quad (D.9a)$$

$$w_{12}^{y(H)*}(k_1, k_2) = w_{12}^{z(H)*}(k_2, k_1) \quad (D.9b)$$

$$\begin{aligned}
\frac{2}{C_z} w_{12}^{z(H)*} = & \left[-\frac{(2\alpha-1)(\alpha+2)}{4\alpha-1} \frac{k_1 k_2}{k^2} - \frac{2\alpha(1-\alpha)}{4\alpha-1} \xi_3 \frac{k_1 k_2}{k} \right. \\
& + \left. \left\{ \frac{6\alpha(2-\alpha)}{4\alpha-1} \frac{k_1 k_2}{k} - \frac{12\alpha^2}{4\alpha-1} \xi_3 k_1 k_2 \right\} H \right] e^{-kC_3} \\
& + \left\{ \left[\frac{\alpha(2\alpha-5)}{4\alpha-1} \frac{k_1 k_2}{k^2} + \frac{2\alpha(1-\alpha)}{4\alpha-1} (\xi_3 - H) \frac{k_1 k_2}{k} \right] e^{-kC_1} \quad (H < \xi_3) \right. \\
& \left. + \left[\frac{\alpha(2\alpha-5)}{4\alpha-1} \frac{k_1 k_2}{k^2} + \frac{6\alpha^2}{4\alpha-1} (H - \xi_3) \frac{k_1 k_2}{k} \right] e^{-kC_2} \quad (H > \xi_3) \right\}
\end{aligned} \quad (D.9c)$$

D2: Contribution from the free surface

$$(kl) = (11)$$

$$\frac{2}{C_x} w_{11}^{x(0)} = -2 \left(-\frac{x}{\rho_1^3} \right) - 2 \left\{ -\frac{1}{4} \frac{x}{\rho_1^3} + \frac{1}{4} \frac{x(3y^2 - x^2)(3\rho_1 + c_1)}{\rho_1^3(\rho_1 + c_1)^3} \right\} \quad (D.10a)$$

$$\frac{2}{C_y} w_{11}^{y(0)} = 2 \left\{ -\frac{1}{4} \frac{y}{\rho_1^3} + \frac{1}{4} \frac{y(3x^2 - y^2)(3\rho_1 + c_1)}{\rho_1^3(\rho_1 + c_1)^3} \right\} \quad (D.10b)$$

$$\frac{2}{C_z} w_{11}^{z(0)} = 2 \left\{ \frac{1}{\rho_1(\rho_1 + c_1)} - \frac{x^2(2\rho_1 + c_1)}{\rho_1^3(\rho_1 + c_1)^2} \right\} \quad (D.10c)$$

$$(kl) = (22)$$

$$w_{22}^{x(0)}(y, x) = w_{11}^{y(0)}(y, x) \quad (D.11a)$$

$$w_{22}^{y(0)}(x, y) = w_{11}^{x(0)}(y, x) \quad (D.11b)$$

$$w_{22}^{z(0)}(x, y) = w_{11}^{z(0)}(y, x) \quad (D.11c)$$

$$(kl) = (33)$$

$$\frac{2}{C_x} w_{33}^{x(0)} = 2 \left(-\frac{x}{\rho_1^3} \right) \quad (D.12a)$$

$$\frac{2}{C_y} w_{33}^{y(0)} = 2 \left(-\frac{y}{\rho_1^3} \right) \quad (D.12b)$$

$$\frac{2}{C_z} w_{33}^{z(0)} = -2 \left(\frac{c_1}{\rho_1^3} \right) \quad (\text{D.12c})$$

$$(kl) = (23)$$

$$\frac{2}{C_x} w_{23}^{x(0)} = 0 \quad (\text{D.13a})$$

$$\frac{2}{C_y} w_{23}^{y(0)} = -2 \left(\frac{c_1}{\rho_1^3} \right) \quad (\text{D.13b})$$

$$\frac{2}{C_z} w_{23}^{z(0)} = -2 \left(-\frac{y}{\rho_1^3} \right) \quad (\text{D.13c})$$

$$(kl) = (31)$$

$$w_{31}^{x(0)}(x, y) = w_{23}^{y(0)}(y, x) \quad (\text{D.14a})$$

$$w_{31}^{y(0)}(x, y) = w_{23}^{x(0)}(y, x) \quad (\text{D.14b})$$

$$w_{31}^{z(0)}(x, y) = w_{23}^{z(0)}(y, x) \quad (\text{D.14c})$$

$$(kl) = (12)$$

$$\frac{2}{C_x} w_{12}^{x(0)} = -2 \left(-\frac{y}{\rho_1^3} \right) + 2 \left\{ -\frac{1}{4} \frac{y}{\rho_1^3} + \frac{1}{4} \frac{y(3x^2 - y^2)(3\rho_1 + c_1)}{\rho_1^3(\rho_1 + c_1)^3} \right\} \quad (\text{D.15a})$$

$$\frac{2}{C_y} w_{12}^{y(0)} = -2 \left(-\frac{x}{\rho_1^3} \right) + 2 \left\{ -\frac{1}{4} \frac{x}{\rho_1^3} + \frac{1}{4} \frac{x(3y^2 - x^2)(3\rho_1 + c_1)}{\rho_1^3(\rho_1 + c_1)^3} \right\} \quad (\text{D.15b})$$

$$\frac{2}{C_z} w_{12}^{z(0)} = 2 \left\{ -\frac{xy(2\rho_1 + c_1)}{\rho_1^3(\rho_1 + c_1)^2} \right\} \quad (\text{D.15c})$$

D3: Contribution from disk surfaces

$$\frac{2}{C_x} w_{11}^{x(K)} = +2 \left(-\frac{x}{\rho_1^3} \right) \quad (\text{D.16a})$$

$$\frac{2}{C_y} w_{11}^{y(K)} = -2 \left(-\frac{y}{\rho_1^3} \right) \quad (\text{D.16b})$$

$$\frac{2}{C_z} w_{11}^{z(K)} = -2 \left(\frac{c_1}{\rho_1^3} \right) \quad (\text{D.16c})$$

$$(kl) = (22)$$

$$w_{22}^{x(K)}(x, y) = w_{11}^{y(K)}(y, x) \quad (\text{D.17a})$$

$$w_{22}^{y(K)}(x, y) = w_{11}^{x(K)}(y, x) \quad (\text{D.17b})$$

$$w_{22}^{z(K)}(x, y) = w_{11}^{z(K)}(y, x) \quad (\text{D.17c})$$

$$(kl) = (33)$$

$$\frac{2}{C_x} w_{33}^{x(K)} = -2 \left(-\frac{x}{\rho_1^3} \right) \quad (\text{D.18a})$$

$$\frac{2}{C_y} w_{33}^{y(K)} = -2 \left(-\frac{y}{\rho_1^3} \right) \quad (\text{D.18b})$$

$$\frac{2}{C_z} w_{33}^{z(K)} = +2 \left(\frac{c_1}{\rho_1^3} \right) \quad (\text{D.18c})$$

$$(kl) = (23)$$

$$\frac{2}{C_x} w_{23}^{x(K)} = 0 \quad (\text{D.19a})$$

$$\frac{2}{C_y} w_{23}^{y(K)} = +2 \left(\frac{c_1}{\rho_1^3} \right) \quad (\text{D.19b})$$

$$\frac{2}{C_z} w_{23}^{z(K)} = +2 \left(-\frac{y}{\rho_1^3} \right) \quad (\text{D.19c})$$

$$(kl) = (31)$$

$$w_{31}^{x(K)}(x, y) = w_{23}^{y(K)}(y, x) \quad (\text{D.20a})$$

$$w_{31}^{y(K)}(x, y) = w_{23}^{x(K)}(y, x) \quad (\text{D.20b})$$

$$w_{31}^{z(K)}(x, y) = w_{23}^{z(K)}(y, x) \quad (\text{D.20c})$$

$$(kl) = (12)$$

$$\frac{2}{C_x} w_{12}^{x(K)} = +2 \left(-\frac{y}{\rho_1^3} \right) \quad (\text{D.21a})$$

$$\frac{2}{C_y} w_{12}^{y(K)} = +2 \left(-\frac{x}{\rho_1^3} \right) \quad (\text{D.21b})$$

$$\frac{2}{C_z} w_{12}^{z(K)} = 0 \quad (\text{D.21c})$$

Appendix E: Piezomagnetic Potential due to Vertical Strike-Slip and Tensile Faults

E1: Vertical strike-slip fault

(a) Horizontal magnetization in the x direction

$$\frac{2}{C_x \Delta U} W_x^{(S)} = W_0^x + \begin{cases} W_I^x & (H \geq D) \\ W_{II}^x & (D > H \geq d) \\ W_{III}^x & (d > H) \end{cases} \quad (\text{E.1a})$$

$$\begin{aligned} W_0^x = & -\frac{3\alpha}{4\alpha-1} \left[\left\{ \tan^{-1} \frac{tp_1}{yS_1} \right\} \parallel_d^D - \left\{ \tan^{-1} \frac{tp_3}{yS_3} \right\} \parallel_d^D \right] \\ & + (2-\alpha) \left[\left\{ \frac{ty}{r^2} \cdot \frac{p_1}{S_1+p_1} \right\} \parallel_d^D - \left\{ \frac{ty}{r^2} \cdot \frac{p_3}{S_3+p_3} \right\} \parallel_d^D \right] \\ & + \frac{2\alpha(1-\alpha)}{4\alpha-1} \left[\left\{ \frac{ty}{r^2} \cdot \frac{p_1^2}{S_1(S_1+p_1)} \right\} \parallel_d^D - z \left\{ \frac{ty}{S_1(S_1+p_1)^2} \right\} \parallel_d^D \right] \\ & - \frac{2\alpha(1-\alpha)}{4\alpha-1} \left[\left\{ \frac{ty}{r^2} \cdot \frac{p_3^2}{S_3(S_3+p_3)} \right\} \parallel_d^D - (z-2H) \left\{ \frac{ty}{S_3(S_3+p_3)^2} \right\} \parallel_d^D \right] \\ & - \frac{6\alpha(2-\alpha)}{4\alpha-1} H \left[\left\{ -\frac{ty}{S_3(S_3+p_3)^2} \right\} \parallel_d^D \right] \\ & + \frac{12\alpha^2}{4\alpha-1} H \left[\left\{ -\frac{ty}{S_3^3} \right\} \parallel_d^D + (z-2H) \left\{ \frac{ty}{r^4} \left(\frac{3p_3}{S_3} - \frac{p_3^3}{S_3^3} \right) \right\} \parallel_d^D \right] \end{aligned} \quad (\text{E.1b})$$

$$\begin{aligned} W_I^x = & \frac{3\alpha}{4\alpha-1} \left[\left\{ \tan^{-1} \frac{tp_1}{yS_1} \right\} \parallel_d^D + \left\{ \tan^{-1} \frac{tp_2}{yS_2} \right\} \parallel_d^D \right] \\ & + \frac{6\alpha}{4\alpha-1} \left[-\left\{ \tan^{-1} \frac{tp_2}{yS_2} \right\} \parallel_d^D \right] \\ & + \alpha \left[\left\{ \frac{ty}{r^2} \cdot \frac{p_1}{S_1+p_1} \right\} \parallel_d^D + \left\{ \frac{ty}{r^2} \cdot \frac{p_2}{S_2+p_2} \right\} \parallel_d^D \right] \\ & - \frac{2\alpha(1-\alpha)}{4\alpha-1} \left[\left\{ \frac{ty}{r^2} \cdot \frac{p_1^2}{S_1(S_1+p_1)} \right\} \parallel_d^D - z \left\{ \frac{ty}{S_1(S_1+p_1)^2} \right\} \parallel_d^D \right] \\ & + \frac{6\alpha^2}{4\alpha-1} \left[\left\{ \frac{ty}{r^2} \cdot \frac{p_2^2}{S_2(S_2+p_2)} \right\} \parallel_d^D - (z-2H) \left\{ \frac{ty}{S_2(S_2+p_2)^2} \right\} \parallel_d^D \right] \\ & - \frac{6\alpha^2}{4\alpha-1} H \left[\left\{ \frac{ty}{S_2(S_2+p_2)^2} \right\} \parallel_d^D \right] \end{aligned} \quad (\text{E.1c})$$

$$W_{II}^x = W_I^x(D \rightarrow H) - \frac{2\alpha(1-\alpha)}{4\alpha-1} H \left[\left\{ -\frac{ty}{S_1(S_1+p_1)^2} \right\} \parallel_d^D \right] \quad (\text{E.1d})$$

$$W_{III}^x = -\frac{2\alpha(1-\alpha)}{4\alpha-1} H \left[\left\{ -\frac{ty}{S_1(S_1+p_1)^2} \right\} \parallel_d^D \right] \quad (\text{E.1e})$$

(b) Horizontal magnetization in the y direction

$$\frac{2}{C_y \Delta U} W_y^{(S)} = W_0^y + \begin{cases} W_I^y & (H \geq D) \\ W_{II}^y & (D > H \geq d) \\ W_{III}^y & (d > H) \end{cases} \quad (\text{E.2a})$$

$$\begin{aligned} W_0^y = & -\frac{3\alpha}{4\alpha-1} \left[-\left\{ \log(S_1 + p_1) \right\} \|_d^D + \left\{ \log(S_3 + p_3) \right\} \|_d^D \right] \\ & + (2-\alpha) \left[-\frac{1}{2} \left\{ \log(S_1 + p_1) + \frac{t^2 - y^2}{r^2} \cdot \frac{p_1}{S_1 + p_1} \right\} \|_d^D \right. \\ & + \left. \frac{1}{2} \left\{ \log(S_3 + p_3) + \frac{t^2 - y^2}{r^2} \cdot \frac{p_3}{S_3 + p_3} \right\} \|_d^D \right] \\ & + \frac{2\alpha(1-\alpha)}{4\alpha-1} \left[\left\{ -\frac{1}{2} \log(S_1 + p_1) + \frac{1}{2} \frac{p_1}{S_1 + p_1} + \frac{y^2}{r^2} \cdot \frac{p_1^2}{S_1(S_1 + p_1)} \right\} \|_d^D \right. \\ & + \left. z \left\{ \frac{1}{S_1 + p_1} - \frac{y^2}{S_1(S_1 + p_1)^2} \right\} \|_d^D \right] \\ & - \frac{2\alpha(1-\alpha)}{4\alpha-1} \left[\left\{ -\frac{1}{2} \log(S_3 + p_3) + \frac{1}{2} \frac{p_3}{S_3 + p_3} + \frac{y^2}{r^2} \cdot \frac{p_3^2}{S_3(S_3 + p_3)} \right\} \|_d^D \right. \\ & + \left. (z-2H) \left\{ \frac{1}{S_3 + p_3} - \frac{y^2}{S_3(S_3 + p_3)^2} \right\} \|_d^D \right] \\ & - \frac{6\alpha(2-\alpha)}{4\alpha-1} H \left[\left\{ \frac{1}{S_3 + p_3} - \frac{y^2}{S_3(S_3 + p_3)^2} \right\} \|_d^D \right] \\ & + \frac{12\alpha^2}{4\alpha-1} H \left[\left\{ \frac{1}{S_3} - \frac{y^2}{S_3^3} \right\} \|_d^D + (z-2H) \left\{ \frac{1}{r^2} \left(\frac{3y^2 - r^2}{r^2} \cdot \frac{p_3}{S_3} - \frac{y^2}{r^2} \cdot \frac{p_3^3}{S_3^3} \right) \right\} \|_d^D \right] \end{aligned} \quad (\text{E.2b})$$

$$\begin{aligned} W_I^y = & \frac{3\alpha}{4\alpha-1} \left[-\left\{ \log(S_1 + p_1) \right\} \|_d^D - \left\{ \log(S_2 + p_2) \right\} \|_d^D \right] \\ & + \frac{6\alpha}{4\alpha-1} \left[-\left\{ \log(S_2 + p_2) \right\} \|_d^D \right] \\ & + \alpha \left[-\frac{1}{2} \left\{ \log(S_1 + p_1) + \frac{t^2 - y^2}{r^2} \cdot \frac{p_1}{S_1 + p_1} \right\} \|_d^D \right. \\ & - \left. \frac{1}{2} \left\{ \log(S_2 + p_2) + \frac{t^2 - y^2}{r^2} \cdot \frac{p_2}{S_2 + p_2} \right\} \|_d^D \right] \\ & - \frac{2\alpha(1-\alpha)}{4\alpha-1} \left[\left\{ -\frac{1}{2} \log(S_1 + p_1) + \frac{1}{2} \frac{p_1}{S_1 + p_1} + \frac{y^2}{r^2} \cdot \frac{p_1^2}{S_1(S_1 + p_1)} \right\} \|_d^D \right. \\ & + \left. z \left\{ \frac{1}{S_1 + p_1} - \frac{y^2}{S_1(S_1 + p_1)^2} \right\} \|_d^D \right] \\ & + \frac{6\alpha^2}{4\alpha-1} \left[\left\{ -\frac{1}{2} \log(S_2 + p_2) + \frac{1}{2} \frac{p_2}{S_2 + p_2} + \frac{y^2}{r^2} \cdot \frac{p_2^2}{S_2(S_2 + p_2)} \right\} \|_d^D \right. \end{aligned}$$

$$\begin{aligned}
& + (z - 2H) \left\{ \frac{1}{S_2 + p_2} - \frac{y^2}{S_2(S_2 + p_2)^2} \right\} \parallel_d^D \Big] \\
& - \frac{6\alpha^2}{4\alpha - 1} H \left[\left\{ -\frac{1}{S_2 + p_2} + \frac{y^2}{S_2(S_2 + p_2)^2} \right\} \parallel_d^D \right]
\end{aligned} \tag{E.2c}$$

$$W_{II}^y = W_I^y(D \rightarrow H) - \frac{2\alpha(1-\alpha)}{4\alpha-1} H \left[\left\{ \frac{1}{S_1 + p_1} - \frac{y^2}{S_1(S_1 + p_1)^2} \right\} \parallel_H^D \right] \tag{E.2d}$$

$$W_{III}^y = -\frac{2\alpha(1-\alpha)}{4\alpha-1} H \left[\left\{ \frac{1}{S_1 + p_1} - \frac{y^2}{S_1(S_1 + p_1)^2} \right\} \parallel_d^D \right] \tag{E.2e}$$

(c) Vertical magnetization

$$\frac{2}{C_s 4U} W_z^{(S)} = W_0^z + \begin{cases} W_I^z & (H \geq D) \\ W_{II}^z & (D > H \geq d) \\ W_{III}^z & (d > H) \end{cases} \tag{E.3a}$$

$$\begin{aligned}
W_0^z = & \frac{(2\alpha-1)(\alpha+2)}{4\alpha-1} \left[\left\{ \frac{y}{S_1 + p_1} \right\} \parallel_d^D - \left\{ \frac{y}{S_3 + p_3} \right\} \parallel_d^D \right] \\
& + \frac{2\alpha(1-\alpha)}{4\alpha-1} \left[\left\{ \frac{y}{S_1} \right\} \parallel_d^D - z \cdot \left\{ \frac{y}{r^2} \cdot \frac{p_1}{S_1} \right\} \parallel_d^D \right] \\
& - \frac{2\alpha(1-\alpha)}{4\alpha-1} \left[\left\{ \frac{y}{S_3} \right\} \parallel_d^D - (z-2H) \cdot \left\{ \frac{y}{r^2} \cdot \frac{p_3}{S_3} \right\} \parallel_d^D \right] \\
& + \frac{6\alpha(2-\alpha)}{4\alpha-1} H \left[\left\{ -\frac{y}{r^2} \cdot \frac{p_1}{S_1} \right\} \parallel_d^D \right] \\
& - \frac{12\alpha^2}{4\alpha-1} H \left[\left\{ -\frac{y}{r^2} \cdot \frac{p_3}{S_3} \right\} \parallel_d^D + (z-2H) \cdot \left\{ \frac{y}{S_3} \right\} \parallel_d^D \right]
\end{aligned} \tag{E.3b}$$

$$\begin{aligned}
W_I^z = & -\frac{\alpha(2\alpha-5)}{4\alpha-1} \left[\left\{ \frac{y}{S_1 + p_1} \right\} \parallel_d^D + \left\{ \frac{y}{S_2 + p_2} \right\} \parallel_d^D \right] \\
& - \frac{2\alpha(1-\alpha)}{4\alpha-1} \left[\left\{ \frac{y}{S_1} \right\} \parallel_d^D - z \cdot \left\{ \frac{y}{r^2} \cdot \frac{p_1}{S_1} \right\} \parallel_d^D \right] \\
& - \frac{6\alpha^2}{4\alpha-1} \left[-\left\{ \frac{y}{S_2} \right\} \parallel_d^D - (z-2H) \cdot \left\{ \frac{y}{r^2} \cdot \frac{p_2}{S_2} \right\} \parallel_d^D \right] \\
& + \frac{6\alpha^2}{4\alpha-1} H \left[\left\{ -\frac{y}{r^2} \cdot \frac{p_2}{S_2} \right\} \parallel_d^D \right]
\end{aligned} \tag{E.3c}$$

$$W_{II}^z = W_I^z(D \rightarrow H) - \frac{2\alpha(1-\alpha)}{4\alpha-1} H \left[\left\{ -\frac{y}{r^2} \cdot \frac{p_1}{S_1} \right\} \parallel_H^D \right] \tag{E.3d}$$

$$W_{III}^z = -\frac{2\alpha(1-\alpha)}{4\alpha-1} H \left[\left\{ -\frac{y}{r^2} \cdot \frac{p_1}{S_1} \right\} \parallel_d^D \right] \tag{E.3e}$$

E2: Vertical tensile fault (intrusive dyke)(a) Horizontal magnetization in the x direction

$$\frac{2}{C_x AU} W_x^{(T)} = W_0^x + \begin{cases} W_I^x & (H \geq D) \\ W_{II}^x & (D > H \geq d) \\ W_{III}^x & (d > H) \end{cases} \quad (\text{E.4a})$$

$$\begin{aligned} W_0^x = & \frac{2(1-2\alpha)(1-\alpha)}{4\alpha-1} \left[-\left\{ \log(S_1+p_1) \right\} \|_d^D + \left\{ \log(S_3+p_3) \right\} \|_d^D \right] \\ & + (2-\alpha) \left[-\frac{1}{2} \left\{ \log(S_1+p_1) + \frac{t^2-y^2}{r^2} \cdot \frac{p_1}{S_1+p_1} \right\} \|_d^D \right. \\ & \left. + \frac{1}{2} \left\{ \log(S_3+p_3) + \frac{t^2-y^2}{r^2} \cdot \frac{p_3}{S_3+p_3} \right\} \|_d^D \right] \\ & + \frac{2\alpha(1-\alpha)}{4\alpha-1} \left[\left\{ -\frac{1}{2} \log(S_1+p_1) + \frac{1}{2} \frac{p_1}{S_1+p_1} + \frac{y^2}{r^2} \cdot \frac{p_1^2}{S_1(S_1+p_1)} \right\} \|_d^D \right. \\ & \left. + z \left\{ \frac{1}{S_1+p_1} - \frac{y^2}{S_1(S_1+p_1)^2} \right\} \|_d^D \right] \\ & - \frac{2\alpha(1-\alpha)}{4\alpha-1} \left[\left\{ -\frac{1}{2} \log(S_3+p_3) + \frac{1}{2} \frac{p_3}{S_3+p_3} + \frac{y^2}{r^2} \cdot \frac{p_3^2}{S_3(S_3+p_3)} \right\} \|_d^D \right. \\ & \left. + (z-2H) \left\{ \frac{1}{S_3+p_3} - \frac{y^2}{S_3(S_3+p_3)^2} \right\} \|_d^D \right] \\ & - \frac{18\alpha^2}{4\alpha-1} H \left[\left\{ \frac{1}{S_3+p_3} - \frac{y^2}{S_3(S_3+p_3)^2} \right\} \|_d^D \right] \\ & + \frac{12\alpha(1-2\alpha)}{4\alpha-1} H \left[\left\{ \frac{1}{S_3+p_3} - \frac{t^2}{S_3(S_3+p_3)^2} \right\} \|_d^D \right] \\ & + \frac{12\alpha^2}{4\alpha-1} H \left[\left\{ \frac{1}{S_3} - \frac{y^2}{S_3^3} \right\} \|_d^D + (z-2H) \left\{ \frac{1}{r^2} \left(\frac{3y^2-t^2}{r^2} \cdot \frac{p_3}{S_3} - \frac{y^2}{r^2} \cdot \frac{p_3^3}{S_3^3} \right) \right\} \|_d^D \right] \end{aligned} \quad (\text{E.4b})$$

$$\begin{aligned} W_I^x = & -\frac{2\alpha(1+2\alpha)}{4\alpha-1} \left[-\left\{ \log(S_1+p_1) \right\} \|_d^D - \left\{ \log(S_2+p_2) \right\} \|_d^D \right] \\ & - \frac{8\alpha(1-\alpha)}{4\alpha-1} \left[\left\{ -\log(S_2+p_2) \right\} \|_d^D \right] \\ & + \alpha \left[-\frac{1}{2} \left\{ \log(S_1+p_1) + \frac{t^2-y^2}{r^2} \cdot \frac{p_1}{S_1+p_1} \right\} \|_d^D \right. \\ & \left. - \frac{1}{2} \left\{ \log(S_2+p_2) + \frac{t^2-y^2}{r^2} \cdot \frac{p_2}{S_2+p_2} \right\} \|_d^D \right] \\ & - \frac{2\alpha(1-\alpha)}{4\alpha-1} \left[\left\{ -\frac{1}{2} \log(S_1+p_1) + \frac{1}{2} \frac{p_1}{S_1+p_1} + \frac{y^2}{r^2} \cdot \frac{p_1^2}{S_1(S_1+p_1)} \right\} \|_d^D \right. \end{aligned}$$

$$\begin{aligned}
& + z \left\{ \frac{1}{S_1 + p_1} - \frac{y^2}{S_1(S_1 + p_1)^2} \right\} \Big\|_d^D \Big] \\
& + \frac{6\alpha^2}{4\alpha - 1} \left[\left\{ -\frac{1}{2} \log(S_2 + p_2) + \frac{1}{2} \frac{p_2}{S_2 + p_2} + \frac{y^2}{r^2} \cdot \frac{p_2^2}{S_2(S_2 + p_2)} \right\} \Big\|_d^D \right. \\
& + (z - 2H) \left\{ \frac{1}{S_2 + p_2} - \frac{y^2}{S_2(S_2 + p_2)^2} \right\} \Big\|_d^D \Big] \\
& \left. - \frac{6\alpha^2}{4\alpha - 1} H \left[\left\{ -\frac{1}{S_2 + p_2} + \frac{y^2}{S_2(S_2 + p_2)^2} \right\} \Big\|_d^D \right] \right] \quad (D.4c)
\end{aligned}$$

$$W_{II}^x = W_I^x(D \rightarrow H) - \frac{2\alpha(1-\alpha)}{4\alpha - 1} H \left[\left\{ \frac{1}{S_1 + p_1} - \frac{y^2}{S_1(S_1 + p_1)^2} \right\} \Big\|_d^D \right] \quad (E.4d)$$

$$W_{III}^x = -\frac{2\alpha(1-\alpha)}{4\alpha - 1} H \left[\left\{ \frac{1}{S_1 + p_1} - \frac{y^2}{S_1(S_1 + p_1)^2} \right\} \Big\|_d^D \right] \quad (E.4e)$$

(b) Horizontal magnetization in the y direction

$$\frac{2}{C_y \Delta U} W_y^{(T)} = W_0^y + \begin{cases} W_I^y & (H \geq D) \\ W_{II}^y & (D > H \geq d) \\ W_{III}^y & (d > H) \end{cases} \quad (E.5a)$$

$$\begin{aligned}
W_0^y = & -\frac{3\alpha}{4\alpha - 1} \left[\left\{ \tan^{-1} \frac{tp_1}{yS_1} \right\} \Big\|_d^D - \left\{ \tan^{-1} \frac{tp_3}{yS_3} \right\} \Big\|_d^D \right] \\
& - (2 - \alpha) \left[\left\{ \frac{ty}{r^2} \cdot \frac{p_1}{S_1 + p_1} \right\} \Big\|_d^D - \left\{ \frac{ty}{r^2} \cdot \frac{p_3}{S_3 + p_3} \right\} \Big\|_d^D \right] \\
& + \frac{2\alpha(1-\alpha)}{4\alpha - 1} \left[\left\{ -\frac{ty}{q_1^2} \cdot \frac{p_1}{S_1} - \frac{ty}{r^2} \cdot \frac{p_1^2}{S_1(S_1 + p_1)} + \tan^{-1} \frac{p_1 t}{yS_1} \right\} \Big\|_d^D \right. \\
& + z \left\{ -\frac{ty}{q_1^2} \cdot \frac{1}{S_1} + \frac{ty}{S_1(S_1 + p_1)^2} \right\} \Big\|_d^D \Big] \\
& - \frac{2\alpha(1-\alpha)}{4\alpha - 1} \left[\left\{ -\frac{ty}{q_3^2} \cdot \frac{p_3}{S_3} - \frac{ty}{r^2} \cdot \frac{p_3^2}{S_3(S_3 + p_3)} + \tan^{-1} \frac{p_3 t}{yS_3} \right\} \Big\|_d^D \right. \\
& + (z - 2H) \left\{ -\frac{ty}{q_3^2} \cdot \frac{1}{S_3} + \frac{ty}{S_3(S_3 + p_3)^2} \right\} \Big\|_d^D \Big] \\
& - \frac{18\alpha^2}{4\alpha - 1} H \left[\left\{ -\frac{ty}{q_3^2} \cdot \frac{1}{S_3} + \frac{ty}{S_3(S_3 + p_3)^2} \right\} \Big\|_d^D \right] \\
& + \frac{12\alpha(1-2\alpha)}{4\alpha - 1} H \left[\left\{ -\frac{ty}{S_3(S_3 + p_3)^2} \right\} \Big\|_d^D \right] \\
& + \frac{12\alpha^2}{4\alpha - 1} H \left[\left\{ -3ty \cdot \frac{p_3^2}{q_3^4} \cdot \frac{1}{S_3} - \frac{t^3 y^3}{q_3^4} \cdot \frac{1}{S_3^3} \right\} \Big\|_d^D \right. \\
& \left. - (z - 2H) \left\{ 2 \left(\frac{ty}{r^4} + \frac{ty}{q_3^4} \right) \frac{p_3}{S_3} + \left(\frac{ty}{r^2} + \frac{ty}{q_3^2} \right) \frac{p_3}{S_3^3} \right\} \Big\|_d^D \right] \quad (E.5b)
\end{aligned}$$

$$\begin{aligned}
W_I^y = & \frac{3\alpha}{4\alpha-1} \left[\left\{ \tan^{-1} \frac{tp_1}{yS_1} \right\} \|_d^D + \left\{ \tan^{-1} \frac{tp_2}{yS_2} \right\} \|_d^D \right] \\
& + \frac{4\alpha(1+2\alpha)}{4\alpha-1} \left[- \left\{ \tan^{-1} \frac{tp_2}{yS_2} \right\} \|_d^D \right] \\
& - \alpha \left[\left\{ \frac{ty}{r^2} \cdot \frac{p_1}{S_1+p_1} \right\} \|_d^D + \left\{ \frac{ty}{r^2} \cdot \frac{p_2}{S_2+p_2} \right\} \|_d^D \right] \\
& - \frac{2\alpha(1-\alpha)}{4\alpha-1} \left[\left\{ -\frac{ty}{q_1^2} \cdot \frac{p_1}{S_1} - \frac{ty}{r^2} \cdot \frac{p_1^2}{S_1(S_1+p_1)} + \tan^{-1} \frac{p_1 t}{yS_1} \right\} \|_d^D \right. \\
& \left. + z \left\{ -\frac{ty}{q_1^2} \cdot \frac{1}{S_1} + \frac{ty}{S_1(S_1+p_1)^2} \right\} \|_d^D \right] \\
& - \frac{6\alpha^2}{4\alpha-1} H \left[\left\{ \frac{ty}{q_2^2} \cdot \frac{1}{S_2} - \frac{ty}{S_2(S_2+p_2)} \right\} \|_d^D \right] \\
& + \frac{6\alpha^2}{4\alpha-1} \left[\left\{ -\frac{ty}{q_2^2} \cdot \frac{p_2^2}{r^2} + \frac{ty}{r^2} \cdot \frac{p_2}{S_2(S_2+p_2)} + \tan^{-1} \frac{p_2 t}{yS_2} \right\} \|_d^D \right. \\
& \left. + (z-2H) \left\{ -\frac{ty}{q_2^2} \cdot \frac{1}{S_2} + \frac{ty}{S_2(S_2+p_2)^2} \right\} \|_d^D \right] \quad (E.5c)
\end{aligned}$$

$$W_{II}^y = W_I^y(D \rightarrow H) - \frac{2\alpha(1-\alpha)}{4\alpha-1} H \left[\left\{ -\frac{ty}{q_1^2} \cdot \frac{1}{S_1} + \frac{ty}{S_1(S_1+p_1)^2} \right\} \|_H^D \right] \quad (E.5d)$$

$$W_{III}^y = -\frac{2\alpha(1-\alpha)}{4\alpha-1} H \left[\left\{ -\frac{ty}{q_1^2} \cdot \frac{1}{S_1} + \frac{ty}{S_1(S_1+p_1)^2} \right\} \|_d^D \right] \quad (E.5e)$$

(c) Vertical magnetization

$$\frac{2}{C_z \Delta U} W_z^{(r)} = W_0^z + \begin{cases} W_I^z & (H \geq D) \\ W_{II}^z & (D > H \geq d) \\ W_{III}^z & (d > H) \end{cases} \quad (E.6a)$$

$$\begin{aligned}
W_0^z = & \frac{(2\alpha-1)(\alpha+2)}{4\alpha-1} \left[\left\{ -\frac{1}{2} \log \frac{S_1-t}{S_1+t} - \frac{t}{S_1+p_1} \right\} \|_d^D \right. \\
& \left. - \left\{ -\frac{1}{2} \log \frac{S_3-t}{S_3+t} - \frac{t}{S_3+p_3} \right\} \|_d^D \right] \\
& + \frac{2(1-2\alpha)(1-\alpha)}{4\alpha-1} \left[\left\{ -\frac{1}{2} \log \frac{S_1-t}{S_1+t} \right\} \|_d^D + \left\{ \frac{1}{2} \log \frac{S_3-t}{S_3+t} \right\} \|_d^D \right] \\
& + \frac{2\alpha(1-\alpha)}{4\alpha-1} \left[\left\{ -\frac{1}{2} \log \frac{S_1-t}{S_1+t} - \frac{ty^2}{q_1^2} \cdot \frac{1}{S_1} \right\} \|_d^D + z \left\{ \left(\frac{1}{r^2} + \frac{1}{q_1^2} \right) \cdot \frac{tp_1}{S_1} \right\} \|_d^D \right] \\
& - \frac{2\alpha(1-\alpha)}{4\alpha-1} \left[\left\{ -\frac{1}{2} \log \frac{S_3-t}{S_3+t} - \frac{ty^2}{q_3^2} \cdot \frac{1}{S_3} \right\} \|_d^D \right. \\
& \left. + (z-2H) \left\{ \left(\frac{1}{r^2} + \frac{1}{q_3^2} \right) \cdot \frac{tp_3}{S_3} \right\} \|_d^D \right]
\end{aligned}$$

$$\begin{aligned}
& + \frac{18\alpha^2}{4\alpha-1} H \left[\left\{ \left(\frac{1}{r^2} + \frac{1}{q_3^2} \right) \cdot \frac{tp_3}{S_3} \right\} \right]_d^p \\
& - \frac{12\alpha(1-2\alpha)}{4\alpha-1} H \left[\left\{ -\frac{t}{r^2} \cdot \frac{p_3}{S_3} \right\} \right]_d^p \\
& - \frac{12\alpha^2}{4\alpha-1} H \left[\left\{ -\left(\frac{1}{r^2} + \frac{1}{q_3^2} \right) \cdot \frac{tp_3}{S_3} + \frac{p_3 y^2}{q_3^4} \cdot \left(\frac{3t}{S_3} - \frac{t^3}{S_3^3} \right) \right\} \right]_d^p \\
& + (z-2H) \left\{ -\frac{1}{q_3^2} \cdot \frac{t}{S_3} + \frac{y^2}{q_3^4} \cdot \left(\frac{3t}{S_3} - \frac{t^3}{S_3^3} \right) \right\} \right]_d^p \quad (\text{E.6b})
\end{aligned}$$

$$\begin{aligned}
W_I^z = & -\frac{2\alpha(1+2\alpha)}{4\alpha-1} \left[-\frac{1}{2} \left\{ \log \frac{S_1-t}{S_1+t} \right\} \right]_d^p - \frac{1}{2} \left\{ \log \frac{S_2-t}{S_2+t} \right\} \right]_d^p \\
& - 4\alpha \left[\left\{ \frac{1}{2} \log \frac{S_2-t}{S_2+t} \right\} \right]_d^p \\
& - \frac{\alpha(2\alpha-5)}{4\alpha-1} \left[\left\{ -\frac{1}{2} \log \frac{S_1-t}{S_1+t} - \frac{t}{S_1+p_1} \right\} \right]_d^p \\
& + \left\{ -\frac{1}{2} \log \frac{S_2-t}{S_2+t} - \frac{t}{S_2+p_2} \right\} \right]_d^p \\
& - \frac{2\alpha(1-\alpha)}{4\alpha-1} \left[\left\{ -\frac{1}{2} \log \frac{S_1-t}{S_1+t} - \frac{ty^2}{q_1^2} \cdot \frac{1}{S_1} \right\} \right]_d^p \\
& + z \left\{ \left(\frac{1}{r^2} + \frac{1}{q_1^2} \right) \cdot \frac{tp_1}{S_1} \right\} \right]_d^p \\
& + \frac{6\alpha^2}{4\alpha-1} H \left[\left\{ -\left(\frac{1}{r^2} + \frac{1}{q_2^2} \right) \cdot \frac{tp_2}{S_2} \right\} \right]_d^p \\
& - \frac{6\alpha^2}{4\alpha-1} \left[\left\{ -\frac{1}{2} \log \frac{S_2-t}{S_2+t} - \frac{ty^2}{q_2^2} \cdot \frac{1}{S_2} \right\} \right]_d^p \\
& + (z-2H) \left\{ \left(\frac{1}{r^2} + \frac{1}{q_2^2} \right) \cdot \frac{tp_2}{S_2} \right\} \right]_d^p \quad (\text{E.6c})
\end{aligned}$$

$$W_{II}^z = W_I^z(D \rightarrow H) - \frac{2\alpha(1-\alpha)}{4\alpha-1} H \left[\left\{ \left(\frac{1}{r^2} + \frac{1}{q_1^2} \right) \cdot \frac{tp_1}{S_1} \right\} \right]_d^p \quad (\text{E.6d})$$

$$W_{III}^z = -\frac{2\alpha(1-\alpha)}{4\alpha-1} H \left[\left\{ \left(\frac{1}{r^2} + \frac{1}{q_1^2} \right) \cdot \frac{tp_1}{S_1} \right\} \right]_d^p \quad (\text{E.6e})$$

where

$$t = x - x_1, \quad r^2 = t^2 + y^2, \quad (\text{E.7a})$$

$$p_1 = x_3 - z, \quad p_2 = 2H - x_3 - z, \quad p_3 = 2H + x_3 - z, \quad (\text{E.7b})$$

$$q_1^2 = y^2 + p_1^2, \quad q_2^2 = y^2 + p_2^2, \quad q_3^2 = y^2 + p_3^2, \quad (\text{E.7c})$$

$$S_1 = \sqrt{r^2 + p_1^2}, \quad S_2 = \sqrt{r^2 + p_2^2}, \quad S_3 = \sqrt{r^2 + p_3^2}, \quad (\text{E.7d})$$

and

$$\{f(x_1, x_2)\} \|_a^b = f(L, b) - f(L, a) - f(-L, b) + f(-L, a) \quad (\text{E.8})$$

In eqs. (E.1d), (E.2d), (E.3d), (E.4d), (E.5d) and (E.6d), the notation $W_I^m(D \rightarrow H)$ implies replacement of the upper limit D in $\|_a^D$ by H .

References

- ABDULLABEKOV, K. N., YE. BERDALIYEV, A. N. PUSHKOV and V. A. SHAPIRO, 1979, Local variations of the geomagnetic field during the filling of a reservoir, *Geomag. Aeron. (English transl.)*, **19**, 204-206.
- AKI, K. and P. G. RICHARDS, 1980, Quantitative Seismology, Theory and Methods, Vol. 1, Chapter 3, W. H. Freeman and Co., San Francisco.
- BONAFEDE, M. and R. SABADINI, 1980, A theoretical approach to the seismomagnetic effect, *Boll. Geof. Teor. Appl.*, **22**, 105-116.
- BONAFEDE, M. and M. DRAGONI, 1986, Selection rules for bulk piezomagnetic coefficients of isotropic titanomagnetite dispersions, *Boll. Geof. Teor. Appl.*, **28**, 251-262.
- BREINER, S., 1964, Piezomagnetic effect at the time of local earthquakes, *Nature*, **202**, 790-791.
- CARMICHAEL, R. S., 1977, Depth calculation of piezomagnetic effect for earthquake prediction, *Earth Planet. Sci. Lett.* **36**, 309-316.
- CHINNERY, M. A., 1963, The stress changes that accompany strike-slip faulting, *Bull. Seism. Soc. Amer.*, **53**, 921-932.
- CORWIN, R. F. and H. F. MORRISON, 1977, Self-potential variations preceding earthquakes in central California, *Geophys. Res. Lett.*, **4**, 171-174.
- COURANT, R. and D. HILBERT, 1937, *Methoden der Mathematischen Physik*, Band 2, Kapitel 4, Springer, Berlin.
- DAVIS, P. M., 1974, The piezomagnetic computation of magnetic anomalies due to ground loading by a man-made lake, *Pageoph*, **112**, 811-818.
- DAVIS, P. M., 1976, The computed piezomagnetic anomaly field for Kilauea Volcano, Hawaii, *J. Geomag. Geoelectr.*, **28**, 113-122.
- DAVIS, P. M., 1986, Surface deformation due to inflation of an arbitrarily oriented triaxial ellipsoidal cavity in an elastic half-space, with reference to Kilauea Volcano, Hawaii, *J. Geophys. Res.*, **91**, 7429-7438.
- DAVIS, P. M. and F. D. STACEY, 1972, Geomagnetic anomalies caused by a man-made lake, *Nature*, **240**, 348-349.
- DAVIS, P. M., D. B. JACKSON, J. FIELD and F. D. STACEY, 1973, Kilauea volcano, Hawaii: A search for volcanomagnetic effect, *Science*, **180**, 73-74.
- DAVIS, P. M., F. D. STACEY, C. J. ZABLOCKI and J. V. OLSON, 1979, Improved signal discrimination in tectonomagnetism: Discovery of a volcanomagnetic effect at Kilauea, Hawaii, *Phys. Earth Planet. Interiors*, **19**, 331-336.
- EASON, G., B. NOBLE and I. N. SNEDDON, 1955, On certain integrals of Lipschitz-Hankel type involving products of Bessel functions, *Phil. Trans. R. Soc., London, Ser. A*, **247**, 529-551.
- ESHELBY, J. D., 1957, The determination of the elastic field of an ellipsoidal inclusion and related problems, *Proc. R. Soc. London, Ser. A*, **241**, 376-396.
- FITTERMAN, D. V., 1978, Electrokinetic and magnetic anomalies associated with dilatant regions in a layered earth, *J. Geophys. Res.*, **83**, 5923-5928.
- FITTERMAN, D. V., 1979, Theory of electrokinetic-magnetic anomalies in a faulted half-space, *J. Geophys. Res.*, **84**, 6031-6040.

- FITTERMAN, D. V., 1981, Correction to "Theory of electrokinetic-magnetic anomalies in a faulted half-space", *J. Geophys. Res.*, **86**, 9585-9588.
- GOKHBERG, M. B., V. A. MORGOUNOV, T. YOSHINO and I. TOMIZAWA, 1982, Experimental measurement of electromagnetic emissions possibly related to earthquakes in Japan, *J. Geophys. Res.*, **87**, 7824-7828.
- HAGIWARA, Y., 1977a, The Mogi model as a possible cause of the crustal uplift in the eastern part of Izu Peninsula and related gravity change, (in Japanese with English abstract), *Bull. Earthq. Res. Inst., Univ. Tokyo*, **52**, 301-309.
- HAGIWARA, Y., 1977b, Matsushiro uplift as a multiple Mogi model, (in Japanese with English abstract), *J. Geod. Soc. Japan*, **23**, 25-35.
- HAMANO, Y., 1983, Experiments on the stress sensitivity of natural remanent magnetization, *J. Geomag. Geoelectr.*, **35**, 155-172.
- HAMANO, Y., R. BOYD, M. FULLER and M. LANHAM, 1989, Induced susceptibility anisotropy of igneous rocks caused by uniaxial compression, *J. Geomag. Geoelectr.*, **41**, 203-220.
- HAMANO, Y., H. UTADA, T. SHIMOMURA, Y. TANAKA, Y. SASAI, I. NAKAGAWA, Y. YOKOYAMA, M. OHNO, T. YOSHINO, S. KOYAMA and T. YUKUTAKE, 1990, Geomagnetic variations observed after the 1986 eruption of Izu-Oshima Volcano, *J. Geomag. Geoelectr.*, **42**, 319-335.
- HAO, J. Q., L. M. HASTIE and F. D. STACEY, 1982, Theory of the seismomagnetic effect: a reassessment, *Phys. Earth Planet. Int.*, **28**, 129-140.
- HAO, J., P. HUANG, T. ZHANG, M. XU, J. ZHOU and X. MA, 1990, The effect of stress on remanent magnetization of rocks, *Acta Seism. Sinica*, **3**, 465-475.
- HASTINGS Jr., C., 1955, Approximations for Digital Computers, 205pp., Princeton.
- HENYEU, T. L., S. J. PIKE and D. F. PALMER, 1978, On the measurement of stress sensitivity of NRM using a cryogenic magnetometer, *J. Geomag., Geoelectr.*, **30**, 607-617.
- HILDENBRAND, T. G., 1975, Seismomagnetism, Ph. D. Thesis, Univ. California, Berkeley, 158pp.
- HODYCH, J. P., 1976, Single domain theory for the reversible effect of small uniaxial stress upon the initial susceptibility of rock, *Can. J. Earth Sci.*, **13**, 2047-2061.
- HODYCH, J. P., 1977, Single domain theory for the reversible effect of small uniaxial stress upon the remanent magnetization of rock, *Can. J. Earth Sci.*, **14**, 1186-1200.
- HONKURA, Y. and S. TAIRA, 1983, Changes in the amplitudes of short-period geomagnetic variations as observed in association with crustal uplift in the Izu Peninsula, Japan, *Earthq. Pred. Res.*, **2**, 115-125.
- ISHIDO, T. and H. MIZUTANI, 1981, Experimental and theoretical basis of electrokinetic phenomena in rock-water systems and its application to geophysics, *J. Geophys. Res.*, **86**, 1763-1775.
- ISIKARA, A. M. and Y. HONKURA (editors), 1986, Electric and magnetic research on active faults in the north Anatolian fault zone, Tokyo Inst. Tech., 139pp.
- ISPIR, Y. and O. UYAR, 1971, An attempt in determining the seismomagnetic effect in N. W. Turkey, *J. Geomag. Geoelectr.*, **23**, 295-305.
- IWASAKI, T. and R. SATO, 1979, Strain field in a semi-infinite medium due to an inclined rectangular fault, *J. Phys. Earth*, **27**, 285-314.
- JOHNSTON, M. J. S., 1978, Local magnetic field observations and stress changes near a slip discontinuity on the San Andreas fault, *J. Geomag. Geoelectr.*, **30**, 607-617.
- JOHNSTON, M. J. S. and F. D. STACEY, 1969, Volcano-magnetic effect observed on Mt. Ruapehu, New Zealand, *J. Geophys. Res.*, **74**, 6541-6544.
- JOHNSTON, M. J. S., F. J. WILLIAMS, J. MCWHIRTER and B. E. WILLIAMS, 1979, Tectono-magnetic anomaly during the southern California downwarp, *J. Geophys. Res.*, **84**, 6026-6030.
- JOHNSTON, M. J. S., R. J. MUELLER and J. DVORAK, 1981, Volcanomagnetic observations during eruptions, May-August 1980, in The 1980 eruptions of Mount St. Helens,

- Washington, U.S. Geol. Sur. professional paper, **1250**, 183-189.
- JOHNSTON, M. J. S. and R. J. MUELLER, 1987, Seismomagnetic observation during the 8 July 1986 magnitude 5.9 North Palm Springs earthquake, *Science*, **237**, 1201-1203.
- KALASHINIKOV, A. G. and S. P. KAPITSA, 1952, Magnetic susceptibility of rocks under elastic stresses, *Dokl. Akad. Nauk. U.S.S.R.*, **86**, 521-523.
- KAPITSA, S. P., 1955, Magnetic properties of eruptive rocks under mechanical stresses, *Izv. Akad. Nauk. U.S.S.R., Ser. Geophys.*, **6**, 489-504.
- KATO, Y., 1939, Investigation of the changes in the earth's magnetic field accompanying earthquakes or volcanic eruptions, *Sci. Rep. Tohoku Imp. Univ.*, Ser. 1, **27**, 1-100.
- KATO, Y., 1940, The changes in the earth's magnetic field accompanying the volcanic eruption of Miyake-zima, *Proc. Imp. Acad., Japan*, **16**, 467-472.
- KATO, Y. and UTASHIRO, 1949, On the changes of the terrestrial magnetic field accompanying the Great Nankaido Earthquake of 1946, *Sci. Rep. Tohoku Univ.*, Ser. 5, **1**, 40-41.
- KEAN, W. F., R. DAY, M. FULLER and V. A. SCHMIDT, 1976, The effect of uniaxial compression on the initial susceptibility of rocks as a function of grain size and composition of their constituent titanomagnetite, *J. Geophys. Res.*, **81**, 861-872.
- KELLOGG, O.D., 1929, Foundation of potential theory, Chapter VI, Springer, Berlin.
- KERN, J. W., 1961, The effect of stress on the susceptibility and magnetization of a partially magnetized multidomain system, *J. Geomag. Geoelectr.*, **66**, 3807-3816.
- KINOSHITA, H., 1968, Studies on piezo-magnetization (III)—PRM and relating phenomena—, *J. Geomag. Geoelectr.*, **20**, 155-167.
- KINOSHITA, H., 1969, Studies on piezo-magnetization (IV)—Interpretation of PRM production for single domain grains—, *J. Geomag. Geoelectr.*, **21**, 409-426.
- MARTIN, III, R. J., R. E. HABERMANN and M. WYSS, 1978, The effect of stress cycling and inelastic volumetric strain on remanent magnetization, *J. Geophys. Res.*, **83**, 3485-3496.
- MARUYAMA, T., 1964, Statical elastic dislocations in an infinite and semi-infinite medium, *Bull. Earthq. Res. Inst., Univ. Tokyo*, **42**, 289-368.
- MAZZELLA, A. and H. F. MORRISON, 1974, Electrical resistivity variations associated with earthquakes on the San Andreas fault, *Science*, **185**, 855-857.
- MINAKAMI, T., 1941, A magnetic dip survey of Miyakesima Island, *Bull. Earthq. Res. Inst.*, **19**, 356-362.
- MINDLIN, R. D., 1936, Force at a point in the interior of a semi-infinite solid, *Physics*, **7**, 195-202.
- MINDLIN, R. D. and D. H. CHENG, 1950, Nuclei of strain in the semi-infinite solid, *J. Applied Phys.*, **21**, 926-930.
- MIYAKOSHI, J., 1986, Anomalous time variation of the self-potential in the fractured zone of an active fault preceding the earthquake occurrence, *J. Geomag. Geoelectr.*, **38**, 1015-1030.
- MIZUTANI, H. and T. ISHIDO, 1976, A new interpretation of magnetic field variation associated with the Matsushiro earthquakes, *J. Geomag. Geoelectr.*, **28**, 179-188.
- MIZUTANI, H., T. ISHIDO, T. YOKOKURA and S. OHNISHI, 1976, Electrokinetic phenomena associated with earthquakes, *Geophys. Res. Lett.*, **3**, 365-368.
- MOGI, K., 1958, Relations between the eruptions of various volcanoes and the deformations of the ground surfaces around them, *Bull. Earthq. Res. Inst., Univ. Tokyo*, **36**, 99-134.
- MURA, T., 1982, *Micromechanics of Defects in Solids*, 494pp., Martinus Nijhoff Publishers, The Hague.
- MURAKAMI, H., 1989, Geomagnetic fields produced by electrokinetic sources, *J. Geomag. Geoelectr.*, **41**, 221-247.
- NAGAOKA, H., 1889, Combined effects of torsion and longitudinal stress on magnetization

- of nickel, *Phil. Mag., Ser. A*, **5**, 27-117.
- NAGATA, T., 1941, Anomalous change in geomagnetism accompanying volcanic activity, *Bull. Earthq. Res. Inst.*, **19**, 335-355.
- NAGATA, T., 1943, The natural remanent magnetism of volcanic rocks and its relation to geomagnetic phenomena, *Bull. Earthq. Res. Inst.*, **21**, 1-196.
- NAGATA, T., 1969, Tectonomagnetism, *I.A.G.A. Bull.*, **27**, 12-43.
- NAGATA, T., 1970a, Basic magnetic properties of rocks under the effect of mechanical stresses, *Tectonophysics*, **9**, 167-195.
- NAGATA, T., 1970b, Anisotropic magnetic susceptibility of rocks under mechanical stresses, *Pageoph*, **78**, 110-122.
- NAGATA, T. 1971, Introductory notes on shock remanent magnetization and shock demagnetization of igneous rocks, *Pageoph*, **89**, 159-177.
- NAGATA, T. and H. KINOSHITA, 1967, Effect of hydrostatic pressure on magnetostriction and magnetocrystalline anisotropy of magnetite, *Phys. Earth. Planet. Int.*, **1**, 44-48.
- NAGATA, T. and B. J. CARLETON, 1968, Notes on piezo-remanent magnetization of igneous rocks, *J. Geomag. Geoelectr.*, **20**, 115-127.
- NAGY, D., 1965, The evaluation of Heuman's lambda function and its application to calculation of the gravitational effect of a right circular cylinder, *Pageoph*, **62**, 5-12.
- NULMAN, A. A., V. A. SHAPIRO, S. I. MAKSIMOVSKIKH, N. A. IVANOV, JOON KIM and R. S. CARMICHAEL, 1978, Magnetite under hydrostatic pressure, and implications for tectonomagnetism, *J. Geomag. Geoelectr.*, **30**, 585-592.
- OHCHI, K., N. IJICHI, M. KUWASHIMA and M. KAWAMURA, 1979, Geomagnetic total force intensity variation associated with the Izu-Oshima Kinkai earthquake, 1978, (in Japanese with English abstract), *Memoirs Kakioka Mag. Obs.*, *JMA*, **18**, 55-64.
- OHNAKA, M. and H. KINOSHITA, 1968, Effects of uniaxial compression on remanent magnetization, *J. Geomag. Geoelectr.*, **20**, 93-99.
- OHSHIMAN, N., 1980, Local magnetic changes associated with fault activity, M. Sc. thesis, Tokyo Inst. Tech., 178pp.
- OKADA, Y., 1985, Surface deformation due to shear and tensile faults in a half-space, *Bull. Seism. Soc. Am.*, **75**, 1135-1154.
- OSHIMAN, N., 1990, Enhancement of tectonomagnetic change due to non-uniform magnetization in the Earth's crust—two dimensional case studies, *J. Geomag. Geoelectr.*, **42**, 607-619.
- OKUBO, S., 1991, Potential and gravity changes raised by a point dislocation, *Geophys. J. Int.*, **105**, 573-586.
- POZZI, J. P., 1977, Effects of stresses on magnetic properties of volcanic rocks, *Phys. Earth Planet. Int.*, **14**, 77-85.
- PRESS, F., 1965, Displacements, strains, and tilts at teleseismic distances, *J. Geophys. Res.*, **70**, 2395-2412.
- REVOL, J., R. DAY and M. FULLER, 1978, Effect of uniaxial stress upon remanent magnetization: Stress cycling and domain state dependence, *J. Geomag. Geoelectr.*, **30**, 593-605.
- RIKITAKE, T., 1951, The distribution of magnetic dip in Ooshima (Oo-sima) Island and its change that accompanied the eruption of Volcano Mihara, 1950, *Bull. Earthq. Res. Inst., Univ. Tokyo*, **29**, 161-181.
- RIKITAKE, T., 1966, Some theoretical aspects of further studies on tectonomagnetic modeling, (in Japanese), in Proceedings of a symposium on "Geomagnetic changes associated with earthquakes and volcanic activities" (Editor: T. NAGATA), Fac. Sci., Tokyo Univ., 105-106.
- RIKITAKE, T., 1968, Geomagnetism and earthquake prediction, *Tectonophysics*, **6**, 59-68.
- RIKITAKE, T., Y. YAMAZAKI, M. SAWADA, Y. SASAI, T. YOSHINO, S. UZAWA and T. SHIMOMURA, 1967, Geomagnetic and geoelectric studies of the Matsushiro earthquake swarm (5), *Bull. Earthq. Res. Inst., Univ. Tokyo*, **45**, 395-416.

- SASAI, Y., 1979, The piezomagnetic field associated with the Mogi model, *Bull. Earthq. Res. Inst., Univ. Tokyo*, **54**, 1-29.
- SASAI, Y., 1980, Application of the elasticity theory of dislocations to tectonomagnetic modelling, *Bull. Earthq. Res. Inst., Univ. Tokyo*, **55**, 387-447.
- SASAI, Y., 1983, A surface integral representation of the tectonomagnetic field based on the linear piezomagnetic effect, *Bull. Earthq. Res. Inst., Univ. Tokyo*, **58**, 763-785.
- SASAI, Y., 1984, Piezomagnetic field caused by intrusion of a dyke, (in Japanese), *Proc. Conductivity Anomaly Symposium (1984)*, 227-241.
- SASAI, Y., 1985, Predominance of piezomagnetic effect in tectonomagnetic field of the Mogi model, *J. Geomag. Geoelectr.*, **37**, 159-167.
- SASAI, Y., 1986a, A Green's function for tectonomagnetic problems in an elastic half-space, *J. Geomag. Geoelectr.*, **38**, 949-969.
- SASAI, Y., 1986b, Multiple tension-crack model for dilatancy: Surface displacement gravity and magnetic change, *Bull. Earthq. Res. Inst.*, **61**, 429-473.
- SASAI, Y., 1988, Correction to the paper "Multiple tension-crack model for dilatancy: Surface displacement gravity and magnetic change", *Bull. Earthq. Res. Inst.*, **63**, 323-326.
- SASAI, Y., 1989, Tectonomagnetism in southern Kanto and Tokai district, central Japan, *J. Geod. Soc. Jpn.*, **35**, 227-242.
- SASAI, Y., 1991, Piezomagnetic field associated with the Mogi model revisited: analytic solution for finite spherical source, *J. Geomag. Geoelectr.*, **43**, 21-64.
- SASAI, Y. and Y. ISHIKAWA, 1980a, Tectonomagnetic event preceding a M5.0 earthquake in the Izu Peninsula—Aseismic slip of a buried fault?, *Bull. Earthq. Res. Inst.*, **55**, 895-911.
- SASAI, Y. and Y. ISHIKAWA, 1980b, Changes in the geomagnetic total force intensity associated with the anomalous crustal activity in the eastern part of the Izu Peninsula (3)—The east off Izu Peninsula earthquake of 1980—, (in Japanese with English abstract), *Bull. Earthq. Res. Inst.*, **55**, 1101-1113.
- SASAI, Y., T. SHIMOMURA, Y. HAMANO, H. UTADA, T. YOSHINO, S. KOYAMA, Y. ISHIKAWA, I. NAKAGAWA, Y. YOKOYAMA, M. OHNO, H. WATANABE, T. YUKUTAKE, Y. TANAKA, T. YAMAMOTO, K. NAKAYA, S. TSUNOMURA, F. MUROMATSU and R. MURAKAMI, 1990, Volcanomagnetic effect observed during the 1986 eruption of Izu-Oshima Volcano, *J. Geomag. Geoelectr.*, **42**, 291-317.
- SASAI, Y. and Y. ISHIKAWA, 1991, Tectonomagnetic signals related to the seismovolcanic activity in the Izu Peninsula, *J. Phys. Earth*, **39**, 299-319.
- SHAMSI, S. and F. D. STACEY, 1969, Dislocation models and seismomagnetic calculations for California 1906 and Alaska 1964 earthquake, *Bull. Seism. Soc. Amer.*, **59**, 1435-1448.
- SHAPIRO, V. A. and K. N. ABDULLABEKOV, 1978, An attempt to observe a seismomagnetic effect during the Gazly 17th May 1979 earthquake, *J. Geomag. Geoelectr.*, **30**, 487-492.
- SHAPIRO, V. A., A. N. PUSHKOV, K. N. ABDULLABEKOV, E. B. BERDALIEV and M. Yu. MIMINOV, 1978, Geomagnetic investigation in the seismoactive regions of middle Asia, *J. Geomag. Geoelectr.*, **30**, 503-509.
- SHAPIRO, V. A. and K. N. ABDULLABEKOV, 1982, Anomalous variations of the geomagnetic field in East Fergana—magnetic precursor of the Alay earthquake with M7.0 (1978 November 21), *Geophys. J. R. astr. Soc.*, **68**, 1-5.
- SMITH, B. E. and M. J. S. JOHNSTON, 1976, A tectonomagnetic effect observed before a magnitude 5.2 earthquake near Hollister, California, *J. Geophys. Res.*, **81**, 3556-3560.
- STACEY, F. D., 1962, Theory of magnetic susceptibility of stressed rocks, *Phil. Mag.*, **7**, 551-556.
- STACEY, F. D., 1964, The seismomagnetic effect, *Pageoph*, **58**, 5-22.
- STACEY, F. D., K. G. BARR and G. R. ROBSON, 1965, The volcanomagnetic effect, *Pageoph*,

- 62, 96-104.
- STACEY, F. D. and M. J. S. JOHNSTON, 1972, Theory of the piezomagnetic effect in titanomagnetite-bearing rocks, *Pageoph*, **97**, 146-155.
- STACEY, F. D. and S. K. BANERJEE, 1974, The physical principles of rock magnetism, Chapter 11, Elsevier, Amsterdam.
- STEKETEE, J. A., 1958a, On Volterra's dislocations in a semi-infinite elastic medium, *Can. J. Phys.*, **36**, 192-205.
- STEKETEE, J. A., 1958b, Some geophysical applications of the elasticity theory of dislocation, *Can. J. Phys.*, **36**, 1168-1198.
- STRATTON, J. A., 1941, Electromagnetic theory, Chapter III, McGraw-Hill, New York.
- SUMITOMO, N. and K. NORITOMI, 1986, Synchronous precursors in the electrical earth resistivity and the geomagnetic field in relation to an earthquake near the Yamasaki fault, southwest Japan, *J. Geomag. Geoelectr.*, **38**, 971-989.
- SUZUKI, Y. and N. OSHIMAN, 1990, A paradox in volcanomagnetism: Disagreement between analytical and numerical estimates of geomagnetic changes due to an underground pressure nucleus, *J. Geomag. Geoelectr.*, **42**, 1291-1308.
- TAKAHASI, R. and K. HIRANO, 1941a, Changes in the vertical intensity of geomagnetism that accompanied the eruption of Miyakezima in 1940, *Bull. Earthq. Res. Inst.*, **19**, 82-103.
- TAKAHASI, R. and K. HIRANO, 1941b, Changes in the vertical intensity of geomagnetism that accompanied the eruption, *Bull. Earthq. Res. Inst.*, **19**, 373-380.
- TAKAHASI, H. and M. MORI, 1974, Double exponential formulas for numerical integration, *Publ. R.I.M.S., Kyoto Univ.*, **9**, 721-741.
- TALWANI, P. and R. L. KOVACH, 1972, Geomagnetic observations and fault creep in California, *Tectonophysics*, **14**, 245-256.
- TANAKADATE, A. and H. NAGAOKA, 1893, The disturbance of isomagnetism attending the Mino-Owari earthquake of 1891, *J. Sci. Coll., Tokyo Imperial Univ.*, **5**, 149-192.
- TAZIMA, M., 1967, Accuracy of recent magnetic survey and a locally anomalous behaviour of the geomagnetic secular variations in Japan, *Bull. Geograph. Sur. Inst. Japan*, **13**, part 2, 1-78.
- TERADA, T., 1931, On luminous phenomena accompanying earthquakes, *Bull. Earthq. Res. Inst.*, **9**, 225-255.
- UHRENBACHER, R., 1988, A new method for interpreting tectonomagnetic field changes using natural geomagnetic stress sensor, *European University Studies, Ser. XVII*, pp. 218, Peter Lang, Frankfurt am Main.
- VAROTSOS, P. and K. ALEXOPOULOS, 1984a, Physical properties of the variations of the electric field of the earth preceding earthquakes, I, *Tectonophysics*, **110**, 73-98.
- VAROTSOS, P. and K. ALEXOPOULOS, 1984b, Physical properties of the variations of the electric field of the earth preceding earthquakes, II Determination of epicenter and magnitude, *Tectonophysics*, **110**, 99-125.
- VLADIMIROV, V. S., 1971, Equations of Mathematical Physics, (English Translation from Russian), Marcel Decker.
- WATSON, G. N., 1922, A treatise on the theory of Bessel functions, 4th ed., Cambridge, 804pp.
- YAMAKAWA, N., 1955, On the strain produced in a semi-infinite elastic solid by an interior source of stress, (in Japanese with English abstract), *J. Seism. Soc. Japan*, (ii), **8**, 84-98.
- YAMAZAKI, Y., 1977, Tectonoelectricity, *Geophys. Surveys*, **3**, 123-142.
- YANAGIHARA, K., 1972, Secular variation of the electrical conductivity anomaly in the central part of Japan, *Mem. Kakioka Mag. Obs., Japan Meteorol. Agency*, **15**, 1-11.
- YOKOYAMA, I., 1956, Geomagnetic studies of Volcano Mihara, the 7th paper, *Bull. Earthq. Res. Inst., Univ. Tokyo*, **34**, 21-32.

- YOKOYAMA, I., 1969, Anomalous changes in geomagnetic field on Oshima Volcano related with its activities in the decade of 1950, *J. Phys. Earth*, **17**, 69-76.
- YUKUTAKE, T., 1990, An overview of the eruptions of Oshima Volcano, Izu, 1986-1987 from the geomagnetic and geoelectric standpoints, *J. Geomag. Geoelectr.*, **42**, 141-150.
- YUKUTAKE, T. and H. TACHINAKA, 1967, Geomagnetic variation associated with stress change within a semi-infinite elastic earth caused by a cylindrical force source, *Bull. Earthq. Res. Inst., Univ. Tokyo*, **45**, 785-798.
- YUKUTAKE, T., T. YOSHINO, H. UTADA, H. WATANABE, Y. HAMANO, Y. SASAI and T. SHIMOMURA, 1987, Changes in the electrical resistivity of the central cone, Miharayama, of Izu-Oshima Volcano, associated with its eruption in November, 1986, *Proc. Japan Acad.*, **63-B**, 55-58.
- YUKUTAKE, T., H. UTADA, T. YOSHINO, E. KIMOTO, K. OTANI and T. SHIMOMURA, 1990, Regional secular change in the geomagnetic field in the Oshima Island area during a tectonically active period, *J. Geomag. Geoelectr.*, **42**, 257-275.
- YUKUTAKE, T., H. UTADA, T. YOSHINO, H. WATANABE, Y. HAMANO, Y. SASAI, E. KIMOTO, K. OTANI and T. SHIMOMURA, 1990, Changes in the geomagnetic total intensity observed before the eruption of Oshima Volcano in 1986, *J. Geomag. Geoelectr.*, **42**, 277-290.
- ZHAN, Z., 1989, Investigation of tectonomagnetic phenomena in China, *Phys. Earth Planet. Interiors*, **57**, 11-22.
- ZLOTNICKI, J., J. P. POZZI and F. H. CORNET, 1981, Investigation of induced magnetization variations caused by triaxial stresses, *J. Geophys. Res.*, **86**, 11899-11909.
- ZLOTNICKI, J. and F. H. CORNET, 1986, A numerical model of earthquake-induced piezomagnetic anomalies, *J. Geophys. Res.*, **91**, 709-718.
- ZLOTNICKI, J. and J. L. LE MOUËL, 1988, Volcanomagnetic effects observed on Piton de la Fournaise Volcano (Reunion Island): 1985-1987, *J. Geophys. Res.*, **93**, 9157-9171.

線形ピエゾ磁気効果に基づく地殻活動磁場のモデル化

地震研究所 笹井 洋一

地震や火山活動、あるいはゆるやかな地殻変動による地殻応力に伴って、地磁気が変化する。これは岩石が応力によって磁化を変えるピエゾ磁気効果を、その原因としている。本論文では様々な地殻活動に伴うピエゾ磁気変化を統一的に扱う方法を定式化する。この理論は基本的には、STACEY (1964) が「地震地磁気効果」を見積る計算で行ったやり方を一般化したものである。

第2章では基礎理論を構築する。まず岩石実験の成果に基づいて、三次元応力状態における応力と磁化の関係を定式化する。これは単軸圧縮の実験結果に重ね合わせの原理を適用して得られる。ここで求めた等方的ピエゾ磁気法則は2つの独立なパラメータから成り、ZLOTNICKI *et al.* (1981) が提案したものと等価である。従来のピエゾ磁気法則 (STACEY, 1964; NAGATA, 1970) は唯一つのパラメータ (磁気応力係数) から成っているが、それはこの拡張された法則の特別な場合に当たる。様々な岩石の集合体についての平均としては、従来の一つのパラメータで記述されたピエゾ磁気法則が成り立つものと考えられるので、以下の計算ではこちらを用いることにする。磁場についてのガウスの法則と静的つりあいのコーシー=ナビエ方程式を、構成法則、即ちピエゾ磁気法則と等方弾性体のフックの法則で結合することによって、磁気弾性体の作る磁場に対する基礎方程式が導かれる。これは変位場で表現された源泉項を持つポアソン方程式になる。この方程式の解についての表現定理は、考えている弾性体の表面の変位とその法線微分に関する面積分で表される。この定理をくい違い面を含む磁気弾性体に適用すると、くい違い面は面磁石として振舞うことが判る。ボルテラ型のくい違いの場

合では、磁気面は単に磁気二重層となり、その磁気モーメントはくい違い変位と磁化ベクトルの内積に媒質定数を掛けたもので与えられる。これを地震地磁気モーメントと呼ぶ。以下の計算において仮定した地球のモデルは最も簡単なもので、均質で等方性の半無限弾性体の地表からある深さまでが一樣に磁帯し、磁気応力係数も一定とする。

第3章では火山学において重要な茂木モデル (Mogi 1958) に伴うピエゾ磁気変化を詳しく調べる。半無限弾性体中の有限半径球が静水圧的に膨張する場合を扱った。二重フーリエ変換 (ハンケル変換) とリップシッツ=ハンケル積分を用いて、解析解が得られた。この二つの手法は、本研究で扱う全ての問題を解析解に帰着させる過程で、くり返し使われる。力源の半径を無限小にした極限として、点力源解が得られる。この操作は以下において、いくつかのグリーン関数を構築する場合の原型をなす。すなわち、応力場の特異点を含む積分においては、境界条件を満たすような閉曲面でこの特異点を囲み、その面を特異点に収れんさせる、という極限操作が必要である。

第4章では単力源 (Single Force) の重ね合わせて作られる力学モデルに伴うピエゾ磁気変化を計算する。一般の方法を考える。半無限弾性体内の一点に作用する変位場を重ね合わせることで、様々な地殻変動モデルが作られる。この単力源の作るピエゾ磁気ポテンシャルを求め、これを基本ピエゾ磁気ポテンシャル (Fundamental Piezomagnetic Potential) と呼ぶ。単力源の線形結合で表される力学的モデルに伴う磁気変化も、基本磁気ポテンシャルの一次結合で与えられる。この方法は地表荷重問題と体積の力源 (塑性変形や熱応力) 問題に適用できる。応用例として、一樣な円形荷重によるダム地磁気効果を計算した。この計算例を世界各地で得られているダム地磁気効果の観測結果と比較したところ、地殻上部の磁気応力係数の平均的な値は、岩石磁気実験で得られる頑丈な岩石のそれよりも一桁大きい、という可能性が示唆された。

第5章においては、くい違いの弾性論を用いたモデルを扱う。半無限弾性体中のくい違い面が作る弾性場を与えるボルテラの公式と、全く同じ形の、ピエゾ磁気変化についてのボルテラ公式が導かれる。グリーン関数は一点における微小くい違いの作るピエゾ磁気ポテンシャルであり、これを要素ピエゾ磁気ポテンシャル (Elementary Piezomagnetic Potential) と呼ぶ。要素ポテンシャルを求める際に、点くい違いの周囲の発散する応力場の影響を正しく評価しなくてはならない。ピエゾ磁気に関するボルテラ公式の導出過程を吟味すると、微小くい違い面に平行な円盤を小さくする、という極限を取るべきことが示される。せん断型くい違いおよび水平な開口型くい違いでは、地表面に現れる等価磁気がくい違い面のそれと完全に相殺しあう、という結果が得られた。一方、垂直なくい違い面の開口の場合は、くい違い面に等価磁気を生じる。そのため、あるタイプの断層運動によるピエゾ磁気変化は、地震地磁気モーメントから期待されるものよりかなり小さくなってしまふ。重要な応用例は複合テンション・クラック・モデルで、これは地殻ダイラタンシーやある種の火山性地殻変動を扱うのに有効である。ここでは複合茂木モデルの地磁気変化を定式化した。断層運動に伴う地磁気変化の例として、垂直な長方形断層による、横ずれ、および開口 (岩脈貫入) 変位の場合の解析解を導いた。